Université de Liège
Faculté des Sciences
I.P.N.A.S.

Academic year 2011–2012

Contribution to Entanglement Theory, Applications in Atomic Systems and Cavity QED

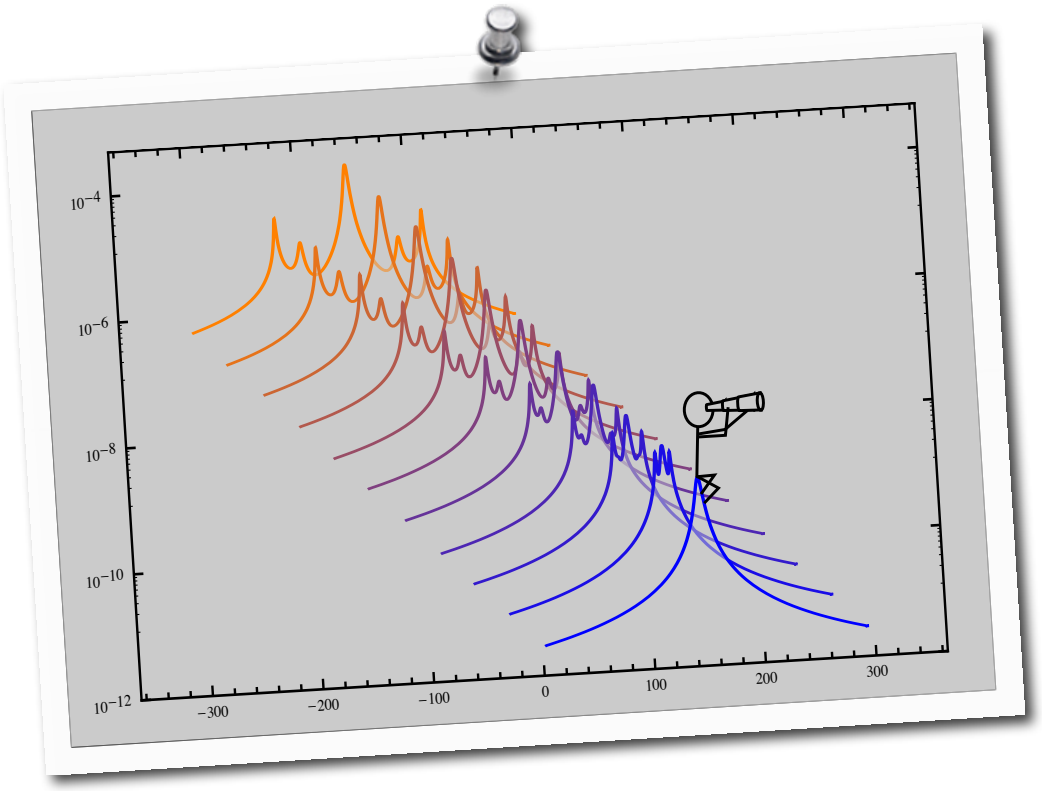

Jérémie Gillet

Advisor:

Thierry Bastin

President of the Jury:

Peter Schlagheck

Members of the Jury:

Girish S. Agarwal
John Martin
Pierre Mathonet
Joachim Von Zanthier

Thesis presented in fulfillment of
the requirements for the Degree of Doctor in Science

October 21st 2011

First of all, I would like to thank to my advisor, Thierry Bastin, who led my efforts for four years. I learned many things on this journey and, more often than not, you were the one teaching them to me.

I want to give many thanks to Girish S. Agarwal, who co-advised me and welcomed me three times to his group in Oklahoma State University for the grand total of one year. That year was synonym of hard work and of many, many breakthroughs. I also want to thank everybody of the Quantum Optics and Quantum Information Science Group at OSU, you guys were an essential part of my adventure, I was lucky to meet you.

I vehemently thank all the members of the IPNAS in Liège, you are amazing, how do you do it? This place is like a second home to me, especially on Fridays. My second family is located elsewhere, though. Cross the street, enter the building, go up four floors. Fourth floorers and affiliated were sometimes the only thing that kept me going, may our friendship never die.

I will keep it short and not mention anybody else by name but chances are, if you are reading this thesis, you had some role to play in its development. I want you to pat yourself on the back and receive all my gratitude, that's probably the least you deserve.

Contents

Introduction

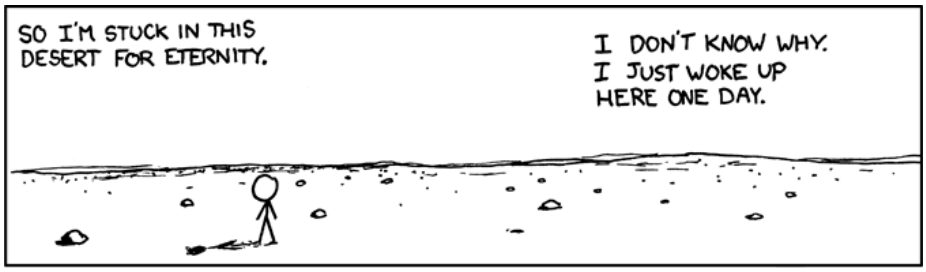

Randall Munroe, *A Bunch of Rocks* (part 1 of 9), `xkcd.com/505/`

Quantum entanglement is by far the most intriguing feature of quantum mechanics compared to any other classical theory. It plays a fundamental role in every apparent paradox or counter-intuitive consequence of quantum theory. Its mind-blowing properties have many, many application in a very large range of fields. In spite of this incredible success, characterization and classification of entanglement in a general state is still an open question of the quantum theory. That is the very issue that motivated this work. The first two chapters of this thesis introduce entanglement criteria of various domains of application that contribute to this search of entanglement characterization. For the rest of the thesis, we set aside the mathematical considerations and consider the fascinating problem of experimentally producing entanglement in physical systems and more particularly in systems of cold atoms. This entanglement production must come from ingredients available in the laboratories today: lasers, cavities, cold atoms in gazes or isolated and, most importantly, interatomic interactions. In chapters 3 to 5, we consider dipole interactions between atoms and the phenomenon of dipole blockade as a mean to produce entanglement in systems of two or more atoms. In chapter 6, we explore the many possibilities of cavity quantum electrodynamics. Every chapter just about stands on its own and will be duly self-introduced and placed into its context in the literature, but we present them briefly here.

Chapter 1 is devoted to *Multipartite Entanglement Criterion from Uncertainty Relations*. In this chapter, we describe a criterion which can experimentally detect the presence of entanglement in a wide variety of quantum states. That criterion is the love child of two great concepts in quantum mechanics, the Schrödinger-Robertson inequality (SRI) and the positive partial transpose (PPT) criterion. The SRI is a generalization of the even

more famous Heisenberg inequality and describes how the product of the variances of two non-commuting operators can never be smaller than some particular minimal value. The PPT criterion shows that under the action of a particular mathematical operation, the partial transpose, the density matrix of a separable state must remain a physical quantity, whereas the density of an entangled state might very well not do so. By bringing those two concepts together, we were able to define the Schrödinger-Robertson partial transpose criterion. This criterion dictates that the product of the variances of two observables modified by the partial transpose operation will always be bounded by a minimal value when acting on a separable state. An entangled state, however, might violate the inequality, a certain sign of its entanglement. We show that in order to satisfy some constraints due to the SRI and the PPT criterion, the observables must obey some specific conditions and we show their general form for bipartite systems. We go on proving that our entanglement criterion is necessary and sufficient for any pure bipartite state or even any pure three-qubit state. We test its performances on a large variety of systems, harmonic oscillators, multi-photon polarization states, Schrödinger cat states and multipartite mixed states.

Chapter 2 is devoted to *Concurrences for N-qubit Systems*. In that chapter, we present another entanglement criterion inspired from the criterion of the concurrence. The concurrence is a mathematical criterion that not only detects entanglement in two-qubit states, but also quantifies the amount of entanglement for pure states or mixed states. We start the chapter by introducing the concurrence. Next, we give a series of nine conditions that a pure three-qubit state must obey to be separable. We prove that those conditions are necessary and sufficient conditions to entanglement with a formalism that can easily be generalized to systems of more qubits. We then take advantage of those conditions to define concurrences for tripartite pure states. We show that those quantities are linked to other values used to evaluate tripartite entanglement. Using the formalism of the original concurrence, we prove that our concurrences can also be evaluated easily on mixed states. Any non-zero concurrence is a sure sign of entanglement. We finally test our criterion on different mixed states and find encouraging results. In the second part of the chapter we generalize the whole process to systems of N-qubits. We show that the number of conditions to separability grows very much with the number of qubits, but we can still compute them and we define generalized concurrences, which are necessary and sufficient conditions for entanglement in pure states. We finally prove that they may also be applied on mixed states.

Chapter 3 is devoted to *Entanglement, Antibunching, and Saturation Effects in Dipole Blockade* and leads the path of quantum information theory into the domain of quantum optics. In this chapter, we study the interaction of two identical two-level atoms immersed in a resonant laser field. The Hamiltonian model for the interaction is specifically chosen to describe the dipole blockade effect. In a blockaded system, one atom in its excited states prevents, with some degree, the other atom to get excited. The interest of such an interaction is the production of entanglement. Indeed, a system of two independent atoms can never be entangled by a laser, however a blockaded system is constrained to deal only with the ground state and a coherent superposition of "first atom excited, second not excited" and of the opposite situation and such a superposition is shown to carry maximal

entanglement. After introducing our Hamiltonian, we introduce the master equation which modelizes dissipation effects in the system, allowing us, after a few considerations about the non-interactive case, to compute the time evolution of the system. We measure the concurrence as well as a quantity able to estimate the blockade on time-evolving states. We show that our model describes the dipole blockade well and also that the strengthening of the laser power has the effect of lifting said blockade. Then, we study the equilibrium case, the steady state of the system and we give its analytical description as well as an analytical expression of its concurrence. That expression allows us to tune the laser power in order to maximize the amount of entanglement for a given interaction strength. Finally, we study another way to experimentally show the blockade effect, the photon-photon correlation.

Chapter 4 is devoted to *Dipole Blockade and Entanglement in Three-Atom Systems* and generalizes the Hamiltonian model for the dipole blockade effect on systems of three two-level atoms. We start by introducing the model, along with a particular basis which takes advantage of the possible symmetries of the system. We also define quantities which measure the blockade effect, which can now be considered for a particular pair of atoms or for the three of them altogether. We then consider several different cases of interaction: no interaction between the atoms, interaction between only two, same interaction between all atoms and aligned atoms with interaction between first neighbors only. For each case, we give an analytical value of the steady state and study their blockades. We observe blockades in the different cases with varying amplitudes except for one particular case where antiblockade is observed. After that, we study the two-atom concurrences by tracing out one atom and find that bipartite entanglement is weakened by the presence of a third interacting atom. Finally, we study tripartite entanglement using the three-qubit concurrences defined in chapter 3 and find indications of bipartite entanglement in the system as well as genuine tripartite entanglement.

Chapter 5 is devoted to *EIT, Dipole Blockade and Dipole-Dipole Interaction*. In this chapter, we introduce the electromagnetically induced transparency (EIT). The EIT is a phenomenon taking place in multi-level systems excited by two non-resonant lasers, the pump and the probe, where under some conditions the absorption of the probe laser is cancelled for a specific window of frequency. We start by quantifying this effect with the steady state of a single three-level atom and check established results. Then we investigated what would happen to the EIT if two atoms were to experience dipole blockade. We introduce our model Hamiltonian and master equation, check the eigenstates of the system with the probe laser turned off. Armed with those weapons, we measure the dipole blockade in the system as well as the effect on EIT. In the second part of the chapter we test the effects of another type of interaction, the dipole-dipole interaction. We introduce our model, Hamiltonian and master equation, find the eigenstates of the unperturbed system and compute the values of the dipole blockade and the effect on EIT in the steady state. We find a strong modification in the behavior of the EIT.

Chapter 6 is the last chapter and is devoted to *Cavity Mediated Two-Photon Processes in Two-Qubit Circuit QED*. In free space, two non-identical two-level atoms may not be simultaneously excited by a laser through a two-photon process. We explore the possibility that this inhibition, due to interference effects, can be beaten by placing the atoms in

a single mode cavity. After briefly checking what happens in free space, we give our model Hamiltonian an master equation which modelize the different atomic frequencies, the cavity mode, the interaction between them, the laser field exciting the cavity modes and the dissipation effects such as the atomic spontaneous emission and the cavity losses. We first make an assumption on the atomic frequencies which allows us to diagonalize the unperturbed Hamiltonian and find the eigenvalues and eigenstates of the bare system. Then, using a perturbative approach, we find that two-photon processes are indeed possible in such a system at some particular frequencies and we calculate the transition rates. We confirm our calculations by producing different atomic and photonic spectra in the steady state of the system. We find that the quality of the cavity has a strong effect on the structure of the spectra and induces behaviors not predicted by perturbation theory. In the last part of the chapter, we lift the constraint of the atomic frequency and confirm our results by numerically checking the same spectra for a most general configuration of the system. We also find a new feature of the system, the cavity induced transparency.

In the conclusion, we summarize all the results we were able to get and finally we give the appendices, which contain calculations not essential to the text as well as steady state results too imposing to fit in the chapters.

Chapter 1

Multipartite Entanglement Criterion from Uncertainty Relations

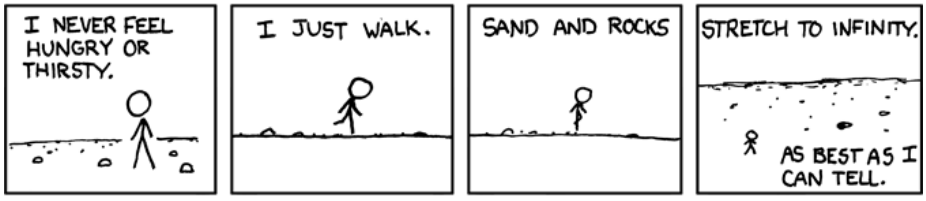

Randall Munroe, *A Bunch of Rocks* (part 2 of 9), `xkcd.com/505/`

In the past few years, many criteria detecting entanglement in bipartite and multipartite systems have been developed [1–3]. The Peres-Horodecki positive partial transpose (PPT) criterion [4] has played a crucial role in the field and provides, in some cases, necessary and sufficient conditions to entanglement. That criteria is formulated in terms of the density operator and any practical application involves state tomography. Other criteria have been proposed so they could be tested experimentally in a direct manner, as the Bell inequalities [5,6] or the entanglement witnesses [7]. More recently, criteria based on variance measurements have been studied for continuous and discrete variable systems [8–20].

In [17] the Heisenberg relation has been used along with the partial transpose operation to obtain a criterion detecting entanglement condition in bipartite non-gaussian states. That idea was generalized in [19,20] with use of the Schrödinger-Robertson relation instead of the Heisenberg inequality. In this chapter, we generalize completely those concepts and prove that the Schrödinger-Robertson type inequality is able to detect entanglement in any pure state of bipartite and tripartite systems. Experimentally, it can be realized by measuring mean values and variances of different observables on a wide range of systems.

We start the chapter by introducing the Schrödinger-Robertson inequality and the PPT criterion in Sec. 1.1 and 1.2. In Sec. 1.3 we introduce our Schrödinger-Robertson partial transpose (SRPT) criterion and study its validity with a few properties of the partial transpose. We find that all observables are not suitable and we yield the general condition

they must satisfy to be eligible. For 2×2 systems, we explicitly give their general form. Finally, we show that the SRPT criterion is necessary and sufficient in the case of bipartite pure states.

In Sec. 1.4, we study various different applications of the SRPT in the bipartite case, including angular momentum states of harmonic oscillators, cat states and multiphoton polarization states. In Sec. 1.5, we prove that our criterion is necessary and sufficient in the case of pure tripartite qubit states. Finally, in Sec. 1.6 we apply the criterion to mixed states and we show that the inequality detects entanglement of bipartite Werner states better than the Bell inequalities [5] and also leads to a good characterization of multipartite Werner states.

1.1 Schrödinger-Robertson Inequality

One of the great results of quantum mechanics is Heisenberg uncertainty principle, actually not a principle at all since it can be demonstrated. That principle states that one cannot measure simultaneously certain pairs of physical quantities with an arbitrarily large precision. More precisely, that uncertainty occurs when the observables corresponding to the physical quantities do not *commute*.

The Heisenberg uncertainty principle can actually be derived from a more general type of inequality, the Schrödinger-Robertson Inequality [21]. Let us consider two observables A and B and a general physical state ρ, expressed in the matrix density formalism. We define the complex quantity

$$z = \mathrm{Tr}\,(\rho AB) = \langle AB \rangle. \tag{1.1}$$

We find that

$$2i\,\mathrm{Im}(z) = \langle AB \rangle - \langle BA \rangle = \langle [A,B] \rangle, \tag{1.2}$$

$$2\,\mathrm{Re}(z) = \langle AB \rangle + \langle BA \rangle = \langle \{A,B\} \rangle, \tag{1.3}$$

where $[A,B] \equiv AB - BA$ and $\{A,B\} \equiv AB + BA$ are respectively the commutator and anticommutator of A and B. We therefore have

$$|\langle [A,B] \rangle|^2 + |\langle \{A,B\} \rangle|^2 = 4|\langle AB \rangle|^2. \tag{1.4}$$

Here, we apply Cauchy-Schwarz inequality and get

$$|\langle AB \rangle|^2 \leq \langle A^2 \rangle \langle B^2 \rangle, \tag{1.5}$$

which combined with Eq. (1.4) gives

$$|\langle [A,B] \rangle|^2 + |\langle \{A,B\} \rangle|^2 \leq 4\langle A^2 \rangle \langle B^2 \rangle. \tag{1.6}$$

Let us define some new observables $C = A - \langle A \rangle$ and $D = B - \langle B \rangle$. Clearly, we have

$$\langle [C,D] \rangle = \langle [A,B] \rangle, \tag{1.7}$$

$$\langle \{C,D\} \rangle = \langle \{A,B\} \rangle - 2\langle A \rangle \langle B \rangle. \tag{1.8}$$

Since we can write Eq. (1.6) for the observables C and D with the *variance*

$$(\Delta A)^2 = \langle (A - \langle A \rangle)^2 \rangle = \langle C^2 \rangle, \tag{1.9}$$

we can finally write the Schrödinger-Robertson Inequality:

$$(\Delta A)^2 (\Delta B)^2 \geq \frac{1}{4} |\langle [A, B] \rangle|^2 + \frac{1}{4} |\langle \{A, B\} \rangle - 2\langle A \rangle \langle B \rangle|^2. \tag{1.10}$$

This result is a remarkable and very general feature of quantum mechanics, which is completely inherent to the physical state being investigated and not at all related to the ability of a researcher to measure the quantities.

The Heisenberg inequality is simply obtained by ignoring the second term on the right-hand side of (1.10), which only accentuates the inequality.

1.2 Positive Partial Transpose Criterion

In 1996, Asher Peres [4] published a criterion able to characterize the entanglement in bipartite systems, either pure or mixed. Let us consider a separable system acting in $\mathcal{H}$ composed of two subsystems described by the individual density matrices ρ_i^1 et ρ_i^2. The state of the system is in general

$$\rho = \sum_i p_i \, \rho_i^1 \otimes \rho_i^2, \tag{1.11}$$

with $p_i \geq 0, \forall i$ et $\sum_i p_i = 1$. The individual matrix elements will be described as

$$\rho_{m\mu,n\nu} = \langle m\mu | \rho | n\nu \rangle = \sum_i p_i \, \left(\rho_i^1\right)_{mn} \left(\rho_i^2\right)_{\mu\nu}, \tag{1.12}$$

where the states described by latin indices are the basis states of the first subsystem and the ones described by the greek indices are those of the second subsystem, which may have a different dimension. Let us form a new density matrix σ defined by

$$\sigma_{m\mu,n\nu} \equiv \rho_{n\mu,m\nu}. \tag{1.13}$$

The matrix σ is defined from ρ where the latin indices have been switched, but not the greek ones. This definition of σ is equivalent to

$$\sigma = \rho^{\mathrm{pt}} \equiv \sum_i p_i \, (\rho_i^1)^{\mathrm{T}} \otimes \rho_i^2, \tag{1.14}$$

where "pt" stands for *partial transpose* and represents the operator that transposes the density matrix of the first subsystem. The partial transpose of a density matrix as defined by Eq. (1.13) is a very general concept which holds for any state, entangled or not. It is also applicable to any bipartite hermitian operator A and we define similarly

$$\left(A^{\mathrm{pt}}\right)_{m\mu,n\nu} \equiv A_{n\mu,m\nu}. \tag{1.15}$$

The transposed density matrices $(\rho_i^1)^{\mathrm{T}}$ of our separable state are still hermitian, positive operators and therefore are legitimate density matrices describing a physical state, which implies that so does σ. In other words, any separable state must have a positive partial transpose. From the physical sense of σ, the Peres criterion is stated.

Criterion 1. Peres Criterion (PPT Criterion) — *If a bipartite state described by the density matrix ρ is separable, then its partial transpose ρ^{pt} is positive.*

Equivalently, if one eigenvalues of ρ^{pt} is found to be negative, then the state ρ is entangled.

This first statement of the criterion is only a necessary condition and was unfortunately proven to remain only necessary for the general case. However, its was proven by the Horodecki [22] that this criterion was indeed necessary and sufficient in the case of systems of dimension 2×2 or 2×3.

Criterion 2. Peres-Horodecki Criterion — *A bipartite state described by the density matrix ρ of dimension 2×2 or 2×3 is separable if and only if its partial transpose ρ^{pt} is positive.*

Although this criterion is very powerful, it cannot be implemented experimentally right away since the operation of partial transposition is a mathematical operator and not a physical one. That is why we found a way to make use of the PPT criterion in an experimental context, namely the measurement of Scrödinger-Robertson inequalities.

1.3 Schrödinger-Robertson Partial Transpose Criterion

For any observables A, B and any density operator ρ, the Schrödinger-Robertson inequality is observed. In this section, we use that property together with the PPT criterion to build a new entanglement criterion.

The partial transpose ρ^{pt} of a bipartite separable density operator must be positive, which implies it does describe some physical state and must therefore obey the Schrödinger-Robertson uncertainty relation for any observables A and B, i.e. Eq. (1.10) also holds with ρ^{pt} if ρ is separable. In the density matrix formalism, this inequality is written

$$\begin{aligned}\left(\mathrm{Tr}\left(\rho^{\mathrm{pt}}A\right)^2 - \mathrm{Tr}\left(\rho^{\mathrm{pt}}A^2\right)\right)\left(\mathrm{Tr}\left(\rho^{\mathrm{pt}}B\right)^2 - \mathrm{Tr}\left(\rho^{\mathrm{pt}}B^2\right)\right) \\ \geq \tfrac{1}{4}\left|\mathrm{Tr}\left(\rho^{\mathrm{pt}}[A,B]\right)\right|^2 + \tfrac{1}{4}\left|\mathrm{Tr}\left(\rho^{\mathrm{pt}}\{A,B\}\right) - 2\mathrm{Tr}\left(\rho^{\mathrm{pt}}A\right)\mathrm{Tr}\left(\rho^{\mathrm{pt}}B\right)\right|^2 .\end{aligned} \tag{1.16}$$

This inequality always holds when applied on separable state, but might not do so when ρ^{pt} represents a non-physical state, i. e. when ρ is entangled. Since we cannot produce a ρ^{pt} states with the experimental tools available, we could think of "switching" the partial

transpose sign from $\mathrm{Tr}\,(\rho^{\mathrm{pt}}A)$ to $\mathrm{Tr}\,(\rho A^{\mathrm{pt}})$ and from $\mathrm{Tr}\,(\rho^{\mathrm{pt}}A^2)$ to $\mathrm{Tr}\,(\rho(A^{\mathrm{pt}})^2)$, which would yield the Scrödinger-Robertson partial transpose (SRPT) inequality

$$(\Delta A^{\mathrm{pt}})^2(\Delta B^{\mathrm{pt}})^2 \geq \frac{1}{4}|\langle[A,B]^{\mathrm{pt}}\rangle|^2+\frac{1}{4}|\langle\{A,B\}^{\mathrm{pt}}\rangle - 2\langle A^{\mathrm{pt}}\rangle\langle B^{\mathrm{pt}}\rangle|^2, \tag{1.17}$$

which would never be violated for separable states and violated by entangled states only. The key result of this chapter is that unlike the PPT criterion in itself, Eq. (1.17) has the property of being experimentally implementable since it deals with observable quantities. However, "switching" the partial transpose sign is not a trivial operation, we need to make sure the operation is valid.

First of all the partial transpose A^{pt} of an observable A must remain an observable; if that is the case then the mean value $\mathrm{Tr}\,(\rho A^{\mathrm{pt}})$ of a partially transposed observable must be equal to the mean value $\mathrm{Tr}\,(\rho^{\mathrm{pt}}A)$ of the observable measured on the partially transposed density matrix and finally the value of the variance $(\Delta A^{\mathrm{pt}})^2$ must also follow that rule. In the next subsection, we investigate those conditions and prove a few properties, which will lead us to believe that not all observables can be considered in order to get a valid SRPT relation.

1.3.1 Properties of the Partial Transposition

In this subsection, we talk about a pair observables A or B that are considered to act on a system composed of two subsystems of size n and n', finite or not. We consider the matrix elements $A^{\dagger}_{i\mu,j\nu}$ with the latin indices i,j referring to the first subsystem taking the values $1,2,\cdots,n$ and the greek indices μ,ν referring to the second subsystem taking the values $1,2,\cdots,n'$.

Property 1.1. *The partial transposition of an observable A is an observable.*

Proof: The only requirement for an operator A to be an observable is to be hermitian, i. e. to verify $A^{\dagger}=A$. We have

$$\begin{aligned}
\left((A^{\mathrm{pt}})^{\dagger}\right)_{i\mu,j\nu} &= (A^{\mathrm{pt}})^{*}_{j\nu,i\mu}, && (1.18)\\
&= A^{*}_{i\nu,j\mu}, && (1.19)\\
&= A_{j\mu,i\nu}, && (1.20)\\
&= (A^{\mathrm{pt}})_{i\mu,j\nu}, && (1.21)
\end{aligned}$$

which concludes the proof.

The next proposition deals with the mean values of observables.

Property 1.2. *For any operators A, B, we have*

$$\mathrm{Tr}\,(A^{\mathrm{pt}}B) = \mathrm{Tr}\,(AB^{\mathrm{pt}})\,. \tag{1.22}$$

Proof: in order to simplify the developments, we use the convention of a repeated index implying a summation over all values of said index. We have

$$\begin{aligned} \mathrm{Tr}\left(A^{\mathrm{pt}}B\right) &= \left(A^{\mathrm{pt}}B\right)_{i\mu,i\mu} = \left(A^{\mathrm{pt}}\right)_{i\mu,l\lambda} B_{l\lambda,i\mu}, & (1.23)\\ &= A_{l\mu,i\lambda} B_{l\lambda,i\mu} = A_{l\mu,i\lambda}\left(B^{\mathrm{pt}}\right)_{i\lambda,l\mu}, & (1.24)\\ &= \left(AB^{\mathrm{pt}}\right)_{l\mu,l\mu} = \mathrm{Tr}\left(AB^{\mathrm{pt}}\right), & (1.25) \end{aligned}$$

which concludes.

Hence, if B represents a density matrix, this result means that the mean value of a partially transposed observable is equal to the mean value of the observable measured on the partially transposed density matrix. The next proposition deals with the variance.

Property 1.3. *For any observable A, we have*

$$\mathrm{Tr}\left(\rho^{\mathrm{pt}}A^2\right) = \mathrm{Tr}\left(\rho\left(A^{\mathrm{pt}}\right)^2\right), \tag{1.26}$$

for any density matrix ρ if and only if

$$\left(A^{\mathrm{pt}}\right)^2 = \left(A^2\right)^{\mathrm{pt}}. \tag{1.27}$$

Proof: if $\left(A^{\mathrm{pt}}\right)^2 = \left(A^2\right)^{\mathrm{pt}}$, then the result is a direct consequence of Prop. 1.2. On the other hand, if the traces are identical

$$\mathrm{Tr}\left(\rho^{\mathrm{pt}}A^2\right) - \mathrm{Tr}\left(\rho\left(A^{\mathrm{pt}}\right)^2\right) = \mathrm{Tr}\left(\rho\left[\left(A^2\right)^{\mathrm{pt}} - \left(A^{\mathrm{pt}}\right)^2\right]\right) = 0, \tag{1.28}$$

and in particular, we must have

$$\langle\psi|\left(A^2\right)^{\mathrm{pt}} - \left(A^{\mathrm{pt}}\right)^2|\psi\rangle = 0, \tag{1.29}$$

for *any* state vector $|\psi\rangle$ including all the eigenstates of the observable, which is only possible if $\left(A^{\mathrm{pt}}\right)^2 = \left(A^2\right)^{\mathrm{pt}}$. This result shows that the variance $(\Delta A^{\mathrm{pt}})^2 = \mathrm{Tr}\left(\rho(A^{\mathrm{pt}})^2\right) - \mathrm{Tr}\left(\rho A^{\mathrm{pt}}\right)^2$ is not always equal to the variance $(\Delta A)^2$ applied on the partially transposed state ρ^{pt}.

This result is the major constraint about using SRPT inequalities. In general, observables do not satisfy Eq. (1.27), which can result in a violation of an SRPT inequality applied on a separable state with unsuitable observables.

To illustrate this, we consider the inequality corresponding to the computational basis vector $|00\rangle$ of a two-qubit system using the observables

$$\begin{aligned} A &= \sigma_x \otimes \sigma_x, & (1.30)\\ B &= \sigma_x \otimes \sigma_y + \sigma_y \otimes \sigma_x, & (1.31) \end{aligned}$$

with σ_x and σ_y the Pauli operators. Even though the state $|00\rangle$ is separable, we find $\Delta B^{\mathrm{pt}} = 0$ and $|\langle[A,B]^{\mathrm{pt}}\rangle| = 2$ which means the SRPT inequality is violated. That violation could happen since $(B^{\mathrm{pt}})^2 \neq (B^2)^{\mathrm{pt}}$. This example illustrates the importance of using suitable observables in the SRPT inequality. Now that we defined the conditions for the SRPT inequality to be used, we can formulate our new criterion.

Criterion 3. Schrödinger-Robertson Partial Transpose Criterion — *If there are two observables A, B satisfying*

$$(A^{\mathrm{pt}})^2 = \left(A^2\right)^{\mathrm{pt}}, \ (B^{\mathrm{pt}})^2 = \left(B^2\right)^{\mathrm{pt}}, \tag{1.32}$$

such that the Schrödinger-Robertson inequality

$$(\Delta A^{\mathrm{pt}})^2(\Delta B^{\mathrm{pt}})^2 \geq \frac{1}{4}|\langle [A,B]^{\mathrm{pt}}\rangle|^2 + \frac{1}{4}|\langle \{A,B\}^{\mathrm{pt}}\rangle - 2\langle A^{\mathrm{pt}}\rangle\langle B^{\mathrm{pt}}\rangle|^2, \tag{1.33}$$

measured on a state ρ is violated, then the ρ is entangled.

1.3.2 Form of the Suitable Observables

The first step into actually being able to use our criterion is getting more information about the specific observables that can be used. If there is no observable A satisfying Eq. (1.27), then the criterion is useless. In the following, we show that such observables do exist and that the criterion is actually necessary and sufficient for bipartite pure states.

Let us now characterize the form of the observables A of dimension $N = n \times n'$ that satisfy $(A^{\mathrm{pt}})^2 = (A^2)^{\mathrm{pt}}$. In order to do so, wee need to define a matrix orthogonal basis that will span all hermitian matrices.

Suitable candidates for that basis are the infinitesimal generators of the special unitary group $\mathrm{SU}(N)$, as they are all hermitian. The number of independent generators of $\mathrm{SU}(N)$ is $N^2 - 1$ and we need to add the identity matrix to the set to obtain the matrix basis we are looking for.

By definition, the $N^2 - 1$ generators S_i are $N \times N$, traceless and hermitian matrices such that

$$S_a S_b = \frac{1}{2N}\delta_{ab} I_N + \frac{1}{2}\sum_{c=1}^{N^2-1} (i f_{abc} + d_{abc}) S_c, \tag{1.34}$$

with $a, b = 1, 2, \cdots, N^2 - 1$ and where I_N is the $N \times N$ identity matrix ,δ_{ab} the Kronecker symbol, the f_{abc} and d_{abc} are structure constants and are respectively antisymmetric and symmetric in all indices. As it follows,

$$\{S_a, S_b\} = \frac{1}{N}\delta_{ab} I_N + \sum_{c=1}^{N^2-1} d_{abc} S_c, \tag{1.35}$$

$$[S_a, S_b] = i\sum_{c=1}^{N^2-1} f_{abc} S_c. \tag{1.36}$$

That basis is orthogonal in the sense of the inner product

$$2\ \mathrm{Tr}\,(S_a S_b) = \delta_{ab}. \tag{1.37}$$

The Pauli matrices

$$\sigma_x = \begin{pmatrix} 0 & 1 \\ 1 & 0 \end{pmatrix}, \quad \sigma_y = \begin{pmatrix} 0 & -i \\ i & 0 \end{pmatrix}, \quad \sigma_z = \begin{pmatrix} 1 & 0 \\ 0 & -1 \end{pmatrix}, \tag{1.38}$$

are (when divided by 2) such examples of generators for $N = 2$, in which case the d constants are all zero and the f constants take the values of the Levi-Civita symbol ϵ_{ijk}. The Gell-Mann matrices

$$\begin{aligned} \lambda_1 &= \begin{pmatrix} 0 & 1 & 0 \\ 1 & 0 & 0 \\ 0 & 0 & 0 \end{pmatrix}, \quad \lambda_2 = \begin{pmatrix} 0 & -i & 0 \\ i & 0 & 0 \\ 0 & 0 & 0 \end{pmatrix}, \quad \lambda_3 = \begin{pmatrix} 1 & 0 & 0 \\ 0 & -1 & 0 \\ 0 & 0 & 0 \end{pmatrix}, \\ \lambda_4 &= \begin{pmatrix} 0 & 0 & 1 \\ 0 & 0 & 0 \\ 1 & 0 & 0 \end{pmatrix}, \quad \lambda_5 = \begin{pmatrix} 0 & 0 & -i \\ 0 & 0 & 0 \\ i & 0 & 0 \end{pmatrix}, \quad \lambda_6 = \begin{pmatrix} 0 & 0 & 0 \\ 0 & 0 & 1 \\ 0 & 1 & 0 \end{pmatrix}, \\ \lambda_7 &= \begin{pmatrix} 0 & 0 & 0 \\ 0 & 0 & -i \\ 0 & i & 0 \end{pmatrix}, \quad \lambda_8 = \tfrac{1}{\sqrt{3}} \begin{pmatrix} 1 & 0 & 0 \\ 0 & 1 & 0 \\ 0 & 0 & -2 \end{pmatrix}, \end{aligned} \tag{1.39}$$

are also matrices of that form for $N = 3$ when divided by 2 for normalization.

Generalizing from the Pauli and Gell-Mann matrices, we can find a general set of SU(N) infinitesimal generators. Written in an operator-like fashion on the basis $\{|1\rangle, |2\rangle, \cdots, |N\rangle\}$ we find the first set of $(N^2 - N)/2$ matrices

$$S^{(1)}_{i,j} = \frac{1}{2}(|i\rangle\langle j| + |j\rangle\langle i|), \tag{1.40}$$

for $i = 1, 2, \cdots, N-1$ and $j = i+1, i+2, \cdots, N$. With the same conditions on i, j we give the second set of $(N^2 - N)/2$ matrices

$$S^{(2)}_{i,j} = \frac{-i}{2}(|i\rangle\langle j| - |j\rangle\langle i|). \tag{1.41}$$

The last set of $N - 1$ matrices is given by

$$S^{(3)}_i = \frac{1}{\sqrt{2(i^2 + i)}} \left(\sum_{k=1}^{i} |k\rangle\langle k| - i|i+1\rangle\langle i+1| \right), \tag{1.42}$$

for $i = 1, 2, \cdots, N-1$. All the matrices are properly normalized, and by relabeling them, one finds a set of $N^2 - 1$ matrices with the coefficients f_{abc}, d_{abc} easily found from the commutation and anticommutation relations.

Let us now consider a general system composed of two subsystems of respective dimensions n and n', with $N = n \times n'$, which are spanned by the base matrices S_i and S'_i with structure constants f, d and f', d'. We add to the basis identity matrices by defining $S_0 \equiv I_n/\sqrt{2n}$ and $S'_0 \equiv I_{n'}/\sqrt{2n'}$ and use once again the convention that any repeated index implies a sum over all of its possible values. We can therefore write a general hermitian matrix A as

$$A = a_{ij} S_i \otimes S'_j, \tag{1.43}$$

with the real coefficients a_{ij} defined as $a_{ij} \equiv 4\mathrm{Tr}\left(AS_i \otimes S'_j\right)$ and i and j running from 0 to n^2-1 and n'^2-1. Hence, we have

$$(A^{\mathrm{pt}})^2 = a_{ij}a_{kl}(S_kS_i)^{\mathrm{T}} \otimes S'_jS'_l, \tag{1.44}$$

$$\left(A^2\right)^{\mathrm{pt}} = a_{kj}a_{il}(S_kS_i)^{\mathrm{T}} \otimes S'_jS'_l. \tag{1.45}$$

We can see that if S_k and S_i commute, one only needs to switch their order in Eq. (1.45) and rename i as k and vice versa for the matrices to be equal. However, given the commutation property (1.36), it is clear that in general they do not do so and the only matrix that is assured to commute with all others is the identity matrix S_0. The same can be said of S'_j and S'_l and therefore, we see that every term with a 0 index in (1.44) will be found exactly the same in (1.45), which means there are no restrictions on the values of the a_{ij} coefficients when i or j is zero. For the rest of the $(n-1)\times(n'-1)$ coefficients, we need to investigate further. Letting go of all the terms including a zero index, we find that the quantities (1.44) and (1.45) are equal if and only if

$$0 = (a_{ij}a_{kl} - a_{kj}a_{il})(S_kS_i)^{\mathrm{T}} \otimes S'_jS'_l, \tag{1.46}$$

$$= \frac{1}{4}(a_{ij}a_{kl} - a_{kj}a_{il})\left(\delta_{ki}\frac{I_n}{n} + (if_{kip} + d_{kip})S_p^{\mathrm{T}}\right) \otimes \left(\delta_{jl}\frac{I_{n'}}{n'} + (if'_{jlq} + d'_{jlq})S'_q\right), \tag{1.47}$$

$$= \frac{1}{4}(a_{ij}a_{kl} - a_{kj}a_{il})\left((if_{kip} + d_{kip})S_p^{\mathrm{T}}\right) \otimes \left((if'_{jlq} + d'_{jlq})S'_q\right), \tag{1.48}$$

$$= -\frac{1}{4}f_{kip}f'_{jlq}(a_{ij}a_{kl} - a_{kj}a_{il})S_p^{\mathrm{T}} \otimes S'_q, \tag{1.49}$$

$$= -\frac{1}{2}f_{kip}f'_{jlq}a_{ij}a_{kl}S_p^{\mathrm{T}} \otimes S'_q, \tag{1.50}$$

$$\tag{1.51}$$

where in the third and fourth step we used the fact that an antisymmetric quantity such as $(a_{ij}a_{kl} - a_{kj}a_{il})$ summed with a symmetric factor δ_{ki} or d_{kip} will amount to zero and in the last step we noted that $f_{kip}f'_{jlq}a_{kj}a_{il} = -f_{kip}f'_{jlq}a_{ij}a_{jl}$. We end up with an null operator expressed in the $S_p^{\mathrm{T}} \otimes S'_q$ basis which is completely legitimate and we find the following result : the matrix A will satisfy $(A^{\mathrm{pt}})^2 = (A^2)^{\mathrm{pt}}$ if and only if

$$f_{kip}f'_{jlq}a_{ij}a_{kl} = 0, \tag{1.52}$$

for all p, q and all indices above 0.

In the case of two-qubit systems, that condition has a simple interpretation. Indeed, for 2×2 systems, the Pauli matrices form the matrix basis and the condition is expressed as

$$\epsilon_{kip}\epsilon_{jlq}a_{ij}a_{kl} = 0, \tag{1.53}$$

for all p, q above 0, which expresses that every 2×2 minor of the 3×3 matrix a_{ij} must be zero. Therefore all the lines (or columns) of that matrix must be linearly dependent and we can write $a_{ij} = a_ib_j$. The general form of the matrices is then

$$A = (\mathbf{a}\cdot\boldsymbol{\sigma})\otimes(\mathbf{b}\cdot\boldsymbol{\sigma}) + I_2\otimes(\mathbf{c}\cdot\boldsymbol{\sigma}) + (\mathbf{d}\cdot\boldsymbol{\sigma})\otimes I_2 + \eta\, I_4, \tag{1.54}$$

where $\boldsymbol{\sigma}$ is the vector composed of the 3 Pauli operators, $\mathbf{a}, \mathbf{b}, \mathbf{c}$ and $\mathbf{d}$ are four real vectors and η is a real number.

As a particular case of this general result, we note that if A can be written as $A_1 \otimes A_2$ with A_1 and A_2 two observables from the two subsystems, then A satisfies Eq. (1.27) immediately.

1.3.3 Necessary and sufficient criterion for pure states

In this subsection we state a necessary and sufficient version of our criterion.

Criterion 4. SRPT Criterion with Pure States — *A bipartite pure state $|\psi\rangle \in \mathcal{H}_1 \otimes \mathcal{H}_2$, with $\mathcal{H}_1$ and $\mathcal{H}_2$ two Hilbert spaces of any dimension is entangled if and only if there are observables A, B acting on $\mathcal{H}_1 \otimes \mathcal{H}_2$ satisfying*

$$(A^{\mathrm{pt}})^2 = \left(A^2\right)^{\mathrm{pt}},\ (B^{\mathrm{pt}})^2 = \left(B^2\right)^{\mathrm{pt}}, \tag{1.55}$$

such that the SRPT inequality

$$(\Delta A^{\mathrm{pt}})^2(\Delta B^{\mathrm{pt}})^2 \geq \frac{1}{4}|\langle[A,B]^{\mathrm{pt}}\rangle|^2 + \frac{1}{4}|\langle\{A,B\}^{\mathrm{pt}}\rangle - 2\langle A^{\mathrm{pt}}\rangle\langle B^{\mathrm{pt}}\rangle|^2, \tag{1.56}$$

is violated.

Proof: Let us consider an entangled state $|\psi\rangle$ and express it in the following decomposition:

$$|\psi\rangle = \sum_i c_i |i\rangle_1 \otimes |i\rangle_2, \tag{1.57}$$

where the $|i\rangle_j$ are a basis of $\mathcal{H}_j$ and the c_i complex numbers. Such a decomposition is always possible, the Schmidt decomposition being a particular one with real c_i coefficients [1]. We will work in the $|ij\rangle \equiv |i\rangle_1 \otimes |j\rangle_2$ basis, expressing operators through that basis.

If there is only one non-zero coefficient c_0, the state is written $|\psi\rangle = |00\rangle$ and is obviously separable. Therefore, since $|\psi\rangle$ is entangled, there are at least two non-zero coefficients; let us assume without loss of generality $c_0 \neq 0 \neq c_1$. We define two observables

$$A = |01\rangle\langle 01|, \tag{1.58}$$
$$B = \sigma_x \otimes \sigma_x,, \tag{1.59}$$

with the Pauli operator $\sigma_x \equiv |0\rangle\langle 1| + |1\rangle\langle 0|$. First, we have $A^{\mathrm{pt}} = A$, $B^{\mathrm{pt}} = B$ and we find that

$$(A^{\mathrm{pt}})^2 = (|01\rangle\langle 01|)^{\mathrm{pt}}(|01\rangle\langle 01|)^{\mathrm{pt}} = |01\rangle\langle 01|, \tag{1.60}$$
$$\left(A^2\right)^{\mathrm{pt}} = (|01\rangle\langle 01|\cdot|01\rangle\langle 01|)^{\mathrm{pt}} = |01\rangle\langle 01|, \tag{1.61}$$
$$(B^{\mathrm{pt}})^2 = B^2 = \sigma_x\sigma_x \otimes \sigma_x\sigma_x = I_4, \tag{1.62}$$
$$\left(B^2\right)^{\mathrm{pt}} = I_4^{\mathrm{pt}} = I_4, \tag{1.63}$$

therefore A and B do satisfy Eq. (1.55). We further find

$$\begin{aligned} A \cdot B &= |01\rangle\langle 10| && (1.64)\\ [A,B]^{\mathrm{pt}} &= (|01\rangle\langle 10| - |10\rangle\langle 01|)^{\mathrm{pt}} = |11\rangle\langle 00| - |00\rangle\langle 11|, && (1.65)\\ \{A,B\}^{\mathrm{pt}} &= (|01\rangle\langle 10| + |10\rangle\langle 01|)^{\mathrm{pt}} = |11\rangle\langle 00| + |00\rangle\langle 11|. && (1.66) \end{aligned}$$

For the mean values,

$$\begin{aligned} \langle A^{\mathrm{pt}}\rangle &= \langle\psi|01\rangle\langle 01|\psi\rangle = 0, && (1.67)\\ (\Delta A^{\mathrm{pt}})^2 &= \langle (A^{\mathrm{pt}})^2\rangle = \langle\psi|01\rangle\langle 01|\psi\rangle = 0, && (1.68) \end{aligned}$$

hence we do not need to calculate $\langle B^{\mathrm{pt}}\rangle$ or $(\Delta B^{\mathrm{pt}})^2$ since they will not appear in the final SRPT inequality. We also have

$$\begin{aligned} \frac{1}{4}|\langle [A,B]^{\mathrm{pt}}\rangle|^2 &= \frac{1}{4}|c_0^* c_1 - c_0 c_1^*|^2 = \mathrm{Im}(c_0^* c_1)^2 && (1.69)\\ \frac{1}{4}|\langle \{A,B\}^{\mathrm{pt}}\rangle - 2\langle A^{\mathrm{pt}}\rangle\langle B^{\mathrm{pt}}\rangle|^2 &= \frac{1}{4}|c_0^* c_1 + c_0 c_1^*|^2 = \mathrm{Re}(c_0^* c_1)^2. && (1.70) \end{aligned}$$

The SRPT inequality is then written

$$0 \geq \mathrm{Re}(c_0^* c_1)^2 + \mathrm{Im}(c_0^* c_1)^2 = |c_0|^2 |c_1|^2, \tag{1.71}$$

and is always violated for non-zero c_0 and c_1. We therefore have an experimentally implementable necessary and sufficient criterion for bipartite entanglement on pure states.

The case of mixed states is a more complicated one. To this date, there is still no general method allowing to show the entanglement of two subsystems of any dimensions. Our original criterion remains: if one can find a couple of observables satisfying Eq. (1.55) and violating a SRPT inequality, then the mixed state is entangled, however there is no general method to find such observables given a particular entangled state or to even prove their existence.

1.4 Applications to Bipartite Systems

We will now discuss some applications of the SRPT inequality starting by the bipartite case.

2D Harmonic Oscillator.

We consider entanglement in states of an isotropic two dimensional oscillator with definite energy and angular momentum (see e.g. Ref. [23] describing the experimental production of entangled angular momentum states of photons). Those states are the common eigenvectors $|\psi_{k,M}\rangle$ (k, M integers) of the hamiltonian

$$H = \hbar\omega(aa^\dagger + bb^\dagger + 1), \tag{1.72}$$

with a and b the oscillator annihilation operators and of the angular momentum

$$L_z = i\hbar(ab^\dagger - a^\dagger b), \tag{1.73}$$

with eigenvalues $\hbar\omega(n+1)$ (with $n = 2k + |M|$) and $\hbar M$, respectively . The states $|\psi_{k,M}\rangle$ is expressed in the number state basis $|n_1, n_2\rangle$ as

$$|\psi_{k,M}\rangle = \sum_{j=0}^{n} c_j |n-j, j\rangle, \tag{1.74}$$

with

$$c_j = (-\mathrm{sign}(M)i)^j \sqrt{\frac{\binom{n}{k}}{2^n \binom{n}{j}}} \sum_{l=0}^{j} (-1)^l \binom{k+|M|}{l} \binom{k}{j-l}. \tag{1.75}$$

The proof of that result is shown in Appendix A. The decomposition (1.74) is already in a Schmidt-like basis (with the c_j complex) hence if there are two non zero coefficients, the state is entangled and it is a simple application of the proof for pure states to find the observables that will detect the entanglement. It is easy to find

$$c_0 = \sqrt{\frac{\binom{n}{k}}{2^n}}, \tag{1.76}$$

and in Appendix A we also show the additional property $|c_j| = |c_{n-j}|$. Therefore, except for the ground state for which $c_0 = 1$, all angular momentum eigenstates are entangled in terms of the number states and the entanglement is well detected by the pair of observables

$$A = |ii\rangle\langle ii|, \tag{1.77}$$
$$B = \sigma_x^{(i,j)} \otimes \sigma_x^{(i,j)}, \tag{1.78}$$

with $\sigma_x^{(i,j)} \equiv |i\rangle\langle j| + |j\rangle\langle i|$ and $i + j = n$ which yields for those states the SRPT inequality

$$|c_i||c_j| = |c_i|^2 \leq 0, \tag{1.79}$$

evidently violated for $i = 0$, but in general for several other values as well.

Multiphoton Polarization State.

For some particular experiments, the SRPT inequality can be particularly efficient. Here, we show that on some multiphoton polarization states, the detection of entanglement only involves the measurement of two projectors. Let us consider the entangled two-photon state

$$|\psi\rangle = \alpha|0, 2\rangle + \beta|1, 1\rangle + \gamma|2, 0\rangle, \tag{1.80}$$

where α, β, γ are arbitrary coefficients such that $\mathrm{Re}(\alpha^*\gamma) \neq 0$ and $|m, n\rangle$ denotes m photons in a given polarization state and n photons orthogonally polarized to the m firsts. The

production and properties of those states have been studied in [24]. Of course, this state is also entangled since it is already in a Schmidt-like basis. Using the observables

$$A = |00\rangle\langle 00|, \tag{1.81}$$
$$B = \sigma_x^{(0,2)} \otimes \sigma_x^{(0,2)}, \tag{1.82}$$

and dropping the commutator term in (1.17), we get the inequality $0 \geq |\mathrm{Re}(\alpha^*\gamma)|$. Since $|\psi\rangle$ is never the vacuum, we have $\langle A^{\mathrm{pt}}\rangle = \Delta A^{\mathrm{pt}} = 0$ and B^{pt} does not need to be measured. All that is needed to detect entanglement is the measurement of

$$\{A, B\}^{\mathrm{pt}} = |02\rangle\langle 20| + |20\rangle\langle 02| = |\psi^+\rangle\langle\psi^+| - |\psi^-\rangle\langle\psi^-|, \tag{1.83}$$

with $|\psi^{\pm}\rangle \equiv (|02\rangle \pm |20\rangle)/\sqrt{2}$. More generally, the entanglement of an N-photon state of the form $\sum_{i=0}^{N} c_i|i, N-i\rangle$ will always be easily detectable with similar observables.

Cat States.

In quantum electrodynamics (QED), a coherent state α is defined to be an eigenstate of the annihilation operator a, with the eigenvalue α, i. e. $a|\alpha\rangle = \alpha|\alpha\rangle$ and can be written as

$$|\alpha\rangle = e^{-\frac{|\alpha|^2}{2}} \sum_{n=0}^{\infty} \frac{\alpha^n}{\sqrt{n!}}|n\rangle, \tag{1.84}$$

with $|n\rangle$ the Fock state basis of the considered mode.

We consider the normalized Schrödinger cat state

$$|\psi\rangle = \frac{1}{\mathcal{N}}(|\alpha, \beta\rangle + |-\alpha, -\beta\rangle), \tag{1.85}$$

where $|\alpha\rangle, |\beta\rangle$ are coherent states and $\mathcal{N} = \sqrt{2 + 2e^{-2|\alpha|^2 - 2|\beta|^2}}$. The state $|\psi\rangle$ is a bipartite even state whose production and properties are discussed in [25]. We want to find operators that will show its entanglement with an SRPT inequality.

Our first step to simplify the problem is to find a basis in which α can be considered real. Let us consider that the cast state $|\alpha\rangle$ is expressed in the electromagnetic field mode a. The quadrature operators are defined as

$$x = \frac{1}{\sqrt{2}}(a^\dagger + a), \tag{1.86}$$
$$p = \frac{i}{\sqrt{2}}(a^\dagger - a), \tag{1.87}$$
$$\tag{1.88}$$

and by remembering that the cat states are eigenvalues of the annihilation operator, we

easily find for the mean values

$$\langle\alpha|x|\alpha\rangle = \frac{1}{\sqrt{2}}(\alpha^* + \alpha) = \sqrt{2}\mathrm{Re}(\alpha), \tag{1.89}$$

$$\langle\alpha|p|\alpha\rangle = \frac{i}{\sqrt{2}}(\alpha^* - \alpha) = \sqrt{2}\mathrm{Im}(\alpha). \tag{1.90}$$

$$\tag{1.91}$$

We can always find a rotated basis such that we do not need to deal with imaginary parts, let us define

$$\begin{aligned} x' &= \cos\theta\, x + \sin\theta\, p = \frac{1}{\sqrt{2}}\left(a^\dagger(\cos\theta + i\sin\theta) + a(\cos\theta - i\sin\theta)\right), \\ &= \frac{1}{\sqrt{2}}\left(b^\dagger + b\right), \end{aligned} \tag{1.92}$$

$$\begin{aligned} p' &= -\sin\theta\, x + \cos\theta\, p = \frac{i}{\sqrt{2}}\left(a^\dagger(\cos\theta + i\sin\theta) - a(\cos\theta - i\sin\theta)\right), \\ &= \frac{i}{\sqrt{2}}\left(b^\dagger - b\right), \end{aligned} \tag{1.93}$$

$$\tag{1.94}$$

with $b \equiv e^{-i\theta}a$. By setting $e^{i\theta} = \alpha/|\alpha|$, we find,

$$\langle\alpha|x'|\alpha\rangle = \frac{1}{\sqrt{2}|\alpha|}(\alpha^*\alpha + \alpha\alpha^*) = \sqrt{2}|\alpha|, \tag{1.95}$$

$$\langle\alpha|p'|\alpha\rangle = \frac{i}{\sqrt{2}|\alpha|}(\alpha^*\alpha - \alpha\alpha^*) = 0, \tag{1.96}$$

$$\tag{1.97}$$

which is the result we were looking for, since expressed in the mode b, the parameter α can be considered real. Even for a state such as the $|\psi\rangle$ state given in (1.85), the same method can be applied since the two cat states $|\pm\alpha\rangle$ have the same imaginary part, up to the sign. We therefore assume that we are working in the electromagnetic modes a and b which treats α and β as real numbers, when measuring quadrature operators, which are precisely the operators we use to find a violation of the SRPT inequality.

Experimentally, it is possible to show the entanglement of $|\psi\rangle$ with

$$A = a_1(a^\dagger + a) + b_1(b^\dagger + b), \tag{1.98}$$

$$B = ia_2(a^\dagger - a) + ib_2(b^\dagger - b), \tag{1.99}$$

where a_i and b_i are real parameters and a and b are the annihilation operators of the fields

of $|\alpha\rangle$ and $|\beta\rangle$ chosen such that they treat α and β as real numbers. We get

$$(\Delta A^{\mathrm{pt}})^2 = a_1^2 + b_1^2 + 4\frac{(a_1\alpha + b_1\beta)^2}{1 + e^{-2(\alpha^2+\beta^2)}}, \tag{1.100}$$

$$(\Delta B^{\mathrm{pt}})^2 = a_2^2 + b_2^2 - 4\frac{(a_2\alpha - b_2\beta)^2}{1 + e^{2(\alpha^2+\beta^2)}}, \tag{1.101}$$

$$\frac{1}{4}|\langle [A,B]^{\mathrm{pt}}\rangle|^2 = (a_1a_2 + b_1b_2)^2, \tag{1.102}$$

$$\frac{1}{4}|\langle \{A,B\}^{\mathrm{pt}}\rangle - 2\langle A^{\mathrm{pt}}\rangle\langle B^{\mathrm{pt}}\rangle|^2 = 0. \tag{1.103}$$

Setting $a_1 = -a_2 = -\beta$ and $b_1 = -b_2 = \alpha$ insures a violation of the SRPT inequality for non-zero α and β, since we get

$$\left(\alpha^2+\beta^2\right)\left(\alpha^2+\beta^2 - \frac{16\alpha^2\beta^2}{1+e^{2\alpha^2+2\beta^2}}\right) \geq \left(\alpha^2+\beta^2\right)^2, \tag{1.104}$$

equivalent to

$$-\frac{\alpha^2\beta^2}{1+e^{2\alpha^2+2\beta^2}} \geq 0, \tag{1.105}$$

which is obviously always violated for non-zero parameters. Numerically speaking, the violation of the inequality is the strongest for values of α and β around 0.74.

In order to compare the results, one may try to apply the entanglement criterion introduced by Duan *et al.* [8] on $|\psi\rangle$. That criterion is a sufficient condition for entanglement and is also necessary when applied on gaussian states. Clearly, the state $|\psi\rangle$ is not gaussian, but the criterion may still be applied. The calculation is very close to the previous on, however it can be shown that the cat state $|\psi\rangle$ never violates Duan *et al.*'s inequality.

1.5 Necessary and Sufficient Criterion for Pure three-qubit States

The SRPT inequality is also a strong criterion in the tripartite case. A tripartite pure state $|\psi\rangle$ is fully separable if it can be written as a combination of three separable subsystems as in $|\psi\rangle = |\psi_1\rangle \otimes |\psi_2\rangle \otimes |\psi_3\rangle$, biseparable if it can be written as a combination of one subsystem separated from the other (entangled) subsystems as in $|\psi\rangle = |\psi_1\rangle \otimes |\psi_{23}\rangle$ in the case of the first system being separable and fully entangled otherwise. In that last case, for three qubit, there are two separate classes of entanglement represented by the states $|\mathrm{GHZ}\rangle = (|000\rangle + |111\rangle)/\sqrt{2}$ and $|\mathrm{W}\rangle = (|001\rangle + |010+\rangle|100\rangle)/\sqrt{3}$ [26].

In the multipartite case, the partial transposition may be defined to act on any number of subsystems. In this chapter, when talking about multipartite states, we will always consider the partial transposition to act on the first subsystem of the state (or of the operator) only.

It has been shown that any three-qubit state can always be written under the form [27]:

$$|\psi\rangle = \lambda_0|000\rangle + \lambda_1|100\rangle + \lambda_2|101\rangle + \lambda_3|110\rangle + \lambda_4|111\rangle, \tag{1.106}$$

where one λ_i is complex and the other ones are real. We get to our next result:

Criterion 5. SRPT Criterion for Three-Qubit case — *A three-qubit pure state is entangled if and only if there are observables satisfying Eq. (1.27) such that a Schrödinger-Robertson partial transpose inequality is violated.*

Proof. We first consider a three-qubit state and express it as in Eq. (1.106). The three sets of observables

$$A = |001\rangle\langle 001| \qquad B = \sigma_x \otimes I_2 \otimes \sigma_x, \tag{1.107}$$
$$A = |010\rangle\langle 010| \qquad B = \sigma_x \otimes \sigma_x \otimes I_2, \tag{1.108}$$
$$A = |011\rangle\langle 011| \qquad B = \sigma_x \otimes \sigma_x \otimes \sigma_x, \tag{1.109}$$

lead to the SRPT inequalities

$$|\lambda_0||\lambda_2| \leq 0, \tag{1.110}$$
$$|\lambda_0||\lambda_3| \leq 0, \tag{1.111}$$
$$|\lambda_0||\lambda_4| \leq 0. \tag{1.112}$$

If $\lambda_0 = 0$ the inequalities are not violated, but in that case

$$|\psi\rangle = |1\rangle \otimes (\lambda_1|00\rangle + \lambda_2|01\rangle + \lambda_3|10\rangle + \lambda_4|11\rangle), \tag{1.113}$$

is biseparable. We already know that every entangled two-qubit state can be detected with the mean of an SRPT inequality. If $\lambda_2 = \lambda_3 = \lambda_4 = 0$, there is no violation of the inequalities either, but in that case

$$|\psi\rangle = (\lambda_0|0\rangle + \lambda_1|1\rangle) \otimes |00\rangle, \tag{1.114}$$

is fully separable. Therefore, there is always an SRPT inequality able to detect the entanglement of $|\psi\rangle$.

An interesting result is the fact that a pair of bipartite operators can never detect a GHZ-type state. Indeed, the expectation value of an observable A on a GHZ-type state expressed as in Eq. (1.106) will be a combination of the terms $\langle 000|A|000\rangle$, $\langle 000|A|111\rangle$, $\langle 111|A|000\rangle$ and $\langle 111|A|111\rangle$. If A is a bipartite observable acting, e.g., on the first two subsystems, we have $\langle 000|A|111\rangle = \langle 00|A_{12}|11\rangle\langle 0|I_2|1\rangle = 0$. Thus, the mean value of the observable A acting on a GHZ-type state is the same as if A were acting on a separable state of the form $\rho = \lambda_0^2|000\rangle\langle 000| + \lambda_4^2|111\rangle\langle 111|$. Therefore there cannot be any violation of an SRPT inequality.

1.6 Application to Mixed States

Let us now investigate the performances of the SRPT criterion on mixed states.

Bipartite Werner States.

The generalization of the SRPT criterion to mixed states is a difficult task. We may try, as an illustrative example, to detect the Werner mixed state [28]

$$\rho_x = x|\psi\rangle\langle\psi| + (1-x)\frac{I_4}{4} \tag{1.115}$$

with the normalized state $|\psi\rangle = a|00\rangle + b|11\rangle$.

The PPT criterion, which is necessary and sufficient for the 2×2 mixed state case may be used to describe the entanglement of the state. We find that the partially transposed state $\rho_x^{\rm pt}$ has the eigenvalues

$$\frac{1-x}{4} + x|a|^2, \tag{1.116}$$

$$\frac{1-x}{4} + x|b|^2, \tag{1.117}$$

$$\frac{1-x}{4} + x|a||b|, \tag{1.118}$$

$$\frac{1-x}{4} - x|a||b|. \tag{1.119}$$

The three first ones can never be negative, but we find that the last one is negative, i. e. the state is entangled, if and only if $x > 1/(1+4|a||b|)$.

Using the pair of observables:

$$A = \sigma_z \otimes \sigma_z, \tag{1.120}$$

$$B = \sigma_x \otimes (\cos\varphi\,\sigma_x + \sin\varphi\,\sigma_y), \tag{1.121}$$

our SRPT inequality detects the entanglement of ρ_W when $x > 2/(1+\sqrt{1+32\,\mathrm{Re}(e^{i\varphi}a^*b)})$.

In the particular case when $|\psi\rangle$ is the Bell state $|\phi^\pm\rangle$, i. e. when $a = \pm b = 1/\sqrt{2}$, and $\varphi = 0$, ρ_x is entangled if and only if $x > 1/3$ whereas it is detected via the SRPT inequality when $x > 1/2$. This result improves the limits of detection given by the Bell inequalities ($x > 1/\sqrt{2}$, see [4]) or by the uncertainty relations of Gühne [16] ($x > 1/\sqrt{3}$).

Multipartite Werner States.

The SRPT inequality can be applied on mixed states of multipartite systems. Let us look at its results on the N-dimensional Werner mixed state

$$\rho(x) = x|\mathrm{GHZ}_N\rangle\langle\mathrm{GHZ}_N| + (1-x)\frac{I_{2^N}}{2^N}, \tag{1.122}$$

with $|\mathrm{GHZ}_N\rangle \equiv (|0\cdots 0\rangle + |1\cdots 1\rangle)/\sqrt{2}$. Using the observables

$$A = |01\cdots 1\rangle\langle 01\cdots 1| + |10\cdots 0\rangle\langle 10\cdots 0|, \tag{1.123}$$

$$B = |0\cdots 0\rangle\langle 1\cdots 1| + |1\cdots 1\rangle\langle 0\cdots 0| + |01\cdots 1\rangle\langle 10\cdots 0| + |10\cdots 0\rangle\langle 01\cdots 1|, \tag{1.124}$$

we find an SRPT inequality violated if $x > 1/(1 + 2^{N-2})$. The PPT criterion gives the sufficient limit of entanglement $x > 1/(1 + 2^{N-1})$ and we can find in [29] a witness giving the detection limit of $x > (2 - 2^{2-N})/(3 - 2^{2-N})$, which is strictly smaller than our result for $N \geq 3$ (also, that limit approaches $2/3$ as N grows, where ours approaches 0). For $N = 3$, the PPT criterion gives $x > 1/5$, we find the limit $x > 1/3$ while in [29] the limit is $x > 3/5$ and another witness in [16] gives the limit $x > 3/7$.

Finally it should be kept in mind that any criterion based on inequalities would be restrictive as these are based on two chosen observables unlike the density operators which contain all the information. One could of course increase the number of observables and work a stronger criterion based on the positivity condition $\langle (\sum_i c_i A_i)^\dagger (\sum_i c_i A_i) \rangle \geq 0$ [30], for any observable A_i. Further possibilities consist of using generalized uncertainty relations which are especially suitable for mixed states [31].

Most of the results from this chapter were published in Phys. Rev. A **78**, 052317 (2008).

Chapter 2

Concurrences for N-qubit Systems

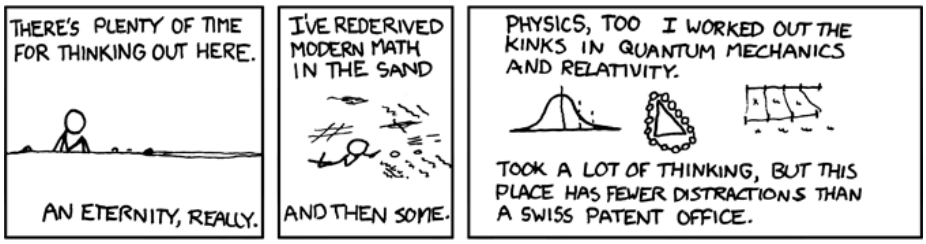

Randall Munroe, *A Bunch of Rocks* (part 3 of 9), `xkcd.com/505/`

Criteria such as the positive partial transpose [4, 22] or Bell's inequalities [5] were originally constructed with the objective to distinguish between separable systems and entangled systems. A question that quickly rose in the following years was the matter of actually *quantifying* the amount of entanglement in a system, since it appeared that states could be strongly or faintly entangled [28]. With that in mind, some entanglement measurement quantities following particular properties were introduced [1, 32].

The concurrence was introduced by Wooters [33] as a measure of entanglement applicable on two-qubit systems, either in a pure state or a mixed state. This very powerful result has been decisive for the comprehension of entanglement in mixed states. The concurrence was quickly modified and generalized to be able to apply on larger systems.

The two-tangle, defined as the square of the concurrence, that can be calculated on any subsets of two qubits within three-qubit pure states was studied and the residual entanglement found was called the three-tangle [34–36]. Other studied bipartite concurrence for states of any dimensions [37] or systems of three or more subsystems and defined a generalized concurrence for pure states [38–41]. Unfortunately, those criteria often do not translate well to mixed state systems and have to rely on convex hulls or lower bounds [36,42]. Although the concurrence in itself is not a experimentally measurable quantity, one of the generalization made the experimental detection possible in a system of two photons [43].

The entanglement in tripartite and multipartite systems has revealed to be quite com-

plex. A pure state of three qubits is known to have two different kinds of genuine tripartite entanglement and an infinite number of ways for more qubits [26]. Nonetheless, many criteria of various application spans were introduced over the years [6, 44–47]. In this chapter, we present our version of generalized concurrences.

We start in Sec. 2.1 by briefly commenting entanglement measures and we define the concurrence as done by Wooters [33]. In Sec. 2.2, we give our definition of generalized concurrences applied to systems of three qubits. We start by listing the conditions under which a three-qubit state is completely separable and we prove it by using tensors composed of the coefficients of the pure state in the computational basis, then we use these conditions to define 9 operators and their 9 associated concurrences. We then briefly discuss the relation between these concurrences and other existing entanglement measures.

In Sec 2.3, we generalize our pure state concurrences to mixed states. We show the proof that our concurrences are well defined for pure states with a demonstration applicable to N-qubit systems, although it is only a sufficient condition to entanglement. We then consider the particular case of symmetric states, in which the number of separability conditions falls down to 3. Finally, we apply the concurrences to several states and find interesting results.

In Sec 2.4, we aim at generalizing three-qubit concurrences to N-qubit systems. For that purpose, we use the tensor algebra that we used in Sec. 2.2 to derive all conditions on the coefficients that a separable state must hold and we give a necessary and sufficient criterion for full separability in pure states.

In Sec 2.5, from the conditions gathered in Sec 2.4, we are able to define the concurrences for an arbitrary number of qubits. In the case of pure states, the concurrences proves themselves to be necessary and sufficient conditions to entanglement, while for mixed states the conditions are merely proven to be sufficient. Finally, we study examples of the application of our concurrences over mixed states.

2.1 Two-qubit Concurrence

In addition to knowing *if* a general mixed state ρ was entangled, the question of *how much* it is entangled stalks the quantum physicist. An operator quantifying the quantity of entanglement in a system is called an *entanglement measure* E. An entanglement measure must obey a few criteria which sometimes differ from author to author [1, 32, 48], of which we cite the most common ones. An entanglement measure $E(\rho)$ must obey the following conditions.

- $\mathbf{E}(\text{æ}) = \mathbf{0}$ if ρ is separable.
- **Normalization** — the entanglement of a maximally entangled state must be finite.
- **Conservation** — the entanglement of a system must be conserved under local unitary operations.

- **Additivity** — the entanglement measure of n copies of a system ρ is n times the entanglement of ρ,
$$E(\rho^{\otimes n}) = nE(\rho). \tag{2.1}$$
- **Sub-additivity** — the entanglement of two subsystems together must not be greater than the sum of the individual entanglements,
$$E(\rho \otimes \sigma) \leq E(\rho) + E(\sigma). \tag{2.2}$$
- **Convexity** — the entanglement is a convex function,
$$E(\lambda\rho + (1-\lambda)\sigma) \leqslant \lambda E(\rho) + (1-\lambda)E(\sigma),\ \forall\, 0 \leqslant \lambda \leqslant 1. \tag{2.3}$$

An example of entanglement measure for a two-qubit pure state $|\psi\rangle$ was introduced by Bennett *et al.* in [48] with a measure using the Von Neumann entropy [49]

$$E(|\psi\rangle) = \mathrm{Tr}\left(\rho_1 \ln \rho_1\right), \tag{2.4}$$

where ρ_1 is the partial trace of $|\psi\rangle\langle\psi|$ on either the first or second subsystem. The entanglement is zero for a separable state and any state reaching the maximum possible value of $E(|\psi\rangle) = \ln(2)$ is called maximally entangled. The Bell states are such examples of maximally entangled states. Any other entangled state finds its entanglement of formation between the two bounds.

The concurrence was originally introduced by Wootters in 1997 [50] as an intermediate step to calculate the Von Neumann entropy E. He proposed in 1998 [33, 50] a formulation that allowed to calculate the entanglement of not only a pure two-qubit state, but of an arbitrary mixed state of two qubits as well.

The definition of any pure state measure of entanglement E must be extended to mixed states as

$$E(\rho) = \min_{\mathcal{P}} \left(\sum_i p_i\, E(|\psi_i\rangle) \right), \tag{2.5}$$

where $\mathcal{P}$ stands for the set of all decompositions p_i and $|\psi_i\rangle$ that allow to write ρ as

$$\rho = \sum_i p_i\, |\psi_i\rangle\langle\psi_i|. \tag{2.6}$$

We start by describing the concurrence applied on pure states. First, let us define the *spin-flip* operation on a qubit in the state $|\psi\rangle$, by

$$|\widetilde{\psi}\rangle = \sigma_y |\psi^*\rangle, \tag{2.7}$$

where the * denotes the complex conjugation of the state.

For a $\frac{1}{2}$-spin particle, this transformation is equivalent to flipping the spin direction. For a two-qubit state $|\psi\rangle$, we define the spin-flip operator as

$$|\widetilde{\psi}\rangle = \sigma_y \otimes \sigma_y |\psi^*\rangle. \tag{2.8}$$

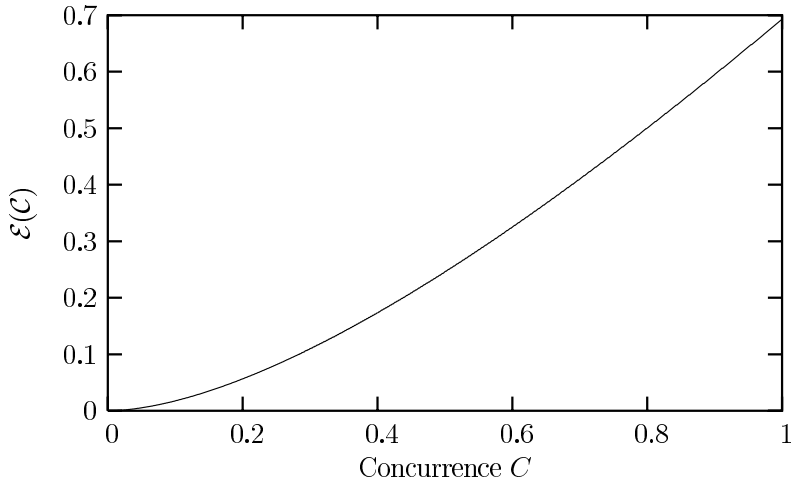

Figure 2.2: The $\mathcal{E}(C)$ function.

The *concurrence* C of a general pure state $|\psi\rangle = a|00\rangle + b|01\rangle + c|10\rangle + d|11\rangle$ is defined by

$$C(|\psi\rangle) = |\langle\psi|\widetilde{\psi}\rangle| = 2|ad - bc|. \tag{2.9}$$

Given the normalization condition $|a|^2+|b|^2+|c|^2+|d|^2 = 1$, the maximal value the concurrence can take is 1, which is realized when either $|a| = |d|$ and $b = c = 0$ or $|b| = |c|$ and $a = d = 0$.

Wootters showed [50] that the Von Neumann entropy (2.4) of $|\psi\rangle$ could be written as

$$E(|\psi\rangle) = \mathcal{E}(C(|\psi\rangle)), \tag{2.10}$$

with

$$\mathcal{E}(C) = h\left(\frac{1+\sqrt{1-C^2}}{2}\right), \tag{2.11}$$

and

$$h(x) = -x\ln x - (1-x)\ln(1-x). \tag{2.12}$$

As shown in Fig. 2.2 the function $h(x)$ is a monotonic function that ranges from zero to 0 to $\ln(2)$ as the concurrence C monotonically grows from 0 to 1, so that the concurrence is a kind of measure of entanglement in its own right.

Keeping his momentum, Wootters generalized his concurrence to mixed states and showed that for a general two-qubit state ρ the minimal value of concurrence over all possible decomposition was

$$C(\rho) = \max\{0, \lambda_1 - \lambda_2 - \lambda_3 - \lambda_4\}, \tag{2.13}$$

where the λ_i are the square root of the ordered eigenvalues (greatest to lowest) of the matrix

$$R = \rho\widetilde{\rho}, \tag{2.14}$$

with the spin-flip transformation generalized on density matrices as

$$\widetilde{\rho} = (\sigma_y \otimes \sigma_y)\rho^*(\sigma_y \otimes \sigma_y). \tag{2.15}$$

The proof of that result, adapted to an arbitrary number of qubits, will be described in Sec. 2.3.

The concurrence is a very strong criterion for entanglement. A two-qubit system is entangled if and only if its concurrence is non zero. Furthermore, it quantifies the amount of entanglement, i. e. when a concurrence is 0 the state is separable and when the concurrence is 1 the state is maximally entangled. We have the following criterion.

Criterion 6. Concurrence — *The two-qubit mixed state ρ is entangled if and only if its concurrence*

$$C(\rho) = \max\{0, \lambda_1 - \lambda_2 - \lambda_3 - \lambda_4\}, \tag{2.16}$$

is greater than zero, with λ_i the square root of the ordered eigenvalues (greatest to lowest) of the matrix

$$(\sigma_y \otimes \sigma_y)\rho^*(\sigma_y \otimes \sigma_y)\rho. \tag{2.17}$$

Furthermore, the concurrence is an entanglement measure which is renders 1 for maximally entangled states.

2.1.1 Illustrative Examples

Let us calculate the concurrence of the Bell states

$$|\psi^{\pm}\rangle = \frac{1}{\sqrt{2}}(|01\rangle \pm |10\rangle). \tag{2.18}$$

We find that

$$|\widetilde{\psi^{\pm}}\rangle = \sigma_y \otimes \sigma_y |(\psi^{\pm})^*\rangle = \pm|\psi^{\pm}\rangle, \tag{2.19}$$

and therefore

$$C(|\psi^{\pm}\rangle) = |\pm\langle\psi^{\pm}|\psi^{\pm}\rangle| = 1, \tag{2.20}$$

and we conclude that the Bell states are maximally entangled.

The concurrence of the state $|01\rangle$ is

$$C(|01\rangle) = |\langle 01|\sigma_y \otimes \sigma_y|01\rangle| = |\langle 01|10\rangle| = 0, \tag{2.21}$$

and the state $|01\rangle$ is (evidently) found to be separable.

Let us consider the noisy Bell state

$$\rho = x|\psi^-\rangle\langle\psi^-| + \frac{1-x}{4}I_4, \tag{2.22}$$

with $0 \leq x \leq 1$ and compute the concurrence. We find that three of the square root of the eigenvalues of $\rho\widetilde{\rho}$ are $\frac{1}{4}(1-x)$ and the last one is $\frac{1}{4}(1+3x)$. Therefore we find a concurrence of

$$C(\rho) = \max\left\{0, \frac{1}{4}(1+3x) - \frac{3}{4}(1-x)\right\} = \max\left\{0, \frac{1}{2}(3x-1)\right\}, \tag{2.23}$$

which is zero when $x \leq \frac{1}{3}$ and positive elsewhere. We conclude that ρ is a separable state for $x \leq \frac{1}{3}$ and is entangled for $\frac{1}{3} < x \leq 1$. The amount of entanglement grows linearly with x and reaches the maximal value of 1 when $x = 1$, which is no surprise since at that point ρ is the pure Bell state $|\psi^-\rangle\langle\psi^-|$.

2.2 Three-qubit Concurrences for Pure States

In this section, we show our efforts to generalize the concurrence to a system composed of three qubit. We will see that several concurrences can be defined and that the entanglement detection criterion remains necessary and sufficient for pure states, whereas for mixed states it becomes merely sufficient.

2.2.1 Necessary and Sufficient Conditions to Separability

We express the general state of a 3-qubit pure state as

$$|\psi\rangle = \sum_{i,j,k} a_{ijk}|ijk\rangle, \tag{2.24}$$

where $\{i, j, k\} \in \{0, 1\}$ and the normalization condition

$$\sum_{i,j,k} |a_{ijk}|^2 = 1. \tag{2.25}$$

First, we express the necessary and sufficient conditions for $|\psi\rangle$ to be separable.

Criterion 7. Conditions for three-qubit pure states separability — *The three-qubit $|\psi\rangle$ state is separable if and only if the following conditions hold,*

$$a_{000}a_{011} = a_{001}a_{010}, \quad a_{100}a_{111} = a_{101}a_{110}, \tag{2.26}$$
$$a_{000}a_{101} = a_{001}a_{100}, \quad a_{010}a_{111} = a_{011}a_{110}, \tag{2.27}$$
$$a_{000}a_{110} = a_{010}a_{100}, \quad a_{001}a_{111} = a_{011}a_{101}, \tag{2.28}$$
$$a_{000}a_{111} = a_{001}a_{110} = a_{010}a_{101} = a_{011}a_{100}. \tag{2.29}$$

And we prove it in two parts.
Necessary condition. If $|\psi\rangle$ is fully separable, it can be written under the form

$$|\psi\rangle = |a\rangle \otimes |b\rangle \otimes |c\rangle, \tag{2.30}$$

with $|a\rangle, |b\rangle$ and $|c\rangle$ single-qubit states with the respective coefficients in the computational basis a_0, a_1, b_0, b_1, c_0 and c_1. Hence, we find that the a_{ijk} coefficients are written

$$a_{ijk} = a_i b_j c_k. \tag{2.31}$$

With that form, Eqs. (2.26) to (2.29) are very easy to verify, i. e. the first condition is transcribed

$$a_{000}a_{011} = a_{001}a_{010} \Leftrightarrow a_0 b_0 c_0 a_0 b_1 c_1 = a_0 b_0 c_1 a_0 b_1 c_0, \tag{2.32}$$

and is trivially verified.

Sufficient condition. To prove this part, we will consider the coefficients a_{ijk} of $|\psi\rangle$ and use them as the elements of a $2 \times 2 \times 2$, three-order tensor. Let us first briefly discuss a few properties of tensors. The order of a tensor is its number of dimensions, or the number of indices needed to describe its elements [51]. Vectors are one-order tensors, matrices are two-order tensors, we will use three-order in our case since we are dealing with three qubits. The rank of a tensor $\boldsymbol{A}$ is defined as the smallest number of rank-one tensors that generate $\boldsymbol{A}$ as their sum [52]. A one-rank tensor $\boldsymbol{A}$ is a tensor that can be written under the form [51],

$$\boldsymbol{A} = \begin{pmatrix} a_0 \\ a_1 \end{pmatrix} \otimes \begin{pmatrix} b_0 \\ b_1 \end{pmatrix} \otimes \begin{pmatrix} c_0 \\ c_1 \end{pmatrix}, \tag{2.33}$$

in the case of a $2 \times 2 \times 2$ tensor. If we can show that the tensor constructed from the a_{ijk} elements is of rank one when the conditions (2.26) to (2.29) are satisfied, it will mean that it can be expressed as the tensor (2.33), which directly corresponds to the coefficients of the separable state (2.30) with the same notations.

The rank of $\boldsymbol{A}$ can be calculated from its three modes *matricization* [51]. Matricization is the process of rearranging the elements of a tensor so that it can be represented as a matrix. The columns of the matrices are build from the a_{ijk} coefficients with two of the three indices i, j or k fixed. Therefore, there are three different ways to matricize the tensor $\boldsymbol{A}$, depending on which coefficients are fixed. If j and k are chosen, then the first matrix $\boldsymbol{A}^{(1)}$ is constructed by considering all possible columns a_{ijk} from the values of j and k. We have

$$\boldsymbol{A}^{(1)} = \begin{pmatrix} a_{000} & a_{001} & a_{010} & a_{011} \\ a_{100} & a_{101} & a_{110} & a_{111} \end{pmatrix}, \tag{2.34}$$

similarly, we construct the two other matrices

$$\boldsymbol{A}^{(2)} = \begin{pmatrix} a_{000} & a_{001} & a_{100} & a_{101} \\ a_{010} & a_{011} & a_{110} & a_{111} \end{pmatrix}, \tag{2.35}$$

and

$$\boldsymbol{A}^{(3)} = \begin{pmatrix} a_{000} & a_{010} & a_{100} & a_{110} \\ a_{001} & a_{011} & a_{101} & a_{111} \end{pmatrix}. \tag{2.36}$$

The rank of $\boldsymbol{A}$ is one if and only if all three matrices are of rank one [51], which is equivalent to saying that all columns within the matrices are linearly dependent. For the two first columns of $\boldsymbol{A}^{(1)}$, it means that we must have

$$a_{000}a_{101} = a_{001}a_{100}, \tag{2.37}$$

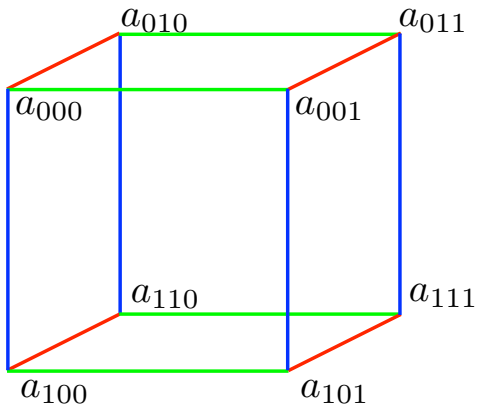

Figure 2.3: Representation of the three-order tensor of the a_{ijk} coefficient. The blue lines form the columns of $\boldsymbol{A}^{(1)}$, the red lines are the columns of $\boldsymbol{A}^{(2)}$ and the green lines are the columns of $\boldsymbol{A}^{(3)}$. The two-term equalities (2.26) to (2.28) are conditions formed on the 6 surfaces of the cube, while the four-term equality (2.29) is formed along the 6 diagonals, through the volume of the cube.

which is the condition expressed in the left hand side of Eq. (2.27). It can be checked that all other conditions inferred from the rank one of $\boldsymbol{A}^{(1)}, \boldsymbol{A}^{(2)}$ and $\boldsymbol{A}^{(3)}$ are included in Eq. (2.26) to (2.29) . Therefore, if those conditions hold, $\boldsymbol{A}$ is of rank one and therefore represents a fully separable state $|\psi\rangle$.

The tensor is represented in Fig. 2.3 as a cube formed with the 8 a_{ijk} coefficient. Another way of picturing the conditions from the matricization of $\boldsymbol{A}$ is to see that the rank of all matrices formed by the 6 faces of the cube and the 6 diagonal planes must be one. We note that the conditions from the "surface" matrices stand alone in Eq. (2.26) to (2.28), and that the ones from the "diagonal" or "volume" matrices can be expressed in a single 4-terms equality (2.29).

2.2.2 Three-qubit Concurrences

The above criterion is a necessary and sufficient condition for separability applying to pure states. For a general three-qubit mixed state, the situation is more complicated since there does not yet exist a criterion detecting the entanglement. For a two-qubit state $|\psi\rangle = a|00\rangle + b|01\rangle + c|10\rangle + d|11\rangle$, there is only one condition for separability, i.e.

$$ad = bc. \tag{2.38}$$

The strength of the original concurrence was the ability to find a way to apply that simple condition to mixed states. Our generalized concurrence follow the same steps by defining several "spin-flip" operations and extending their use to mixed states.

Let us define the following operators:

$$S_1 = -P_0 \otimes \sigma_y \otimes \sigma_y, \qquad S_2 = -P_1 \otimes \sigma_y \otimes \sigma_y, \tag{2.39}$$
$$S_3 = -\sigma_y \otimes P_0 \otimes \sigma_y, \qquad S_4 = -\sigma_y \otimes P_1 \otimes \sigma_y, \tag{2.40}$$
$$S_5 = -\sigma_y \otimes \sigma_y \otimes P_0, \qquad S_6 = -\sigma_y \otimes \sigma_y \otimes P_1, \tag{2.41}$$

$$S_7 = -\sigma_x \otimes \sigma_y \otimes \sigma_y, \tag{2.42}$$
$$S_8 = -\sigma_y \otimes \sigma_x \otimes \sigma_y, \tag{2.43}$$
$$S_9 = -\sigma_y \otimes \sigma_y \otimes \sigma_x, \tag{2.44}$$

with $P_0 \equiv |0\rangle\langle 0|$, $P_1 \equiv |1\rangle\langle 1|$ and σ_j the Pauli matrices.

We can now define our 9 concurrences C_i of a three-qubit state $|\psi\rangle$:

$$C_\alpha(|\psi\rangle) = |\langle\psi^*|S_\alpha|\psi\rangle|\,, \tag{2.45}$$

with $\alpha = \{1, \cdots, 9\}$ and where the star denotes the complex conjugation in the computational basis. We get, for a general $|\psi\rangle$

$$C_1(|\psi\rangle) = 2|a_{000}a_{011} - a_{001}a_{010}|, \qquad C_2(|\psi\rangle) = 2|a_{100}a_{111} - a_{101}a_{110}|, \tag{2.46}$$
$$C_3(|\psi\rangle) = 2|a_{000}a_{101} - a_{001}a_{100}|, \qquad C_4(|\psi\rangle) = 2|a_{010}a_{111} - a_{011}a_{110}|, \tag{2.47}$$
$$C_5(|\psi\rangle) = 2|a_{000}a_{110} - a_{010}a_{100}|, \qquad C_6(|\psi\rangle) = 2|a_{001}a_{111} - a_{011}a_{101}|, \tag{2.48}$$
$$C_7(|\psi\rangle) = 2|a_{000}a_{111} - a_{001}a_{110} \;-\; a_{010}a_{101} + a_{011}a_{100}|, \tag{2.49}$$
$$C_8(|\psi\rangle) = 2|a_{000}a_{111} - a_{001}a_{110} \;+\; a_{010}a_{101} - a_{011}a_{100}|, \tag{2.50}$$
$$C_9(|\psi\rangle) = 2|a_{000}a_{111} + a_{001}a_{110} \;-\; a_{010}a_{101} - a_{011}a_{100}|. \tag{2.51}$$

Note that the S_α matrices were normalized in such a way that the highest possible value of each concurrence is 1. In general, if the goal is simply to detect entanglement, the matrices do not need to be normalized, as a non-zero concurrence is enough to show the entanglement. However, if the value of different concurrences are to be compared the concurrences must be normalized and the absolute value of the concurrences must be considered. We get the following criterion.

Criterion 8. Three-qubit concurrence for pure states — *The three-qubit state $|\psi\rangle$ is separable if and only if*

$$C_\alpha(|\psi\rangle) = |\langle\psi^*|S_\alpha|\psi\rangle| = 0, \tag{2.52}$$

for all $1 \leq \alpha \leq 9$.

Proof. The conditions $C_\alpha(|\psi\rangle) = 0$ for $\alpha = 1$ to $\alpha = 6$ are identical to Eq. (2.26) to (2.28), and the conditions in (2.29) can be retrieved easily by adding or subtracting two of the $C_7(|\psi\rangle) = 0$ to $C_9(|\psi\rangle) = 0$ conditions.

Incidentally, it may be useful to linearly combine the 9 operators S_α to make up new operators, which need to be normalized is the amount of entanglement between two states is to be compared. For example, we may add or subtract any pair from the S_7, S_8 and S_9 matrices to obtain the following pairs of operator/concurrence

$$S_{10} = (S_8 + S_9)/2 \qquad C_{10} = 2|a_{000}a_{111} - a_{011}a_{100}|, \tag{2.53}$$
$$S_{11} = (S_8 - S_9)/2 \qquad C_{11} = 2|a_{010}a_{101} - a_{001}a_{110}|, \tag{2.54}$$
$$S_{12} = (S_7 + S_9)/2 \qquad C_{12} = 2|a_{000}a_{111} - a_{001}a_{110}|, \tag{2.55}$$
$$S_{13} = (S_7 - S_9)/2 \qquad C_{13} = 2|a_{011}a_{100} - a_{001}a_{110}|, \tag{2.56}$$
$$S_{14} = (S_7 + S_8)/2 \qquad C_{14} = 2|a_{000}a_{111} - a_{001}a_{110}|, \tag{2.57}$$
$$S_{15} = (S_7 - S_8)/2 \qquad C_{15} = 2|a_{011}a_{100} - a_{010}a_{101}|, \tag{2.58}$$

where we simplified the $C_\alpha(|\psi\rangle)$ into C_α for visibility. Once again, those concurrences do not bring extra information or constraints to the systems since the set of conditions $C_\alpha(|\psi\rangle) = 0$ for α from 7 to 9 is strictly equivalent to the set of the same conditions for α from 10 to 15. However, these may be easier to handle in a variety of situations. For example checking the correspondence of the conditions $C_\alpha(|\psi\rangle) = 0$ with the conditions of (2.29) is easier with α from 10 to 15.

In general, we may define any matrix S through a linear combination $S = \sum_\alpha c_\alpha S_\alpha$ with c_α real coefficients normalized such that the general concurrence $C_S(|\psi\rangle) = |\langle\psi^*|S|\psi\rangle|$ has a highest possible value of 1.

Relations with other entanglement criteria

Unfortunately, none of the concurrences can individually pretend to be a measure of entanglement, as they do not remain invariant under local transformations. However, a combination of those quantities might.

Let us write the three-tangle equation [34]:

$$C^2_{A(BC)} = C^2_{AB} + C^2_{AC} + \tau. \tag{2.59}$$

In that equation τ is the three-tangle, $C^2_{AB}(C^2_{AC})$ are the square of concurrence of the pure state $|\psi\rangle$ after the third (second) subsystem was traced out and

$$C^2_{A(BC)} = 4\,\mathrm{det}\rho_A \tag{2.60}$$

with ρ_A is the system with the second and third subsystems traced out. $C^2_{A(BC)}$ is defined the square of the concurrence between the subsystem A and the other two subsystems.

All those quantities can be calculated form the a_{ijk} coefficients, and it is easy to show that

$$C^2_{A(BC)} = C^2_3 + C^2_4 + C^2_5 + C^2_6 + C^2_{10} + C^2_{11}, \tag{2.61}$$
$$C^2_{B(AC)} = C^2_1 + C^2_2 + C^2_5 + C^2_6 + C^2_{12} + C^2_{13}, \tag{2.62}$$
$$C^2_{C(AB)} = C^2_1 + C^2_2 + C^2_3 + C^2_4 + C^2_{14} + C^2_{15}. \tag{2.63}$$

Those quantities are invariant under local transformation although they are only applicable to pure states, which prevents the from being legitimate entanglement measures. If, only for a second, we consider a definition of the concurrence without the absolute value bars, i. e. $C_\alpha(|\psi\rangle) = \langle\psi^*|S_\alpha|\psi\rangle$, we can show that the three-tangle can be expressed as

$$\tau = \left|C_7^2 - 4C_1C_2\right| = \left|C_8^2 - 4C_3C_4\right| = \left|C_9^2 - 4C_5C_6\right|. \tag{2.64}$$

A definition of generalized concurrence $C^G(|\psi\rangle)$ for a three-qubit pure state $|\psi\rangle$ is given in [41] by

$$C^G(|\psi\rangle) = \sqrt{3 - \mathrm{Tr}\left(\rho_1^2 + \rho_2^2 + \rho_3^2\right)}, \tag{2.65}$$

where the reduced density matrices ρ_i are obtained by tracing out every subsystem expect the i-th. We find that

$$\mathrm{Tr}\left(\rho_1^2\right) = 1 - \frac{1}{2}\left(C_3^2 + C_4^2 + C_5^2 + C_6^2 + C_{10}^2 + C_{11}^2\right), \tag{2.66}$$

$$\mathrm{Tr}\left(\rho_2^2\right) = 1 - \frac{1}{2}\left(C_1^2 + C_2^2 + C_5^2 + C_6^2 + C_{12}^2 + C_{13}^2\right), \tag{2.67}$$

$$\mathrm{Tr}\left(\rho_3^2\right) = 1 - \frac{1}{2}\left(C_1^2 + C_2^2 + C_3^2 + C_4^2 + C_{14}^2 + C_{15}^2\right), \tag{2.68}$$

which are in fact the values $1 - C_{A(BC)}^2/2, 1 - C_{B(AC)}^2/2$ and $1 - C_{C(AB)}^2/2$. We finally express the generalized concurrence in function of our concurrences

$$C^G(|\psi\rangle) = \sqrt{\sum_{i=1}^{9} C_i^2}, \tag{2.69}$$

as we find that $\sum_{i=7}^{9} C_i^2 = \sum_{i=10}^{15} C_i^2$.

2.3 Three-qubit Concurrences for Mixed States

We now generalize the concurrences to mixed states. As we wrote earlier, a measure of entanglement C of a mixed state of any dimension $\rho = \sum_i p_i|\psi_i\rangle\langle\psi_i|$with $p_i > 0$, must be written as

$$C_S(\rho) = \inf \sum_i p_i C_S(|\psi_i\rangle), \tag{2.70}$$

with the concurrence related to the normalized matrix $S = \sum_{\alpha=1}^{9} c_\alpha S_\alpha$ and where the "inf" means that the decomposition $\{p_i, |\psi_i\rangle\}$ should be chosen in such a way that the sum reaches its minimal value possible. We show that the minimal value possible of $\sum_i p_i C_S(|\psi_i\rangle)$ is

$$C_S(\rho) = \mathrm{Max}[0, \lambda_1^S - \sum_{k=2}^{8} \lambda_k^S], \tag{2.71}$$

where the λ_k^S are the square roots of the 8 eigenvalues of the matrix

$$\rho S \rho^* S, \tag{2.72}$$

with $\lambda_1^S \geq \lambda_2^S \geq \cdots \geq \lambda_8^S$. The following result does not depend on the $N = 3$ condition and can easily be generalized to a N-qubit state, we therefore consider operators of dimension 2^N. In Sec. 2.5 we will define generalized N-qubit S_α operators.

To show that the definition of that concurrence is valid, let us go through all the details of the development. Except for a (very) few modification, the development that follow can be found entirely in Wootters' paper [50].

First of all, consider a general $N-$qubit density matrix ρ. Find a complete set of orthogonal eigenvectors $|v_i\rangle$ corresponding the non-zero eigenvalues of ρ and "normalize" them such a way that $\langle v_i|v_i\rangle$ is equal to the i-th eigenvalue so that we have $\rho = \sum_i |v_i\rangle\langle v_i|$.

A general decomposition $\{|w_i\rangle\}$ of ρ is given by

$$|w_i\rangle = \sum_{j=1}^{n} U_{ij}^* |v_i\rangle, \tag{2.73}$$

where n is the rank of ρ, and U is a $m \times m$ unitary matrix with $m \geq n$. The rank n of the matrix can be any value from 1 to 2^N. Alternatively, we can consider U as a $m \times n$ matrix whose columns are orthonormal. Then we have $\rho = \sum_i |w_i\rangle\langle w_i|$.

Let us now consider two classes of density matrices: the ones that hold $\lambda_1^S - \sum_{k=2}^n \lambda_k^S \geq 0$ and the ones that do not. We consider the former class first.

We seek a decomposition with states $\{|x_i\rangle\}$, $1 \leq i \leq n$ such that

$$\langle x_i^*|S|x_j\rangle = \lambda_i^S \delta_{ij}. \tag{2.74}$$

To obtain that particular decomposition, we need to find the appropriate transformation matrix U. For a general matrix U we have

$$\langle x_i^*|S|x_j\rangle = (U\tau^S U^T)_{ij}, \tag{2.75}$$

with $\tau_{ij}^S \equiv \langle v_i^*|S|v_j\rangle$. The goal is then to find the transformation U that diagonalizes $U\tau^S U^T$, which is always possible since τ^S is symmetric (thanks to the symmetry of S) and its diagonal elements can be made non-negative reals, in which case they are the square root of the eigenvalues of $\tau^S(\tau^S)^*$. The eigenvalues correspond to the λ_i^S and we get the wanted decomposition. Also, we can always modify U by switching its rows and columns so that the λ_i^S appear in ordered fashion.

Let us define another decomposition $\{|y_i\rangle\}$ as

$$|y_1\rangle = |x_1\rangle, \tag{2.76}$$

$$|y_i\rangle = i|x_i\rangle \qquad \text{for } i > 1, \tag{2.77}$$

which will later produce the sign difference between λ_1^S and the other eigenvalues.

Let us now define the pre-concurrence

$$c_S(|\psi\rangle) = \frac{\langle\psi^*|S|\psi\rangle}{\langle\psi|\psi\rangle}, \tag{2.78}$$

and calculate the average normalizing concurrence in the decomposition $\{|y_i\rangle\}$:

$$\langle c_S\rangle = \sum_i \langle y_i|y_i\rangle \frac{\langle y_i^*|S|y_i\rangle}{\langle y_i|y_i\rangle} = \sum_i \langle y_i^*|S|y_i\rangle = \lambda_1^S - \sum_{k=2}^{n} \lambda_k^S = C_S(\rho). \tag{2.79}$$

We can see that the average pre-concurrence is equal to the concurrence announced above. The last decomposition $\{|z_i\rangle\}$ that we are going to find is the one that will set the value of the pre-concurrence of every single state $|z_i\rangle$ equal to $C_S(\rho)$. To find it, let us write

$$|z_i\rangle = \sum_{j=1}^{n} V_{ij}^* |y_i\rangle, \tag{2.80}$$

and note that the average pre-concurrence becomes

$$\langle c_S\rangle = \sum_i \langle y_i^*|S|y_i\rangle = \sum_i (VY^SV^T)_{ii} = \mathrm{Tr}\left(VY^SV^T\right), \tag{2.81}$$

where $Y_{ij}^S \equiv \langle y_i^*|S|y_i\rangle$. We can see that if Y^S is an orthogonal matrix (i.e., $V^T = V^{-1}$) the average pre-concurrence does not change, therefore we will settle for such a matrix transformation. To equalize the pre-concurrences of the different states $|z_i\rangle$, we find two states $|z_a\rangle$, $|z_b\rangle$ that have respectively a higher and lower pre-concurrence than $C_S(\rho)$. We know that there is a V that could let them unchanged, another one that could exchange them, therefore by continuity, there must me one that gets the pre-concurrence of $|z_a\rangle$ to $C_S(\rho)$. Proceeding with one vector at a time, we can get the decomposition wanted.

We have a decomposition $\{|z_i\rangle\}$ whose average pre-concurrence is equal to the concurrence. Let us now show that there is no decomposition that can lead to a smaller concurrence of ρ. We have an average value of the concurrence of the decomposition of

$$\langle C\rangle = \sum_i |(VY^SV^T)_{ii}|, \tag{2.82}$$

where V is an $m \times n$ matrix whose columns are orthonormal. We can write

$$\langle C\rangle = \sum_i \left| \sum_j (V_{ij})^2 Y_{jj}^S \right|, \tag{2.83}$$

and make use of the fact that $\sum_i |(V_{ij})^2| = 1$. Indeed, for any complex number $\alpha_{ij} = (V_{ij})^2$ such that $\sum_i |\alpha_{ij}| = 1$ with all α_{i1} reals (the phases of the other α_{ij} may be changed accordingly) we have

$$\sum_i \left| \sum_j \alpha_{ij} Y_{jj}^S \right| \geq \left| \sum_{ij} \alpha_{ij} Y_{jj}^S \right| = \left| \lambda_1^S - \sum_{j=2} \left(\sum_i \alpha_{ij} \right) \lambda_j^S \right| \geq \lambda_1^S - \sum_{k=2} \lambda_k^S = C_S(\rho), \tag{2.84}$$

and no decomposition may have a better average concurrence than the one that was realized by the decomposition $\{|y_i\rangle\}$.

We still have to consider the case where $\lambda_1^S - \sum_{k=2}^n \lambda_k^S \leq 0$. In that situation the concurrence C_S should not detect any entanglement in any of the terms of the decomposition of ρ. We only have to find one decomposition that realizes that condition. We can get it directly with the decomposition

$$|z_i\rangle = \sum_j O_{ij} e^{i\theta_j} |x_j\rangle \tag{2.85}$$

where the $e^{i\theta_i}$ phases are chosen in such a way that $\sum_j e^{2i\theta_j}\lambda_j^S = 0$ and O is an real orthonormal matrix composed exclusively of elements equal to 1 or -1. It is always possible to find such phases when $\lambda_1^S \leq \sum_{k=2}^n \lambda_k^S$ as illustrated on Fig. 2.4. The matrix O can be defined as the tensor product

$$O = \frac{1}{\sqrt{n}} \begin{pmatrix} 1 & 1 \\ 1 & -1 \end{pmatrix}^{\otimes N}. \tag{2.86}$$

With that decomposition, we can calculate the concurrence of any state $|z_i\rangle$ and we find

$$\begin{aligned} C_S(|z_i\rangle) &= \langle z_i^*|S|z_i\rangle, & (2.87)\\ &= \sum_{jk} e^{i\theta_k} e^{i\theta_j} O_{ki} O_{ij} \langle x_k^*|S|x_j\rangle, & (2.88)\\ &= \sum_j e^{2i\theta_j} \lambda_j^S, & (2.89)\\ &= 0, & (2.90) \end{aligned}$$

and therefore no entanglement is detected in the system, which does not mean that the system is fully separable. However, with that result, we get a necessary criterion to entanglement.

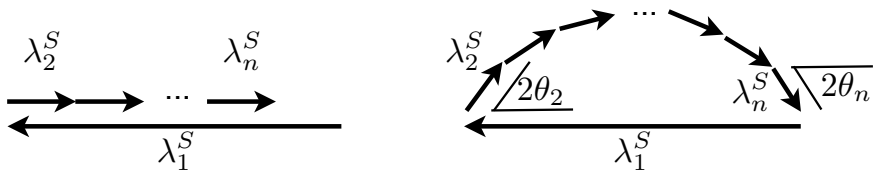

Figure 2.4: On the left, the situation where $\lambda_1^S > \sum_{k=2}^n \lambda_k^S$, the state is entangled. On the right, $\lambda_1^S \leq \sum_{k=2}^n \lambda_k^S$ and it is always possible to find a set of phases θ_k such that $\sum_j e^{2i\theta_j}\lambda_j^S = 0$ and a decomposition $\{|z_i\rangle\}$ where no entanglement detected by the spin-flip S can be found.

Criterion 9. Three-qubit Concurrence — *If a three-qubit mixed state ρ is fully separable, then for all linear combinations $S = \sum_\alpha c_\alpha S_\alpha$ we find $C_S(\rho) = 0$.*

Equivalently, if we find a combination S such that $C_S(\rho) \neq 0$, then ρ is entangled.

2.3.1 Particular Case for Symmetric States

In the particular case of three-qubit symmetric states, i. e. states that can be written as

$$|\psi_s\rangle = a|000\rangle + b(|001\rangle + |010\rangle + |100\rangle) + c(|011\rangle + |101\rangle + |110\rangle) + d|111\rangle, \tag{2.91}$$

with $|a|^2+3|b|^2+3|c|^2+|d|^2= 1$. Note that such a state is either completely separable or has the three subsystems entangled together, biseparability cannot occur due to the symmetry of the state. For such a symmetry, the number of separability conditions drops down to the following three

$$ad = bc, \tag{2.92}$$
$$ac = b^2 \tag{2.93}$$
$$ab = c^2, \tag{2.94}$$

and the three independent S^s matrices associated with those are

$$S_1^s = -\frac{1}{3}\sum_{\nu=\{x,y,y\}} \sigma_{\nu_1}\otimes\sigma_{\nu_2}\otimes\sigma_{\nu_3}, \tag{2.95}$$

$$S_2^s = -\frac{1}{6}\sum_{\nu=\{y,y,z\}} \sigma_{\nu_1}\otimes\sigma_{\nu_2}\otimes\sigma_{\nu_3} - \frac{1}{6}\sum_{\nu=\{y,y,I\}} \sigma_{\nu_1}\otimes\sigma_{\nu_2}\otimes\sigma_{\nu_3}, \tag{2.96}$$

$$S_3^s = -\frac{1}{6}\sum_{\nu=\{y,y,z\}} \sigma_{\nu_1}\otimes\sigma_{\nu_2}\otimes\sigma_{\nu_3} + \frac{1}{6}\sum_{\nu=\{y,y,I\}} \sigma_{\nu_1}\otimes\sigma_{\nu_2}\otimes\sigma_{\nu_3}, \tag{2.97}$$

where the sum over $\nu = \{i, j, k\}$ means the sum over each distinct permutations of $\{i, j, k\}$ and σ_I stands for the identity matrix. Please note that all matrices are also completely symmetric with the exchange of any two subsystems. Expressed as a combination of the original 9 matrices, we have

$$S_1^s = \frac{1}{3}\left(S_7 + S_8 + S_9\right), \tag{2.98}$$

$$S_2^s = \frac{1}{3}\left(S_1 + S_3 + S_5\right), \tag{2.99}$$

$$S_3^s = -\frac{1}{3}\left(S_2 + S_4 + S_6\right). \tag{2.100}$$

The concurrences associated are

$$C_1^s(|\psi_s\rangle) = 2|ad - bc|, \tag{2.101}$$
$$C_2^s(|\psi_s\rangle) = 2|ac - b^2|, \tag{2.102}$$
$$C_3^s(|\psi_s\rangle) = 2|bd - c^2|. \tag{2.103}$$

2.3.2 Illustrative Examples

Let us first apply the criterion to the entangled bipartite state

$$|\psi\rangle = |\phi^+\rangle \otimes (\alpha|0\rangle + \beta|1\rangle), \tag{2.104}$$

with $|\alpha|^2+|\beta|^2= 1$ and

$$|\phi^+\rangle = \frac{1}{\sqrt{2}}(|00\rangle + |11\rangle). \tag{2.105}$$

Among the 15 defined concurrences C_α, we find that the only non zero concurrences are

$$\begin{aligned} C_5(|\psi\rangle) &= |\alpha|^2, & (2.106)\\ C_6(|\psi\rangle) &= |\beta|^2, & (2.107)\\ C_9(|\psi\rangle) &= 2|\alpha\beta|, & (2.108)\\ C_{10}(|\psi\rangle) &= C_{11}(|\psi\rangle) = C_{12}(|\psi\rangle) = C_{13}(|\psi\rangle) = |\alpha\beta|, & (2.109) \end{aligned}$$

which shows that the tripartite concurrence does detect bipartite entanglement as well. Note that $C_5^2 + C_6^2 + C_9^2$

The two classes of genuine tripartite entanglement are represented by the W state and the Greenberger-Horne-Zeilinger state

$$|\mathrm{W}\rangle \equiv \frac{1}{\sqrt{3}}(|001\rangle + |010\rangle + |100\rangle), \tag{2.110}$$

$$|\mathrm{GHZ}\rangle \equiv \frac{1}{\sqrt{2}}(|000\rangle + |111\rangle). \tag{2.111}$$

Those states are completely symmetric, therefore if we use the C_α^s concurrences we find

$$\begin{aligned} C_1^s(|\mathrm{GHZ}\rangle) &= 1, & (2.112)\\ C_2^s(|\mathrm{W}\rangle) &= \frac{2}{3}, & (2.113) \end{aligned}$$

and C_3^s is also found to be 2/3 when applied on the W-type state $(|011\rangle+|101\rangle+|110\rangle)/\sqrt{3}$.

Let us now consider a family of mixed state called Dür-Cirac-Tarrach states ρ_D [44], into which by the mean of using probabilistic spin-flips and phase-shift operations any N-qubit state can be depolarized. That family of states reads as

$$\rho_D = \sum_{\sigma=\pm} \lambda_0^\sigma |\psi_0^\sigma\rangle\langle\psi_0^\sigma| + \sum_{j=1}^{2^{N-1}-1} \lambda_j (|\psi_j^+\rangle\langle\psi_j^+| + |\psi_j^-\rangle\langle\psi_j^-|), \tag{2.114}$$

with j understood in binary notations, with all λ positive numbers and the GHZ basis

$$|\psi_j^\pm\rangle = \frac{1}{\sqrt{2}}(|j,0\rangle \pm |2^{N-1}-1-j,1\rangle). \tag{2.115}$$

In the case of $N = 3$, ρ_D is fully separable if and only if its partial transpose with respect to the first, second and third subsystem are all positive [44]. Those conditions are respectively fulfilled when

$$|\lambda_0^+ - \lambda_0^-| \leq 2\lambda_2, \tag{2.116}$$
$$|\lambda_0^+ - \lambda_0^-| \leq 2\lambda_1, \tag{2.117}$$
$$|\lambda_0^+ - \lambda_0^-| \leq 2\lambda_3. \tag{2.118}$$

Let us chose the C_{10} concurrence. We proceed as in Eq. (2.72), compute the $\rho_D S_{10} \rho_D^* S_{10}$ matrix and calculate the square roots is eigenvalues. The non-zero eigenvalues found are λ_0^+, λ_0^-, and λ_2 repeated twice. We then have the concurrence

$$C_{S_{10}}(\rho_D) = \text{Max}[0, 2\,\text{Max}[\lambda_0^+, \lambda_0^-, \lambda_2] - \lambda_0^+ - \lambda_0^- - 2\lambda_2]. \tag{2.119}$$

If λ_2 is the greatest value, then the concurrence is $\text{Max}[0, -\lambda_0^+ - \lambda_0^-] = 0$ and no entanglement is detected. In the case of $\lambda_0^\pm$ being the greatest value, we have a concurrence of $\text{Max}[0, |\lambda_0^+ - \lambda_0^-| - 2\lambda_2]$, which can be greater than zero when $|\lambda_0^+ - \lambda_0^-| > 2\lambda_2$. Finally, we find

$$C_{S_{10}}(\rho_D) > 0 \Leftrightarrow |\lambda_0^+ - \lambda_0^-| \leq 2\lambda_2, \tag{2.120}$$
$$C_{S_{12}}(\rho_D) > 0 \Leftrightarrow |\lambda_0^+ - \lambda_0^-| \leq 2\lambda_1, \tag{2.121}$$
$$C_{S_{14}}(\rho_D) > 0 \Leftrightarrow |\lambda_0^+ - \lambda_0^-| \leq 2\lambda_3, \tag{2.122}$$

the three exact conditions for full separability.

One particular case of the ρ_D case is the noisy GHZ state given by

$$\rho_{\text{GHZ}} = x|\text{GHZ}\rangle\langle\text{GHZ}| + \frac{1-x}{8} I_8. \tag{2.123}$$

Our concurrence, applied with S_{10}, finds that the state is entangled when $x > 1/5$, which is also the upper limit of x for full separability [44].

Let us consider now another type of state: the noisy W state, given by

$$\rho_{\text{W}} = x|\text{W}\rangle\langle\text{W}| + \frac{1-x}{8} I_8. \tag{2.124}$$

That state has a negative partial transpose when

$$x > \frac{3}{3 + 8\sqrt{2}} \approx 0.21, \tag{2.125}$$

which is not this time, a necessary and sufficient condition for separability. Indeed, by using the combination S

$$S = S_1 + S_3 + S_5, \tag{2.126}$$

we are able to calculate that the concurrence $C_S(\rho_{\text{W}})$ is non zero if

$$x > \frac{\sqrt{3}}{8 + \sqrt{3}} \approx 0.18, \tag{2.127}$$

which is actually a better limit than the one given by the PPT criterion. We can conclude that in the range $x \in [0.18, 0.21]$, the state ρ_{W} is actually entangled, but that entanglement is not detected by the PPT criterion, which makes it a bound entangled state [53].

2.4 N-qubit Concurrences for Pure States

Let us now generalize the notion of three-qubit concurrences to N-qubit systems. Just like what we did on tripartite states, we will always be able to detect entanglement in any pure state and we get a necessary condition to entanglement for mixed states.

2.4.1 Necessary and Sufficient Conditions to Separability

We express a general state N-qubit pure state as

$$|\psi\rangle = \sum_{j=0}^{2^N-1} a_j |j\rangle, \tag{2.128}$$

where $j = j_1 j_2 \cdots j_N$ is interpreted as a binary number with N digits.

We generalize the approach we used on $N = 3$. To find the conditions a fully separable state must hold, we consider a $2 \times \cdots \times 2$ N-order tensor $\boldsymbol{A}$ whose elements are the 2^N coefficients a_j. Finding the conditions for which $\boldsymbol{A}$ can be expressed as a rank-one tensor of the form

$$\boldsymbol{A} = \begin{pmatrix} a_0^{(1)} \\ a_1^{(1)} \end{pmatrix} \otimes \begin{pmatrix} a_0^{(2)} \\ a_1^{(2)} \end{pmatrix} \otimes \cdots \otimes \begin{pmatrix} a_0^{(N)} \\ a_1^{(N)} \end{pmatrix}, \tag{2.129}$$

will insure that, once the conditions obeyed, the state $|\psi\rangle$ can be written as a separable state

$$|\psi\rangle = |\psi^{(1)}\rangle \otimes |\psi^{(2)}\rangle \otimes \cdots \otimes |\psi^{(N)}\rangle, \tag{2.130}$$

with $|\psi^{(i)}\rangle \equiv a_0^{(i)}|0\rangle + a_1^{(i)}|1\rangle$.

Just like in the $N = 3$ case, the tensor $\boldsymbol{A}$ will be of rank one if and only if its N-mode matricizations are all of rank one [51]. The columns of the matricization matrices are build from the $a_{j_1 j_2 \cdots j_N}$ coefficients with all indexes fixed but one. Therefore, there are N different matrices each containing 2^{N-1} columns. For illustrative purposes, we represented the case of $N = 4$ in Fig. 2.5 with a (pseudo-)hypercube formed by the coefficients of $\boldsymbol{A}$. The columns of one matrix obtained through the matricization process are the couples of coefficients linked by a the lines of one color.

If the fixed coefficients are the last $N - 1$ coefficients, we find

$$\boldsymbol{A}^{(1)} = \begin{pmatrix} a_{00\cdots00} & a_{00\cdots01} & \cdots & a_{01\cdots1} \\ a_{10\cdots00} & a_{10\cdots01} & \cdots & a_{11\cdots1} \end{pmatrix}, \tag{2.131}$$

and in general, for all but the k-th coefficient (represented in bold) fixed

$$\boldsymbol{A}^{(k)} = \begin{pmatrix} a_{0\cdots0\mathbf{0}0\cdots0} & a_{0\cdots0\mathbf{0}0\cdots01} & \cdots & a_{1\cdots1\mathbf{0}1\cdots1} \\ a_{0\cdots0\mathbf{1}0\cdots0} & a_{0\cdots0\mathbf{1}0\cdots01} & \cdots & a_{1\cdots1\mathbf{1}1\cdots1} \end{pmatrix}. \tag{2.132}$$

For the k-th matrix to be of rank one, all columns must be linearly dependent and the $2^{N-1} - 1$ following conditions needs to be fulfilled

$$a_{j_1 j_2 \cdots \mathbf{0} \cdots j_N} a_{j'_1 j'_2 \cdots \mathbf{1} \cdots j'_N} = a_{j_1 j_2 \cdots \mathbf{1} \cdots j_N} a_{j'_1 j'_2 \cdots \mathbf{0} \cdots j'_N}, \tag{2.133}$$

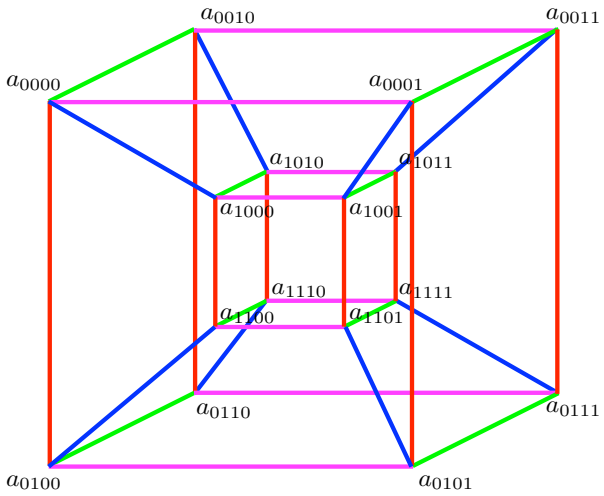

Figure 2.5: Representation of the four-order tensor of the $a_{j_1j_2j_3j_4}$ coefficient. The blue lines form the columns of $\boldsymbol{A}^{(1)}$, the red lines are the columns of $\boldsymbol{A}^{(2)}$, the green lines are the columns of $\boldsymbol{A}^{(3)}$ and the magenta lines are the columns of $\boldsymbol{A}^{(4)}$.

for every possible pairs of number $j_1j_2\cdots j_N \neq j'_1j'_2\cdots j'_N$ (where there is no j_k nor j'_k), which makes $\binom{2^{N-1}}{2} = 2^{N-2}(2^{N-1}-1)$ different conditions[1]. For the whole tensor to be of rank one, those conditions must also hold for every k.

Those N series of $2^{N-2}(2^{N-1}-1)$ conditions yield a huge number of equations, however many of them are redundant and we wish to reduce that number by sorting them into different classes.

- **Two-term equalities**

  This class of conditions is the one that deals with products that appear only once among all the conditions (2.133). Just like in Eq. (2.26) to (2.28), they come from "surface" matrices on the N-cube of the coefficients. They are the class of conditions

  $$a_{j_1j_2\cdots0\cdots0\cdots j_N}a_{j_1j_2\cdots1\cdots1\cdots j_N} = a_{j_1j_2\cdots1\cdots0\cdots j_N}a_{j_1j_2\cdots0\cdots1\cdots j_N}, \tag{2.134}$$

  with the $(N-2)$-digit number $j_1j_2\cdots j_N$, where j_k and j_l $(i \neq j)$ are missing. There are as many such conditions as there are ways to find the k,l pair, i. e. $\binom{N}{2}$ ways, multiplied by the number of different values for a $(N-2)$-digit number $j_1j_2\cdots j_{N_2}$, i. e. 2^{N-2}.

- **Four-term equalities**

[1] That is the number of possible choices of two columns among the 2^{N-1} columns of $\boldsymbol{A}^{(k)}$.

This next class of conditions deals with products that appear in three times in the conditions (2.133), just like Eq. (2.29). They come from "volume" matrices on the N-cube of the coefficients. They are written

$$a_{000j_4\cdots j_N}a_{111j_4\cdots j_N} = a_{001j_4\cdots j_N}a_{110j_4\cdots j_N} = a_{010j_4\cdots j_N}a_{101j_4\cdots j_N} = a_{100j_4\cdots j_N}a_{011j_4\cdots j_N}, \tag{2.135}$$

where we chose to single out the first three indices, but all possible placements must be considered. This time we have $\binom{N}{3}$ ways to find the three indices, multiplied by the 2^{N-3} possible ways to write a $(N-3)$-digit number and lastly one four-term equality is verified by three different two-term equalities.

- **2^{k-1}-term equalities**

  This class of conditions deals with products that appears $(2^{k-1}-1)$ times in the conditions (2.133). They are the terms coming from matrices going through volumes of dimension k of the N-cube. All the terms of those equalities are written

$$a_{J_1\cdots J_k j_{k+1}\cdots j_N}a_{J'_1\cdots J'_k j_{k+1}\cdots j_N}, \tag{2.136}$$

  for all possible values of $J_1\cdots J_k$ and $J'_1\cdots J'_k$ such that $J_l + J'_l = 1$ for $l = 1, 2, \cdots, k$. The number of two-term equalities obtained is then the number of ways to chose k digits $\binom{N}{k}$ multiplied by the 2^{N-k} ways to write a $(N-k)$-digit number multiplied by the $(2^{k-1}-1)$ two-term equalities in one 2^{k-1}-term equality.

The number k of ways to single out indices goes from 2 (two-term equalities) to N (single 2^{N-1}-term equality). The total number $\mathrm{Num}(N)$ of two-term conditions for a N-qubit tensor $\boldsymbol{A}$ to be of rank one is then

$$\mathrm{Num}(N) = \sum_{k=2}^{N}\binom{N}{k}2^{N-k}\left(2^{k-1}-1\right) = 2^{N-1} + 2^{2N-1} - 3^N, \tag{2.137}$$

which asymptotically grows as 2^{2N-1}.

Criterion 10. Conditions for N-qubit pure states separability — *The N-qubit $|\psi\rangle = \sum_j a_j|j\rangle$ state is separable if and only if for every $k = 2, 3, \cdots N$, for every choice of $(N-k)$-digit binary number $j_{k+1}\cdots j_N$ and for every way of choosing k indices J_l $(l = 1, 2, \cdots k)$ among the N, the 2^{k-1} terms*

$$a_{J_1\cdots J_k j_{k+1}\cdots j_N}a_{J'_1\cdots J'_k j_{k+1}\cdots j_N}, \tag{2.138}$$

are all equal for every possible value of $J_1\cdots J_k$ and $J'_1\cdots J'_k$, such that $J_l + J'_l = 1$.

Necessary condition. If $|\psi\rangle$ is fully separable, it can be written as

$$|\psi\rangle = |\psi^1\rangle \otimes |\psi^2\rangle \otimes \cdots \otimes |\psi^N\rangle, \tag{2.139}$$

with N single-qubit states $|\psi^i\rangle \equiv a_0^{(i)}|0\rangle + a_1^{(i)}|1\rangle$. By identifying the coefficients of $|\psi\rangle$ with the $a_{j_1 j_2 \cdots j_N}$ we find

$$a_{j_1 j_2 \cdots j_N} = a_{j_1}^{(1)} a_{j_2}^{(2)} \cdots a_{j_N}^{(N)}, \tag{2.140}$$

and conditions of the type of (2.133) are trivial to verify.

Sufficient condition. If all conditions hold, the tensor of the a_j coefficients is of rank one, can therefore be factorized and $|\psi\rangle$ is fully separable.

2.5 N-qubit Concurrences for Mixed States

It is quite simple to define the S_α operators once all the conditions are listed and numbered. Let us consider the α-th condition, written in general as

$$a_i a_j = a_k a_l, \tag{2.141}$$

with the indices once again understood as N-digit binary numbers taken corresponding the terms (2.138). We define the symmetric operator

$$S_\alpha = |j\rangle\langle i| + |i\rangle\langle j| - |k\rangle\langle l| - |l\rangle\langle k|. \tag{2.142}$$

We can define the N-qubit concurrences:

$$C_\alpha(|\psi\rangle) = |\langle\psi^*|S_\alpha|\psi\rangle| = 2|a_i a_i - a_k a_l|, \tag{2.143}$$

and we get the criterion:

Criterion 11. **N-qubit concurrence for pure states** — *The N-qubit state $|\psi\rangle$ is separable if and only if*

$$C_\alpha(|\psi\rangle) = |\langle\psi^*|S_\alpha|\psi\rangle| = 0, \tag{2.144}$$

for all $1 \leq \alpha \leq Num(N)$.

We now consider a N-qubit mixed state written ρ, and we define the mixed state concurrences as

$$C_S(\rho) = \mathrm{Max}[0, \lambda_1^S - \sum_{k=2}^{N} \lambda_k^S], \tag{2.145}$$

with S any symmetric N-partite operator made from a linear combination of the S_α and the λ_k^S are the square roots of the eigenvalues of the matrix $\rho S \rho^* S$ with $\lambda_1^S \geq \lambda_2^S \geq \cdots \geq \lambda_N^S$.

The proof for the validity of such a definition is exactly the same one as the one shown above for the case $N = 3$. Just like the case $N = 3$, we get a necessary criterion to entanglement.

Criterion 12. ***N*-qubit Concurrence** — *If a N-qubit mixed state ρ is fully separable, for all normalized linear combinations $S = \sum_\alpha c_\alpha S_\alpha$ we find*

$$C_S(\rho) = Max[0, \lambda_1^S - \sum_{k=2}^{N} \lambda_k^S] = 0. \tag{2.146}$$

Equivalently, if we find a combination S such that $C_S(\rho) \neq 0$, then ρ is entangled.

2.5.1 Illustrative Examples

Let us once again consider the Dür-Cirac-Tarrach ρ_D state

$$\rho_D = \sum_{\sigma=\pm} \lambda_0^\sigma |\psi_0^\sigma\rangle\langle\psi_0^\sigma| + \sum_{j=1}^{2^{N-1}-1} \lambda_j (|\psi_j^+\rangle\langle\psi_j^+| + |\psi_j^-\rangle\langle\psi_j^-|), \tag{2.147}$$

with

$$|\psi_j^\pm\rangle = \frac{1}{\sqrt{2}}(|j,0\rangle \pm |2^{N-1}-1-j,1\rangle), \tag{2.148}$$

or equivalently

$$|\psi_j^\pm\rangle = \frac{1}{\sqrt{2}}(|2j\rangle \pm |2^N-1-j\rangle), \tag{2.149}$$

since in binary notations, adding a 0 to the back of a number doubles it, while adding a 1 doubles it and adds one.

it can be shown [44] that the state is fully separable if and only if

$$|\lambda_0^+ - \lambda_0^-| \leq 2\lambda_k, \tag{2.150}$$

for all $1 \leq k \leq 2^{N-1}-1$. We use the S_{α_k}

$$S_{\alpha_k} = |0\rangle\langle 2^N-1| + |2^N-1\rangle\langle 0| - |2k\rangle\langle 2^N-1-2k| - |2k\rangle\langle 2^N-1-2k|. \tag{2.151}$$

The S_{α_k} are operators obtained from the the type of conditions in Eq. (2.136) since 0 and 2^N-1 share no digits in binary form (all 0's and all 1's respectively) and neither do $2k$ and 2^N-1-2k, which means they all refer to the conditions where all indices were chosen to be the J_l. and J_l'.

The operator can also be written

$$S_{\alpha_k} = |\psi_0^+\rangle\langle\psi_0^+| - |\psi_0^-\rangle\langle\psi_0^-| - |\psi_k^+\rangle\langle\psi_k^+| + |\psi_k^-\rangle\langle\psi_k^-|, \tag{2.152}$$

Since all coefficients of ρ_D are real, we have $\rho_D = \rho_D^*$ and therefore We find

$$\begin{aligned}
\rho_D S_{\alpha_k} \rho_D^* S_{\alpha_k} &= (\rho_D S_{\alpha_k})^2, && (2.153)\\
&= \left(\lambda_0^+ |\psi_0^+\rangle\langle\psi_0^+| - \lambda_0^- |\psi_0^-\rangle\langle\psi_0^-| - \lambda_k |\psi_k^+\rangle\langle\psi_k^+| + \lambda_k |\psi_k^-\rangle\langle\psi_k^-|\right)^2, && (2.154)\\
&= (\lambda_0^+)^2 |\psi_0^+\rangle\langle\psi_0^+| + (\lambda_0^+)^2 |\psi_0^-\rangle\langle\psi_0^-| \\
&\quad + \lambda_k^2 (|\psi_k^+\rangle\langle\psi_k^+| + |\psi_k^-\rangle\langle\psi_k^-|), && (2.155)
\end{aligned}$$

and since $\rho_D S_{\alpha_k} \rho_D^* S_{\alpha_k}$ is already in diagonal form, we immediately find the concurrence

$$C_{S_{\alpha_k}}(\rho_D) = \text{Max}[0, 2\,\text{Max}[\lambda_0^+, \lambda_0^-, \lambda_k] - \lambda_0^+ - \lambda_0^- - 2\lambda_k], \tag{2.156}$$

and with exactly the exactly the same reasoning as with the $N = 3$ case, we find that

$$C_{S_{\alpha_k}}(\rho_D) > 0 \Leftrightarrow |\lambda_0^+ - \lambda_0^-| \leq 2\lambda_k, \tag{2.157}$$

for all possible values of k.

Once again, our generalized concurrence was able to find the exact conditions for separability.

Chapter 3

Entanglement, Antibunching, and Saturation Effects in Dipole Blockade

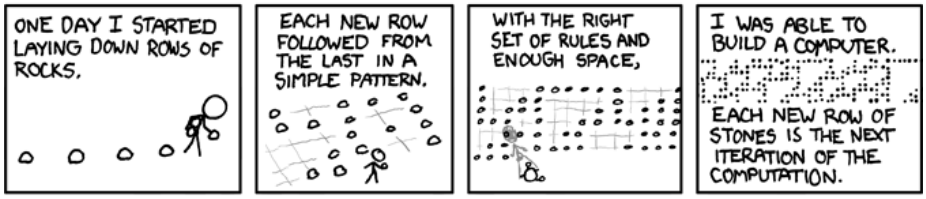

Randall Munroe, *A Bunch of Rocks* (part 4 of 9), `xkcd.com/505/`

Dipole-dipole interactions between atoms or molecules affect profoundly the light absorption that occurs in matter [54]. They have been known for several years to give rise to fascinating applications in quantum information science like quantum logic operations in neutral atoms [55, 56] or entanglement production in mesoscopic ensembles [57–59]. The level shifts associated with those interactions can strongly modify the laser excitation of adjacent atoms, up to a complete suppression of more than one excitation in nearby atoms.

In this so-called *dipole blockade* effect, the first excited atom prevents any further excitation in a confined volume by shifting the resonance for its non-excited neighbors, resulting in production of singly excited collective states [57]. In the past years, evidence for the dipole blockade effect has been obtained with samples of Rydberg atoms because of their strong long-range interaction [60–63].

An analogous photon blockade effect in an optical cavity has also been reported [64]. Recently Rabi oscillations between the ground state of a pair of Rydberg atoms and the single excited symmetric collective state has been observed for atoms located more than a few micrometers away [65, 66]. In all those fascinating achievements, the residual effects resulting from possible multiple excitations of the atomic sample are usually not discussed although they cannot be eliminated totally. This motivates a deeper quantitative analysis of the dipole blockade phenomenon to optimize its occurrence and understand its possible limitations in particular in entanglement production [63, 67].

We start this chapter with Sec. 3.1, where we define our theoretical model Hamiltonian and master equation. In Sec. 3.2, we justify the master equation approach by first considering a single atoms excited by a laser and subject to dissipation effects. We solve the time-dependent equations describing its evolution for any time and also at the equilibrium, which is not possible with a Shcrödinger equation approach. The problem of two independent atoms is merely the adjunction of twice the solution of the single atom problem.

In Sec. 3.3, we give the time-dependent equations of our model and we solve them numerically for three different regimes: weakly interacting atoms, strongly interacting atoms and strongly driven interacting atoms. The dipole blockade effect appears clearly. Next, we study the time-dependence of concurrence of the system in the three previously mentioned regimes. It appears that the amount of entanglement is directly related to the strength of the blockade.

In Sec. 3.4, we give the analytical form of the steady state of our model. We also give the analytical form of the ratio between the populations of two excited state and the populations of singly excited states. We derive the analytical form of the concurrence of the steady state and check the maximal amount of entanglement possibly found in the system by studying limit cases. We also show that for a given interaction strength, the laser strength can be tuned to give an optimal quantity of entanglement in the system and that for a laser strength above a given value the entanglement vanishes.

In Sec. 3.5, we report how a continuous monitoring of the dipole blockade could be obtained with help of the photon-photon correlation signal of the scattered light in a regime where the spontaneous emission would dominate the dissipation effects of the sample and finally we conclude.

3.1 Theoretical Model

We consider two atoms at fixed positions $\mathbf{x}_1$ and $\mathbf{x}_2$ with internal levels $|e\rangle$ and $|g\rangle$, dipolar transition frequency $\omega = 2\pi c/\lambda$, and single atom spontaneous emission rate $2\gamma_s$. We consider that the two atoms strongly interact when in state $|ee\rangle$ resulting in a shift $\hbar\delta$ of this doubly excited state. They are driven by a resonant external laser field with wave vector $\mathbf{k}_L$ and Rabi frequency 2Ω.

In the rotating-wave approximation, the coherent evolution of the system is described by the interaction Hamiltonian

$$H = \hbar\delta|ee\rangle\langle ee| + \hbar\Omega\left(e^{i\mathbf{k}_L\cdot\mathbf{x}_1}S_1^+ + e^{i\mathbf{k}_L\cdot\mathbf{x}_2}S_2^+ + \text{h.c.}\right), \tag{3.1}$$

where $S_i^+ = (S_i^-)^\dagger$ $(i = 1, 2)$ is the atom raising operator $|e\rangle_i\langle g|$ and the term $\hbar\delta|ee\rangle\langle ee|$ accounts for the shift of the doubly excited state of the system induced by the dipole-dipole interaction.

The system is best described in the Dicke basis $\{|ee\rangle, |s\rangle, |gg\rangle, |a\rangle\}$ with

$$|s\rangle \equiv \frac{1}{\sqrt{2}}(e^{i\mathbf{k}_L\cdot\mathbf{x}_1}|eg\rangle + e^{i\mathbf{k}_L\cdot\mathbf{x}_2}|ge\rangle), \tag{3.2}$$

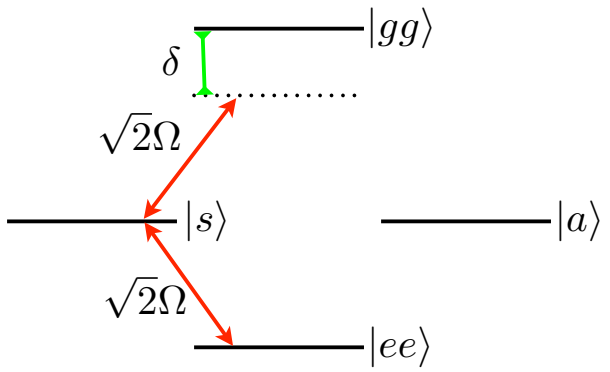

Figure 3.2: Energy diagram of the system. The resonant laser populates the $|ee\rangle$ state from the symmetric state $|s\rangle$, itself populated from the ground state with a Rabi frequency $\sqrt{2}\Omega$. However, $|ee\rangle$ is shifted from its usual energy level by a quantity $\hbar\delta$. The antisymmetric state $|a\rangle$ is left alone.

and

$$|a\rangle \equiv \frac{1}{\sqrt{2}}(e^{i\mathbf{k}_L\cdot\mathbf{x}_1}|eg\rangle - e^{i\mathbf{k}_L\cdot\mathbf{x}_2}|ge\rangle), \tag{3.3}$$

as the symmetric and antisymmetric state, respectively. Quantum interference effects from the variation of the phases $e^{i\mathbf{k}_L\cdot\mathbf{x}_i}$ coming from the geometry of the system were studied in [68] but in this chapter we assume $\mathbf{k}_L$ to be perpendicular to the two-atom line and the reference frame is properly chosen so as $\mathbf{k}_L \cdot \mathbf{x}_1 = \mathbf{k}_L \cdot \mathbf{x}_2 = 0$ and all phase terms in H, $|a\rangle$ or $|s\rangle$ are dropped. In the Dicke basis, the Hamiltonian then becomes

$$H = \hbar\delta|ee\rangle\langle ee| + \sqrt{2}\hbar\Omega\left(|ee\rangle\langle s| + |s\rangle\langle gg| + \text{h.c.}\right). \tag{3.4}$$

We see that in this particular configuration, the $|a\rangle$ state does not appear in the Hamiltonian and its population should therefore be a constant provided no other process is involved. The system is therefore completely symmetric under the exchange of the two atoms. We represented the system in that form in Fig. 3.2.

When considering dissipation in the Markov and Born approximation, the time evolution of the system is governed by the master equation [69]

$$\dot{\rho} = -\frac{i}{\hbar}[H,\rho] - \gamma\sum_{i=1}^{2}(S_i^+S_i^-\rho + \rho S_i^+S_i^- - 2S_i^-\rho S_i^+), \tag{3.5}$$

where $\gamma = \gamma_s + \gamma_d$ with $2\gamma_d$ the dissipation rate modeling non-radiative dissipative effects in the sample. We consider that the two atoms are separated by more than the transition wavelength λ so that we can neglect the imbalance among the decay rates of the Dicke states $|s\rangle$ and $|a\rangle$ [70]. This situation is encountered in most recent experiments, like in Ref. [65] where the atoms are located more than 20λ away.

One of the effects of dissipative processes in the system modelized by 3.5 is to populate the antisymmetric state $|a\rangle$ through the decay of the $|ee\rangle$ state, even though the Hamiltonian has no effect on it.

3.2 Non-interactive Case

Let us first investigate the non-interactive case $\delta = 0$. Physically, this case corresponds to two two-level atoms far from each other, both excited by a laser field, or two distant identical laser fields, such that the atoms never see each other. Such a case can be easily analytically solved by realizing that the system does not need to be solved as a whole, instead each atom can be treated independently and the state of the whole system will be the tensor product of both atomic states.

The Hamiltonian for one atom excited by a laser field on resonance H_s, where the s stands for *single atom*, is

$$H_s = \hbar\Omega(S^+ + S^-), \tag{3.6}$$

with the previously introduced notations. The time evolution of a pure state $|\psi_s\rangle$ describing the atom is dictated by a Schrödinger equation whose solution is, assuming the state was in the ground state at time $t = 0$,

$$|\psi_s\rangle = \cos(\Omega t)|g\rangle - i\sin(\Omega t)|e\rangle, \tag{3.7}$$

which is the well-known Rabi oscillation.

Let us now consider a more complete physical approach by adding to the model dissipation effects. The excited atom, left alone, is susceptible to de-excite itself either through a non-radiative process (for example after a collision or other experimental factor) at the rate $2\gamma_d$ or through a radiative process (spontaneous emission of a photon) with the rate $2\gamma_s$, for a total rate of 2γ. In a model taking these effects into account, a pure state approach does not allow to follow the evolution of the single-atom system, as we only know the stochastic probability of the atom to de-excite and we must consider a mixed state ρ_s instead. The time evolution of the system is then given by the master equation

$$\dot{\rho}_s = -\frac{i}{\hbar}[H_s, \rho_s] - \gamma(S^+S^-\rho_s + \rho_s S^+S^- - 2S^-\rho_s S^+), \tag{3.8}$$

or, considering the mixed state time-dependent coefficients represented in a matrix form with the $\{|e\rangle, |g\rangle\}$ basis

$$\rho_s = \begin{pmatrix} \rho_e & \rho_{eg} \\ \rho_{eg}^* & \rho_g \end{pmatrix}, \tag{3.9}$$

with $\mathrm{Tr}\,(\rho_s) = \rho_e + \rho_g = 1$. The master equation (3.8) translates as

$$\begin{aligned} \dot{\rho}_e &= -2\Omega\,\mathrm{Im}(\rho_{eg}) - 2\gamma\rho_e, & (3.10)\\ \dot{\rho}_{eg} &= i\Omega\,(\rho_e - \rho_g) - \gamma\rho_{eg}, & (3.11)\\ \dot{\rho}_g &= 2\Omega\,\mathrm{Im}(\rho_{eg}) + 2\gamma\rho_e. & (3.12) \end{aligned}$$

The general solution to this system of differential equations is, assuming that the initial

state at $t = 0$ is the ground state $|g\rangle$,

$$\rho_e = \frac{\Omega^2}{2\Omega^2+\gamma^2}\left[1 - e^{-\frac{3}{2}\gamma t}\left(3\frac{\gamma}{\lambda}\sinh\left(\frac{\lambda t}{2}\right) + \cosh\left(\frac{\lambda t}{2}\right)\right)\right], \tag{3.13}$$

$$\rho_{eg} = \frac{-i\Omega\gamma}{2\Omega^2+\gamma^2}\left[1 - e^{-\frac{3}{2}\gamma t}\left(\frac{\gamma^2-4\Omega^2}{\gamma\lambda}\sinh\left(\frac{\lambda t}{2}\right) + \cosh\left(\frac{\lambda t}{2}\right)\right)\right], \tag{3.14}$$

$$\rho_g = \frac{1}{2\Omega^2+\gamma^2}\left[(\Omega^2+\gamma^2) + \Omega^2 e^{-\frac{3}{2}\gamma t}\left(3\frac{\gamma}{\lambda}\sinh\left(\frac{\lambda t}{2}\right) + \cosh\left(\frac{\lambda t}{2}\right)\right)\right], \tag{3.15}$$

with $\lambda = \sqrt{\gamma^2 - 16\Omega^2}$. When the dissipative effects are strong enough, i. e. when $\gamma > 4\Omega$, λ takes a real value and the populations exponentially tend to their equilibrium value, which will be low the the excited state since the laser is weak. When the laser strength is stronger, i. e. when $4\Omega > \gamma$, λ will be imaginary and the populations will undergo damped Rabi oscillations (since $\sinh(ix) = i\sin(x)$ and $\cosh(ix) = \cos(x)$) and finally settle to their equilibrium values.

The steady state solution ρ_s^S of that system, where the upper S stands for *steady state*, is the equilibrium value of ρ_s at $t \to \infty$. We find, still in the $\{|e\rangle, |g\rangle\}$ basis,

$$\rho_s^S = \rho_s(t \to \infty) = \frac{1}{2\Omega^2+\gamma^2}\begin{pmatrix} \Omega^2 & -i\Omega\gamma \\ i\Omega\gamma & \Omega^2+\gamma^2 \end{pmatrix}. \tag{3.16}$$

We see that at the equilibrium, it is always more probable to find the atom in the ground state than in the excited state, due to the dissipation processes. In the strong field limit $\Omega \gg \gamma$, the probabilities equalize.

The steady state ρ_s^S may also be written as a mixed state of two pure states

$$\rho_s^S = \frac{\Omega^2+\gamma^2}{2\Omega^2+\gamma^2}\,|\phi\rangle\langle\phi| + \frac{\Omega^2}{2\Omega^2+\gamma^2}\,|g\rangle\langle g|, \tag{3.17}$$

with

$$|\phi\rangle \equiv \frac{1}{\sqrt{\Omega^2+\gamma^2}}\left(\Omega|e\rangle - i\gamma|g\rangle\right), \tag{3.18}$$

which approaches $|e\rangle$ when γ becomes negligible.

The steady state ρ^S to the two non-interacting, identical atoms system is simply given by

$$\rho^S = \rho_s^S \otimes \rho_s^S. \tag{3.19}$$

For that state, the probability to find both atoms excited is

$$P_{ee} = \langle ee|\rho^S|ee\rangle = \frac{\Omega^4}{(2\Omega^2+\gamma^2)^2}, \tag{3.20}$$

which is exactly the square of the probability $P_e = \langle e|\rho_s^S|e\rangle$ to find either atom excited. In other words,

$$P_{ee} = P_e^2, \tag{3.21}$$

and no bunching or antibunching behavior is expected from the system. Of course, no entanglement can be found in that system since it is written as a tensor product, the very definition of a separable state.

In the Dicke basis $\{|ee\rangle, |s\rangle, |gg\rangle, |a\rangle\}$, the steady state is written

$$\rho = \frac{1}{(2\Omega^2+\gamma^2)^2}\begin{pmatrix} \Omega^4 & -i2\sqrt{2}\Omega^3\gamma & -\Omega^2\gamma^2 & 0 \\ i2\sqrt{2}\Omega^3\gamma & \Omega^4+2\Omega^2\gamma^2 & -i\sqrt{2}\Omega\gamma(\Omega^2+\gamma^2) & 0 \\ -\Omega^2\gamma^2 & i\sqrt{2}\Omega\gamma(\Omega^2+\gamma^2) & (\Omega^2+\gamma^2)^2 & 0 \\ 0 & 0 & 0 & \Omega^4 \end{pmatrix}. \tag{3.22}$$

We see that although the state cannot be entangled, the population in the maximally entangled state $|s\rangle$ is not zero, which shows that the matrix elements of a density matrix should not be interpreted naively. Also, even though the state is completely symmetric, the population of the antisymmetric state $|a\rangle$ is not zero either as it has been populated by the dissipation effects. The global system is still symmetrical because even though $|a\rangle$ becomes $-|a\rangle$ when the atoms are permuted, in the mixed state formalism the term $|a\rangle\langle a|$ does not change its sign (or rather, changes it *twice)*. However that does not happen with the $|a\rangle\langle i|$ terms, where $|i\rangle$ is any symmetric state, therefore those terms must all be null.

3.3 Time Dependent Behavior

In this section, we use the master equation (3.5) to compute the time-behavior of the density matrix and evaluate the dipole blockade and the concurrence in the system.

3.3.1 Dipole Blockade

In presence of the dipole blockade mechanism, the doubly excited state $|ee\rangle$ is out of resonance and expected to be poorly populated, therefore affecting the balance between P_{ee} and P_e^2 that existed without the interaction. The time evolution of the whole system is given by the master equation (3.5) and we may express it in function of the terms of the symmetric density matrix ρ expressed in the Dicke basis

$$\rho(t) = \begin{pmatrix} \rho_e & \rho_{es} & \rho_{eg} & 0 \\ \rho_{se} & \rho_s & \rho_{sg} & 0 \\ \rho_{ge} & \rho_{gs} & \rho_g & 0 \\ 0 & 0 & 0 & \rho_a \end{pmatrix}. \tag{3.23}$$

We can now express the master equation as

$$\begin{aligned}
\dot{\rho}_e &= -2\sqrt{2}\Omega\,\mathrm{Im}(\rho_{es}) - 4\gamma\rho_e, && (3.24)\\
\dot{\rho}_s &= 2\sqrt{2}\Omega\,\mathrm{Im}(\rho_{es} - \rho_{sg}) + 2\gamma(\rho_e - \rho_s), && (3.25)\\
\dot{\rho}_g &= 2\sqrt{2}\Omega\,\mathrm{Im}(\rho_{sg}) + 2\gamma(\rho_a + \rho_s), && (3.26)\\
\dot{\rho}_a &= 2\gamma(\rho_e - \rho_a), && (3.27)\\
\dot{\rho}_{es} &= i\sqrt{2}\Omega\,(\rho_e - \rho_s + \rho_{eg}) - (3\gamma + i\delta)\rho_{es}, && (3.28)\\
\dot{\rho}_{eg} &= -i\sqrt{2}\Omega\,(\rho_{sg} - \rho_{es}) - (2\gamma + i\delta)\rho_{eg}, && (3.29)\\
\dot{\rho}_{sg} &= -i\sqrt{2}\Omega\,(\rho_{eg} + \rho_g - \rho_s) + \gamma(2\rho_{es} - \rho_{sg}), && (3.30)
\end{aligned}$$

and the remaining equation are the complex conjugates of the last three. Posing an initial state, say $|gg\rangle$ at time $t = 0$, it is possible to numerically follow the evolution of the state and compare the quantities P_e and P_e^2 . When $\delta \simeq 0$, we expect the system to be just about separable, in which case $P_{ee} \simeq P_e^2$. When δ grows, the state $|ee\rangle$ gets out of resonance and we expect a diminution of P_{ee} which might not be matched in P_e, therefore effectively seeing the dipole blockade effect.

In Fig. 3.3, We illustrate quantitatively the time evolution of the excitation probabilities for a system initially in the ground state with three different configurations. As expected, when the dipole-dipole interaction is not strong enough, as in case (a), it has negligible effect and the atoms act as independent systems : $P_{ee} \simeq P_e^2$.

For greater dipole-dipole interaction, in case (b), the doubly excited state is blocked and its population remains at very small levels, though not zero. More importantly the double excitation probability P_{ee} is much lower than P_e^2, giving a direct signature of the blockade mechanism.

When the laser intensity is increased, in case (c), we observe that P_{ee} is again very similar to P_e^2. The population blockade is lifted and the atoms behave once again as if they were independent without mutual influence. The dipole blockade effect can thus be circumvented by using strong laser fields. Case (b) exhibits a similar behavior of the system to the one observed experimentally in Ref. [66].

3.3.2 Concurrence

The experimental results reported in Refs. [65, 66] clearly imply the entanglement in the two-atom system. We can quantify such an entanglement: from the master equation (3.5) we obtain the complete time-dependent density matrix which then can be used to compute the concurrence [33].

We show the results in Fig 3.4. The concurrence is maximized when the dipole blockade mechanism is itself optimized. In case (a), the dipole-dipole interaction is too weak and the two-atom system behaves as a collection of independent atoms. No significant entanglement is produced. In case (b), the dipole blockade prevents the doubly excited state to be significantly populated and the two-atom system shares a collective single excitation. More population in the entangled $|s\rangle$ state is expected and significant amounts of entanglement

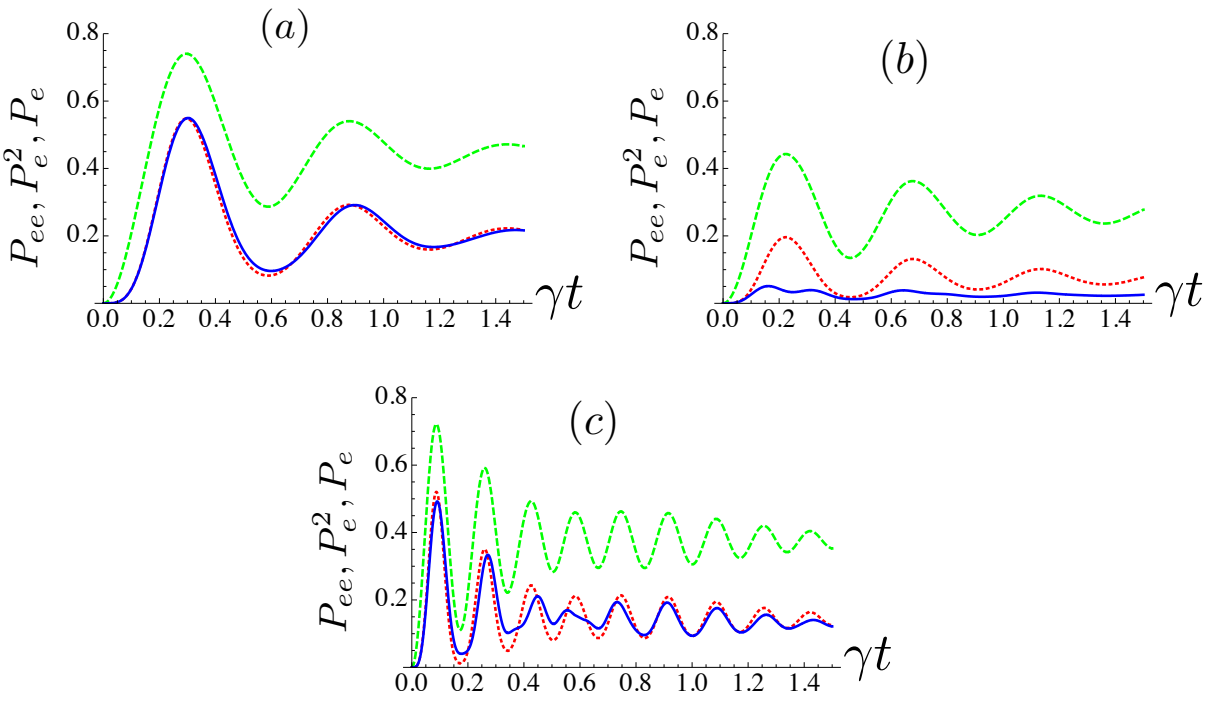

Figure 3.3: Time evolution of the excitation probability P_e (dashed green curve), its square (dotted red curve) and the probability P_{ee} of having both atoms excited (blue curve). The numerical parameters are (*a*) $\Omega/\gamma = 5$, $\delta/\gamma = 5$, (*b*) $\Omega/\gamma = 5$, $\delta/\gamma = 30$ and (*c*) $\Omega/\gamma = 15$, $\delta/\gamma = 30$. The dipole blockade effect is well marked in case (*b*) where $P_{ee} \ll P_e^2$.

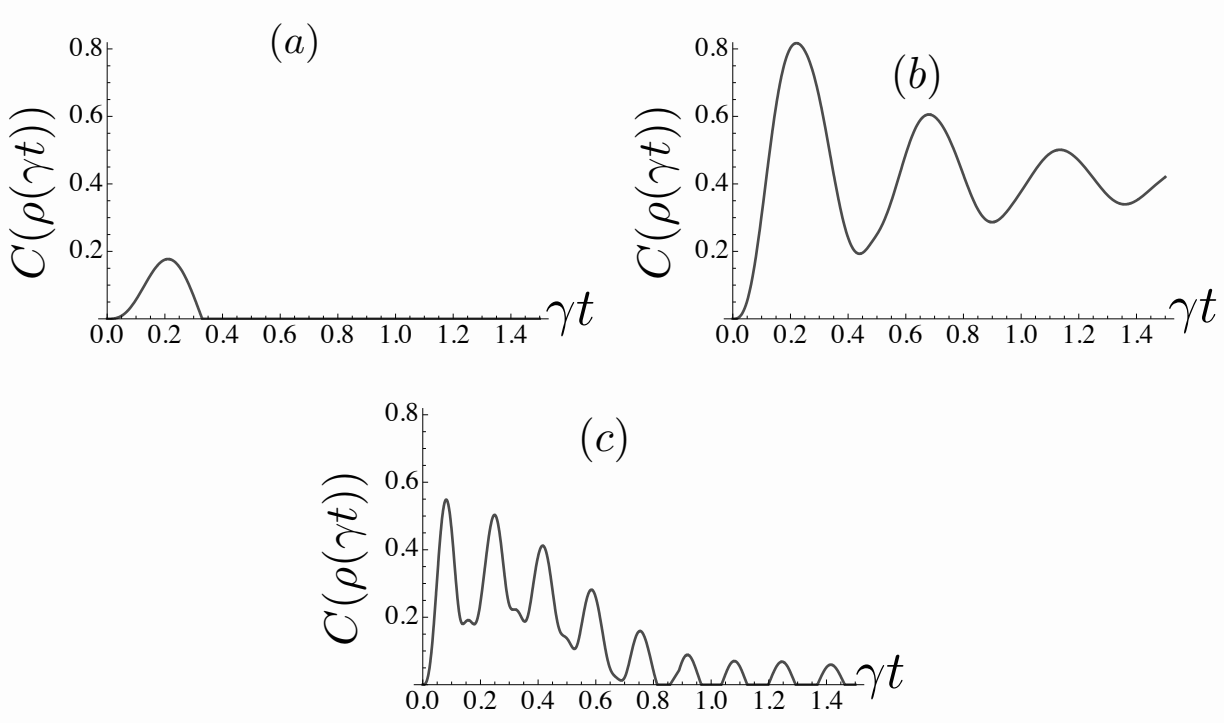

Figure 3.4: Time evolution of the concurrence C of the two-atom system. The numerical parameters are (a) $\Omega/\gamma = 5$, $\delta/\gamma = 5$, (b) $\Omega/\gamma = 5$, $\delta/\gamma = 30$ and (c) $\Omega/\gamma = 15$, $\delta/\gamma = 30$. The most concurrence registered in in case (b), where the blockade is strong.

are produced. In case (c), the dipole blockade is lifted and more population in the separable doubly excited state $|ee\rangle$ is expected. The concurrence is again less important than in case (b).

3.4 Steady State Behavior

The two-atom state ρ subjected to the master equation (3.5) always stabilizes after a finite time around a steady state that we denote ρ^S. The steady state is found by equating the right-hand term of Eq. (3.5) to zero, or equivalently, Eq. (3.24) to (3.30). We get in the Dicke basis

$$\rho^S = \frac{1}{\mathcal{N}} \begin{pmatrix} 4\Omega^4 & 2\sqrt{2}\Omega^3\alpha & -2i\Omega^2\gamma\alpha & 0 \\ 2\sqrt{2}\Omega^3\alpha^* & 2\Omega^2(2\Omega^2+|\alpha|^2) & \sqrt{2}\Omega\alpha(2\Omega^2-i\gamma\alpha^*) & 0 \\ 2i\Omega^2\gamma\alpha^* & \sqrt{2}\Omega\alpha^*(2\Omega^2+i\gamma\alpha) & 4\Omega^4+(2\Omega^2+\gamma^2)|\alpha|^2 & 0 \\ 0 & 0 & 0 & 4\Omega^4 \end{pmatrix}, \tag{3.31}$$

with $\alpha = -(\delta + 2i\gamma)$ and $\mathcal{N} = 16\Omega^4 + (4\Omega^2+\gamma^2)|\alpha|^2$. We may want to write ρ^S as a mixed state of several pure states as

$$\rho^S = \frac{1}{\mathcal{N}}\,|\phi_1\rangle\langle\phi_1| + \frac{1}{\mathcal{N}}\,|\phi_2\rangle\langle\phi_2| + \frac{4\Omega^4}{\mathcal{N}}\left(|a\rangle\langle a| + |gg\rangle\langle gg|\right), \tag{3.32}$$

with the unnormalized states

$$|\phi_1\rangle \equiv 2\Omega^2|ee\rangle + \sqrt{2}\Omega\alpha^*|s\rangle + i\gamma\alpha^*|gg\rangle, \tag{3.33}$$

$$|\phi_2\rangle \equiv 2\Omega^2|s\rangle + \sqrt{2}\Omega\alpha^*|gg\rangle. \tag{3.34}$$

3.4.1 Dipole Blockade

In the steady state regime, the population of the doubly excited state $|ee\rangle$ decreases when δ increases. This is the usual dipole blockade effect where one excited atom prevents the excitation of a nearby atom. This effect is counterbalanced by an increase in the laser intensity and eventually gets lifted with a strong enough laser intensity.

The ratio between the steady state double excitation probability P_{ee} and the square of the single excitation probability P_e reads

$$\left.\frac{P_{ee}}{P_e^2}\right|_S = \frac{64\Omega^4 + 16\Omega^2|\alpha|^2 + 4\gamma^2|\alpha|^2}{64\Omega^4 + 16\Omega^2|\alpha|^2 + |\alpha|^4}. \tag{3.35}$$

In absence of the dipole-dipole interaction ($\delta = 0$) this ratio is trivially equal to 1. This is obviously expected from the absence of correlation in the two-atom system in this case. When increasing $|\delta|$ the ratio monotonically decreases. This is a clear signature of the increasing correlation induced by the stronger and stronger dipole-dipole interaction shifting more and more the doubly excited state.

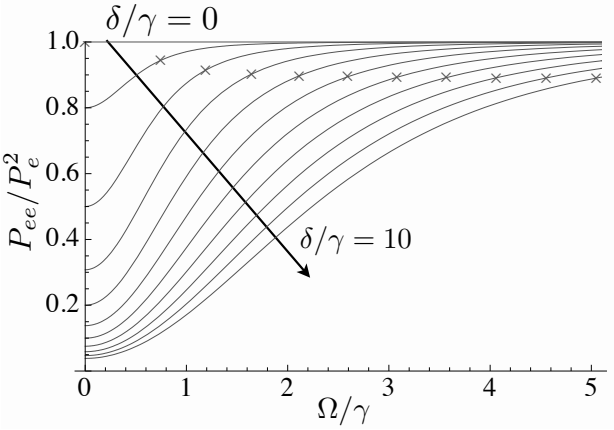

Figure 3.5: Plots of P_{ee}/P_e^2 with respect to Ω/γ for all integer values of δ/γ from 0 to 10. The crosses indicate for each curve the values of Ω/γ above which the steady state is separable.

We show more quantitatively the behavior of this ratio for different values of δ/γ with respect to the field intensity in Fig. 3.5. It is quite clear that for weak intensities of the field, the dipole blockade regime is dominant as there is less and less population in the $|ee\rangle$ state as δ/γ increases.

3.4.2 Concurrence

This dipole blockade model has the great advantage of being analytically solvable. We can even calculate the exact form of the concurrence of the system. The concurrence $C(\rho^S)$ of the steady state reads

$$C(\rho^S) = \text{Max}\left\{0, \frac{\sqrt{2}\Omega^2(\lambda_+ - \lambda_-) - 8\Omega^4}{16\Omega^4 + (4\Omega^2 + \gamma^2)|\alpha|^2}\right\}, \tag{3.36}$$

with

$$\lambda_\pm = \sqrt{8\Omega^4 + \delta^2|\alpha|^2 \pm \delta|\alpha|\sqrt{16\Omega^4 + \delta^2|\alpha|^2}}. \tag{3.37}$$

In absence of dipole-dipole interaction ($\delta = 0$), the steady state is not entangled. No entanglement is produced in this configuration since the two atoms behave as independent systems. This highlights the fundamental role of the dipole blockade mechanism for long-term entanglement production of the two-atom system.

For increasing values of δ, we show in Fig. 3.6 the concurrence of the steady state with respect to the field intensity. We may try to calculate the largest possible value of the concurrence as δ grows. We have

$$\lim_{\delta\to\infty} C(\rho^S) = \frac{2\Omega^2}{4\Omega^2 + \gamma^2}, \tag{3.38}$$

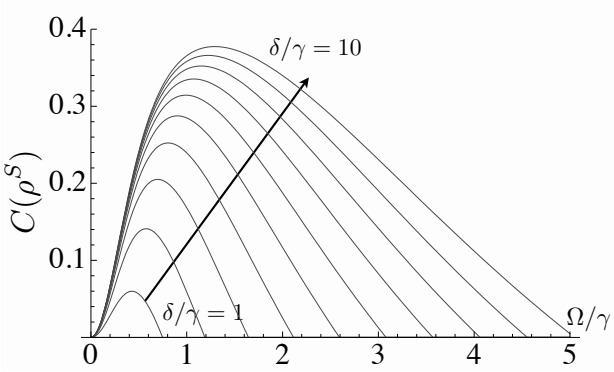

Figure 3.6: Plots of $C(\rho^S)$ with respect to Ω/γ for integer values of δ/γ from 1 to 10. For each value of the interaction δ, there is a value of Ω which maximizes the entanglement.

which approaches $1/2$ if $\Omega \gg \gamma$. This can be understood easily by noting that $\delta \to \infty$ means $|ee\rangle$ is completely out of resonance, hence it is never populated and the resulting system is an equal mixture (when $\Omega \gg \gamma$) of the $|s\rangle$ and $|gg\rangle$ states of respective concurrence 1 and 0. Indeed, we find

$$\lim_{\delta\to\infty} \rho^S = \frac{2\Omega^2+\gamma^2}{4\Omega^2+\gamma^2}\,|\phi\rangle\langle\phi| + \frac{2\Omega^2}{4\Omega^2+\gamma^2}\,|gg\rangle\langle gg|, \tag{3.39}$$

with

$$|\phi\rangle \equiv \frac{1}{\sqrt{2\Omega^2+\gamma^2}}\left(\sqrt{2}\Omega|s\rangle + i\gamma|gg\rangle\right), \tag{3.40}$$

which approaches $|s\rangle$ when γ becomes negligible.

Therefore the long-term entanglement in the system may be reasonably high. For finite values of δ, the value of Ω may be adjusted so that the amount of entanglement in the system is optimized. That can be done by numerically finding the maximum value of $C(\rho^S)$ in Eq. (3.36) with a given δ. When the intensity of the field increases above the optimized value and lifts the dipole blockade, the amount of entanglement decreases accordingly. The steady state is entangled as long as

$$0 < 4\Omega^2 < \delta|\alpha|. \tag{3.41}$$

That upper limit on Ω is pointed on each plot of Fig. 3.5.

3.5 Photon-Photon Correlation

The photon-photon correlation signal gives information that is not contained in intensity measurements and is a good probe for the quantum nature of the investigated processes.

The first and second correlation functions can be written as [70, 71]

$$G^{(1)}(\mathbf{r},t) = \sum_{\mu,\nu=1}^{2} e^{ik_L\hat{\mathbf{r}}\cdot\mathbf{x}_{\mu,\nu}}\langle S_\mu^+(t)S_\nu^-(t)\rangle, \tag{3.42}$$

with $\mathbf{r}$ the position of the photon detector, $\hat{\mathbf{r}} = \mathbf{r}/|\mathbf{r}|$ and

$$G^{(2)}(\mathbf{r}_1,t;\mathbf{r}_2,t+\tau) = \sum_{\mu,\nu,\lambda,\kappa=1}^{2} e^{ik_L(\hat{\mathbf{r}}_1\cdot\mathbf{x}_{\mu,\nu}+\hat{\mathbf{r}}_2\cdot\mathbf{x}_{\lambda,\kappa})}\langle S_\mu^+(t)S_\lambda^+(t+\tau)S_\kappa^-(t+\tau)S_\nu^-(t)\rangle, \tag{3.43}$$

with $\mathbf{x}_{\mu,\nu} = \mathbf{x}_\mu - \mathbf{x}_\nu$. The $G^{(2)}$ correlation can also be normalized and written as

$$g^{(2)}(\mathbf{r}_1,t;\mathbf{r}_2,t+\tau) = \frac{P(\mathbf{r}_2,t+\tau|\mathbf{r}_1,t)}{P(\mathbf{r}_2,t)}, \tag{3.44}$$

where $P(\mathbf{r},t)$ is the probability of detecting a photon at position $\mathbf{r}$ and time t, and $P(\mathbf{r}_2,t+\tau|\mathbf{r}_1,t)$ the conditional probability of finding a photon at $\mathbf{r}_2$ and $t+\tau$ assuming that a photon at $\mathbf{r}_1$ and t has been recorded.

The probabilities can be calculated using the quantum regression theorem from the dynamical behavior of the density matrix [72] via

$$P(\mathbf{r},t) = \left\langle D^\dagger(\mathbf{r})D(\mathbf{r})\right\rangle_{\rho(t)}, \tag{3.45}$$

$$P(\mathbf{r}_2,t+\tau|\mathbf{r}_1,t) = \left\langle D^\dagger(\mathbf{r}_2)D(\mathbf{r}_2)\right\rangle_{\rho'(t+\tau;\mathbf{r}_1,t)}, \tag{3.46}$$

where $\rho(t)$ is the density operator of the two-atom system at time t, $\rho'(t+\tau;\mathbf{r}_1,t)$ is the density operator at time $t+\tau$ assuming a photon has been detected at point $\mathbf{r}_1$ and time t, and $D(\mathbf{r})$ is the photon detector operator [73]

$$D(\mathbf{r}) = S_1^- + e^{i\phi(\mathbf{r})}S_2^-, \tag{3.47}$$

where $\phi(\mathbf{r}) = k_L\hat{\mathbf{r}}\cdot\mathbf{x}_{12}$. The second order correlation function can be calculated by considering that a state ρ just prior to a photon detection at position $\mathbf{r}_1$ and time t will be reduced, according to the von Neumann projection postulate, to

$$\rho'(\mathbf{r}_1,t) = \frac{D(\mathbf{r}_1)\rho D^\dagger(\mathbf{r}_1)}{\langle D^\dagger(\mathbf{r}_1)D(\mathbf{r}_1)\rangle}, \tag{3.48}$$

and will evolve following the master equation (3.5). After a time τ, the second measurement is made and $g^{(2)}$ can be calculated.

We show in Fig. 3.7 the photon-photon correlation function (3.44) with respect to τ in a time t when the system is in the steady state and where the two detectors are located such that $\phi(\mathbf{r}_1) = \phi(\mathbf{r}_2) = 2n\pi$ with n an integer number.

Although this is not yet the case in the first experimental observations of the dipole blockade manifestations [65, 66], we consider here a regime where the spontaneous emission

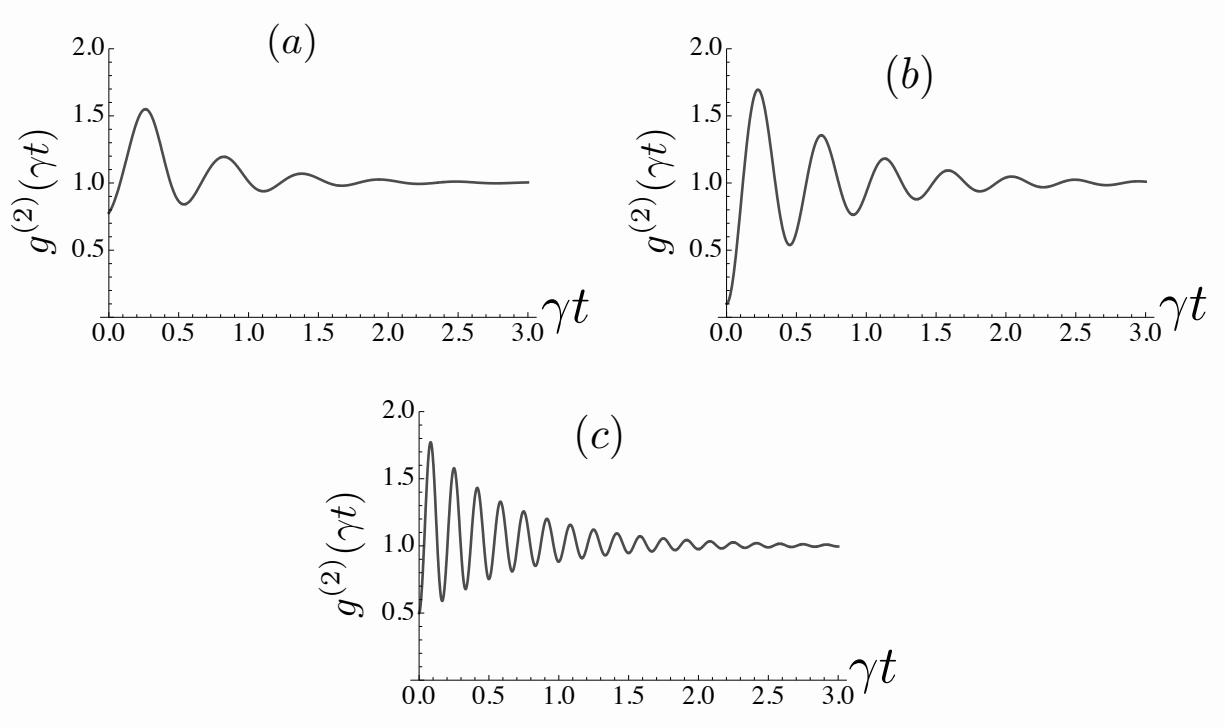

Figure 3.7: Second order correlation function $g^{(2)}(\tau)$. (a : $\Omega/\gamma = 5$, $\delta/\gamma = 5$; b : $\Omega/\gamma = 5$, $\delta/\gamma = 30$; c : $\Omega/\gamma = 15$, $\delta/\gamma = 30$).

dominates all dissipative effects in the atomic sample ($\gamma \approx \gamma_s$). Similar experimental parameters to those used in Figs. 3.3 and 3.4 have been considered.

For low dipole-dipole interaction (case a), an usual antibunching behavior of the scattered photons is observed [71]. For higher dipole-dipole interaction (case b), the antibunching of the scattered photons is much more marked as the value of the correlation function for $\tau = 0$ is much smaller with a much higher slope with respect to τ. The dipole blockade enhances the antibunching behavior. For higher laser intensities (case c), $g^{(2)}(\tau = 0)$ increases again and the dipole blockade effect is less marked and the period of the oscillations shortens.

For $\tau = 0$ and considering the time $t = 0$ when the system is in the steady state, we get

$$g^{(2)}(\mathbf{r}_1, 0; \mathbf{r}_2, 0) = \frac{4(16\Omega^4 + (4\Omega^2 + \gamma^2)|\alpha|^2)\cos^2((\phi_1 - \phi_2)/2)}{(8\Omega^2 + |\alpha|^2(1 + \cos\phi_1))(8\Omega^2 + |\alpha|^2(1 + \cos\phi_2))}, \tag{3.49}$$

with $\phi_i \equiv \phi(\mathbf{r}_i)$ $(i = 1, 2)$. Some particular detector positions are worth investigating. When $\phi_1 = \phi_2 = (2n + 1)\pi$ with n an integer, the photon-photon correlation function reads

$$g^{(2)}(\mathbf{r}_1, 0; \mathbf{r}_2, 0) = 1 + \frac{(4\Omega^2 + \gamma^2)|\alpha|^2}{16\Omega^4}, \tag{3.50}$$

which exhibits a simple quadratic dependence to the dipole blockade parameter δ.

The most interesting regime is reached when $\phi_1 = \phi_2 = (2n+1)\pi/2$. In this case,

$$g^{(2)}(\mathbf{r}_1, 0; \mathbf{r}_2, 0) = \left.\frac{P_{ee}}{P_e^2}\right|_S \tag{3.51}$$

and the photon-photon correlation function identifies to the ratio (3.35) between the steady state double excitation probability and the square of the single excitation probability. This ratio is a direct measure of the dipole blockade effect. The more it diverges from 1, the more intense the dipole-dipole interactions are. For those particular detector positions, the coincident photon-photon correlation signal monitors quantitatively the dipole blockade in the two-atom sample. This monitoring works continuously as long as the system is permanently driven in its steady state and scatters the laser light.

As a conclusion, we have provided a model able to analyze quantitatively the dipole blockade effect on the dynamical evolution of a two two-level atom system. We have shown that the dipole blockade is an efficient mechanism for production of significant long-term entanglement in the steady state of the system when it is continuously driven by a resonant laser field. This long-term entanglement non-existent in absence of dipole blockade is tunable with the laser intensity. We have proven that the effect of the dipole blockade can be lifted in strong driving conditions.

Finally we have shown that for particular detector positions, the photon-photon correlation function could continuously monitor the dipole-dipole interaction between the two atoms in a regime where the spontaneous emission would dominate all dissipative effects in the atomic sample. That would provide an efficient tool in the analysis of the occurrence of the dipole blockade.

The results from this chapter were published in Phys. Rev. A **81**, 013837 (2010).

Chapter 4

Dipole Blockade and Entanglement in Three-Atom Systems

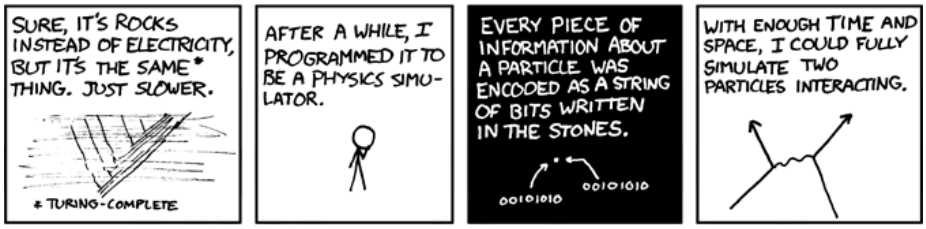

Randall Munroe, *A Bunch of Rocks* (part 5 of 9), `xkcd.com/505/`

In the previous chapter, we introduced a model used to yield quantitative results to the question of dipole blockade for a system composed of two two-level atoms. This dipole blockade effect is seen in systems in which the excitation of an atom prevents any further excitation in neighboring atoms by shifting their resonance, resulting in potential entanglement production and manipulation [57].

Multipartite Rydberg interaction has been studied in the literature for a few atoms [67, 74] or ultracold gazes [60–63]. In some conditions, the gazes showed sign of antiblockade [75, 76]. The possibility of creating multipartite entanglement [77] or its transport through chains of Rydberg atoms [78] was also studied recently.

Our goal in this chapter is to expand our bipartite model to a multipartite system three two-level atoms interacting with each other with the very same interaction potential and studying the system blockade and its entanglement with analytical values whenever possible. Our theoretical model in given in Sec. 4.1 in the regular, atomic basis as well as in a mixed symmetry basis and we define the measure of the different excited states we consider to investigate the blockade in such a system.

In Sec. 4.2, we briefly investigate the non-interactive case, where all atoms are independent. In Sec. 4.3 we consider a system of two atoms interacting and of a third, independent atoms. We measure the blockades and note that there is no difference with the two-atom case studied in the previous chapter. In Sec. 4.4, we introduce the first genuine three-atom

model in which all atoms interact with each other with the same amplitude. We give the analytical form of the steady state of such a system, as well as the limit case for an infinite interaction and we note that the production of entanglement through the presence of a W-type state is possible. We also investigate the three-atom and two-atom blockades. In Sec. 4.5, we introduce the second three-atom interaction setup, the case of aligned atoms interacting only with their neighbor. The solution of the steady state problem is given in appendix B and we measure the three-atom blockade as well as the two-atom blockades which behaves very differently depending on the pair of atoms investigated.

In Sec. 4.6, the two-atom concurrences of all the different setups are measured by tracing out one of the three atoms. We generally note that the entanglement between two atoms decreases in amplitude as a third atom is set to interact with them. In Sec. 4.7, we use our criterion of the tripartite concurrences defined in chapter 3 to investigate the entanglement in the present system. We find that bipartite entanglement is detected as well and we propose a few interpretation of other non-zero tripartite concurrences. Finally, we discuss the results and conclude in Sec. 4.8.

4.1 Theoretical Model

We consider three identical atoms at fixed positions $\mathbf{x}_i$ with internal levels $|e_i\rangle$, with $i = 1, 2, 3$. They are all driven by the same resonant external laser field with wave vector $\mathbf{k}_L$ and Rabi frequency 2Ω. When two atoms i, j are in their excited states, they interact through a van der Waals interaction dependent on the interatomic distance r_{ij}. Just as in the two-atom problem, the interaction is modelized by the Hamiltonian term $\delta_{ij}|e_ie_j\rangle\langle e_ie_j|$.

In the rotating-wave approximation, the coherent evolution of the system is described by the interaction Hamiltonian

$$\begin{aligned} H &= \sum_{j=1}^{3} \hbar\Omega \left(e^{i\mathbf{k}_L\cdot\mathbf{x}_j} S_j^+ + e^{-i\mathbf{k}_L\cdot\mathbf{x}_j} S_j^-\right) \\ &\quad +\hbar\delta_{12}|e_1e_2\rangle\langle e_1e_2| + \hbar\delta_{13}|e_1e_3\rangle\langle e_1e_3| + \hbar\delta_{23}|e_2e_3\rangle\langle e_2e_3|, \end{aligned} \tag{4.1}$$

where $S_i^+ = (S_i^-)^\dagger$ $(i = 1, 2, 3)$ is the atomic raising operator $|e_i\rangle\langle g_i|$. For simplicity, we will consider the wave vector $\mathbf{k}_L$ to be perpendicular to the plane (or the line) formed by the three atoms and the reference frame is properly chosen such that $\mathbf{k}_L \cdot \mathbf{x}_1 = \mathbf{k}_L \cdot \mathbf{x}_2 = \mathbf{k}_L \cdot \mathbf{x}_3 = 0$.

Depending on the position of the atoms, the terms δ_{ij} are allowed to take any value. If all atoms are away from each others, the interaction between them vanishes and we have $\delta_{12} = \delta_{13} = \delta_{23} = 0$ in which case the system can be described by the density matrix $\rho_s \otimes \rho_s \otimes \rho_s$ where ρ_s represents the state of one independent atom driven by a laser. If the third atom is far away from the two first ones, which is modelized by $\delta_{13} = \delta_{23} = 0$, the system can be described with the density matrix $\rho_t \otimes \rho_s$ where ρ_t represents a system with two atoms interacting through the δ_{12} term, which is a system described in the previous chapter.

Let us describe the system in the mixed symmetry basis

$$
\begin{aligned}
|g\rangle &= |ggg\rangle, && (4.2)\\
|W_1\rangle &= \frac{1}{\sqrt{3}}(|egg\rangle + |geg\rangle + |gge\rangle), && (4.3)\\
|W_2\rangle &= \frac{1}{\sqrt{3}}(|eeg\rangle + |ege\rangle + |gee\rangle), && (4.4)\\
|e\rangle &= |eee\rangle, && (4.5)\\
|\psi_1\rangle &= \frac{1}{\sqrt{6}}(|egg\rangle + |geg\rangle - 2|gge\rangle), && (4.6)\\
|\psi_2\rangle &= \frac{1}{\sqrt{6}}(2|eeg\rangle - |ege\rangle - |gee\rangle), && (4.7)\\
|\phi_1\rangle &= \frac{1}{\sqrt{2}}(|egg\rangle - |geg\rangle), && (4.8)\\
|\phi_2\rangle &= \frac{1}{\sqrt{2}}(|ege\rangle - |gee\rangle). && (4.9)
\end{aligned}
$$

The first four elements of that basis are completely symmetric under the exchange of any pair of atoms, $|\psi_1\rangle$ and $|\psi_2\rangle$ are symmetric under the exchange of the first two atoms only, $|\phi_1\rangle$ and $|\phi_2\rangle$ are antisymmetric under the exchange of the first two atoms and the third subsystem can be factored out; all other exchanges bear no particular symmetry.

In that basis, the Hamiltonian is written

$$
\begin{aligned}
H = {} & \hbar\delta_{123}|e\rangle\langle e| + \frac{\hbar\delta_{123}}{3}|W_2\rangle\langle W_2| + \frac{\hbar\delta_{123}+3\delta_{12}}{6}|\psi_2\rangle\langle\psi_2| + \frac{\hbar\delta_{13}+\delta_{23}}{2}|\phi_2\rangle\langle\phi_2| \\
& + \left(\frac{\hbar(\delta_{23}-\delta_{13})}{2\sqrt{3}}|W_2\rangle\langle\psi_2| + \frac{\hbar(\delta_{13}-\delta_{23})}{\sqrt{6}}|W_2\rangle\langle\phi_2| + \frac{\hbar(3\delta_{12}-\delta_{123})}{3\sqrt{2}}|\psi_2\rangle\langle\phi_2| + \text{h.c.}\right) \\
& + \left(\sqrt{3}\hbar\Omega(|e\rangle\langle W_2| + |W_1\rangle\langle g|) + 2\hbar\Omega|W_2\rangle\langle W_1| + \hbar\Omega(|\psi_2\rangle\langle\psi_1| + |\phi_2\rangle\langle\phi_1|) + \text{h.c.}\right), \quad (4.10)
\end{aligned}
$$

with $\delta_{123} \equiv \delta_{12} + \delta_{13} + \delta_{23}$. Let us discuss the energy levels and Hamiltonian terms, which are all represented in Fig. 4.2 for a better understanding of all the processes in the system. We first focus our attention on the states that are being blockaded, which are the states $|\phi\rangle$ with a $\hbar\delta|\phi\rangle\langle\phi|$ type term in the Hamiltonian. The maximally excited state $|e\rangle$ is strongly blockaded with an interaction strength equal to the sum of all three pair-interaction strengths δ_{ij}. The symmetrical, twice excited state $|W_2\rangle$ is also being blockaded with an interaction strength equal to the mean value of all three pair-interaction strengths δ_{ij}. We also find that the two non-symmetrical, twice excited states $|\psi_2\rangle$ and $|\phi_2\rangle$ are being blockaded with a different interaction strengths. The singly excited (and entangled) state $|W_1\rangle$ and the ground state $|g\rangle$ are not blockaded at all, a property that could be used to produce entanglement, just like entanglement was produced from mixing the separable $|gg\rangle$ and the entangled state $|s\rangle$ in the two-atom problem.

The interaction terms also have the effect of coupling all the twice excited states together, as the second line in H shows. For some particular geometrical symmetries of

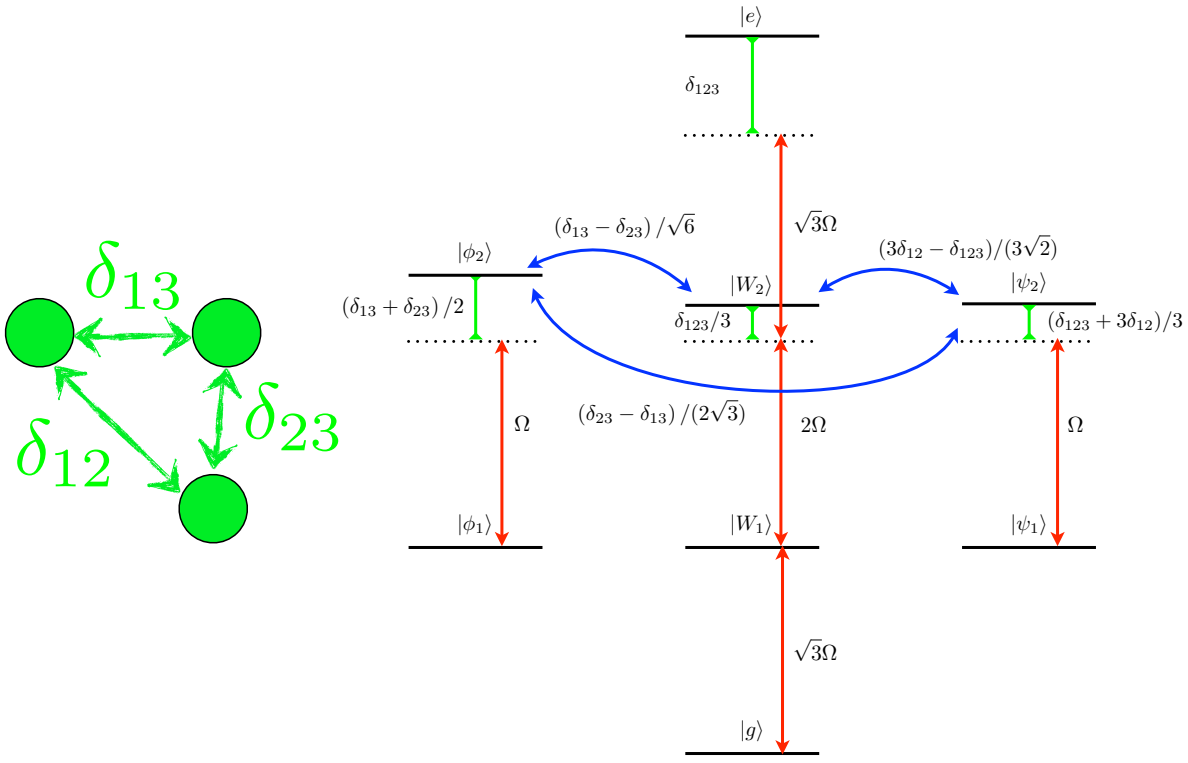

Figure 4.2: Representation and energy levels of the three-atom system in a general configuration. The dashed lines show the position the levels would have if there was no dipole-dipole interaction, instead here they are shifted with different amplitudes. The straight, red arrows indicates pairs of states that are coupled through the tuned laser. Note that the laser only couples states with the same kind of symmetry. The bent, blue arrows indicates the states coupled through the dipole interaction. All terms from the Hamiltonian (4.10) are represented.

the system, the coupling terms may vanish. For example, when all atoms are equidistant from each other we have $\delta_{13} = \delta_{23} = \delta_{12}$ and the all coupling terms disappear, leaving a completely symmetrical system. When the first two atoms are at the same distance from the third one we have $\delta_{13} = \delta_{23}$ and the $|\phi_2\rangle$ state is decoupled from the rest of the system, leaving a system symmetrical under the permutation of the first two atoms.

Let us now discuss the laser field coupling the different states. We note that the states with different symmetries are decoupled: the laser allows the successive transitions $|g\rangle \leftrightarrow |W_1\rangle \leftrightarrow |W_2\rangle \leftrightarrow |e\rangle$ but there is no transition to the unsymmetrical states, however the laser also couples the mixed symmetry states together, with the allowed transitions $|\psi_1\rangle \leftrightarrow |\psi_2\rangle$ and $|\phi_1\rangle \leftrightarrow |\phi_2\rangle$.

We see that the choice of the mixed symmetry basis is very well adapted to a completely symmetrical system, however it may complicate some interpretations for a lesser symmetry. In the case of permutational symmetry of only the first two atoms, it becomes more convenient to replace the basis vectors $|W_2\rangle$ and $|\psi_2\rangle$ by the vectors $|eeg\rangle$ and

$$|\psi^+\rangle \equiv \frac{1}{\sqrt{2}} \left(|ege\rangle + |gee\rangle\right). \tag{4.11}$$

When considering dissipation in the Markov and Born approximation [69], the time evolution of the system is governed by the master equation

$$\dot{\rho} = -i[H, \rho] - \gamma \sum_{i=1}^{3} (S_i^+ S_i^- \rho + \rho S_i^+ S_i^- - 2 S_i^- \rho S_i^+), \tag{4.12}$$

where $2\gamma = 2\gamma_s + 2\gamma_d$ is the total dissipation rate including the single atom spontaneous emission rates $2\gamma_s$ and the non-radiative dissipative effects rate $2\gamma_d$ in the experimental sample. Those dissipation processes insure that even the states completely decoupled from from the others by the Hamiltonian will be populated.

Just as in the two-atom problem, the intensity of the blockades will be studied on steady states with ratios of probabilities to find some excited states. In general, for a three-atom state ρ, we define the probabilities P_{e_i} to find the i-th atom in an excited states as

$$P_{e_i} = \langle e_i | \mathrm{Tr}_{j,k}(\rho) | e_i \rangle, \tag{4.13}$$

with $\mathrm{Tr}_{j,k}(\rho)$ the trace of ρ over the j-th and k-th subsystems (with i, j, k all different), leaving a single-atom density matrix. The probabilities $P_{e_i e_j}$ to find the i-th and j-th atoms simultaneously excited is

$$P_{e_i e_j} = \langle e_i e_j | \mathrm{Tr}_k(\rho) | e_i e_j \rangle, \tag{4.14}$$

with $\mathrm{Tr}_k(\rho)$ the trace of ρ over the k-th subsystem, leaving a two-atom density matrix. Finally, the probability P_e of finding all three atoms excited is simply

$$P_e = \langle e | \rho | e \rangle. \tag{4.15}$$

In this chapter, we will consider two different kinds of blockades, the three-atom blockade

$$\frac{P_e}{P_{e_1} P_{e_2} P_{e_3}}, \tag{4.16}$$

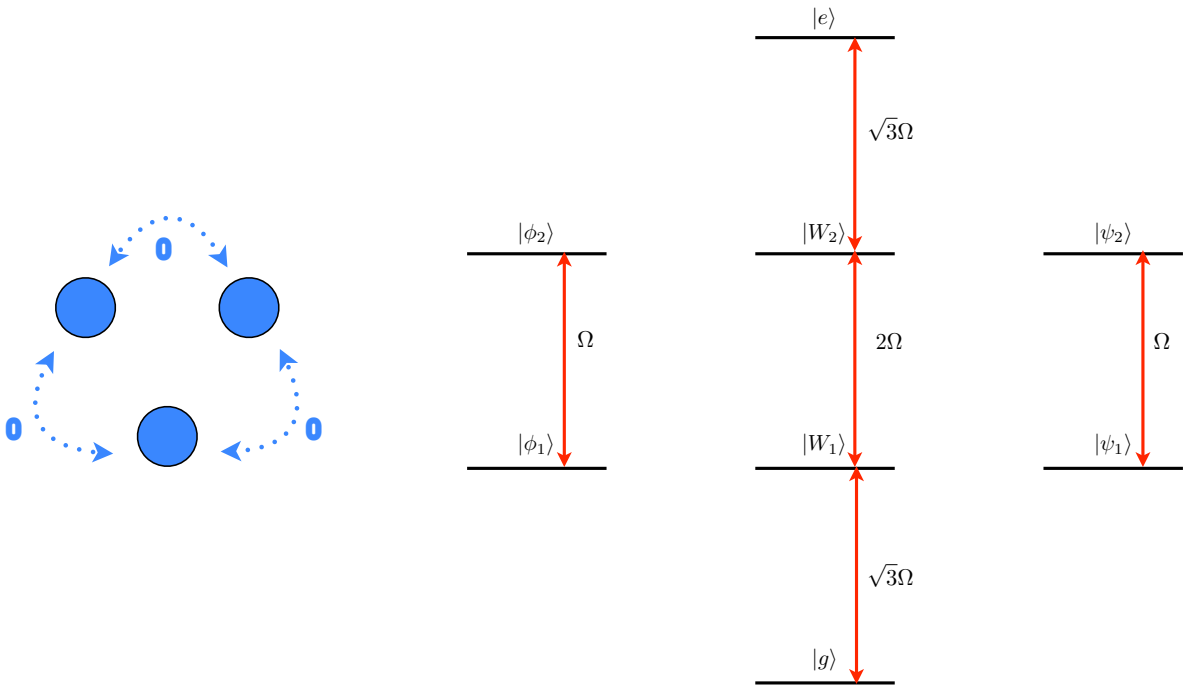

Figure 4.3: Representation and energy levels of the three-atom system when completely independent. There is no shift nor interaction between the atoms. The straight, red arrows indicates pairs of states that are coupled through the tuned laser. The states that are not completely symmetrical are decoupled from the symmetrical states by the laser.

and two-atom blockades

$$\frac{P_{e_i e_j}}{P_{e_i} P_{e_j}}, \tag{4.17}$$

which traces out the k-th subsystem and measure the blockade in the remaining two atoms. In general, there is three different two-atom blockades, there may be less when considering different symmetries.

In the following, we will study the behavior of the system in its steady state in different geometrical configurations. We start by the cases of no-interaction and two-atom interaction only and we continue with two genuine three-atom interaction configurations, the case of three equidistant atoms and of three aligned atoms. For each case, complete analytical solutions for the steady states were found.

4.2 Non-interactive Case

We first consider the case of three non-interacting atoms, obtained by posing $\delta_{12} = \delta_{13} = \delta_{23} = 0$. With that condition, the steady state equations may simply be solved by considering the one-atom problem. Following the same process as in section 3.2, we find

the form of the steady state with no interaction term ρ_0^S to be

$$\rho_0^S = \rho_s^S \otimes \rho_s^S \otimes \rho_s^S, \tag{4.18}$$

with the single-atom steady state

$$\rho_s^S = \frac{1}{4\Omega^2 + \gamma^2} \begin{pmatrix} \Omega^2 & -i\gamma\Omega \\ i\gamma\Omega & \gamma^2 + \Omega^2 \end{pmatrix}, \tag{4.19}$$

in the $\{|e\rangle, |g\rangle\}$ basis.

Once again, since there is no interaction, there can be no blockade process nor any entanglement in the system. We find that the probabilities to find the first, second and third atom in their excited state are

$$P_{e_j} = \frac{\Omega^2}{2\Omega^2 + \gamma^2}, \tag{4.20}$$

for $j = (1, 2, 3)$. The probability to find two atoms excited is merely

$$P_{e_i e_j} = P_{e_i} P_{e_j}, \tag{4.21}$$

for any $i \neq j$ in $(1, 2, 3)$. Finally, the probability to find the three atoms completely excited is

$$P_e = P_{e_1} P_{e_2} P_{e_3}. \tag{4.22}$$

It is apparent that there can be no blockade in the system, neither from considering a pair of atoms nor considering all three. Of course, there can be no entanglement in the system either since the atoms are independent.

When ρ_0^S is written in a matrix form expressed in the mixed symmetry basis, it can be seen that the 8×8 matrix ρ_0^S is composed of three diagonal blocks, one of size 4×4 corresponding to the four completely symmetric states of the basis and of two identical 2×2 blocks respectively corresponding to the $|\psi_j\rangle$ and $|\phi_j\rangle$ states. That particular form is actually dictated from the symmetry constraints in the system and is observed for every completely symmetric mixed state. For a lesser symmetry relative to the permutation of the first two particles, the density matrix is then composed of a 6×6 block matrix corresponding to the symmetric states of the basis with the $|\psi_i\rangle$ and a 2×2 block corresponding to the $|\phi_j\rangle$.

4.3 Two-Atom Interaction

Let us now consider a system of two interacting atoms and the addition of a third, non-interacting atom, which is obtained in the model by posing $\delta_{12} = \delta$ and $\delta_{13} = \delta_{23} = 0$. Since the third atom is independent, the steady state ρ_{12-3}^S of the system is easily found to be

$$\rho_{12-3}^S = \rho_t^S \otimes \rho_s^S, \tag{4.23}$$

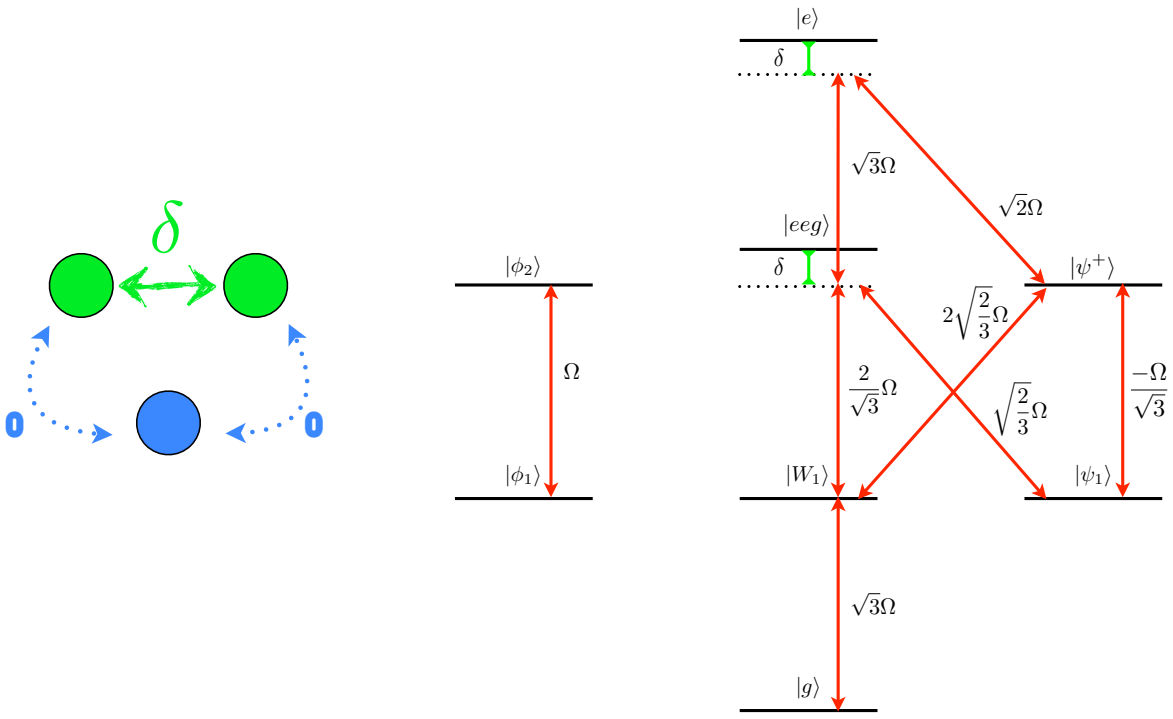

Figure 4.4: Representation and energy levels of the three-atom system when only two are interacting. Only the two energy states involving the excitation of the interacting atoms are shifted by δ. The straight, red arrows indicates pairs of states that are coupled through the tuned laser, their higher number being due to the lesser symmetry of the system.

with ρ_s^S the single-atom steady state (4.19) and ρ_t^S the two-atom steady state already studied and defined in Eq. (3.31).

We represented the energy levels of the system in Fig. 4.4. In that figure, we chose to represent the system in the modified mixed basis in order to eliminate any coupling existing between states of the same level and at the same time single out the $|eeg\rangle$ state, which is the only twice excited state being blockaded. The action of the laser is more complicated to describe in that basis, but allows an easier interpretation of the behavior of the system.

For that situation, considering results from previous chapter 3, we calculate the probabilities of single excitations

$$P_{e_1} = P_{e_2} = \frac{\Omega^2(8\Omega^2 + |\alpha_t|^2)}{16\Omega^2 + (4\Omega^2 + \gamma^2)|\alpha_t|^2}, \tag{4.24}$$

$$P_{e_3} = \frac{\Omega^2}{2\Omega^2 + \gamma^2}, \tag{4.25}$$

with $|\alpha_t|^2 = \delta^2 + 4\gamma^2$. The probabilities for two excitations are

$$P_{e_1e_2} = \frac{\Omega^4}{16\Omega^2 + (4\Omega^2 + \gamma^2)|\alpha_t|^2}, \tag{4.26}$$

$$P_{e_1e_3} = P_{e_1}P_{e_3}, \tag{4.27}$$

$$P_{e_2e_3} = P_{e_2}P_{e_3}, \tag{4.28}$$

and finally the probability to find the system completely excited is

$$P_e = P_{e_1e_2}P_{e_3}. \tag{4.29}$$

We see from those values that the $|e_1e_2\rangle$ state is blockaded as we already know, but the states $|e_1e_3\rangle$ and $|e_2e_3\rangle$ are not at all, since we have

$$\frac{P_{e_1e_3}}{P_{e_1}P_{e_3}} = 1, \tag{4.30}$$

and similarly for $P_{e_1e_2}$.

The completely excited state $|e\rangle$ is indeed blockaded, the amplitude of the blockade is the same as the one between the first two atoms since we have

$$\frac{P_e}{P_{e_1}P_{e_2}P_{e_3}} = \frac{P_{e_1e_2}}{P_{e_1}P_{e_2}}, \tag{4.31}$$

and we conclude that, as we could expect, there is no change at all in the behavior of the system derived from the addition of a third, non-interacting atom. We show in Fig. 4.5 the behavior of both the two and three-atom blockade for different interaction values in function of Ω/γ. All conclusion that were drawn in the previous chapter also fully apply to this case.

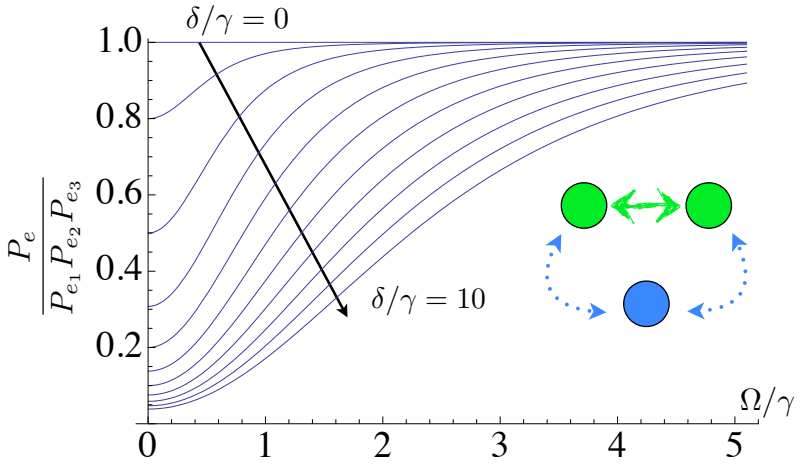

Figure 4.5: Plots of $P_e/P_{e_1}P_{e_2}P_{e_3}$ and $P_{e_1e_2}/P_{e_1}P_{e_2}$ applied to the ρ^S_{12-3} state for increasing values of δ/γ from 0 to 10 in function of Ω/γ. The system is not modified by the adjunction of a third, non-interacting atom.

4.4 Equidistant Atoms

The first genuine three-atom interaction we consider is the case of all atoms being equidistant from each other, which is achieved when they form an equilateral triangle. In that case, we have $\delta_{12} = \delta_{13} = \delta_{23} = \delta$. The energy levels of that system are represented in Fig. 4.6 in the mixed symmetry basis. Thanks to the complete symmetry of equidistant atoms, the representation is very clean and easy to interpret. The first excited state is $|W_1\rangle$ and is not shifted in any way, unlike $|W_2\rangle$ and $|e\rangle$ which are being blockaded. The other two pairs of states $|\psi_i\rangle$ and $|\phi_i\rangle$ are only populated through the dissipation processes and never by the laser directly, and each of their twice excited state is blockaded as well.

Since that system is completely symmetrical, we may use the mixed symmetry basis to express the analytical form of the steady state ρ^S_e, where e stands for *equilateral*. We find

$$\begin{aligned}\rho^S_e &= \frac{1}{\mathcal{N}}\left[|\varphi_1\rangle\langle\varphi_1| + \Omega^2|\varphi_2\rangle\langle\varphi_2| + 4\Omega^4(|\varphi_3\rangle\langle\varphi_3| + |\varphi_4\rangle\langle\varphi_4| + |\varphi_5\rangle\langle\varphi_5|)\right. \\ &\quad \left. + 4\Omega^6(|\psi_1\rangle\langle\psi_1| + |\phi_1\rangle\langle\phi_1| + |g\rangle\langle g|)\right], \end{aligned} \tag{4.32}$$

with $\alpha = \gamma + i\delta$,

$$\mathcal{N} = 32\Omega^6 + 48\Omega^4|\alpha|^2 + \left(\gamma^2 + 6\Omega^2\right)|\alpha|^2\left(3\gamma^2 + |\alpha|^2\right), \tag{4.33}$$

and with the unnormalized states

$$|\varphi_1\rangle = 2\Omega^3|e\rangle + 2i\sqrt{3}\Omega\alpha|W_2\rangle - \alpha(\alpha+\gamma)(\sqrt{3}\Omega|W_1\rangle + i\gamma|g\rangle) \tag{4.34}$$

$$|\varphi_2\rangle = 2\Omega^2|W_2\rangle + 4i\Omega\alpha|W_1\rangle - \sqrt{3}\alpha(\alpha+\gamma)|g\rangle \tag{4.35}$$

$$|\varphi_3\rangle = \Omega|W_1\rangle + i\sqrt{3}\alpha|g\rangle \tag{4.36}$$

$$|\varphi_4\rangle = \Omega|\psi_2\rangle + i\alpha|\psi_1\rangle \tag{4.37}$$

$$|\varphi_5\rangle = \Omega|\phi_2\rangle + i\alpha|\phi_1\rangle. \tag{4.38}$$

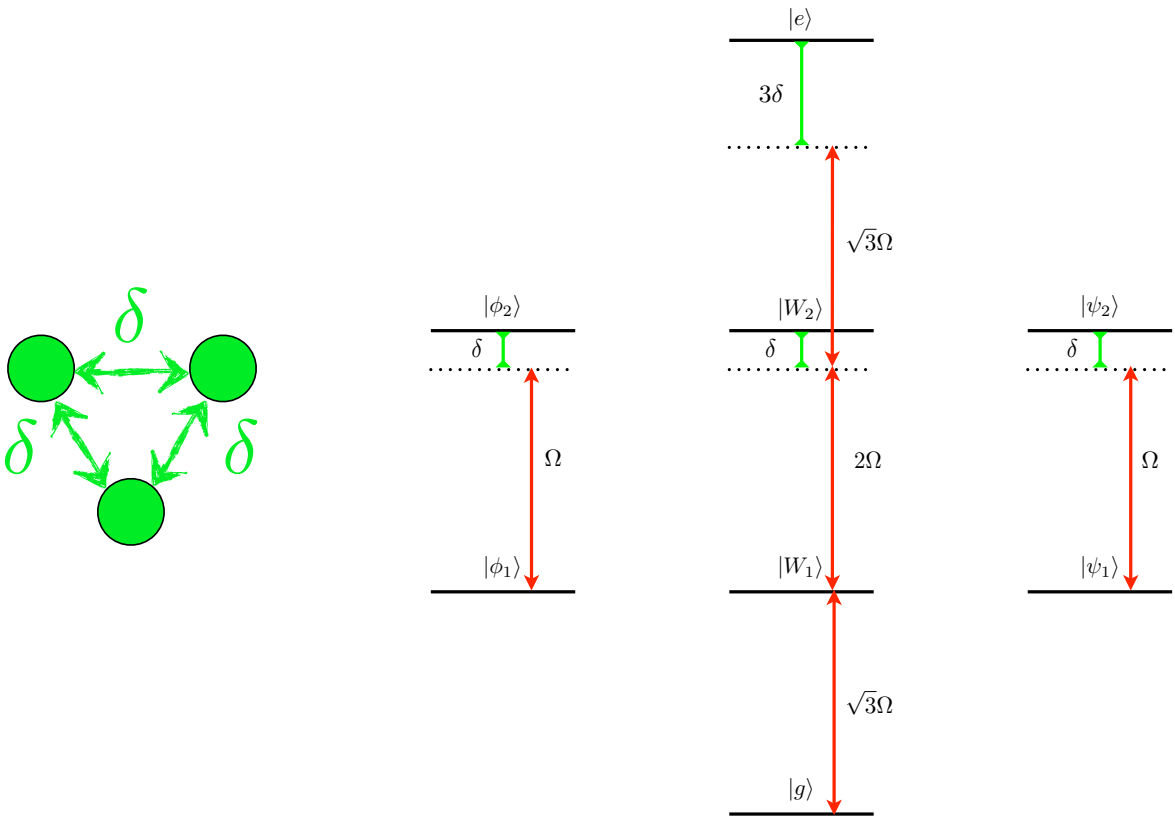

Figure 4.6: Representation and energy levels of the three-atom system when equidistant from each other. The energy levels of the states involving two excited atoms are shifted by δ and the one involving all three exited atoms by 3δ. The straight, red arrows indicates pairs of states that are coupled through the tuned laser. The system is completely symmetric under the exchange of any pair of atoms. All coupling between the states involving two excited atoms are gone.

Let us consider the steady state in the limit case where the interaction term becomes much larger than the Rabi frequency and the dissipation term. In those conditions, it becomes impossible to populate the states $|W_2\rangle$ and $|e\rangle$ and the only two states remaining in tune with the laser are the ground state $|g\rangle$ and the completely symmetric state $|W_1\rangle$. Indeed, taking the limit, we see that

$$\lim_{\delta\to\infty}\rho_e^S = \frac{3\Omega^2+\gamma^2}{6\Omega^2+\gamma^2}\,|\phi\rangle\langle\phi| + \frac{3\Omega^2}{6\Omega^2+\gamma^2}\,|g\rangle\langle g|, \tag{4.39}$$

with

$$|\phi\rangle \equiv \frac{1}{\sqrt{3\Omega^2+\gamma^2}}\left(\sqrt{3}\Omega|W_1\rangle + i\gamma|g\rangle\right), \tag{4.40}$$

which approaches $|W_1\rangle$ when γ is negligible. Therefore we see that in the limit $\delta \gg \Omega, \gamma$, the steady state is an equal mixture between the ground state and $|W_1\rangle$, therefore we conclude that a reasonable amount of entanglement can be obtained in that system, which will be studied later in this chapter.

For that equidistant atoms, the probability of observing an excited atom reads

$$P_{e_j} = \frac{\Omega^2}{\mathcal{N}}\left(16\Omega^4 + 16\Omega^2|\alpha|^2 + (3\gamma^2+|\alpha|^2)|\alpha|^2\right), \tag{4.41}$$

for $j = (1,2,3)$. The probability to find two atoms excited is

$$P_{e_ie_j} = \frac{4\Omega^4}{\mathcal{N}}\left(2\Omega^2+|\alpha|^2\right), \tag{4.42}$$

for any $i \neq j$ in $(1,2,3)$. Finally, the probability to find the three atoms completely excited is

$$P_e = \frac{4\Omega^6}{\mathcal{N}}. \tag{4.43}$$

From those analytical expressions, we can probe the strength of the dipole blockade in the system by computing the values of $P_e/P_{e_1}^3$ to see how much the totally excited state $|e\rangle$ is blocked, or the values of $P_{e_1e_2}/P_{e_1}^2$ for the two-atom blockade of any pair of atoms. In Fig. 4.7 and 4.8, we plotted the quantities in function of Ω/γ for different values of δ/γ. We can see that the three-atom blockade acting on the $|e\rangle$ state is quite strong even for low values of δ/γ, which might be expected since $|e\rangle$ is set off resonance by a quantity of $\delta_{123} = 3\delta$, as shown in the Hamiltonian (4.10), which means even a weak interaction between the atoms may still provide a sizable population of the entangled states $|W_1\rangle$ and $|W_2\rangle$.

The blockade acting on any pair of atoms with the third is traced out remains largely similar to a system of two isolated interacting atoms, which indicates that the addition of a third equidistant atom in the system does not help the two-atom blockade phenomenon. The study of our three-qubit concurrences of the system is done later in the text and will confirm that there is no gain in bipartite entanglement from the addition of a third atom.

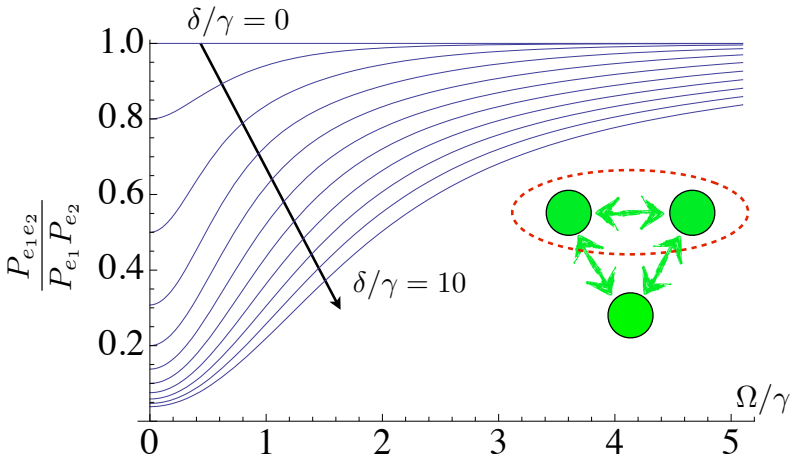

Figure 4.7: Plots of $P_{e_1e_2}/P_{e_1}P_{e_2}$ applied to the ρ_e^S state for the completely symmetric case for increasing values of δ/γ from 0 to 10 in function of Ω/γ.

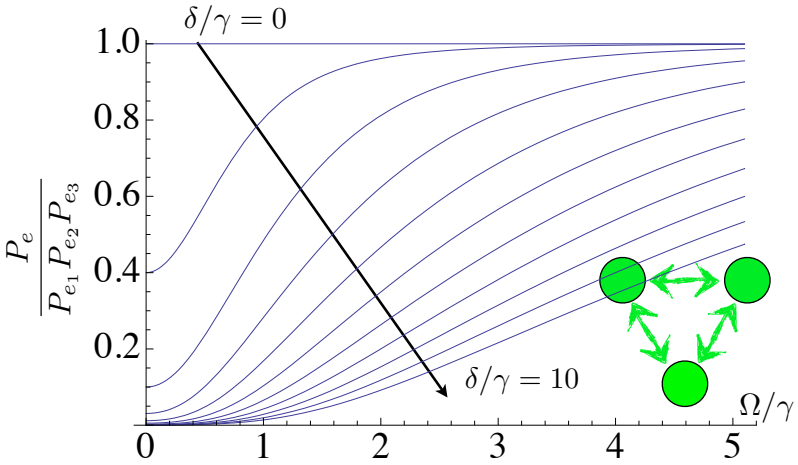

Figure 4.8: Plots of $P_e/P_{e_1}P_{e_2}P_{e_3}$ applied to the ρ_e^S state for increasing values of δ/γ from 0 to 10 in function of Ω/γ.

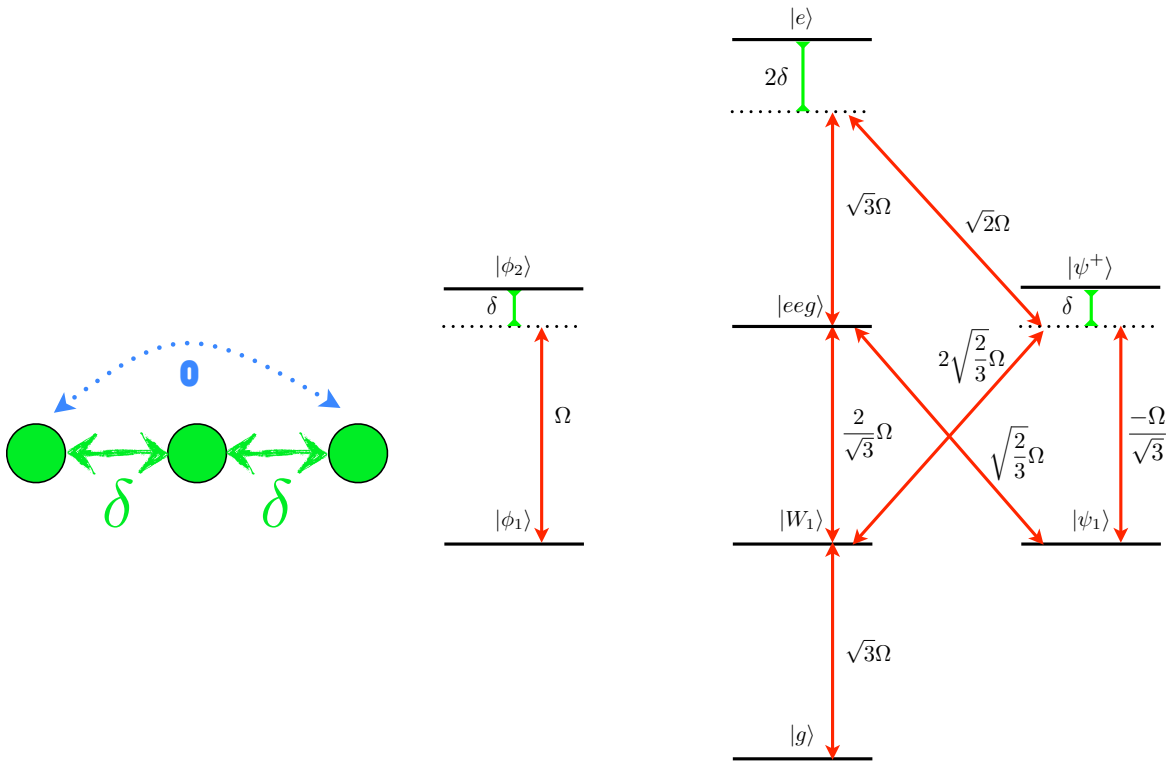

Figure 4.9: Representation and energy levels of the three atoms when aligned. The extremity atoms, numbered first and second, are assumed not to interact. The $|eeg\rangle$ energy level is untouched while the others involving any other pair of excited atoms are shifted by δ and and the one involving all three exited atoms by 2δ. The straight, red arrows indicates pairs of states that are coupled through the tuned laser, their higher number being due to the lesser symmetry of the system.

4.5 Aligned Atoms

The last case of genuine three-atom interaction we consider is the alignment of the three atoms at equal distance. We label the atom in the middle as the third one, so that we can consider permutational symmetry of the first two subsystems. We modelize the fact that the first two atoms are at an equal distance from the third with $\delta_{13} = \delta_{23} = \delta$. We also consider that the interaction between the atoms at the extremities is inexistent, i. e. $\delta_{12} = 0$. This approximation is justified if we consider that the interaction potential is of the van der Waals type, which usually goes as $1/r^6$ [74], meaning that for equidistant atoms, δ_{12} is 64 times smaller than δ and we choose to neglect it for the sake of finding an analytical value for the steady state. The energy levels of the system are represented in Fig. 4.9 in the modified mixed symmetry basis, where $|eeg\rangle$ and $|\psi^+\rangle$ replaced $|W_2\rangle$ and $|\psi_2\rangle$.

Since the system is still symmetrical under the exchange of the first two atoms, the form of the density matrix of the steady state ρ_a^S, where a stands for *aligned*, expressed in the mixed symmetry basis is composed of a 6×6 and a 2×2 diagonal blocks. The analytical expression of ρ_a^S was found but because of the complexity of the full expression, involving ratios between two polynoms of the 32^{nd} degree in Ω, δ and γ, we do not present it here but rather in Appendix B.

When considering the limit for a large interaction δ, the three states $|e\rangle, |\psi^+\rangle$ and $|\phi_2\rangle$ become completely unpopulated, but the excited state $|eeg\rangle$ is unblocked and still populated since $\delta_{12} = 0$. The steady state therefore does not take a simple form as it did in 4.39 and we do not show it here.

To investigate the blockade properties, thanks to the symmetry we are able to find the following simplifications

$$P_{e_1} = P_{e_2} \neq P_{e_3}, \tag{4.44}$$

as well as

$$P_{e_1e_2} \neq P_{e_1e_3} = P_{e_2e_3}. \tag{4.45}$$

Those relations shows that there are two quantities of interest when investigating the two-atom dipole blockade, the ratio $P_{e_1e_3}/P_{e_1}P_{e_3}$ for the first and third atoms, the blockade for the second and third atoms being identical, and the ratio $P_{e_1e_2}/P_{e_1}P_{e_2}$ for the non-interacting first and second atoms. The three-atom blockade P_e should also be investigated but no *a priori* knowledge about it can be found.

In Fig. 4.10, we show the three-atom blockade. The system behaves in a similar fashion than the case of three interacting atoms represented in Fig. 4.8, however the strength of the blockade is smaller for similar δ and Ω, coming from the fact that the $|e\rangle$ state in only in this case shifted from its usual energy level by $\delta_{123} = 2\delta$.

In Fig. 4.11, we show the blockade when considering only two neighboring atoms. This time for equal δ at small Ω, the values of the blockade are very close to the other two considered cases shown in Fig. 4.5 and Fig. 4.7, however it seems that compared to the other cases the blockade remains stronger as laser power increases.

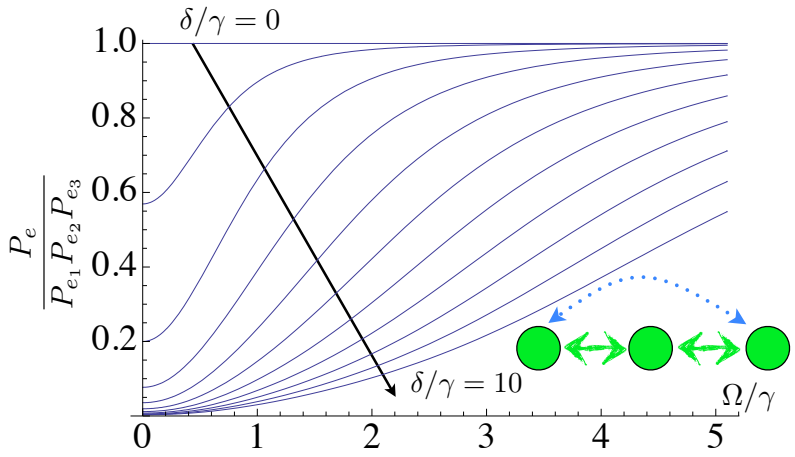

Figure 4.10: Plots of $P_e/P_{e_1}P_{e_2}P_{e_3}$ applied to the ρ_a^S state for increasing values of δ/γ from 0 to 10 in function of Ω/γ.

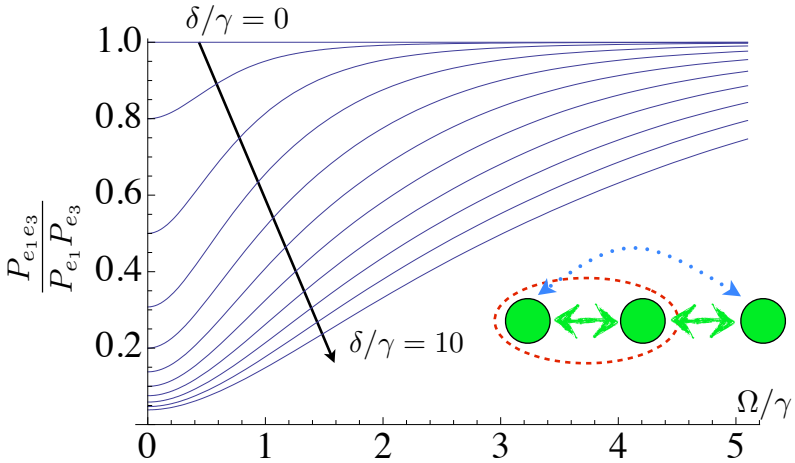

Figure 4.11: Plots of $P_{e_1e_3}/P_{e_1}P_{e_3}$ applied to the ρ_a^S state for increasing values of δ/γ from 0 to 10 in function of Ω/γ.

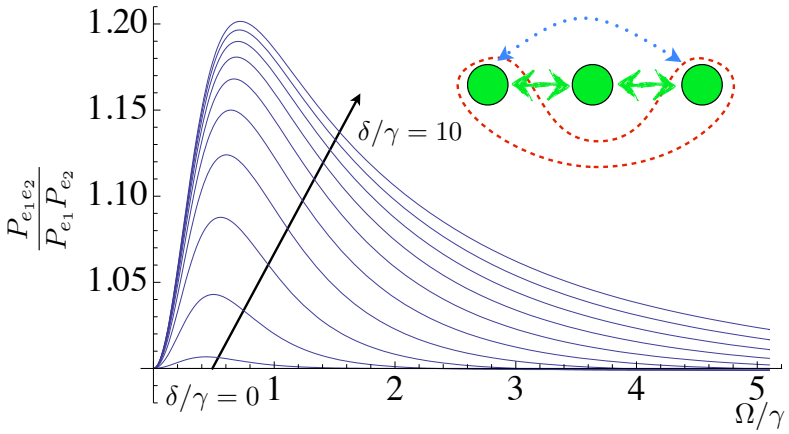

Figure 4.12: Plots of $P_{e_1e_2}/P_{e_1}P_{e_2}$ applied to the ρ_a^S state for increasing values of δ/γ from 0 to 10 in function of Ω/γ. Instead of being blockaded, the $|eeg\rangle$ state is being enhanced.

Finally, in 4.12, we show the two-atom blockade $P_{e_1e_2}/P_{e_1}P_{e_2}$ and we observe that instead of a blockade behavior, we observe that the $|eeg\rangle$ state is actually enhanced, i. e. finding the first two atoms simultaneously excited is more probable than to finding them independently excited. This non-classical behavior can be understood by noting that $|eeg\rangle$ is still on resonance with the laser, unlike $|ege\rangle$ and $|gee\rangle$ which are being shifted out by a quantity δ, however the laser still populates the three singly excited states $|e_i\rangle$ normally, including $|e_3\rangle$, which means that $|e_3\rangle$ "steals" the population that $|e_1\rangle$ and $|e_2\rangle$ would need to equalize $P_{e_1e_2}$ and $P_{e_1}P_{e_2}$. For larger values of Ω, we find that the system becomes very slightly blockaded again but only to asymptotically reach a non-blockade status.

4.6 Two-Atom Concurrence

In this section, we study the entanglement existing between two atoms only, by tracing out the third atom from the system and plotting the values of the concurrence of the remaining atoms.

The first case that was considered in this chapter was the non-interactive case, which obviously may contain no entanglement since the density matrix ρ_0^S is written as a separable state, for either the traced out or the complete system.

The next case is the two-atom interaction density matrix ρ_{12-3}^S, which does contain entanglement. If the third atom is traced out, then we find a system identical to the one previously studied and we have a concurrence of

$$C(\mathrm{Tr}_3\rho_{12-3}^S) = C(\rho_t^S) = \mathrm{Max}\left\{0, \frac{\sqrt{2}\Omega^2(\lambda_+ - \lambda_-) - 8\Omega^4}{16\Omega^4 + (4\Omega^2+\gamma^2)|\alpha_t|^2}\right\}, \tag{4.46}$$

with $\alpha_t = -(\delta + 2i\gamma)$ and

$$\lambda_\pm = \sqrt{8\Omega^4 + \delta^2|\alpha_t|^2 \pm \delta|\alpha_t|\sqrt{16\Omega^4 + \delta^2|\alpha_t|^2}}. \tag{4.47}$$

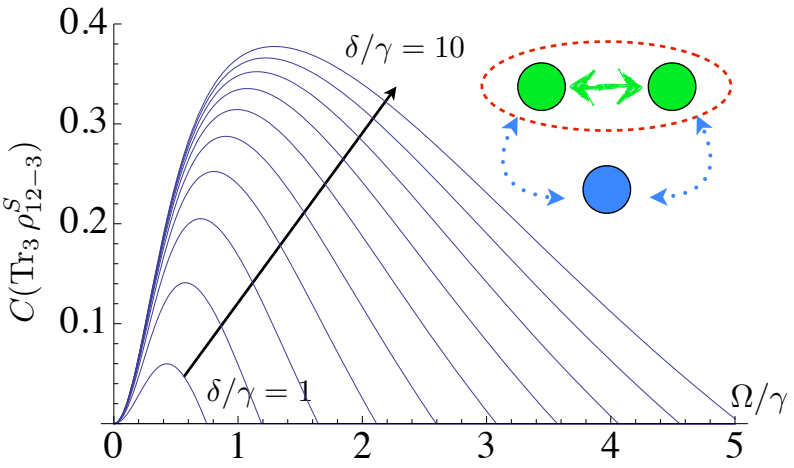

Figure 4.13: Plots of the bipartite concurrence of $\mathrm{Tr}_3\rho^S_{12-3}$.

In Fig. 4.13, we see the plot of the concurrence. Like in the bipartite case, there is entanglement as long as $0 < 4\Omega^2 < \delta|\alpha_t|$ and the biggest possible entanglement value happens when $\delta \gg \Omega \gg \gamma$ and is 1/2. The concurrence of ρ^S_{12-3} when the first or the second atom is traced out of the system is zero, as the third atom shares no interaction with the rest of the system and the process of tracing it out does not create one.

Let us now consider the case of the three equidistant atoms described by the matrix ρ^S_e. The trace can be chosen to act on any three atoms. We first examine the limit where the interaction is much greater than the laser power or the dissipation in the system. We find

$$\lim_{\delta\to\infty} \mathrm{Tr}_3\left(\rho^S_e\right) = \frac{2\Omega^2+\gamma^2}{6\Omega^2+\gamma^2}\,|\phi\rangle\langle\phi| + \frac{4\Omega^2}{6\Omega^2+\gamma^2}\,|g_1g_2\rangle\langle g_1g_2|, \tag{4.48}$$

with

$$|\phi\rangle \equiv \frac{1}{\sqrt{2\Omega^2+\gamma^2}}\left(\sqrt{2}\Omega|\psi^+_{12}\rangle + i\gamma|g_1g_2\rangle\right), \tag{4.49}$$

and

$$|\psi^+_{12}\rangle \equiv \frac{1}{\sqrt{2}}\left(|e_1g_2\rangle + |g_1e_2\rangle\right). \tag{4.50}$$

In the limit $\gamma \ll \Omega$, we see that the system becomes a mixture of the entangled state $|\psi^+_{12}\rangle$ with a 1/3 proportion and of the ground state $|g_1g_2\rangle$ with a 2/3 proportion. Therefore, the maximum value the concurrence can take is 1/3. We see that adding a third interacting atoms to a bipartite system actually decreases the amount of bipartite entanglement in the system. In Fig. 4.14, we plotted the bipartite concurrence of ρ^S_e and we see that even though the behavior of the concurrence is similar, its amplitude is generally smaller than in the bipartite case.

Finally, we consider the case of the aligned atom described by the matrix ρ^S_a. There are two ways to obtain a bipartite system by tracing one out, either by tracing out an extremity atom or the middle one. It turns out that when the third atom is traced out,

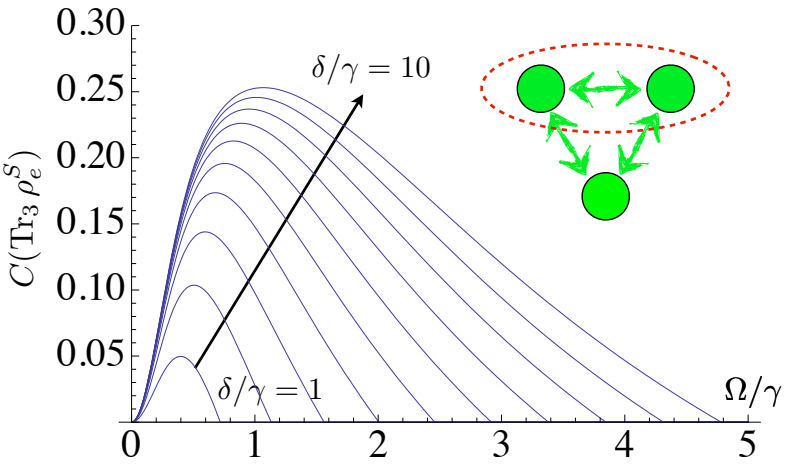

Figure 4.14: Plots of the bipartite concurrence of $\mathrm{Tr}_3\rho_e^S$.

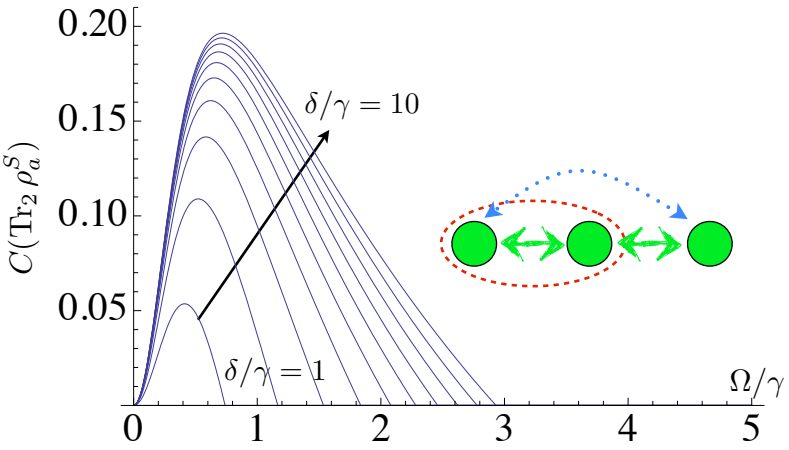

Figure 4.15: Plots of the bipartite concurrence of $\mathrm{Tr}_2\rho_a^S$.

the concurrence of the system is always zero, even though we observed an enhancement of the state $|eeg\rangle$. We see that even though both the first and second atoms are entangled with the third one, they remain unentangled with each other.

In Fig. 4.15, we show the concurrence of ρ_a^S when the second atom is traced out. The behavior of the concurrence is still similar to the other observed cases, but the amount of entanglement is yet smaller. We see that even though the strength of interaction between to atoms is unchanged when a third atoms is set to interact with either one or both of them, the amount of entanglement is significantly decreased, as if the entanglement has to be "shared" among all the subsystems.

4.7 Three-Atom Concurrences

This last section studies the tripartite entanglement of the system in different configurations. Since there is no well-established measure of entanglement for tripartite mixed states, we will put our tripartite concurrences introduced in chapter 2 to the test. Let us briefly replace our criterion in its context. We defined nine basis concurrences[1] or three in the particular case of symmetric states, which can each take values from 0 to 1. Separable states will always have a zero concurrence and if any non-zero concurrence is found, the state is entangled. A state with a concurrence 1 will be said maximally entangled with respect to the particular concurrence measured. However a zero concurrence does not mean that the state is entangled.

The concurrence relative to the matrix S_α, with $\alpha = 1, \cdots, 9$ is given by

$$C_\alpha(\rho) = \mathrm{Max}[0, \lambda_1^{S_\alpha} - \sum_{k=2}^{8} \lambda_k^{S_\alpha}], \tag{4.51}$$

with the $\lambda_k^{S_\alpha}$ the ordered square roots of the 8 eigenvalues of $\rho S_\alpha \rho^* S_\alpha$. The list of matrices S_α is given in Sec. 2.2.2. We gave in Sec. 2.3.2 the example of a pure state with its two first atoms maximally entangled and a separable third atom given by

$$|\psi\rangle = \frac{1}{\sqrt{2}}(|00\rangle + |11\rangle) \otimes (\alpha|0\rangle + \beta|1\rangle), \tag{4.52}$$

with $|\alpha|^2 + |\beta|^2 = 1$. We showed that all concurrences were found to be zero except for $C_5 = |\alpha|^2, C_6 = |\beta|^2$ and $C_9 = 2|\alpha\beta|$. Depending on the values α and β those concurrences might be zero, but we find that in this particular case $C_5^2 + C_6^2 + C_9^2/2 = 1$ and all in all we conclude that C_5, C_6 and C_9 detect entanglement in the first two subsystems. With the same reasoning, we see that C_1, C_2 and C_7 detect entanglement in the second and third subsystems and C_3, C_4 and C_8 detect entanglement in the first and third subsystems.

Talking about symmetric states only, we see that the concurrence C_1^s detects entanglement of GHZ-type states, like the states $\alpha|e\rangle + \beta|g\rangle$ or $\alpha|W_1\rangle + \beta|W_2\rangle$, while C_2^s and C_3^s detect entanglement of W-type states like respectively $|W_2\rangle$ and $|W_1\rangle$ (we identified the computational states $|0\rangle$ and $|1\rangle$ of chapter 2 with the respective states $|e\rangle$ and $|g\rangle$).

Let us now consider the measurement of the concurrences in our physical system of three atoms, starting with the symmetrical setup of the equidistant atoms in the steady state ρ_e^S. With this setup, the presence of tripartite entanglement is strongly expected. To measure it, we use concurrence associated with the three matrices (2.95) to (2.97). If we first consider the expression of the steady state in the $\delta \to \infty$ limit defined in Eq. (4.39), we find that the only non-zero concurrence is

$$C_3^s(\lim_{\delta\to\infty} \rho_e^S) = \frac{2\Omega^2}{6\Omega^2 + \gamma^2}, \tag{4.53}$$

[1] More than nine if linear combinations are considered, which is not the case in this chapter.

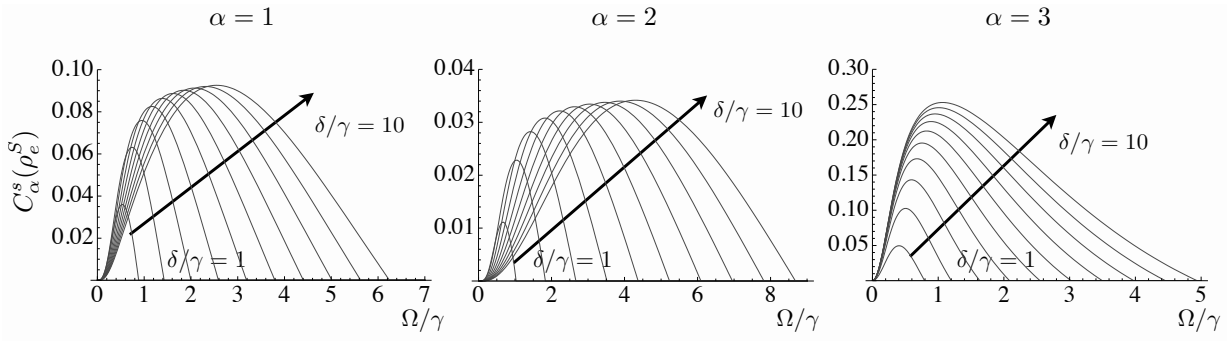

Figure 4.16: Plots of non-zero tripartite concurrences of ρ_e^S, corresponding to the symmetric S_1^s, S_2^s and S_7^s. Please note that the scales of the plots are different. The highest value of concurrence is C_3^s which is the concurrence in which the $|W_1\rangle$ state participates in.

which tends to 1/3 when $\Omega \gg \gamma$. This result could have been expected since we showed in Eq. (4.39) that the mixed state was an equal mixture of $|W_1\rangle$ of concurrence $C_3^s = 1/3$ and $|g\rangle$ of concurrence zero.

In Fig. 4.16 we plotted the value of the three symmetrical concurrences C_α^s of the system for different values of the interaction in function of the laser power. Notice that we adjusted the scales of each plot to capture the zone of interest. Not surprisingly, the highest values of concurrence are found in C_3^s, which is due to the presence of $|W_1\rangle$. The state $|W_2\rangle$ is typically detected by the concurrence C_2^s but because of the blockade, its population is quite low and the concurrence negligible. The presence of C_1^s is due to the mixture between $|W_1\rangle$ and $|W_2\rangle$, which produces an intermediate amount of entanglement.

We note on the first two plots that the behavior of the curves is a bit different from the third one and in general all other bipartite concurrence we ran into. For small, fixed values of Ω/γ, the concurrence weakens when the interaction parameter grows. This can be explained by the fact than when the interaction grows, one source of entanglement which is $|W_2\rangle$ is being depleted as the state becomes more and more blockaded for a fixed laser power. Wee see that once again, the amount of entanglement is laser tunable since there is an optimal value of the laser power which maximizes the entanglement for a given interaction strength.

Let us now inquire the case of the two-atom interaction in the steady state ρ_{12-3}^S. We insisted on the fact that for a bipartite entangled state with a third, separable subsystem, the only non-zero concurrences in the basic first 9 concurrences could be C_5, C_6 and C_9. The very same behavior is numerically observed for ρ_{12-3}^S, which can be verified in Fig. 4.17. The concurrences C_5 and C_6 detect the entanglement of the entangled bipartite system associated with respectively $|e_3\rangle$ and $|g_3\rangle$, which explains the difference in amplitude since a single atom in a steady state will always have more population in its ground state due to the dissipation effects. The concurrences C_9 detects the entanglement with an amplitude linked to both $|e_3\rangle$ and $|g_3\rangle$ populations.

The last setup we investigate is the aligned atoms with the steady state ρ_a^S. We already

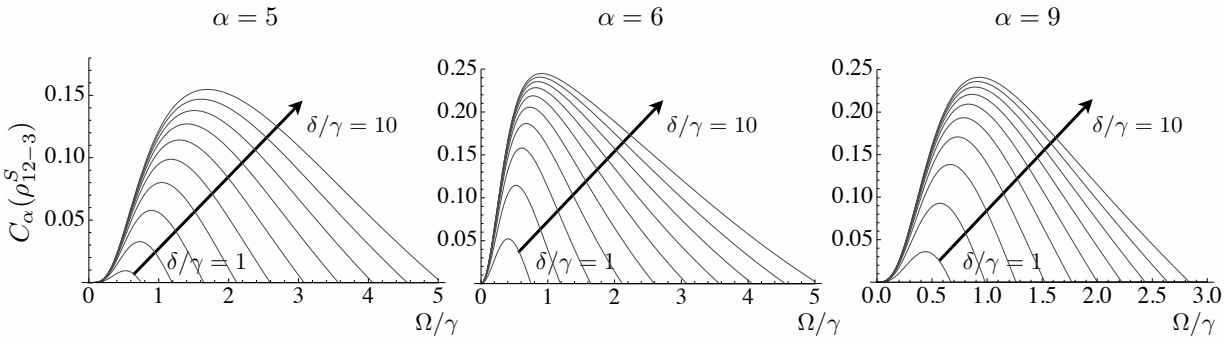

Figure 4.17: Plots of non-zero tripartite concurrences of ρ^S_{12-3}, corresponding to S_5, S_6 and S_9 with different scales. Those concurrences are typically used to find entanglement between the first two subsystems. All other concurrences not using a combination of S_5, S_6 and S_9 were found to be null, as expected since the system is biseparable.

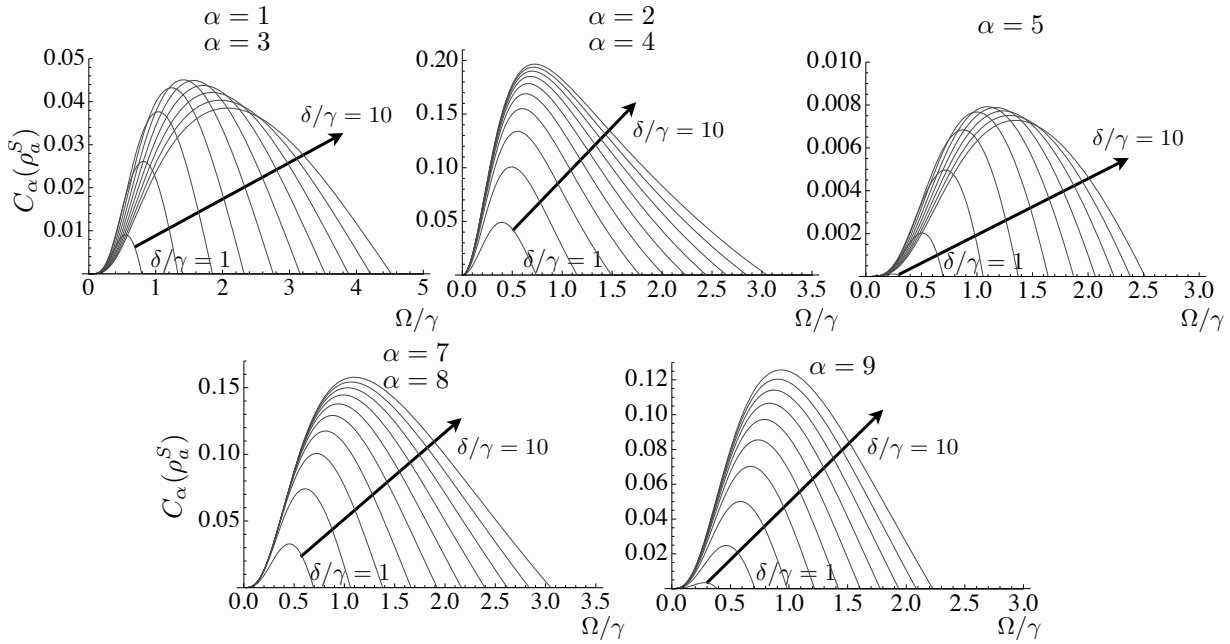

Figure 4.18: Plots of tripartite concurrences of ρ^S_a, corresponding to different values of α with different scales. Due to the symmetry, some concurrences have the same values for different α, we showed them in one plot.

know that the first two atoms are not entangled, which is the direct opposite situation to the two-atom interaction, where all the entanglement was shared between the first two atoms. We plotted the values of the non-zero concurrence in Fig. 4.18. We see that C_6 is always zero and C_5 has negligible values, which is compatible with the idea that the first two atoms are not entangled. We also see that we have $C_1 = C_3$, $C_2 = C_4$ and $C_7 = C_8$ which is due to the permutational symmetry of the first two atoms. Those concurrences are associated with bipartite entanglement of the third atom with the other two, which is definitely being detected. The values of C_1 and C_3 are smaller since they are associated with the populations of two exited states, including $|e_3\rangle$, which is being doubly blockaded. We also note the behavior of decrease of the concurrences as the interaction grows for a small fixed laser power, which is due to the fact that the source of the entanglement, the population of $|e_3\rangle$ is being blockaded. This behavior is not seen in C_2 and C_4 since those concurrences are associated with singly-excited states.

The concurrences C_7 to C_9 not only detect bipartite entanglement but are also associated with genuine tripartite entanglement, such as the one that found in the GHZ-type state $(|eeg\rangle + |gge\rangle)/\sqrt{2}$ which should be populated since the $|eeg\rangle$ state is not shifted out of resonance. The difference of amplitude between $C_{7,8}$ and C_9 is due to the absence of the bipartite entanglement detected by C_9.

4.8 Summary and Discussion

In this chapter, we generalized the model used to describe dipole blockade in two two-level atoms to three atoms, considering the interaction as a Van der Waals-type potential. We considered different configurations chosen to give us a larger understanding of the phenomena of blockade and entanglement.

We saw that the addition of a third, non-interactive atoms had no effect on the blockade levels or on the bipartite entanglement of the system, no tripartite entanglement was created either. Adding a third interacting atom did not significantly change the behavior or amplitude of the two-atom blockade of two directly interacting atoms. However, we saw that in the case of the two non-interacting atoms in the case of the aligned atoms, the system was not blockaded, but instead was boosted. However, this behavior was not associated with entanglement, even though both atoms were entangled to the same atom.

The three-atom blockade was significantly modified by the addition of a third interacting atom and showed persistence to the increase of the laser power, probably due to the maximally excited state being shifted by the sum of all pair-interactions.

The effect of a third interacting atom on the bipartite concurrence was a decrease in its amplitude, though compensated by the apparition of tripartite concurrence. Bipartite entanglement is best produced with only two atoms in this kind of interaction model. The signs of tripartite entanglement were very clear in the case of the equidistant atoms, with the concurrence due to $|W_1\rangle$ rising in amplitude with the interaction, unlike the concurrence due to $|W_2\rangle$ which tends to decrease as the state is being blockaded. For the aligned atoms, the interpretation is a bit more difficult, as there seems to be genuine

tripartite entanglement even though there is none between the first two atoms.

A clearer view of the system might be obtained by generalizing the model to a chain of N atoms. For a great number number of atoms, a linear chain would only marginally differ to a closed one and under the simplification of complete permutational symmetry, more could be understood of the relations between atoms not in direct contact. Our criterion for multipartite concurrences could easily be used in such a context.

Chapter 5

EIT, Dipole Blockade and Dipole-Dipole Interaction

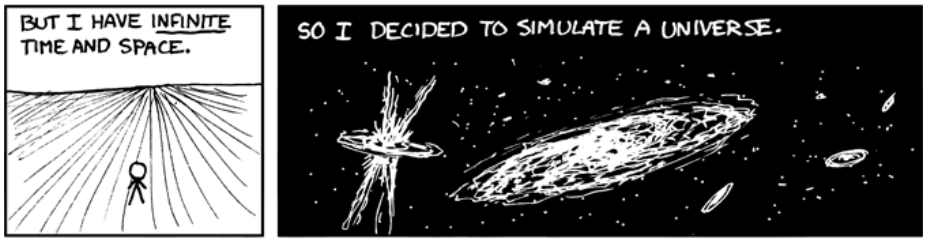

Randall Munroe, *A Bunch of Rocks* (part 6 of 9), `xkcd.com/505/`

The electromagnetically induced transparency (EIT) is a non-linear process which renders a medium transparent to an electric field over a specific range of frequency. A three-level atom is being excited by two lasers, each tuned to a particular transition. There are three different schemes for the configuration of the energy levels and allowed transitions in the atom [79], the V scheme [80], the Λ scheme [81, 82] and the *ladder*, or Ξ scheme [83]. Here, we will consider the latter. A strong laser, the *pump*, is tuned near resonance of two of the levels, while a weaker laser, the *probe*, measures the absorption spectrum of another transition. If its frequency and strength are chosen carefully, the pump laser may create a spectral window of transparency which will be detected by the probe [84, 85]. Associated with the transparency is a radical change of the refractive index of the medium, which is one of the mechanisms used to produce slow light, along with the possibilities of numerous applications in non-linear optics [86]. An experiment found in [87] managed to slow a pulse of light down to 17 m/s. Recently, EIT was even observed on a single atom [88].

In [89] the authors use the EIT effect to detect the presence of a Rydberg state. As we know, two Rydberg states interact though long-range van de Waals potential [60] and in this chapter, we try to answer the question of whether this very interaction might have an influence on the EIT itself. Pushing the question further, we wondered what the effects of another type of interaction might have on EIT and we investigate the case of dipole-dipole

interaction [69].

The structure of this chapter is as follows. In Sec. 5.1 we introduce in detail the EIT in the ladder configuration. We give the Hamiltonian of the system as well as the master equation of the system which we use to compute the steady state of the system and we show the analytical form of the density matrix term responsible for the EIT in the lowest order of the probe strength. The full steady state is shown in appendix C. We graphically show the effect of the EIT with two plots, one in the EIT regime and one not. Finally we treat the probe laser as a perturbation and compute the eigenstates and eigenvalues of the unperturbed Hamiltonian, which allows us to better understand the structure of the system and to interpret the EIT effect.

In Sec. 5.2, we consider two three-level atoms with the top energy state blockaded by a van de Waals-type interaction. We first introduce our Hamiltonian and master equation which modelize the lasers, the atoms interacting with the same interaction term we used in the previous two chapters. We start by treating the probe laser as a perturbation and calculate the eigenstates and eigenvalues of the unperturbed Hamiltonian. That knowledge allows us to predict what one-photon transitions are allowed within the system and we use perturbation theory to check what two-photon transitions are also allowed. Then we confirm the predictions by measuring the dipole blockade effect by comparing different atomic populations in the steady state. Finally, we study the effect of dipole blockade on EIT in the steady state by comparing it to the non-interactive case and we summarize our results so far.

In Sec. 5.3, we disregard van der Waals interactions and consider another model of interaction, the dipole-dipole interaction. We first give our model Hamiltonian and master equation and we briefly comment the nature of the dipole-dipole interaction. Then we investigate the eigenstates and eigenvalues of the Hamiltonian when the probe laser is turned off. We turn it back on and comment on all the possible one-photon transitions it allows, as well as the two-photon transitions using perturbation theory. We then study the blockade in the steady state by comparing atomic populations as well the strong effects of the interaction on EIT and we finally discuss the results.

5.1 Electromagnetically Induced Transparency

First, let us show that it is possible to relate macroscopic, measurable quantities of a medium such as absorption and refractive index to terms of the density matrix of the medium. The induced polarization of a medium can be expressed as [90]

$$P = N\mu_{ij}\rho_{ij}, \tag{5.1}$$

with μ_{ij} the dipole matrix element for the $i \to j$ transition, ρ_{ij} the off-diagonal term of the matrix associated with that transition and N the number of atoms in the medium. We can relate the expression to the macroscopic polarization equation [91]:

$$P = \epsilon_0 \chi E = \epsilon_0(\chi' + i\chi'')E, \tag{5.2}$$

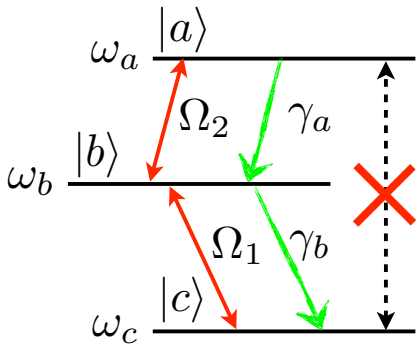

Figure 5.2: Illustration of the one-atom system, in its bare representation.

where ϵ_0 is the permittivity of free space, χ is the electric susceptibility and E is the optical field strength inducing the polarization. The real and imaginary part of χ are respectively related to the refractive index and the absorption of the electric field in the medium. Those two quantities are related through the Kramers-Kronig relations and are therefore not independent [92, 93]. Eq. (5.1) and (5.2) allow us to write

$$\chi' = \frac{N\mu_{ij}^2 \mathrm{Re}(\rho_{ij})}{2\hbar\epsilon_0\Omega_{ij}}, \tag{5.3}$$

$$\chi'' = -\frac{N\mu_{ij}^2 \mathrm{Im}(\rho_{ij})}{2\hbar\epsilon_0\Omega_{ij}}, \tag{5.4}$$

with

$$\Omega_{ij} \equiv \frac{\mu_{ij}E}{2\hbar}, \tag{5.5}$$

as the half Rabi frequency of the transition. In this chapter, we study the behavior of $\mathrm{Re}(\rho_{ij})$ and $\mathrm{Im}(\rho_{ij})$, knowing that they are directly proportional to macroscopical observables.

In order to observe EIT, the three-level system must be such that only two of the possible dipole transitions are allowed and the third is forbidden. The two lasers are near resonance with the two allowed transitions. There are three schemes that can be used to define the system [79], we will only refer to one, the so-called *ladder* scheme or Ξ scheme, which we represent in Fig. 5.2. In this scheme, the forbidden transition is the one between the highest in energy, which we call $|a\rangle$, and the lowest in energy, called $|c\rangle$. The ground level $|c\rangle$ is strongly coupled by the pump laser to the intermediary level $|b\rangle$, itself lightly coupled to $|a\rangle$ by the probe laser. Therefore we study the transparency of the medium near the resonance of the $|b\rangle \rightarrow |a\rangle$ transition.

We consider a three-level atom of decreasing energy levels $\hbar\omega_a$, $\hbar\omega_b$ and $\hbar\omega_c$ respectively associated with the states $|a\rangle$, $|b\rangle$ and $|c\rangle$. The system is driven by a pump laser of Rabi frequency $2\Omega_1$ and by a probe laser of Rabi frequency $2\Omega_2$, with $\Omega_1 \gg \Omega_2$. The pump laser frequency ω_1 is close to $\omega_b - \omega_c$, while the probe laser frequency ω_2 is close to $\omega_a - \omega_b$, and

we define the detunings

$$\Delta \equiv \omega_1 - (\omega_b - \omega_c), \tag{5.6}$$
$$\delta \equiv \omega_2 - (\omega_a - \omega_b), \tag{5.7}$$

for future simplifications and where the capital Δ is associated with the strong, pump laser. The $|a\rangle$ and $|b\rangle$ states respectively decay to the states $|b\rangle$ and $|c\rangle$ with the dissipative rates $2\gamma_a$ and $2\gamma_b$. The $|a\rangle$ state never decays directly to $|c\rangle$, as that transition is forbidden. That system is represented in Fig. 5.2 (a). The time-dependent Hamiltonian H_t of the system is given by

$$\begin{aligned} H_t &= \hbar\omega_a|a\rangle\langle a| + \hbar\omega_b|b\rangle\langle b| + \hbar\omega_c|c\rangle\langle c| \\ &\quad + \hbar\Omega_1\left(|b\rangle\langle c|e^{-i\omega_1 t} + |c\rangle\langle b|e^{i\omega_1 t}\right) + \hbar\Omega_2\left(|a\rangle\langle b|e^{-i\omega_2 t} + |b\rangle\langle a|e^{i\omega_2 t}\right), \end{aligned} \tag{5.8}$$

and the time evolution of a state $|\psi\rangle$ is given by the Schrödinger equation

$$i\hbar\frac{d}{dt}|\psi\rangle = H_t|\psi\rangle. \tag{5.9}$$

First, let us first find a rotating frame in which the Hamiltonian is time-independent. By applying the unitary transformation

$$|\psi\rangle = e^{it(\omega_1|b\rangle\langle b| + (\omega_1+\omega_2)|a\rangle\langle a|)}|\phi\rangle, \tag{5.10}$$

we are able to find an equivalent Schrödinger equation

$$i\hbar\frac{d}{dt}|\phi\rangle = H|\phi\rangle, \tag{5.11}$$

with the time-independent Hamiltonian H given by

$$H = -\hbar(\delta+\Delta)|a\rangle\langle a| - \hbar\Delta|b\rangle\langle b| + \hbar\Omega_1\left(|b\rangle\langle c| + |c\rangle\langle b|\right) + \hbar\Omega_2\left(|a\rangle\langle b| + |b\rangle\langle a|\right). \tag{5.12}$$

We see that we got rid of all the time-dependent phase terms existing in H_t, at the cost of introducing the detunings δ and Δ, and we also set the the energy of the ground state $|c\rangle$ to $\omega_c = 0$.

When considering dissipation in the Markov and Born approximation, the time evolution of the density operator ρ of the system is no longer governed by the Schrödinger equation, but rather by the master equation [69]

$$\dot{\rho} = \frac{-i}{\hbar}[H,\rho] - \gamma_a(|a\rangle\langle a|\rho - 2|b\rangle\langle a|\rho|a\rangle\langle b| + \rho|a\rangle\langle a|) + \gamma_b(|b\rangle\langle b|\rho - 2|c\rangle\langle b|\rho|b\rangle\langle c| + \rho|b\rangle\langle b|). \tag{5.13}$$

We found the general, analytical expression of the steady state following this master equation and due to its complexity, we transcribed it in App. C. That general solution does not make the distinction pump/probe since both lasers are treated as equals. The

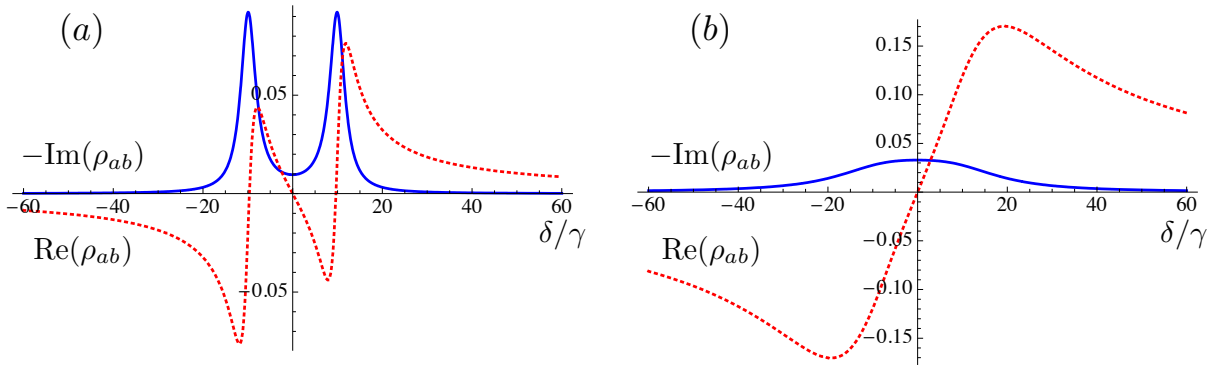

Figure 5.3: The imaginary and real part of ρ_{ab} respectively corresponding to the absorption and the refraction index, in function of δ/γ with $\Delta/\gamma = 0, \Omega_1/\gamma = 10$ and (a) $\Omega_2/\gamma = 1$, (b) $\Omega_2/\gamma = 10$. When Ω_2/γ is small, the absorption becomes minimal on resonance and the medium becomes transparent in a window around $\delta/\gamma = 0$.

quantity we are interested in is $\rho_{ab} \equiv \langle a|\rho|b\rangle$ when Ω_2 is weak. From our solution, we can write it in the EIT regime, i. e. in terms of the lowest order of Ω_2, as

$$\rho_{ab} \simeq \frac{i\Omega_2\rho_b}{i(\delta+\Delta) - \gamma_a - \frac{\Omega_1^2}{(\gamma_a+\gamma_b)-i\delta}}, \tag{5.14}$$

which a the familiar expression for ρ_{ab} [79], with ρ_b the population of the state $|b\rangle$, given to the lowest order of Ω_2 by

$$\rho_b \simeq \frac{\Omega_1^2}{\Delta^2 + \gamma_b^2 + 2\Omega_1^2}. \tag{5.15}$$

We get an idea from Eq. (5.14) of how the absorption, given by the imaginary part of ρ_{ab} behaves when the probe field is turned on. For a strong, resonant pump laser ($\Delta = 0$), whenever the probe is on resonance as well ($\delta = 0$), the absorption strongly weakens and the transparency is obtained. As the probe field grows stronger, the above approximation is not valid anymore and the absorption becomes maximum on resonance. Both situations are shown in Fig. 5.3 with the real imaginary part of ρ_{ab} in function of the detuning δ.

Let us now interpret this behavior through another angle. If we treat the probe laser as a perturbation, we may turn it off for now, setting Ω_2 and ω_2 to zero, and check the eigenvalues of the unperturbed Hamiltonian in order to understand the structure of the system. We find the three eigenvalues

$$-\hbar(\omega_b - \omega_a + \Delta),\ \hbar\lambda_\pm \equiv \frac{-\hbar}{2}\left(\Delta \pm \sqrt{\Delta^2 + 4\Omega_1^2}\right), \tag{5.16}$$

associated with the respective eigenstates $|a\rangle$ and

$$|\lambda_\pm\rangle \equiv \frac{1}{\sqrt{\lambda_\pm^2 + \Omega_1^2}}\left(\lambda_\pm|b\rangle + \Omega_1|c\rangle\right). \tag{5.17}$$

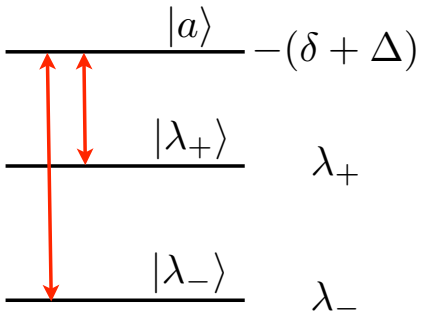

Figure 5.4: Illustration of the one-atom system in its eigenvalue structure when the probe laser is considered a small perturbation. The possible transitions induced by the perturbation are represented in red.

In that eigenstate basis, we may write the full Hamiltonian as

$$\begin{aligned} H &= -\hbar(\delta+\Delta)|a\rangle\langle a| + \hbar\lambda_+|\lambda_+\rangle\langle\lambda_+| + \hbar\lambda_-|\lambda_-\rangle\langle\lambda_-| \\ &\quad + \frac{\hbar\lambda_+\Omega_2}{\sqrt{\Omega_1^2+\lambda_+^2}}\left(|a\rangle\langle\lambda_+| + |\lambda_+\rangle\langle a|\right) + \frac{\hbar\lambda_-\Omega_2}{\sqrt{\Omega_1^2+\lambda_-^2}}\left(|a\rangle\langle\lambda_-| + |\lambda_-\rangle\langle a|\right), \end{aligned} \tag{5.18}$$

from which we can see that there are two types of possible transitions, from $|\lambda_\pm\rangle$ to $|a\rangle$ and no allowed transition from $|\lambda_+\rangle$ to $|\lambda_-\rangle$. The eigenvalues and the possible transitions are represented on Fig. 5.4. The frequencies at which the transitions are optimal are $-\delta-\Delta=\lambda_\pm$, or in other terms

$$\delta = \lambda_\pm, \tag{5.19}$$

which are exactly the frequencies of the maximal absorption for low Ω_2 in Fig. 5.3, in that case we have $\Delta=0$ and the transitions are located at $\pm\Omega_1/\gamma=\pm 10$. When Ω_2 grows stronger, the structure of the system becomes different and the resonant peaks are lost.

5.2 EIT and Dipole Blockade

In this section, we consider two three-level atoms, make them interact with each other by a van der Waals-type interaction and observe the influence on the blockade and on EIT in the system. We already used the van der Waals interaction in the previous chapters to predict dipole blockade in systems two-level atoms and we generalize it here for three-level systems.

5.2.1 Theoretical Model

We consider a system of two three-level atoms excited by the pump and probe lasers, described earlier in the chapter. The two atoms of internal states $|a_i\rangle, |b_i\rangle$ and $|c_i\rangle$ $(i=1,2)$ are located at fixed positions $\mathbf{x}_i$, they are driven by two lasers fields of wave vector $\mathbf{k}_1$ and $\mathbf{k}_2$. For simplicity, $\mathbf{k}_1$ and $\mathbf{k}_2$ are supposed to be perpendicular to the two-atom line and

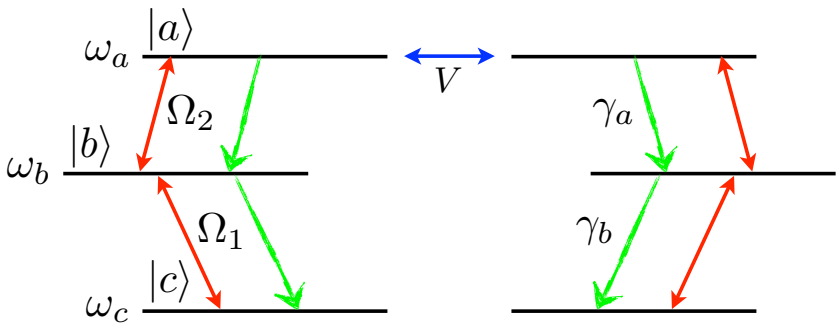

Figure 5.5: Illustration of the system. Both atoms are identical and interact through a van de Waals potential V.

the reference frame is properly chosen so as $\mathbf{k}_i \cdot \mathbf{x}_1 = \mathbf{k}_i \cdot \mathbf{x}_2 = 0$ for $i = 1, 2$. All phase terms that would appear in the driving term in the Hamiltonian H may therefore be dropped. We consider that the two atoms strongly interact when they are in the state $|aa\rangle = |a\rangle_1 \otimes |a\rangle_2$, resulting in a shift $\hbar V$ of this doubly excited state. Fig. 5.5 illustrates this two-atom system.

The time-independent Hamiltonian of the system reads

$$\begin{aligned} H &= \hbar V|aa\rangle\langle aa| + \sum_{i=1}^{2}[-\hbar(\delta+\Delta)|a_i\rangle\langle a_i| - \hbar\Delta|b_i\rangle\langle b_i| \\ &\quad \hbar\Omega_1\left(|b_i\rangle\langle c_i| + |c_i\rangle\langle b_i|\right) + \hbar\Omega_2\left(|a_i\rangle\langle b_i| + |b_i\rangle\langle a_i|\right)]. \end{aligned} \tag{5.20}$$

When considering dissipation in the Markov and Born approximation, the time evolution of the density operator ρ of the system is governed by the master equation [69]

$$\begin{aligned} \dot{\rho} &= \frac{-i}{\hbar}[H,\rho] - \sum_{i=1}^{2}\gamma_a(|a_i\rangle\langle a_i|\rho - 2|b_i\rangle\langle a_i|\rho|a_i\rangle\langle b_i| + \rho|a_i\rangle\langle a_i|) \\ &\quad + \sum_{i=1}^{2}\gamma_b(|b_i\rangle\langle b_i|\rho - 2|c_i\rangle\langle b_i|\rho|b_i\rangle\langle c_i| + \rho|b_i\rangle\langle b_i|). \end{aligned} \tag{5.21}$$

5.2.2 Structure and Eigenstates

We can find the eigenvalues of the problem if we consider that the second laser is only a perturbation W written as

$$W = \sum_{i=1}^{2}\hbar\Omega_2\left(|a_i\rangle\langle b_i| + |b_i\rangle\langle a_i|\right). \tag{5.22}$$

When we set the perturbation to zero we can find the nine eigenstates of the system. These eigenstates are closely related to the $|a\rangle, |\lambda_\pm\rangle$ states, and we will describe them in

that basis. Since the atoms are identical, the Hamiltonian is symmetrical with respect of their exchange, so we should be able to describe the system in a symmetric/antisymmetric basis. We find the set of eigenvalues $\hbar V - 2\hbar(\delta+\Delta), -\hbar(\delta+\Delta)+\hbar\lambda_\pm, 2\hbar\lambda_\pm, -\hbar\Delta$ and again $-\hbar(\delta+\Delta)+\hbar\lambda_\pm, -\hbar\Delta$ respectively associated with the following eigenstates

$$|\psi_1\rangle = |aa\rangle, \tag{5.23}$$

$$|\psi_2^\pm\rangle = \frac{1}{\sqrt{2}}(|a,\lambda_\pm\rangle + |\lambda_\pm, a\rangle), \tag{5.24}$$

$$|\psi_3^\pm\rangle = |\lambda_\pm,\lambda_\pm\rangle \tag{5.25}$$

$$|\psi_4\rangle = \frac{1}{\sqrt{2}}(|\lambda_+,\lambda_-\rangle + |\lambda_-,\lambda_+\rangle), \tag{5.26}$$

$$|\psi_5^\pm\rangle = \frac{1}{\sqrt{2}}(|a,\lambda_\pm\rangle - |\lambda_\pm, a\rangle), \tag{5.27}$$

$$|\psi_6\rangle = \frac{1}{\sqrt{2}}(|\lambda_+,\lambda_-\rangle - |\lambda_-,\lambda_+\rangle). \tag{5.28}$$

Note that states $|\psi_1\rangle$ through $|\psi_4\rangle$ are symmetrical while $|\psi_5^\pm\rangle$ and $|\psi_6\rangle$ are antisymmetrical. The only state affected by the interaction term V is the maximally excited state $|aa\rangle$.

Once the basis found, we may turn the probe field back on and list the non-diagonal terms of the Hamiltonian. We find that the only non-zero terms are

$$\langle\psi_1|W|\psi_2^\pm\rangle = \langle\psi_2^\pm|W|\psi_3^\pm\rangle = \frac{\sqrt{2}\hbar\lambda_\pm\Omega_2}{\sqrt{\lambda_\pm^2+\Omega_1^2}}, \tag{5.29}$$

$$\langle\psi_2^\pm|W|\psi_4\rangle = \pm\frac{\hbar\Omega_1\Omega_2}{\sqrt{\lambda_\pm^2+\Omega_1^2}}, \tag{5.30}$$

$$\langle\psi_5^\pm|W|\psi_6\rangle = \frac{\hbar\Omega_1\Omega_2}{\sqrt{\lambda_\pm^2+\Omega_1^2}}, \tag{5.31}$$

and their complex conjugates.

Since both the Hamiltonian and the perturbation are symmetrical under the exchange of the atoms, we see that the probe laser does not couple the symmetric states with the antisymmetric states. Furthermore, the only authorized one-photon transitions within those two groups are transitions of the type $|\lambda_\pm\rangle_i \to |a\rangle_i$, which amounts to 6 one-photon transitions within the symmetric states and 2 within the antisymmetric states. The eigenstates and possible transitions are represented in Fig. 5.6 as well as the three two-photon transitions that may occur in the system.

The conditions for the one-photon resonant transitions are

$$\delta = V - \Delta - \lambda_\pm, \tag{5.32}$$

$$\delta = \lambda_\pm, \tag{5.33}$$

$$\delta = -\Delta - \lambda_\pm, \tag{5.34}$$

where condition (5.32) refers to transitions to the maximally excited state $|aa\rangle$ and the others transitions to states with only one atom in the state $|a\rangle$. When the pump laser is on

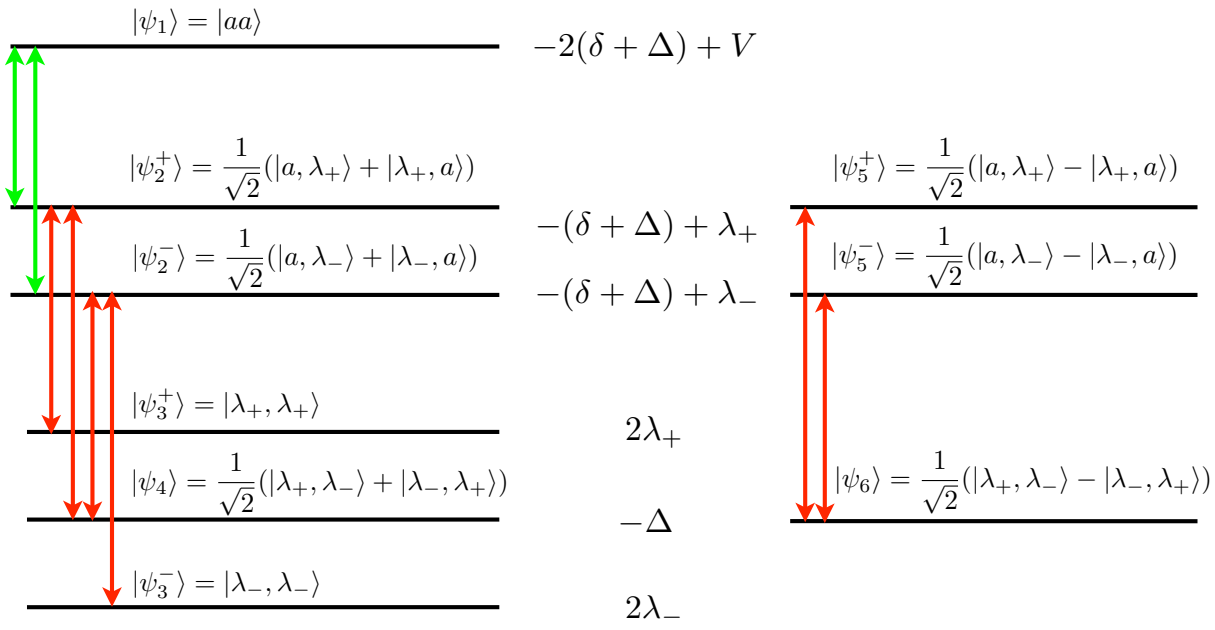

Figure 5.6: Energy levels of the problem. On the left the symmetrical eigenstates, and on the right the antisymmetrical ones. The transitions allowed by the perturbation W are shown, others are not permitted. In green, the transitions that contribute to the $|aa\rangle$ level and in red the other one-photon transitions.

resonance, we have $\Delta = 0$ and $\lambda_\pm = \mp|\Omega_1|$ and the number of resonance conditions falls to four. There are also three conditions for two-photon resonances:

$$2\delta = V - 2\Delta - 2\lambda_\pm, \tag{5.35}$$

$$2\delta = V - \Delta. \tag{5.36}$$

5.2.3 Perturbation Theory

In this section, we investigate the possibilities of two-photon processes within our system. According to Fermi's Golden Rule of the standard second-order perturbation theory [94], assuming that initially the system is in the $|\psi_i\rangle$ state, the transition rate to $|\psi_f\rangle$ through a two-photon process reads

$$R_{\psi_i\to\psi_f} = \frac{2\pi}{\hbar^2}\left|\sum_j \frac{\langle\psi_f|W|\psi_j\rangle\langle\psi_j|W|\psi_i\rangle}{\lambda^{(j)} - \lambda^{(i)}}\right|^2 \delta_D(\lambda^{(f)} - \lambda^{(i)}), \tag{5.37}$$

where δ_D is a Dirac δ-function which yields the condition for resonance for the two-photon process, $|\psi_j\rangle$ are all the states that are simultaneously coupled to $|\psi_i\rangle$ and $|\psi_f\rangle$ and the $\lambda^{(j)}$ are the state eigenfrequencies. The only possible final state is $|\psi_1\rangle$ while there are three possibilities for the initial states, $|\psi_4\rangle$ and $|\psi_3^\pm\rangle$, while the intermediary states are $|\psi_2^\pm\rangle$.

We are not mainly interested in the transition rates but rather in the possibility of the process itself, so we only calculate the term with the perturbation matrix elements. For the transition $|\psi_4\rangle \to |\psi_1\rangle$, with the resonance condition $2\delta = V - \Delta$, we find

$$\sum_{j=\pm} \frac{\langle\psi_1|W|\psi_2^j\rangle\langle\psi_2^j|W|\psi_4\rangle}{-\delta + \lambda_j} = \frac{2\hbar^2\Omega_1\Omega_2^2\lambda_+}{(\lambda_-^2 + \Omega_1^2)(\lambda_+ - \delta)} - \frac{2\hbar^2\Omega_1\Omega_2^2\lambda_-}{(\lambda_-^2 + \Omega_1^2)(\lambda_- - \delta)}, \tag{5.38}$$

$$= \frac{2\hbar^2\Omega_1\Omega_2^2(2\delta + \Delta)}{(\delta(\delta + \Delta) - \Omega_1^2)\sqrt{\Delta^2 + 4\Omega_1^2}}. \tag{5.39}$$

We see that this quantity is non-zero only when $V \neq 0$, since we have the resonance condition $2\delta = V - \Delta$. This ensures that the presence of two non-interacting atoms does not add a new transition frequency in the system. Therefore the transition rate will be zero for the non-interactive case and for a weak probe field. For any other value of the interaction, the rate will be non-zero.

Let us now examine the possible transition $|\psi_3^\pm\rangle \to |\psi_1\rangle$ of resonance condition $2\delta = V - 2\Delta - 2\lambda_\pm$. We see that the term $\langle\psi_2^\pm|W|\psi_3^\pm\rangle$ is not in the list of the non-zero terms of the perturbation and is therefore zero. This means that the sum over j reduces to a single term, in other words only the paths $|\psi_3^\pm\rangle \to |\psi_2^\pm\rangle \to |\psi_1\rangle$ are possible. We therefore have

$$\frac{\langle\psi_1|W|\psi_2^\pm\rangle\langle\psi_2^\pm|W|\psi_3^\pm\rangle}{-(\delta + \Delta)} = \frac{2\hbar^2\lambda_\pm^2\Omega_2^2}{-(\delta + \Delta)(\lambda_\pm^2 + \Omega_1^2)}, \tag{5.40}$$

which will always be non-zero. For the non-interactive case $V = 0$, the resonance conditions reads $\delta = -\Delta - \lambda_\pm$ and corresponds to one-photon transitions pre-existing in the one-atom problem, which means that such a transition is not a real two-photon process but rather two stepwise one-photon processes.

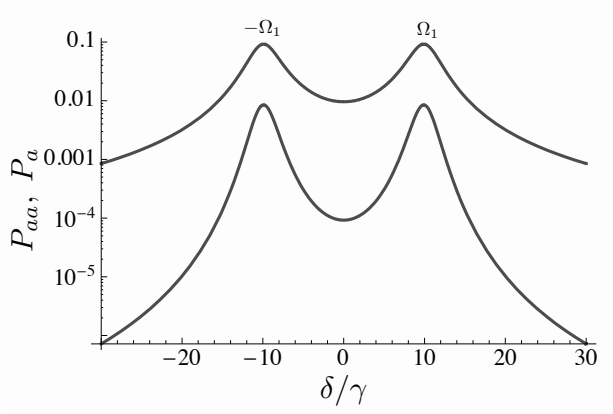

Figure 5.7: Plot of P_{aa} in function of δ/γ. We set $\gamma_a = \gamma_b = \gamma$, $\Omega_1/\gamma = 10$, $\Omega_2/\gamma = 1$, $\Delta = 0$ and $V/\gamma = 0$. The most population of $|aa\rangle$ is found when the probe is set at the resonance $\delta = \pm\Omega_1$. For every value of δ/γ, we have $P_{aa} = P_a^2$ as the two atoms are independent. All values labeling regions of the plot are in units of γ.

5.2.4 Dipole Blockade in the Steady State

Let us now investigate the blockade that may exist in the steady state ρ^S of the system by measuring the population $P_{aa} = \langle aa|\rho^S|aa\rangle$ of the $|aa\rangle$ state in function of the detuning δ, compared to the populations $P_a = \langle a_1|\rho^S|a_1\rangle$ in $|a_1\rangle$, or $|a_2\rangle$ since the system is symmetrical. We do this process numerically. For simplicity, every numerical calculations we do in the rest of the chapter consider identical dissipation rates for the $|a\rangle$ and $|b\rangle$ levels, $\gamma_a = \gamma_b = \gamma$, as well as a pump laser on resonance, i. e. $\Delta = 0$, which implies simplifies the expression of the on-atom eigenvalues to $\lambda_\pm = \mp|\Omega_1|$.

Let us first consider the non-interactive case $V = 0$. In that situation, the two atoms behave independently and no particular behavior such as blockades are expected. We plotted the values of P_{aa} and P_a in Fig. 5.7. For any value of δ, the ratio P_{aa}/P_a^2 is found to be 1, which is an expected result for independent atoms. On the plot, we can observe two peaks located at $\delta = \pm\Omega_1$, but no peak at $\delta = 0$ which confirms that the $|\psi_4\rangle \to |\psi_1\rangle$ transition is prohibited, as we showed earlier using perturbation theory.

We then consider a non-zero value of V. We plotted in Fig. 5.8 both the values of P_{aa} and of the ratio P_{aa}/P_a^2 in function of the detuning δ. On the first plot, we see all predicted transition peaks on the spectrum of P_{aa}, except for the $\delta = V - \Omega_1$ resonance. That absence and the small amplitude of the peak at $\delta = V + \Omega_1$ might be explained by the fact that those transitions arise from the $|\psi_2^\pm\rangle$ states which are poorly populated for small values of Ω_2. Indeed, we can show numerically that for $\Omega_1 \gg \Omega_2, \gamma$, about the totality of the population is shared almost evenly by the four least excited states $|\psi_4\rangle, |\psi_3^\pm\rangle$ and $|\psi_6^\pm\rangle$. The states $|\psi_2^\pm\rangle$ and $|\psi_5\rangle$ are in general poorly populated and $|aa\rangle$ even less.

On the right plot of Fig. 5.8, we see that the $|aa\rangle$ state can be blockaded or enhanced depending on the detuning. The strongest values of enhancing are seen at the two-photon processes resonance frequencies. The two-photon processes excite both atoms simultane-

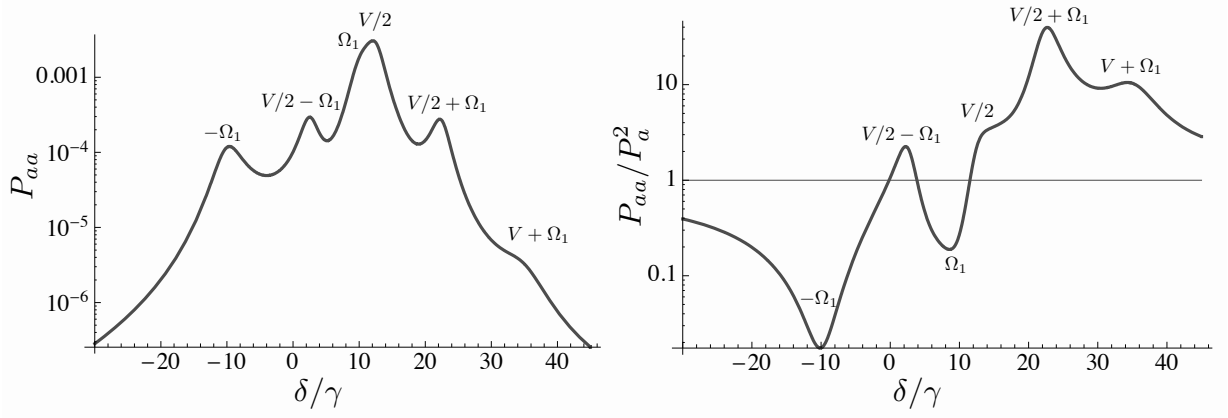

Figure 5.8: Plot of P_{aa} (left) and P_a (right) in function of δ/γ. We set $\gamma_a = \gamma_b = \gamma$, $\Omega_1/\gamma = 10$, $\Omega_2/\gamma = 1$, $\Delta = 0$ and $V/\gamma = 25$. The peaks appear at the expected values of δ and the transitions associated to the $|aa\rangle$ states give out a correlation greater than 1. All values labeling regions of the plots are in units of γ.

ously to the $|aa\rangle$ state without relying on processes exciting the atoms one by one, which has the effect of boosting the population P_{aa} without contributing much to P_a, explaining the enhancing. The strongest values of blockade are seen at the two one-photon transition frequencies which populate the $|\psi_2^{\pm}\rangle$ states, which contain one exited atom $|a\rangle$. Those transitions contribute greatly to P_a and barely to P_{aa}, hence the blockade. We can distinguish a small enhancing peak at the frequency $\delta = V + \Omega_1$ that allows the $|\psi_2^{+}\rangle \to |aa\rangle$ transition which contribute directly to P_{aa}. However since the $|\psi_2^{\pm}\rangle$ states are poorly populated, the amplitude of these peaks is small (the theoretical peak due to $|\psi_2^{+}\rangle \to |aa\rangle$ does not even appear), unlike the peaks due to two-photon excitations which take their roots in the very populated lower states.

5.2.5 EIT in the Steady State

Finally, let us study the EIT in the steady state. The quantity we chose to measure is the absorption and refractive index of one atom with the other atom traced out of the system, i. e. $\rho_{ab} \equiv \langle a_1|\mathrm{Tr}_2\rho|a_1\rangle$. With that definition, we study the amount of absorption and contribution to the refractive index per atom, which allows us to compare our result to the one-atom system.

We plotted on Fig. 5.9 (a) the absorption and refractive index of the two atoms. The two quantities are very similar to the ones found in the non-interactive case shown in Fig. 5.3, with two peaks located at the values of the one-photon transitions conditions and no pronounced new feature. In order to compare the amplitude of the transparency effect with the one-atom case, we plotted in Fig. 5.9 (b) the quantity z defined by

$$z \equiv \mathrm{Im}\left(\frac{\rho_{ab}(V) - \rho_{ab}(V=0)}{\rho_{ab}(V=0)}\right). \tag{5.41}$$

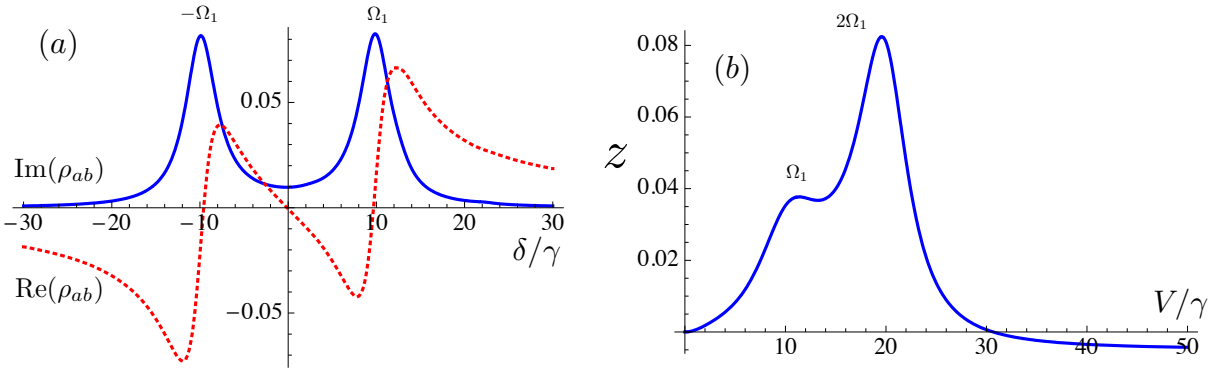

Figure 5.9: On (a) the imaginary and real part of ρ_{ab} in function of δ/γ with $\Delta/\gamma = 0, \Omega_1/\gamma = 10, \Omega_2/\gamma = 1$ and $V = 25$. There is not much difference with the non-interactive case. On (b) we show the ratio z (see text for definition) in function of the interaction V/γ on resonance $\delta = \Delta = 0$ with $\Omega_1/\gamma = 10, \Omega_2/\gamma = 1$. For $V/\gamma \leq 30$ the transparency effect is weakened, although not by a lot, while above that value it is negligibly strengthened. All values labeling regions of the plots are in units of γ.

This quantity represents the relative difference that the apparition of interaction made in the transparency window $\delta = \Delta = 0$. We see that the transparency effect is actually reduced a bit by the presence of the interaction, by a maximum percentage up to about 8% at the position $V = 2\Omega_1$, which corresponds to the two-photon transition resonance (5.35), a process that does not involve the excitation of one atom at a time. For greater values of V/γ, the transparency is stronger by a very small amount. This small contribution of the dipole blockade is explained by the fact that the EIT is not a effect of saturation [84], i. e. it happens even for small populations of $|a\rangle$, which means that manipulating the energy level of $|aa\rangle$ will have little effects on it.

5.2.6 Summary and Discussion

We added to a system of two three-level atoms a van der Waals interaction term and investigated the effects on the blockade of the $|aa\rangle$ state as well as the EIT effect. We found that the only contribution of this interactive term to the global structure of the system was to shift the energy level of the $|aa\rangle$ state, which is what this interaction was designed to do. Its effect on the blockade of the $|aa\rangle$ state was important, as we saw that the system could be either blockaded or enhanced, depending on the detuning of the probe laser. On one-photon transition resonances not involving $|aa\rangle$, the system had a tendency to be blockaded, while on the resonances involving $|aa\rangle$ and especially on the two-photon transition resonances the state was enhanced, sometimes greatly. The effect of increasing the strength of the probe laser was not investigated in order to stay in the EIT regime, but it is expected that strengthening the laser would decrease the amplitude of the blockades and enhancements.

The behavior of the EIT effect was only slightly affected by the interaction. This may

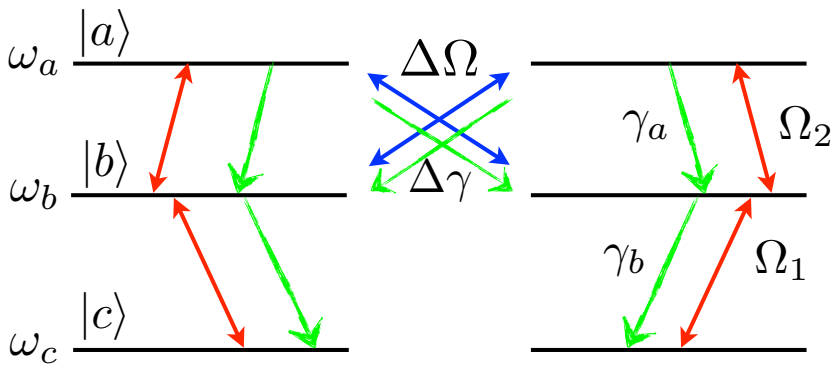

Figure 5.10: Illustration of the system. The dipole-dipole interaction couples the $|a\rangle$ and $|b\rangle$ states of the different atoms.

be explained by the fact that ρ_{ab} is affected by $|b\rangle \rightarrow |a\rangle$, one-photon transitions only, which primarily happen between the four lower states and the states containing one $|a\rangle$. Since that last set of states is not very populated, due to the low value of Ω_2 in the EIT regime, the fact that their own transitions to the $|aa\rangle$ state is being tampered on is of globally small importance on the EIT effect.

A way to affect the EIT more might be to consider another type of interaction. For example, we might consider a three-level atom following a lambda scheme with the highest level being the state $|b\rangle$ which would be largely populated by the pump and interacting with other atoms. In the next section, we consider another type of possible interaction, the dipole-dipole interaction, which will make states $|a\rangle$ and $|b\rangle$ interact.

5.3 EIT and Dipole-Dipole Interaction

In this section, we consider another type of interaction with the dipole-dipole interaction between the $|a\rangle$ and $|b\rangle$ levels of the two atoms. Unlike the van der Waals interaction, this interaction should change more profoundly the eigenstate structure of the unperturbed system and therefore affect the behavior of the EIT.

5.3.1 Theoretical Model

We now consider a system made of two identical three-level atoms excited by the pump and probe lasers. Those atoms interact through a dipole-dipole potential which couples the states $|a\rangle$ and $|b\rangle$ of the first atom with those of the second with a coupling strength $\Delta\Omega$. The interaction also has an effect on the spontaneous emission terms since it rends possible spontaneous transitions from the $|a\rangle$ state of an atom to the $|b\rangle$ state of the other with a cross rate $2\Delta\gamma$. Fig. 5.10 illustrates the system with the dipole dipole interaction.

The Hamiltonian, already expressed in a time-independent frame and with the same

conventions as earlier, then reads

$$\begin{aligned} H &= \hbar\Delta\Omega(|ab\rangle\langle ba|+|ba\rangle\langle ab|) + \sum_{i=1}^{2}[-\hbar(\delta+\Delta)|a_i\rangle\langle a_i|-\hbar\Delta|b_i\rangle\langle b_i| \\ &\quad \hbar\Omega_1\left(|b_i\rangle\langle c_i|+|c_i\rangle\langle b_i|\right) + \hbar\Omega_2\left(|a_i\rangle\langle b_i|+|b_i\rangle\langle a_i|\right)]. \end{aligned} \tag{5.42}$$

When considering dissipation in the Markov and Born approximation, the time evolution of the density operator ρ of the system is governed by the master equation

$$\begin{aligned} \dot{\rho} &= \frac{-i}{\hbar}[H,\rho] - \sum_{i,j=1}^{2}\gamma_{ij}(|a_i\rangle\langle b_i|\otimes|b_j\rangle\langle a_j|\rho - 2|b_i\rangle\langle a_i|\rho|a_j\rangle\langle b_j|+\rho|a_i\rangle\langle b_i|\otimes|b_j\rangle\langle a_j|) \\ &\quad -\sum_{i=1}^{2}\gamma_b(|b_i\rangle\langle b_i|\rho - 2|c_i\rangle\langle b_i|\rho|b_i\rangle\langle c_i|+\rho|b_i\rangle\langle b_i|), \end{aligned} \tag{5.43}$$

with $\gamma_{11} = \gamma_{22} = \gamma_a$ and $\gamma_{12} = \gamma_{21} = \Delta\gamma$.

The dipole-dipole interaction terms $\Delta\Omega$ and $\Delta\gamma$ are not independent since they are determined by the interatomic distance normalized to the wavelength of the transition $r \equiv r_{12}/\lambda$ and the angle θ between the atomic dipole moments [69]. We have

$$\Delta\Omega(r,\theta) = \gamma_a\frac{3}{2}\left[(1-3\cos^2\theta)\left(\frac{\sin(2\pi r)}{(2\pi r)^2}+\frac{\cos(2\pi r)}{(2\pi r)^3}\right) - \sin^2\theta\frac{\cos(2\pi r)}{2\pi r}\right], \tag{5.44}$$

and

$$\Delta\gamma(r,\theta) = \frac{\gamma_a}{2\pi r}\left[\sin(2\pi r) - \frac{1}{2}(1-3\cos^2\theta)\left(\sin(2\pi r)\left(\frac{3}{(2\pi r)^2}-1\right) - 3\frac{\cos(2\pi r)}{2\pi r}\right)\right]. \tag{5.45}$$

We plotted in Fig. 5.11 $\Delta\Omega(r,\theta)$ and $\Delta\gamma(r,\theta)$ in function of r for $\theta = 0$. For values of r over 1, the interaction is quite weak, therefore we settled for the rest of the chapter on the parameter values of $r = 0.1$ and $\theta = 0$, which yields the values of $\Delta\Omega/\gamma \simeq -14.25$ and $\Delta\gamma/\gamma \simeq 0.96$.

5.3.2 Structure and Eigenstates

We can find the eigenvalues of the problem if we consider that the probe laser is only a perturbation W. When we set $\Omega_2 = 0$ we can find the nine eigenstates of the system. Once again, these eigenstates are related to the $|a\rangle, |\lambda_\pm\rangle$ states, except for the states which involve both $|a\rangle$ and $|b\rangle$ since they are now coupled by the interaction. The permutational symmetry of the atoms is preserved, so we can describe the system in a symmetric/antisymmetric

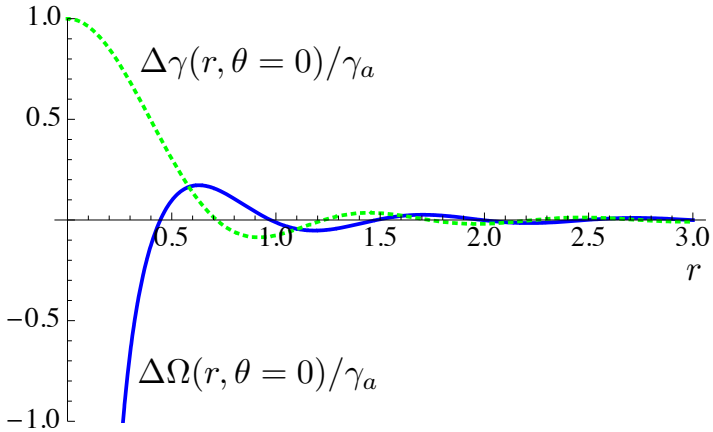

Figure 5.11: Plot of $\Delta\Omega(r,\theta)/\gamma_a$ in blue and $\Delta\gamma(r,\theta)/\gamma_a$ in dotted green as functions of r for $\theta = 0$. As r approaches zero, $\Delta\Omega(r,\theta)$ behaves like $1/r^3$.

basis. We find the following eigenstate basis

$$|\psi_1\rangle = |aa\rangle, \tag{5.46}$$

$$|\psi_2^{\pm}\rangle = \frac{1}{\sqrt{2}}(|a,\Lambda_{\pm}^s\rangle + |\Lambda_{\pm}^s,a\rangle), \tag{5.47}$$

$$|\psi_3^{\pm}\rangle = |\lambda_{\pm},\lambda_{\pm}\rangle \tag{5.48}$$

$$|\psi_4\rangle = \frac{1}{\sqrt{2}}(|\lambda_+,\lambda_-\rangle + |\lambda_-,\lambda_+\rangle), \tag{5.49}$$

$$|\psi_5^{\pm}\rangle = \frac{1}{\sqrt{2}}(|a,\Lambda_{\pm}^a\rangle - |\Lambda_{\pm}^a,a\rangle), \tag{5.50}$$

$$|\psi_6\rangle = \frac{1}{\sqrt{2}}(|\lambda_+,\lambda_-\rangle - |\lambda_-,\lambda_+\rangle) \tag{5.51}$$

$$\tag{5.52}$$

with the states

$$|\Lambda_{\pm}^{s/a}\rangle \equiv \frac{1}{\sqrt{(\Lambda_{\pm}^{s/a})^2+\Omega_1^2}}\left(\Lambda_{\pm}^{s/a}|b\rangle + \Omega_1|c\rangle\right), \tag{5.53}$$

and the frequencies

$$\Lambda_{\pm}^s \equiv \frac{-1}{2}\left((\Delta-\Delta\Omega) \pm \sqrt{(\Delta-\Delta\Omega)^2+4\Omega_1^2}\right), \tag{5.54}$$

$$\Lambda_{\pm}^a \equiv \frac{-1}{2}\left((\Delta+\Delta\Omega) \pm \sqrt{(\Delta+\Delta\Omega)^2+4\Omega_1^2}\right). \tag{5.55}$$

We find that for the non-interactive case $\Delta\Omega = 0$ these last values simplify to $\Lambda_{\pm}^{s/a} = \lambda_{\pm}$ and $|\Lambda_{\pm}^{s/a}\rangle = |\lambda_{\pm}\rangle$. The respective set of energies associated to theses eigenstates are

$-2\hbar(\delta+\Delta), -\hbar(\delta+\Delta)+\hbar\Lambda^s_\pm, 2\hbar\lambda_\pm, -\hbar\Delta$ and $-\hbar(\delta+\Delta)+\hbar\Lambda^a_\pm, -\hbar\Delta$. Note that once again, states $|\psi_1\rangle$ through $|\psi_4\rangle$ are symmetrical while $|\psi_5^\pm\rangle$ and $|\psi_6\rangle$ are antisymmetrical. The state affected by the dipole-dipole interaction terms are the $|\psi_2^\pm\rangle$ and $|\psi_5^\pm\rangle$, which are the states containing one atom in the state $|a\rangle$.

Once the basis found, we may turn the perturbative probe field back on and list the non-diagonal terms of the Hamiltonian in the unperturbed eigenstate basis. We find that the only non-zero terms are

$$\langle\psi_1|W|\psi_2^\pm\rangle = \frac{\sqrt{2}\hbar\Lambda^s_\pm\Omega_2}{\sqrt{(\Lambda^s_\pm)^2+\Omega_1^2}}, \tag{5.56}$$

$$\langle\psi_2^\pm|W|\psi_3^\pm\rangle = \frac{\sqrt{2}\hbar\lambda_\pm(\lambda_\pm\Lambda^s_\pm+\Omega_1^2)\Omega_2}{\sqrt{(\Lambda^s_\pm)^2+\Omega_1^2}(\lambda_\pm^2+\Omega_1^2)}, \tag{5.57}$$

$$\langle\psi_2^\pm|W|\psi_3^\mp\rangle = \frac{\sqrt{2}\hbar\lambda_\mp(\lambda_\mp\Lambda^s_\pm+\Omega_1^2)\Omega_2}{\sqrt{(\Lambda^s_\pm)^2+\Omega_1^2}(\lambda_\mp^2+\Omega_1^2)}, \tag{5.58}$$

$$\langle\psi_2^\pm|W|\psi_4\rangle = \frac{-\hbar(\Delta+2\Lambda^s_\pm)\Omega_1\Omega_2}{\sqrt{(\Lambda^s_\pm)^2+\Omega_1^2}\sqrt{\Delta^2+4\Omega_1^2}}, \tag{5.59}$$

$$\langle\psi_5^\pm|W|\psi_6\rangle = \frac{\hbar\Omega_1\Omega_2}{\sqrt{(\Lambda^a_\pm)^2+\Omega_1^2}}, \tag{5.60}$$

and their complex conjugates. We see that the introduction of the interaction allowed the $|\psi_2^\pm\rangle \to |\psi_3^\mp\rangle$ transitions, which were forbidden before.

The 10 conditions for the one-photon resonant transitions are

$$\delta = -\Delta - \Lambda^s_\pm, \tag{5.61}$$

$$\delta = \Lambda^{s/a}_\pm, \tag{5.62}$$

$$\delta = -\Delta + \Lambda^s_\pm - \lambda_+, \tag{5.63}$$

$$\delta = -\Delta + \Lambda^s_\pm - \lambda_-, \tag{5.64}$$

$$\tag{5.65}$$

and the 3 conditions for two-photon resonances are

$$\delta = \Delta - \lambda_\pm, \tag{5.66}$$

$$2\delta = -\Delta. \tag{5.67}$$

When the pump laser is on resonance, we have $\Delta = 0$, $\lambda_\pm = \mp|\Omega_1|$, $\Lambda^s_\pm = -\Lambda^a_\mp$ and the number of resonance conditions falls to 8 since the resonance condition for $|\psi_1\rangle \to |\psi_2^\pm\rangle$ and $|\psi_5^\pm\rangle \to |\psi_6\rangle$ become identical.

5.3.3 Perturbation Theory

In this section, we investigate the possibilities of two-photon processes within our system. According to Fermi's Golden Rule of the standard second-order perturbation theory [94], assuming that initially the system is in the $|\psi_i\rangle$ state, the transition rate to $|\psi_f\rangle$

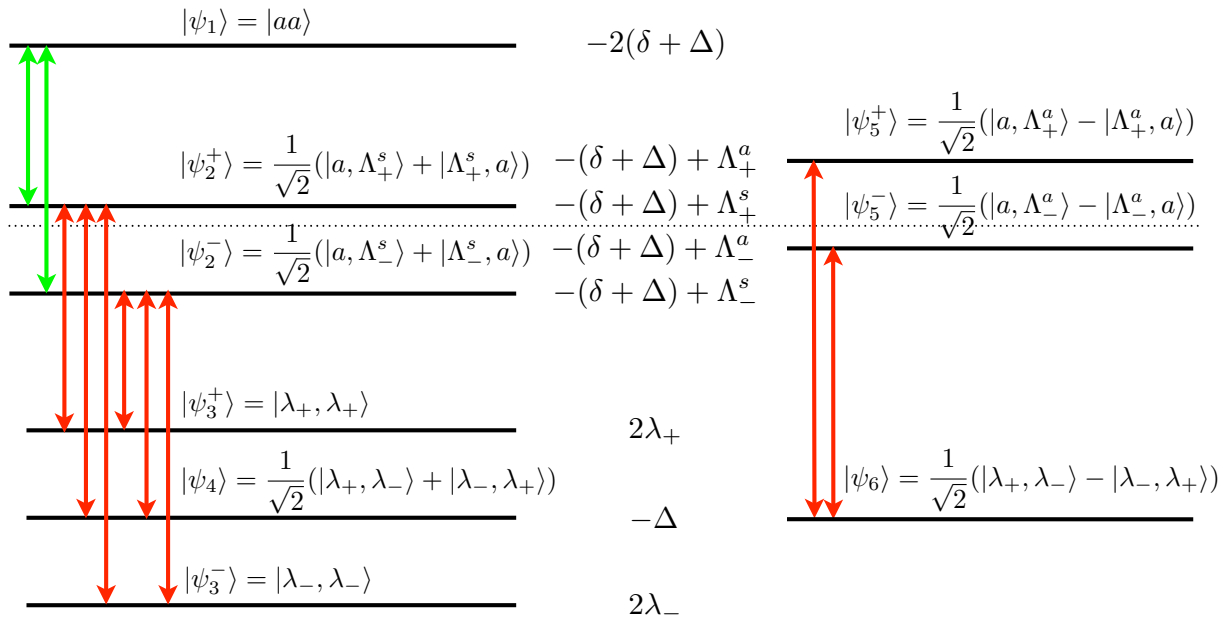

Figure 5.12: Energy levels of the problem. On the left the symmetrical eigenstates, and on the right the antisymmetrical ones. The transitions allowed by the Hamiltonian are shown, others are not permitted. In green, the transitions that contribute to the $|aa\rangle$ level and in red the other one-photon transitions.

through a two-photon process reads one again

$$R_{\psi_i\to\psi_f} = \frac{2\pi}{\hbar^2}\left|\sum_j \frac{\langle\psi_f|W|\psi_j\rangle\langle\psi_j|W|\psi_i\rangle}{\lambda^{(j)}-\lambda^{(i)}}\right|^2 \delta_D(\lambda^{(f)}-\lambda^{(i)}), \tag{5.68}$$

with the same notations as before. Once again, we are not mainly interested in knowing if the transitions are possible and not in the transition rates. For the transition $|\psi_4\rangle \to |\psi_1\rangle$, with the resonance condition $2\delta = -\Delta$, we find

$$\sum_{j=\pm}\frac{\langle\psi_1|W|\psi_2^j\rangle\langle\psi_2^j|W|\psi_4\rangle}{-(\delta+\Delta)+\Lambda_j^s-2\lambda_\pm} = \sum_{j=\pm}\frac{-\sqrt{2}\Omega_1\Omega_2^2\Lambda_j^s(\Delta+2\Lambda_j^s)}{\left((\Lambda_j^s)^2+\Omega_1^2\right)(\Lambda_j^s-\delta-\Delta)\sqrt{\Delta^2+4\Omega_1^2}}, \tag{5.69}$$

$$= \frac{\sqrt{2}\Omega_1\Omega_2^2(2\delta+\Delta)}{(\delta(\delta+\Delta-\Delta\Omega)-\Omega_1^2)\sqrt{\Delta^2+4\Omega_1^2}}, \tag{5.70}$$

which is always zero one the resonance condition. Therefore the transition rate will be zero for any strength of interaction, the destructive interference is preserved from the non-interactive case.

Let us now examine the possible transition $|\psi_3^\pm\rangle \to |\psi_1\rangle$ of resonance condition $\delta =$

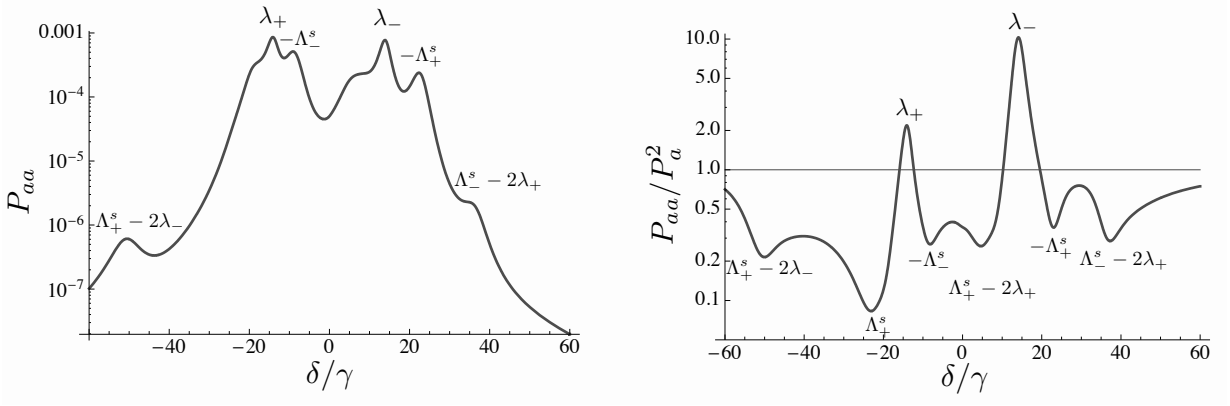

Figure 5.13: Behavior of ρ_{aa} for $\Delta = 0, \Omega_1/\gamma = 14, \Omega_2/\gamma = 1, \gamma_a = \gamma_b = \gamma, \theta = 0, r = 1/10$. The highest peaks appear for the two-photon transitions. All values labeling regions of the plots are in units of γ.

$\Delta - \lambda_\pm$. We have

$$\sum_{j=\pm} \frac{\langle\psi_1|W|\psi_2^j\rangle\langle\psi_2^j|W|\psi_3^\pm\rangle}{\Lambda_j^s - 2\lambda_\pm - (\delta+\Delta)} = \frac{-2\lambda_\pm\Omega_2^2(3\Omega_1^2 + (\Delta-\delta)\lambda_\pm)}{(\lambda_\pm^2+\Omega_1^2)\left(2\lambda_\mp^2 - 2(2\delta-\Delta\Omega)\lambda_\mp + (\delta-\Delta)(\delta-\Delta\Omega) + \Omega_1^2\right)}, \tag{5.71}$$

which are always non-zero when $\delta = \Delta - \lambda_\pm$ for a non-zero Ω_2. Therefore we can always expect those transition to happen in the system.

5.3.4 Dipole Blockade in the Steady State

Let us now measure the dipole blockade in the steady state by measuring P_{aa} and P_{aa}/P_a^2 in function of the detuning δ. Since they are many possible transitions with this system, we chose a value of $\Omega_1/\gamma = 14$ which spreads out as evenly as possible all the resonance conditions, although since we also chose to consider the pump laser on resonance $\Delta = 0$ some of the conditions are already degenerated. We also considered identical dissipation rates $\gamma_a = \gamma_b = \gamma$.

We plotted in Fig. 5.13 both the values of P_{aa} and of the ratio P_{aa}/P_a^2 in function of δ. On the first plot, we labeled the 7 peaks which were clearly visible. The strongest peaks, at $\delta = \lambda_\pm$ are those associated with two-photon processes which populate the $|aa\rangle$ state directly from the less excited states. The next strongest peaks are at the frequencies $\delta = -\Lambda_\pm^s$ which corresponds to both the one-photon transitions populating the $|aa\rangle$ state and the transitions within the antisymmetric states. The other transitions also produce peaks, although some are barely visible, especially the ones associated with the $|\psi_3^\pm\rangle \to |\psi_2^\mp\rangle$ transitions. We also confirm what perturbation theory showed us, i. e. that there is no peak at the frequency $2\delta = -\Delta = 0$.

On the right plot of Fig. 5.13 we represented the quantity P_{aa}/P_a^2. We can easily discriminate the different frequencies for which the system is blockaded or enhanced. Indeed,

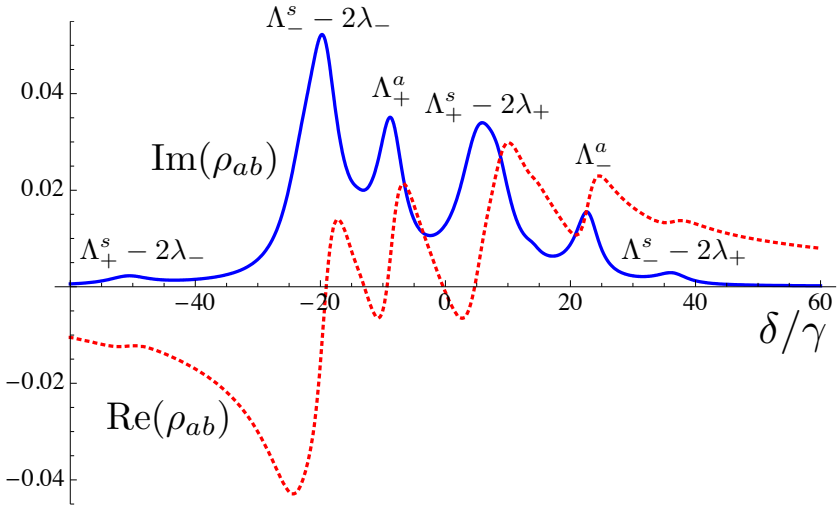

Figure 5.14: The imaginary and real part of ρ_{ab} in function of δ/γ with $\Delta/\gamma = 0, \Omega_1/\gamma = 14, \Omega_2/\gamma = 1, \gamma_a = \gamma_b = \gamma, \theta = 0, r = 1/10$. The number of significant peaks went up to four and we see that there are three windows of transparency, located around the two-photon processes resonance frequencies (not shown). All values labeling regions of the plots are in units of γ.

the only enhanced regions are the one associated with the two two-photon resonances, all the other regions are blockaded. We might have expected an enhancement region around the $|\psi_2^{\pm}\rangle \to |aa\rangle$ transition conditions, but we have already shown that when $\Delta = 0$, the transition conditions happen to coincide with the transitions in the antisymmetric states and since the latter are much more present due to the high population in $|\psi_5\rangle$ the blockade regime prevails.

5.3.5 EIT in the Steady State

Let us now investigate the EIT effect. We plotted the real and imaginary values of ρ_{ab} in function of δ/γ in Fig. 5.14. We see that the addition of the dipole-dipole interaction considerably modified the structure of the EIT effect. Instead of the two peaks and single window of transparency, we observe four main peaks and three windows of transparency. The main two peaks are associated with the $|\psi_3^{\pm}\rangle \to |\psi_2^{\pm}\rangle$ transitions and are also reinforced by the $|\psi_4\rangle \to |\psi_2^{\pm}\rangle$ transitions which are numerically very close and not differentiated on the plot. The next two peaks are associated with the antisymmetric transitions $|\psi_6\rangle \to |\psi_5^{\pm}\rangle$ and the transitions $|\psi_2^{\pm}\rangle \to |\psi_1\rangle$ which play very little role here. Finally, we can make out two very small peaks which are associated with the $|\psi_3^{\pm}\rangle \to |\psi_2^{\mp}\rangle$ transitions, which are weak due to the small coupling term (5.58) in the Hamiltonian.

In between those transition frequencies, in the windows of transparency, we find the frequencies for the two-photon processes which tend to deplete the populations of the $|\psi_2^{\pm}\rangle$

states and therefore lower the number of $|b\rangle \rightarrow |a\rangle$ transitions in the system.

5.3.6 Summary and Discussion

We added to a system of two three-level atoms a dipole-dipole interaction and investigated the effects on the blockade of the $|aa\rangle$ state as well as the EIT effect. The dipole-dipole interaction made a deep change to the structure of the eigenstates of the unperturbed Hamiltonian by modifying the energy levels and definitions of the $|\psi_2^{\pm}\rangle$ and $|\psi_5^{\pm}\rangle$ states. The interaction also allowed an extra transition which added the possibility of two new one-photon transition. It was also shown that the interaction did not modify the inhibition of the $|\psi_4\rangle \rightarrow |\psi_1\rangle$ two-photon transition. Globally, the number of possible transitions in the system grew.

Concerning the blockade, we saw that the dipole-dipole interaction also had the effect of blockading the $|aa\rangle$ state except at the the frequencies associated with the resonance of the two-photon processes. The frequencies associated with the $|\psi_2^{\pm} \rightarrow |aa\rangle\rangle$ would probably have induced some enhancement as well if they were not degenerated with the frequencies of transition within the antisymmetric states when $\Delta = 0$. The amplitude of the blockades in the case of the van der Waals seems a little more intense, which is expected since that interaction directly acts on $|aa\rangle$ and therefore strongly influences its population, unlike the dipole-dipole interaction which only modifies states with a single atom in $|a\rangle$. However, the nature of the interactions being different, such a comparison may not be appropriate. The absence of the two-photon transition $|\psi_4\rangle \rightarrow |\psi_1\rangle$ is most remarked in the study of the blockade of the system.

Unlike previous results obtained with the van der Waals interaction, we found that the dipole-dipole interaction had a very strong effect on EIT. The number of EIT windows grew up to three thanks to the increased number of one-photon resonances provided by the interaction. The main factor for this strong effect was the fact that the interaction spread out the energy levels of the states $|\psi_2^{\pm}\rangle$ and $|\psi_5^{\pm}\rangle$ to four distinct values instead of two. Since those four states are directly coupled with the very populated lower states by one-photon processes, the effects on EIT was strong and the number of absorption peaks was upped from two to four.

Chapter 6

Cavity Mediated Two-Photon Processes in Two Qubits Circuit QED

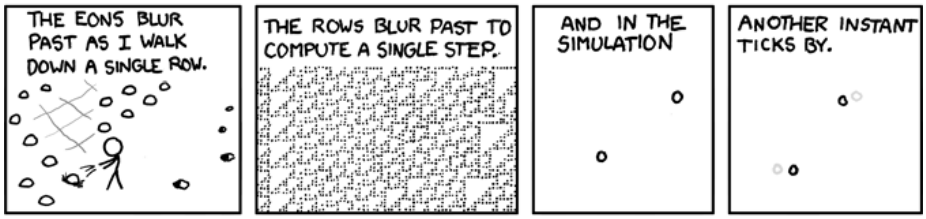

Randall Munroe, *A Bunch of Rocks* (part 7 of 9), `xkcd.com/505/`

In free space, two non-interacting and non-identical atoms immersed in a laser field will never be excited simultaneously. This results from a destructive interference phenomenon in the two-photon absorption process of the two atoms in the laser. The two quantum paths underlying the double excitation (one atom excited first, then the second, and vice-versa) interfere destructively precisely when the laser frequency matches the resonance condition for the excitation of the two atoms [95]. This interference effect can be interestingly annulled if the two atoms are within a distance much smaller than the wavelength of the transition [54, 58, 96]. In this case dipole-dipole interaction comes into play and breaks the destructive character of the interference, resulting in a possible simultaneous excitation of the two atoms.

In Ref. [95], the indirect interaction between two atoms placed in a lossless single mode cavity is exploited to obtain a similar cancellation of the destructive interference effect. Here, we wish to extend significantly that initial proposal by considering the huge potentialities offered by circuit-QED systems. Our model is intended to provide realistic experimental predictions by considering dissipation and steady-state regimes using a driving field. A perturbative approach is first proposed to grasp the essentials of the underlying physics in an idealized case.

The organization of the chapter is as follows. In Section 6.1, we introduce the free space case for future comparison with the cavity case and show why simultaneous excitation is not possible in free space. In Sec. 6.2 we give our Hamiltonian for the atoms imbedded in the cavity which includes the modelization of two internal states and transitional frequency for each atom, the electromagnetic field mode of the cavity, the coupling between the atoms and the field and finally the driving laser field. We also introduce the master equation which modelizes spontaneous emission or dissipation effects in the atoms as well as the photon loss of the cavity.

In Sec. 6.3, we introduce a constraint that allows the diagonalization of the undriven Hamiltonian. Thanks to the diagonalization we are able to understand the structure of the dressed states and we can use perturbation theory to predict two-photon transition rates in the system. Then, after discussing some numerical issues, we study one and two-photon spectra as well as the population of the excited atoms in the steady states of the system numerically found with the master equation. We study some effects of the cavity decay rate that could not be including in the perturbation theory analysis.

In Sec. 6.4, we drop the constraint previously used, which lifts degeneracies, and although we lose the analytical description of the system (except for the particular case of identical atoms) we still use the master equation to calculate atomic, one and two-photon spectra of the system. We compare the general system with the constrained one and confirm several observations. We also observe a new effect in the system, the cavity induced transparency.

In Sec. 6.5, we give a summary of all the theoretical predictions we could make and we discuss the possibility of experimental observation of said predictions.

6.1 Atoms in Free Space

Before considering two atoms immersed in a cavity and two-photon processes, we first consider the problem of two atoms in free space excited by a laser and show that in that kind of system, two-photon processes are prohibited.

Let us consider two non-interacting atoms with internal levels $|e_i\rangle$ and $|g_i\rangle$ $(i = 1, 2)$ of transition frequency ω_1 and ω_2 and single atom spontaneous emission rate $2\gamma_i$. They are excited by a non-resonant laser field of wave vector $\mathbf{k}_L$, Rabi frequency 2ϵ and driving frequency ω. The Hamiltonian H_f of the system, where f stands for *free*, is

$$H_f = \sum_{i=1}^{2} \left(\hbar(\omega_i - \omega)\sigma_i^z + \hbar\epsilon \left(e^{i\mathbf{k}_L\cdot\mathbf{x}_i}\sigma_i^+ + e^{-i\mathbf{k}_L\cdot\mathbf{x}_i}\sigma_i^- \right) \right), \tag{6.1}$$

where $\sigma_i^+ = (\sigma_i^-)^\dagger$ is the atom raising operator $|e_i\rangle\langle g_i|$ and σ_i^z the atomic inversion operator $(|e_i\rangle\langle e_i| - |g_i\rangle\langle g_i|)/2$. We assume that the atoms are placed such that $\mathbf{k}_L \cdot \mathbf{x}_1 = \mathbf{k}_L \cdot \mathbf{x}_2 = 0$.

When considering dissipation in the Markov and Born approximation, the time evolu-

tion of the system is governed by the master equation

$$\dot{\rho} = -\frac{i}{\hbar}[H,\rho] - \sum_{i=1}^{2} \gamma_i(\sigma_i^+\sigma_i^-\rho + \rho\sigma_i^+\sigma_i^- - 2\sigma_i^-\rho\sigma_i^+), \tag{6.2}$$

We now treat the laser as a perturbation by considering a small ϵ. According to Fermi's Golden Rule of the standard second-order perturbation theory [94], the $|gg\rangle \to |ee\rangle$ transition rate through a strict two-photon process reads

$$R_{gg\to ee} = \frac{2\pi}{\hbar^4}|W^{(2)}_{(gg,ee)}|^2\delta(\omega_1+\omega_2-2\omega), \tag{6.3}$$

with

$$W^{(2)}_{(gg,ee)} = \sum_{j=eg,ge} \frac{\langle ee|H|j\rangle\langle j|H|gg\rangle}{\omega_j - \omega}, \tag{6.4}$$

where here the sum is restricted to the one-excitation $|eg\rangle$ and $|ge\rangle$ states, since they are the only ones to be simultaneously coupled by the perturbation to the $|gg\rangle$ and $|ee\rangle$ states.

Calculating $W^{(2)}_{(gg,ee)}$ is straightforward, we find

$$\begin{aligned} W^{(2)}_{(gg,ee)} &= \frac{\langle ee|H|eg\rangle\langle eg|H|gg\rangle}{\omega_1-\omega} + \frac{\langle ee|H|ge\rangle\langle ge|H|gg\rangle}{\omega_2-\omega}, &(6.5)\\ &= \frac{\hbar^2\epsilon^2}{\omega_1-\omega} + \frac{\hbar^2\epsilon^2}{\omega_2-\omega}, &(6.6)\\ &= \hbar^2\epsilon^2\frac{2\omega-\omega_1-\omega_2}{(\omega_1-\omega)(\omega_2-\omega)}, &(6.7)\end{aligned}$$

which is equal to zero when $2\omega = \omega_1 + \omega_2$. We can see that, due to the destructive interference between the two possible excitation paths $|gg\rangle \to |eg\rangle \to |ee\rangle$ and $|gg\rangle \to |ge\rangle \to |ee\rangle$, the simultaneous excitation of both atoms is prohibited.

The system in its steady state can be can be found posing that the master equation (6.2) is zero. The system can actually be decomposed in two subsystems whose master equation can be solved individually. The steady state solution of two atoms excited in free space is

$$\rho_f^S = \rho_1^S \otimes \rho_2^S, \tag{6.8}$$

with

$$\rho_i^S = \frac{1}{2\epsilon^2+\gamma_i^2+(\omega_i-\omega)^2}\left(|\phi_i\rangle\langle\phi_i| + \epsilon^2|g_i\rangle\langle g_i|\right), \tag{6.9}$$

with the unnormalized

$$|\phi_i\rangle = \epsilon|e_i\rangle - (\omega_i - \omega + i\gamma)|g_i\rangle. \tag{6.10}$$

The populations of each excited atoms are

$$P_{e_i} = \frac{\epsilon^2}{2\epsilon^2+\gamma_i^2+(\omega_i-\omega)^2}, \tag{6.11}$$

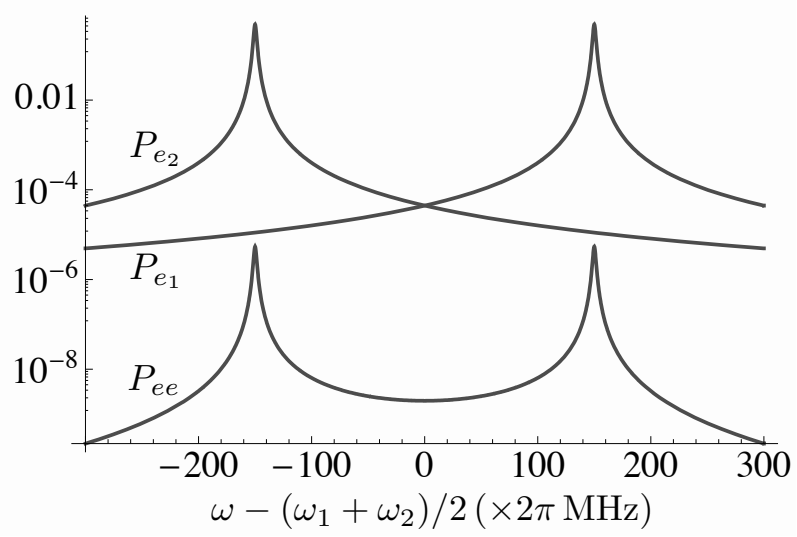

Figure 6.2: Populations of $|e_1\rangle, |e_2\rangle$ and $|ee\rangle$ in the steady state with $(\omega_1 - \omega_2)/2 = 150 \times 2\pi\,\mathrm{MHz}, \epsilon = 2\pi\,\mathrm{MHz}, \gamma = 0.2 \times 2\pi\,\mathrm{MHz}$. There are two peaks located at the frequencies of the individual atoms and none at the frequency $2\omega = \omega_1 + \omega_2$.

and the population in the $|ee\rangle$ state is $P_{ee} = P_{e_1} P_{e_2}$ since the atoms are independent.

We represented in Fig. 6.2 those populations. We see that there is no particular peak at the two-photon transition frequency 2ω, which was expected since due to the interference, there can be no two-photon process there. The numerical values and units do not actually apply to real atomic frequencies, but rather to superconducting qubits frequencies existing in circuit QED experiments, as in [97]. Such qubits are modelized exactly the same way as two-level atoms and are easily manipulated when embedded in a microwave resonator, which is the setup we investigate in the rest of the chapter.

It has been shown that some kind of interaction may counteract the interference and allow two-photon processes to happen [54]. In the next sections, we investigate the possibility of allowing two-photon processes by immersing the atoms in a cavity and letting them interact through the cavity coupling.

6.2 Atoms Embedded in a Cavity

We now consider two atoms 1 and 2 with internal levels $|e_i\rangle$ and $|g_i\rangle$ $(i = 1, 2)$ of transition frequency ω_i and spontaneous emission rate 2γ (identical for both atoms). The two atoms are embedded in a single mode cavity of resonance frequency ω_c and decay rate 2κ. The two atoms are supposed to be identically coupled to the cavity with a coupling constant α. The cavity is driven by a non-resonant laser field of amplitude ϵ and driving frequency ω (see Fig. 6.3). The two atoms are considered sufficiently far apart so that there is no direct interaction of any kind between them but through the cavity coupling. That situation is encountered in most circuit-QED systems, like, e.g., in the experimental

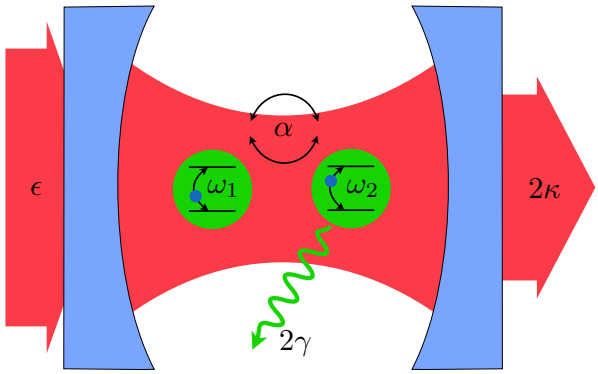

Figure 6.3: Schematic of the two-atom system immersed in a single-mode cavity. Two two-level atoms of transition frequencies ω_1 and ω_2 are identically coupled to the cavity mode of frequency ω_c with a coupling constant α. The cavity has a photon decay rate 2κ, while the atoms have a spontaneous emission rate 2γ. The cavity mode is being driven by a laser of strength ϵ and frequency ω.

setup reported in Ref. [97] where the qubits are several hundred micrometers apart.

In the rotating-wave approximation, the coherent evolution of the system is described by the interaction Hamiltonian

$$H = \hbar(\omega_c - \omega)a^\dagger a + \sum_{i=1}^{2} \hbar(\omega_i - \omega)\sigma_i^z + \sum_{i=1}^{2} \hbar\alpha(a\sigma_i^+ + a^\dagger\sigma_i^-) + i\hbar\epsilon(a^\dagger - a), \tag{6.12}$$

where a [$a^\dagger$] is the photon annihilation [creation] operator for the cavity field mode, $\sigma_i^+ = (\sigma_i^-)^\dagger$ $(i = 1, 2)$ is the atom raising operator $|e_i\rangle\langle g_i|$, and σ_i^z is the atomic inversion operator $(|e_i\rangle\langle e_i| - |g_i\rangle\langle g_i|)/2$.

When considering dissipation in the Markov and Born approximation, the time evolution of the density operator ρ of the system is governed by the master equation [69]

$$\dot{\rho} = \frac{1}{i\hbar}[H, \rho] - \kappa(a^\dagger a\rho - 2a\rho a^\dagger + \rho a^\dagger a) - \sum_{i=1}^{2} \gamma(\sigma_i^+\sigma_i^-\rho - 2\sigma_i^-\rho\sigma_i^+ + \rho\sigma_i^+\sigma_i^-). \tag{6.13}$$

This time evolution leads invariably to a steady-state ρ^S of the system that is determined by equating the left-hand side term of Eq. (6.13) to zero. We denote hereafter by $|N, xy\rangle \equiv |N\rangle \otimes |x_1\rangle \otimes |y_2\rangle$ the bare basis elements of the atom-cavity system, with N the photon number and $x, y \in \{e, g\}$.

First, we may want to study the Hamiltonian of the system using a perturbative approach to grasp the essentials of the physics of the system. The driving laser field defines the perturbation and the unperturbed Hamiltonian is given by Eq. (6.12) with ϵ and ω set to 0. Let us show that H commutes with the global excitation number operator $\hat{n} \equiv a^\dagger a + \sum_i \sigma_i^z + 1$, which counts the number of photons in the system plus the number

of excited atoms. Obviously, $\hat{n}$ commutes with the first two terms of the Hamiltonian, we are left with

$$\begin{aligned}
[\hat{n}, H] &= [a^\dagger a + \sum_i \sigma_i^z, \hbar\alpha \sum_i (a\sigma_i^+ + a^\dagger \sigma_i^-)], && (6.14)\\
&= \hbar\alpha \sum_i [a^\dagger a, a\sigma_i^+ + a^\dagger \sigma_i^-] + \hbar\alpha \sum_i [\sigma_i^z, a\sigma_i^+ + a^\dagger \sigma_i^-], && (6.15)\\
&= \hbar\alpha \sum_i \left(-a\sigma_i^+ + a^\dagger \sigma_i^-\right) + \hbar\alpha \sum_i \left(a\sigma_i^+ - a^\dagger \sigma_i^-\right), && (6.16)\\
&= 0, && (6.17)
\end{aligned}$$

where we used the properties $[a^\dagger a, a] = [a^\dagger, a]a = -a$, $[a^\dagger a, a^\dagger] = a^\dagger [a, a^\dagger] = a^\dagger$ and $[\sigma_i^z, \sigma_j^\pm] = \pm\delta_{ij}\sigma_i^\pm$. It follows that in the $|N, xy\rangle$ bare basis of the atom-cavity system, the unperturbed Hamiltonian has a block-diagonal form, with blocks associated with the global excitation number $n = N + m(x, y)$, where $m(x, y)$ is the number of excited atoms in the $|x, y\rangle$ state ($m = 0$, 1, or 2).

For $n = 0$, the dimension of the diagonal block is 1×1, in association with the only bare basis element $|0\rangle \equiv |0, gg\rangle$. For $n = 1$, the diagonal block is of 3×3 dimension with the 3 basis elements $|1, gg\rangle$, $|0, eg\rangle$, and $|0, ge\rangle$. From $n \geq 2$, the diagonal blocks are of 4×4 dimension in association with the 4 basis elements $|n, gg\rangle$, $|n-1, eg\rangle$, $|n-1, ge\rangle$, and $|n-2, ee\rangle$. The eigenstates and eigenvalues of the unperturbed Hamiltonian yield, respectively, the dressed states of the two-atom-cavity system and their energy. They follow immediately from the block diagonalization.

6.3 Even Atomic Frequency Spread

The diagonalization of the unperturbed Hamiltonian is possible to realize analytically if we make the assumption that

$$\omega_1 + \omega_2 = 2\omega_c, \tag{6.18}$$

in which case we define the frequency difference $\Delta \equiv (\omega_1 - \omega_2)/2$. This means that the frequencies of the atoms are evenly spread around the cavity mode frequency, at the frequencies $\omega_c \pm \Delta$.

6.3.1 Eigenstates and Eigenvalues

Let us now show the results of the block diagonalizations. For $n = 0$, $|0\rangle$ is the only eigenstate with an eigenvalue 0. For $n \geq 1$, the eigenvalues read with respect to the ground state energy

$$\hbar\lambda^{(n,0)} = n\hbar\omega_c, \quad \hbar\lambda^{(n,\pm)} = n\hbar\omega_c \pm \hbar\lambda_n, \tag{6.19}$$

with $\hbar\lambda^{(n,0)}$ twice degenerated for $n \geq 2$ and where

$$\lambda_n = \sqrt{2(2n-1)\alpha^2 + \Delta^2}. \tag{6.20}$$

For $n = 1$, the three associated eigenvectors are, respectively,

$$|1,0\rangle = \frac{1}{\lambda_1}\left(\Delta|1,gg\rangle - \sqrt{2}\alpha|\psi_1^-\rangle\right), \tag{6.21}$$

$$|1,\pm\rangle = \frac{1}{\sqrt{2}\lambda_1}\left(\sqrt{2}\alpha|1,gg\rangle + \Delta|\psi_1^-\rangle \pm \lambda_1|\psi_1^+\rangle\right), \tag{6.22}$$

and, for $n \geq 2$, respectively,

$$|n,0_a\rangle = \sqrt{\frac{n-1}{2n-1}}|n,gg\rangle - \sqrt{\frac{n}{2n-1}}|n-2,ee\rangle, \tag{6.23}$$

$$|n,0_b\rangle = \frac{1}{\lambda_n}\left(\Delta|\phi_n\rangle - \sqrt{2(2n-1)}\alpha|\psi_n^-\rangle\right), \tag{6.24}$$

$$|n,\pm\rangle = \frac{1}{\sqrt{2}\lambda_n}\left(\sqrt{2(2n-1)}\alpha|\phi_n\rangle + \Delta|\psi_n^-\rangle \pm \lambda_n|\psi_n^+\rangle\right), \tag{6.25}$$

with, for $n \geq 1$,

$$|\psi_n^\pm\rangle = \frac{1}{\sqrt{2}}\left(|n-1,eg\rangle \pm |n-1,ge\rangle\right), \tag{6.26}$$

and, for $n \geq 2$,

$$|\phi_n\rangle = \sqrt{\frac{n}{2n-1}}|n,gg\rangle + \sqrt{\frac{n-1}{2n-1}}|n-2,ee\rangle. \tag{6.27}$$

The energy structure is shown on Fig. 6.4. If we turn on the laser perturbation term W of the Hamiltonian defined as

$$W = i\hbar\epsilon(a^\dagger - a), \tag{6.28}$$

the structure of H ceases to be diagonal in the eigenstate basis. The off-diagonal, perturbation terms coming from the laser are expressed, in the unperturbed Hamiltonian eigenstates base, as, for the $n = 0 \to n = 1$ transitions

$$\langle 0|W|1,0\rangle = -i\frac{\Delta}{\lambda_1}\epsilon, \tag{6.29}$$

$$\langle 0|W|1,\pm\rangle = -i\frac{\alpha}{\lambda_1}\epsilon. \tag{6.30}$$

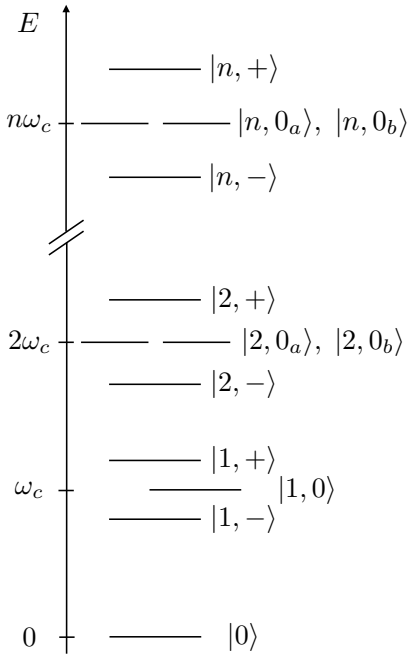

Figure 6.4: Energy diagram for the dressed states of the two-atom-cavity system when $\omega_1 + \omega_2 = 2\omega_c$.

The $n = 1 \rightarrow n = 2$ transitions are written

$$\langle 1,0|W|2,0_a\rangle = -i\sqrt{\frac{2}{3}}\,\frac{\Delta}{\lambda_1}\,\epsilon, \tag{6.31}$$

$$\langle 1,0|W|2,0_b\rangle = -\frac{2i}{\sqrt{3}}\,\frac{3\alpha^2+\Delta^2}{\lambda_1\lambda_2}\,\epsilon, \tag{6.32}$$

$$\langle 1,0|W|2,\pm\rangle = -i\,\frac{\alpha\Delta}{\lambda_1\lambda_2}\,\epsilon, \tag{6.33}$$

$$\langle 1,\pm|W|2,0_a\rangle = -i\sqrt{\frac{2}{3}}\,\frac{\alpha}{\lambda_1}\,\epsilon, \tag{6.34}$$

$$\langle 1,\pm|W|2,0_b\rangle = \frac{i}{\sqrt{3}}\,\frac{\alpha\Delta}{\lambda_1\lambda_2}\,\epsilon, \tag{6.35}$$

$$\langle 1,\pm|W|2,\pm\rangle = -\frac{i}{4}\,\frac{(\lambda_1+\lambda_2)^2}{\lambda_1\lambda_2}\,\epsilon, \tag{6.36}$$

$$\langle 1,\pm|W|2,\mp\rangle = -\frac{i}{4}\,\frac{(\lambda_1-\lambda_2)^2}{\lambda_1\lambda_2}\,\epsilon. \tag{6.37}$$

Finally, the $n \to n+1$ transitions with $n \geq 2$ are written

$$\langle n, 0_a|W|n+1, 0_a\rangle = -2i\sqrt{\frac{n(n^2-1)}{4n^2-1}}\,\epsilon, \tag{6.38}$$

$$\langle n, 0_a|W|n+1, 0_b\rangle = -i\sqrt{\frac{n-1}{4n^2-1}}\,\frac{\Delta}{\lambda_{n+1}}\,\epsilon, \tag{6.39}$$

$$\langle n, 0_a|W|n+1, \pm\rangle = -i\sqrt{\frac{n-1}{2n-1}}\,\frac{\alpha}{\lambda_{n+1}}\,\epsilon, \tag{6.40}$$

$$\langle n, 0_b|W|n+1, 0_a\rangle = -i\sqrt{\frac{n+1}{4n^2-1}}\,\frac{\Delta}{\lambda_n}\,\epsilon, \tag{6.41}$$

$$\langle n, 0_b|W|n+1, 0_b\rangle = -i\sqrt{\frac{n}{4n^2-1}}\,\frac{(n+1)\lambda_n^2+(n-1)\lambda_{n+1}^2}{\lambda_n\lambda_{n+1}}\,\epsilon, \tag{6.42}$$

$$\langle n, 0_b|W|n+1, \pm\rangle = -i\,\frac{\alpha\Delta}{\lambda_n\lambda_{n+1}}\,\epsilon, \tag{6.43}$$

$$\langle n, \pm|W|n+1, 0_a\rangle = -i\sqrt{\frac{n+1}{2n+1}}\,\frac{\alpha}{\lambda_n}\,\epsilon, \tag{6.44}$$

$$\langle n, \pm|W|n+1, 0_b\rangle = i\sqrt{\frac{n}{2n+1}}\,\frac{\alpha\Delta}{\lambda_n\lambda_{n+1}}\,\epsilon, \tag{6.45}$$

$$\langle n, \pm|W|n+1, \pm\rangle = -i\frac{\sqrt{n}}{4}\,\frac{(\lambda_n+\lambda_{n+1})^2}{\lambda_n\lambda_{n+1}}\,\epsilon, \tag{6.46}$$

$$\langle n, \pm|W|n+1, \mp\rangle = -i\frac{\sqrt{n}}{4}\,\frac{(\lambda_n-\lambda_{n+1})^2}{\lambda_n\lambda_{n+1}}\,\epsilon. \tag{6.47}$$

$$\tag{6.48}$$

From the matrix elements, we identify three one-photon transitions from the ground state at frequencies ω_c and $\omega_c \pm \lambda_1$ and two two-photon transitions $|0\rangle \to |2, \pm\rangle$ at frequencies $\omega_c \pm \lambda_2/2$. Unlike the free space case, the transition at $2\omega = \omega_1 + \omega_2 = 2\omega_c$ which corresponds to $|0\rangle \to |2, 0_{a,b}\rangle$ does not identify as two-photon processes but rather to stepwise one-photon transitions through the intermediate state $|1, 0\rangle$ with photons at frequency ω_c.

In general, n-photon transitions to the states $|n, \pm\rangle$ at the frequencies $\omega_c \pm \lambda_n/n$ are conceivable, although the transition rates are proportional to ϵ^{2n} in the perturbation regime.

6.3.2 Perturbative Approach

We now consider the action of the driving field at frequency ω and investigate the possibility of getting both atoms excited through strict two-photon processes, a result that is not achievable when the two atoms are solely in free space. Here, the two-photon transitions $|0\rangle \to |2, \pm\rangle$ make this possible because of the $|0, ee\rangle$ component of the upper states $|2, \pm\rangle$.

According to Fermi's Golden Rule of the standard second-order perturbation theory [94], the $|0\rangle \to |0, ee\rangle$ transition rate through a strict two-photon process reads

$$R_{gg\to ee} = \frac{2\pi}{\hbar^4}|\langle 0, ee|2, \pm\rangle|^2 |W^{(2)}_{0,(2,\pm)}|^2 \delta(\lambda^{(2,\pm)} - 2\omega), \tag{6.49}$$

with

$$W^{(2)}_{0,(2,\pm)} = \sum_{j=0,\pm} \frac{\langle 2, \pm|W|1, j\rangle\langle 1, j|W|0\rangle}{\lambda^{(1,j)} - \omega}, \tag{6.50}$$

where here the sum is only restricted to the one-excitation $|1, j\rangle$ states, since they are the only ones to be simultaneously coupled by the perturbation W to the $|0\rangle$ and $|2, \pm\rangle$ states.

In Eq. (6.49), the δ-function yields the two-photon resonance condition $\omega = \omega_c \pm \lambda_2/2$ that must be fulfilled to get the sought double-excitation process. Let us first calculate

$$\langle 2, \pm|W|1, 0\rangle\langle 1, 0|W|0\rangle = -\frac{\alpha\Delta^2}{\lambda_1^2\lambda_2}\,\epsilon^2, \tag{6.51}$$

$$\langle 2, \pm|W|1, \pm\rangle\langle 1, \pm|W|0\rangle = -\frac{1}{4}\,\frac{\alpha(\lambda_1 + \lambda_2)^2}{\lambda_1^2\lambda_2}\,\epsilon^2, \tag{6.52}$$

$$\langle 2, \pm|W|1, \mp\rangle\langle 1, \mp|W|0\rangle = -\frac{1}{4}\,\frac{\alpha(\lambda_1 - \lambda_2)^2}{\lambda_1^2\lambda_2}\,\epsilon^2. \tag{6.53}$$

We then have

$$W^{(2)}_{0,(2,\pm)} = -\frac{\alpha\epsilon^2}{\lambda_1^2\lambda_2}\left(\frac{\Delta^2}{\omega_c - \omega} + \frac{(\lambda_1 \pm \lambda_2)^2}{4(\omega_c - \omega + \lambda_1)} + \frac{(\lambda_1 \mp \lambda_2)^2}{4(\omega_c - \omega - \lambda_1)}\right), \tag{6.54}$$

$$= -\frac{\alpha\epsilon^2}{\lambda_2}\,\frac{\Delta^2 + (\omega_c - \omega)\,(\lambda_2 \mp 2(\omega_c - \omega))}{(\omega_c - \omega)(\omega_c - \omega + \lambda_1)(\omega_c - \omega - \lambda_1)}, \tag{6.55}$$

which gives, at the resonance condition $\omega = \omega_c \pm \lambda_2/2$ and after a few simplifications

$$R_{gg\to ee} = 2\pi f(r)\frac{\epsilon^4}{\Delta^2}\delta(\lambda^{(2,\pm)} - 2\omega), \tag{6.56}$$

where $r = \alpha/\Delta$ and

$$f(r) = \frac{2304 r^8}{(1 + 6r^2)^3(3 + 2r^2)^2}. \tag{6.57}$$

As expected, this rate is strongly dependent on the coupling constant α and on the spread 2Δ in atomic frequencies, but there will be two-photon transitions as long as the atoms are coupled with the cavity. For $r \ll 1$, the rate behaves as r^8, while it behaves as r^{-2} for $r \gg 1$. The optimal rate is obtained for $r \sim 1.51$ that yields $2\pi f(r) \sim 2.16$.

When the atoms are identical, i. e. when $\Delta = 0$, the $|0\rangle \to |2, \pm\rangle$ transitions still take place, at the transition rate

$$R_{gg\to ee}(\Delta = 0) = 2\pi\frac{8\epsilon^4}{3\alpha^2}\delta(\lambda^{(2,\pm)} - 2\omega). \tag{6.58}$$

Let us examine the possible transitions at $\omega = \omega_c$ when the atoms are identical. We note that when this is the case, the system becomes symmetric with the exchange of the two atoms. It is easy to see that the states $|1,0\rangle$ and $|n,0_b\rangle$ are now antisymmetric with the exchange of the atoms while the other states are symmetric. It is apparent from the perturbation terms in the Hamiltonian that the antisymmetric states only couple to each other and are completely decoupled from the symmetric states, including the ground state, and should therefore never be populated. In other words, since $\langle 0|W|1,0\rangle = 0$, the only one-photon transition from the ground state at $\omega = \omega_c$ is impossible. The two-photon process $|0\rangle \to |2,0_b\rangle$ is also impossible since $W^{(2)}_{0,(2,0_b)}$ is always zero, as we have $\langle 2,0_b|W|1,\pm\rangle = 0$.

There might still remain the possibility of a transition at $\omega = \omega_c$ if the $|2,0_a\rangle$ state is populated from the ground state by a two-photon process. The rate of this process is proportional to $|W^{(2)}_{0,(2,0_a)}|^2$, with

$$
\begin{aligned}
W^{(2)}_{0,(2,0_b)} &= \sum_{j=\pm} \frac{\langle 2,0_b|W|1,j\rangle\langle 1,j|W|0\rangle}{\lambda^{(1,j)} - \omega}, && (6.59)\\
&= \frac{\langle 2,0_a|W|1,+\rangle\langle 1,+|W|0\rangle}{\omega_c - \omega + \lambda_1} + \frac{\langle 2,0_a|W|1,-\rangle\langle 1,-|W|0\rangle}{\omega_c - \omega + \lambda_1}, && (6.60)\\
&= -\sqrt{\frac{2}{3}}\frac{\alpha^2\epsilon^2}{\lambda_1^2\lambda_2}\left(\frac{1}{\omega_c - \omega + \lambda_1} + \frac{1}{\omega_c - \omega + \lambda_1}\right), && (6.61)\\
&= -\sqrt{\frac{2}{3}}\frac{\alpha^2\epsilon^2}{\lambda_1^2\lambda_2}\frac{2(\omega_c - \omega)}{(\omega_c - \omega + \lambda_1)(\omega_c - \omega - \lambda_1)}, && (6.62)\\
& && (6.63)
\end{aligned}
$$

which is always zero on the resonance condition $\omega = \omega_c$. Therefore no transition takes place at the atomic frequencies when they are identical.

Here, we investigated the transition rates for both atoms to simultaneously go from their ground state to their excited state. We may also be interested in the possibility of the number of photons in the cavity going from $N = 0$ to $N = 2$ instantly. The golden rule (6.49) may be modified to calculate such a two-photon process. Since the ground state is the same for atoms or photons, one just needs to replace the $|\langle 0, ee|2,\pm\rangle|^2$ term which calculates the proportion of $|ee\rangle$ state in $|2,\pm\rangle$ by $\langle 2,\pm|(a^\dagger)^2a^2|2,\pm\rangle$ which calculates the number of pairs of photons in $|2,\pm\rangle$. The $W^{(2)}_{0,(2,\pm)}$ needs no modification, therefore all qualitative result on $|gg\rangle \to |ee\rangle$ also applies to the photon sates $|N=0\rangle \to |N=2\rangle$.

6.3.3 Master Equation Approach

In this section, we refine our analysis by using a more general, although numerical, method to investigate the behavior of the system. A master equation approach is used, into which dissipations such as atomic spontaneous emission and cavity loss are considered. We numerically solve the master equation for the steady state of the system and measure different observables. The results obtained will be interpreted in light of the perturbative

Parameter	Value ($\times 2\pi$ MHz)
Δ	0, 150
α	85
ϵ	6
κ	6.8
γ	0.2

Table 6.1: Numerical values used in the numerical processes, unless stated otherwise.

approach of the previous section and we will show that two-photon processes are indeed allowed in the present system.

Numerical Considerations

Here, we discuss the numerical methods used to calculate the following results. In order to obtain results as realistic as possible, we chose to give to our parameters values close to what has been used in recent circuit QED experiments, as in [97]. The typical values we used are listed in Tab. 6.1, unless stated otherwise.

Our goal in this chapter is to highlight the two-photon processes, which are proportional to ϵ^4, compared to the one-photon processes, proportional to ϵ^2 in the perturbation regime. With that in mind, it makes sense to choose a high laser power in order to increase the visibility of the two-photon transitions. However, as the strength of the laser probing the system is increased, more and more excitation modes are being populated and for numerical purposes we cannot use an infinite vector basis for the photon number $|N\rangle$. Therefore, we need to make approximations in order to solve the master equation by cutting off the excitation number to a maximum $n_{\max}$. Unfortunately, with a truncated basis for high laser power the populations come numerically to a saturation and harmonization of all the different populations in the density matrix. We need a way to evaluate this effect in order to chose a laser power as high as possible which still minimizes numerical errors.

It would possible to estimate the saturation effect in the numerical process by comparing the number of photons calculated for an empty cavity to the number it should really have, which can be calculated analytically for an infinite basis. Indeed, the master equation relating to an empty cavity is written

$$\dot{\rho} = \frac{1}{i\hbar}[H_0, \rho] - \kappa(a^\dagger a\rho - 2a\rho a^\dagger + \rho a^\dagger a), \tag{6.64}$$

with the excited empty cavity Hamiltonian

$$H_0 = \hbar(\omega_c - \omega)a^\dagger a + i\hbar\epsilon(a^\dagger - a). \tag{6.65}$$

The time variation of any operator A is calculated using Eq. (6.64) as

$$\begin{aligned}
\frac{d}{dt}\langle A\rangle &= \mathrm{Tr}\left(A\dot{\rho}\right), && (6.66)\\
&= -i(\omega_c-\omega)\mathrm{Tr}\left(Aa^\dagger a\rho - A\rho a^\dagger a\right) + \epsilon\mathrm{Tr}\left(Aa^\dagger\rho - A\rho a^\dagger - Aa\rho + A\rho a\right)\\
&\quad -\kappa\mathrm{Tr}\left(Aa^\dagger a\rho\right) + 2\kappa\mathrm{Tr}\left(Aa\rho a^\dagger\right) - \kappa\mathrm{Tr}\left(A\rho a^\dagger a\right), && (6.67)\\
&= -i(\omega_c-\omega)\langle[A,a^\dagger a]\rangle + \epsilon\left(\langle[A,a^\dagger]\rangle - \langle[A,a]\rangle\right)\\
&\quad -\kappa\left(\langle Aa^\dagger a - 2a^\dagger Aa + a^\dagger aA\rangle\right), && (6.68)
\end{aligned}$$

where we used the invariance of the trace under cyclic permutations of the operators it act on. If we want to calculate the time variation of the mean number of photons, we have $A = a^\dagger a$ and we calculate

$$[A,a^\dagger a] = 0,\ \ [A,a^\dagger] = a^\dagger[a,a^\dagger] = a^\dagger,\ \ [A,a] = -[a,a^\dagger]a = a, \quad (6.69)$$

$$Aa^\dagger a - 2a^\dagger Aa + a^\dagger aA = 2(a^\dagger aa^\dagger a - a^\dagger a^\dagger aa) = 2a^\dagger[a,a^\dagger]a = 2a^\dagger a, \quad (6.70)$$

where we used the commutation relation $[a,a^\dagger] = 1$. We finally find

$$\frac{d}{dt}\langle a^\dagger a\rangle = \epsilon(\langle a^\dagger\rangle + \langle a\rangle) - 2\kappa\langle a^\dagger a\rangle. \quad (6.71)$$

Let us also calculate the time variation of the annihilation operator $A = a$. We have

$$[A,a^\dagger a] = [a,a^\dagger]a = -a,\ \ [A,a^\dagger] = 1,\ \ [A,a] = 0, \quad (6.72)$$

$$Aa^\dagger a - 2a^\dagger Aa + a^\dagger aA = aa^\dagger a - a^\dagger aa = a[a,a^\dagger] = a, \quad (6.73)$$

and we find

$$\frac{d}{dt}\langle a\rangle = -i(\omega_c-\omega)\langle a\rangle + \epsilon - \kappa\langle a\rangle, \quad (6.74)$$

and $\frac{d}{dt}\langle a^\dagger\rangle$ is the complex conjugate of $\frac{d}{dt}\langle a\rangle$. At the system equilibrium, the time variations are null and as we solve the system we find for the steady state

$$\langle a^\dagger a\rangle = \frac{\epsilon^2}{\kappa^2 + (\omega_c-\omega)^2}. \quad (6.75)$$

Now we can compare the value we numerically obtain from the steady state using a truncated basis to (6.75) to get an idea of the saturation effect. In this work, we always consider excitation numbers going up to $n_{\max} = 5$. When the cavity is empty and on resonance, which is obtained by setting $\alpha = 0$ and $\omega_c = \omega$, we find, using the parameter values shown in Table 6.1, a difference with Eq. (6.75) of $\sim 0.5\%$. We did not use a higher power laser, to prevent going beyond that margin of error.

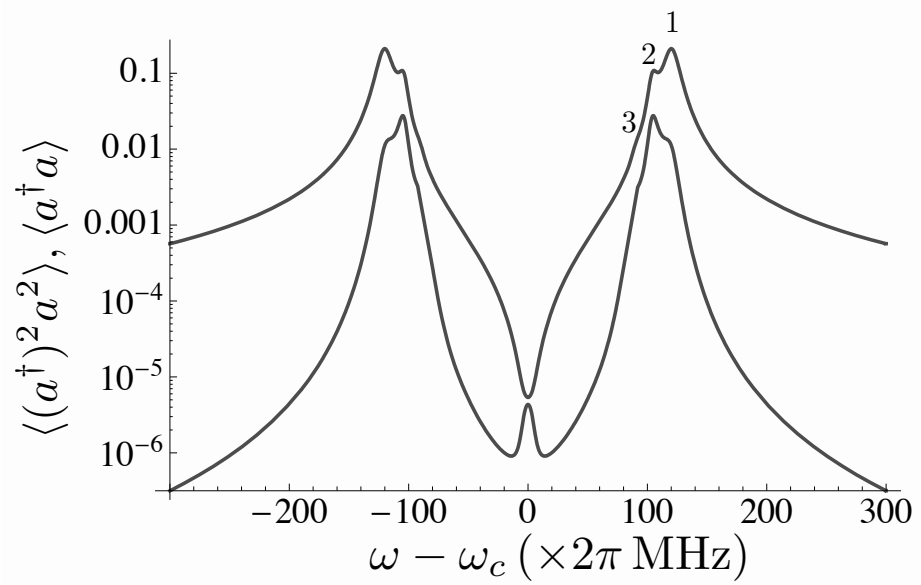

Figure 6.5: Spectra of $\langle a^\dagger a\rangle$ (top) and $\langle (a^\dagger)^2 a^2\rangle$ (bottom) in function of $\omega - \omega_c$ for the values in Tab. 6.1 and $\Delta = 0$. Note the absence of peak at $\omega = \omega_c$. The other peaks are numbered as the order of the n-photon transition $|0\rangle \to |n, +\rangle$ at $\omega - \omega_c = \lambda_n/n$: one-photon, two-photon and an embryo of the three-photon transition can be made out. The symmetrical peaks on the left side correspond to the n-photon transition $|0\rangle \to |n, -\rangle$.

One and two-photon Spectroscopy

The transmission T of an optical cavity of decay rate κ is the quantity of photons that filter out of one of the mirrors of the cavity and is given by $T = \kappa\langle a^\dagger a\rangle$. The second order transmission $T^{(2)}$ consider the events involving more than one photon detected at the same time by a photodetector and is given by $T^{(2)} = \kappa^2\langle (a^\dagger)^2 a^2\rangle$. In the following section, we study the values of the populations $\langle a^\dagger a\rangle$ and $\langle (a^\dagger)^2 a^2\rangle$ inside the cavity for the steady state ρ^S in function of the laser frequency ω_c, the transmissions being directly proportional.

First we study the resonant case. When the atoms have the same internal frequency than the cavity, i. e. when $\Delta = 0$, we found that the state $|1, 0\rangle$ does not get populated, since $\langle 1, 0|W|0, gg\rangle$ vanishes and neither do the states $|2, 0_{a,b}\rangle$. Hence, we should not expect to see a one photon transition peak at the frequency $\omega = \omega_c$. We plotted the photon spectrum in Fig. 6.5, and we see that, indeed, on the top curve the photon population at $\omega = \omega_c$ is highly inhibited, the main peaks of the spectrum are those due to the $|n, \pm\rangle$ transitions, for $n = 1, 2$ and slightly $n = 3$.

We see the peaks due to the one-photon processes $|0\rangle \to |1, \pm\rangle$ in the $\langle (a^\dagger)^2 a^2\rangle$ spectrum, but the laser power is strong enough for the amplitude of the two-photon $|0\rangle \to |2, \pm\rangle$ transition peak to dominate it and to bring a non-negligible contribution in the spectrum of $\langle a^\dagger a\rangle$. That dominance grows as the laser power increases, since the n photons transitions rates scale as $\sim \epsilon^{2n}$. We note a small peak at $\omega = \omega_c$ for $\langle (a^\dagger)^2 a^2\rangle$. That peak might be explained by higher order transitions ($n \geq 3$) which are not inhibited, but also not strong

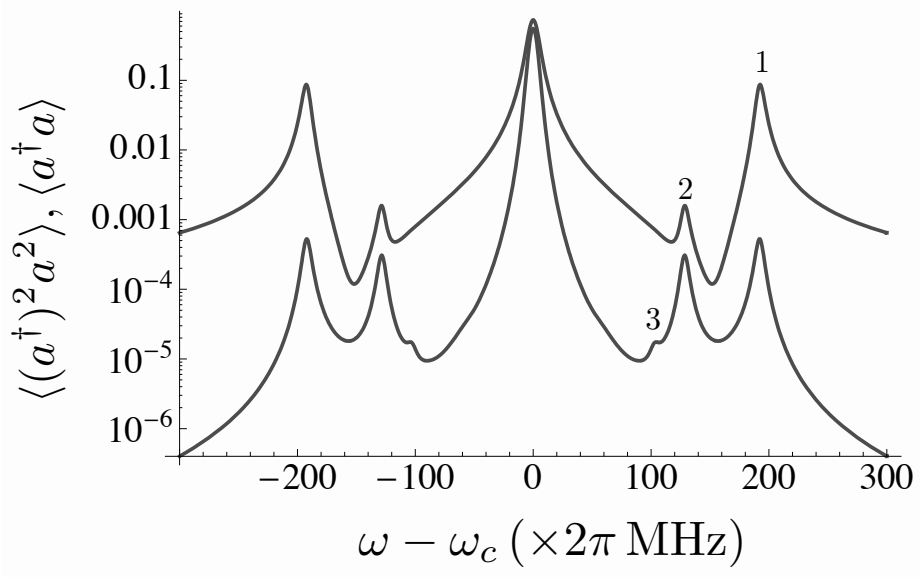

Figure 6.6: Spectra of $\langle a^\dagger a \rangle$ (top) and $\langle (a^\dagger)^2 a^2 \rangle$ (bottom) in function of $\omega - \omega_c$ for the values in Tab. 6.1 and $\Delta = 150 \times 2\pi\,\mathrm{MHz}$. The transition at $\omega = \omega_c$ is not inhibited anymore, on the contrary it yields the most important peak. The other peaks are numbered as the order of the n-photon transition $|0\rangle \to |n, +\rangle$ at $\omega - \omega_c = \lambda_n/n$: one-photon, two-photon and three-photon (not visible on the $\langle a^\dagger a \rangle$ spectrum). The symmetrical peaks on the left side correspond to the n-photon transitions $|0\rangle \to |n, -\rangle$.

enough to show on $\langle a^\dagger a \rangle$.

Then we study the non-resonant case by setting $\Delta = 150 \times 2\pi\,\mathrm{MHz}$ in Fig. 6.6. In that situation, the matrix element $\langle 1, 0|W|0\rangle$ is no longer zero and the transitions at $\omega = \omega_c$ are allowed again, hence the observed peak at the cavity resonance frequency which largely dominates the other transition peaks. The transition at $\omega = \omega_c$ is the condition for the consecutive one-photon transitions $|0\rangle \to |1, 0\rangle \to \cdots \to |n, 0_{a,b}\rangle$, which is why the peak is also very important on $\langle (a^\dagger)^2 a^2 \rangle$, unlike the peak corresponding to the $|0\rangle \to |1, \pm\rangle$, which does not correspond to a two-photon process and is henceforth comparatively much weaker on the $\langle (a^\dagger)^2 a^2 \rangle$ spectrum. Once again, we note that in the two-photon spectrum the two-photon transmission to $|2, \pm\rangle$ is of the same order of magnitude than the transmission to $|1, \pm\rangle$, due to the strength of the laser power. Also, we note the emergence of two new peaks, only visible on $\langle (a^\dagger)^2 a^2 \rangle$, which are due to three-photon transitions.

Cavity quality

In this section, we study the influence of the quality of the cavity on various possible spectra by superposing plots or the same quantity for different values of the decay rate κ. A theoretical, perfect cavity is characterized by $\kappa = 0$ (in which case the transmission actually vanishes) while an imperfect cavity will have κ greater than zero. The greater κ is, the closer the cavity will mimic free space.

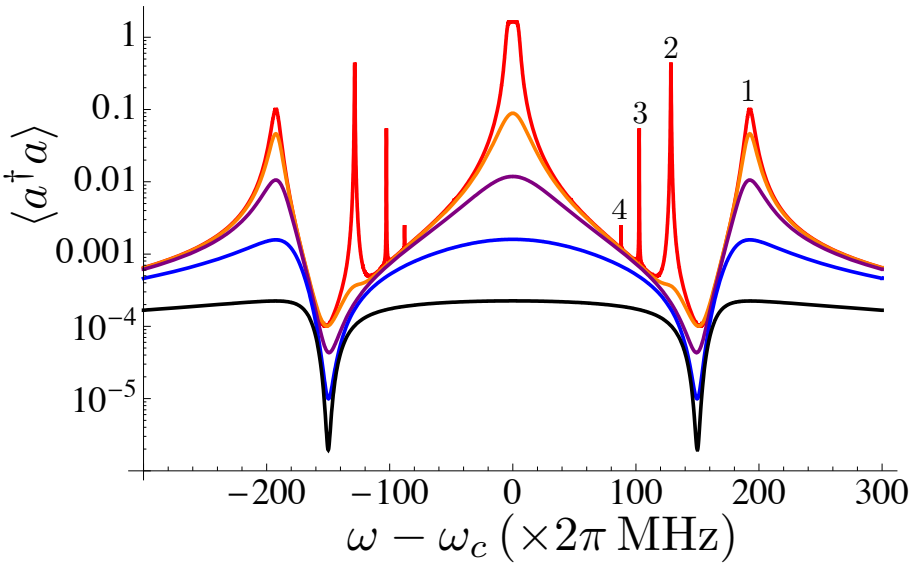

Figure 6.7: Spectra of $\langle a^\dagger a \rangle$ in function of $\omega - \omega_c$ for the values in Tab. 6.1, $\Delta = 150 \times 2\pi\,\mathrm{MHz}$ and different values of κ (in 2π MHz): 0 (Red); 20 (Orange); 55 (Purple); 150 (Blue); 400 (Black). The peaks are numbered in function of the order of the transitions at $\omega - \omega_c = \lambda_n/n$.

First we study the transmission spectra, shown in Fig 6.7, for different values of κ and $\Delta = 150 \times 2\pi\,\mathrm{MHz}$. When the cavity decay rate is great, the $\langle a^\dagger a \rangle$ spectrum obtained is a typical one-photon absorption spectrum, with dips located at the two atomic frequencies, $\omega_c \pm \Delta$, which is similar to the case of two atoms in a vacuum. There is no other visible structure for cavities of such low quality.

When the cavity quality increases, peaks progressively start to appear at the frequencies of all the allowed transitions. In a perfect cavity, the amplitude of the peaks becomes very important and we observe several peaks numbered on the plot, corresponding to the n-photon processes $|0\rangle \to |n, \pm\rangle$ at $\omega - \omega_c = \lambda_n/n$ for $n = 1, 2, 3, 4$. We also note the amplitude of the central peak at $\omega = \omega_c$, which corresponds to all the consecutive one-photon transitions $|0\rangle \to |1, 0\rangle \to \cdots \to |n, 0_{a,b}\rangle$.

Let us now study another aspect of the system and measure the populations of the excited states $|e_1\rangle$ and $|ee\rangle$ in the steady state ρ^S in function of the laser frequency ω. The quantities $\langle e_1|\rho^S|e_1\rangle$ and $\langle ee|\rho^S|ee\rangle$ will be considered, where the traces over the subsystems of no direct interest, namely the photon field and the second atom, is implied. Those atomic populations can be measured in circuit-QED [98].

In Fig. 6.8 we plotted the spectrum of $\langle ee|\rho^S|ee\rangle$. For a lossless cavity (in red) we observe transition peaks corresponding to the n-photon processes $|0\rangle \to |n, \pm\rangle$ at $\omega - \omega_c = \lambda_n/n$ for n up to 5, all numbered on the figure. Between the peak number five and the central peak we can distinguish a few small peaks. It can be shown that those peaks correspond to the transitions $|1, \pm\rangle \to |n, \pm\rangle$ with $n \geq 2$, which happen at the frequencies $\omega = \omega_c \pm (\lambda_n - \lambda_1)/(n-1)$. That second series of excitations is made possible thanks to

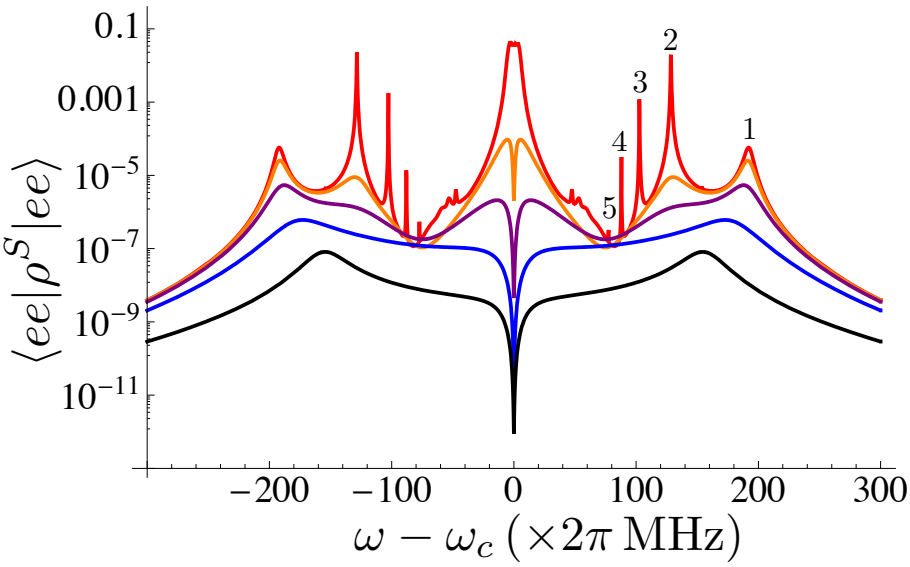

Figure 6.8: Spectra of $\langle ee|\rho^S|ee\rangle$ in function of $\omega - \omega_c$ for the values in Tab. 6.1, $\Delta = 150 \times 2\pi\,\mathrm{MHz}$ and different values of κ (in 2π MHz): 0 (Red); 20 (Orange); 55 (Purple); 150 (Blue); 400 (Black). The peaks are numbered in function of the order of the transitions at $\omega - \omega_c = \lambda_n/n$.

the strength of the laser which populates the $|1,\pm\rangle$ states even away from resonance.

For cavities of lesser quality, the peaks quickly start to fade away. For the worst cavity we considered (in black), we see the apparition of two peaks, who are actually centered on the atomic frequencies $\omega - \omega_c = \pm 150 \times 2\pi\,\mathrm{MHz}$, a behavior we would expect from the ionization spectrum of two atoms in free space, as in Fig. 6.2. We also note the apparition of a dip at the frequency $\omega = \omega_c$. We saw in Sec. 6.1 that in free space the transition are $2\omega = \omega_1 + \omega_2$ was prohibited by Fermi's golden rule, although that prohibition in the perturbation theory did not translate in the steady state behavior by an interference or a dip, but rather simply by an absence of peak. In our case, for a low quality cavity, the $\omega = \omega_c$ transition to the $|ee\rangle$ state is strictly prohibited unlike the photonic transitions shown in Fig. 6.6, even though they are both predicted to happen by perturbation theory. At this stage, we can only assume that this behavior is induced by the cavity decay mechanisms which are not considered in Fermi's golden rule and more calculations should be made in order to understand this phenomenon completely.

In Fig. 6.9, we study the diminution of the peak amplitude of $\langle ee|\rho^S|ee\rangle$ at the frequency $\omega = \omega_c + \lambda_2/2$ in function of κ/γ. Clearly, when $\kappa \ll \gamma$ the amplitude saturates, i. e. the population of the doubly excited atoms is limited by the spontaneous emission, but another regime is reached when $\kappa \gg \gamma$ where the amplitude is decreased following a power law. We therefore see that the best amplitudes are reached for the cavity decay rate smaller or of the order of the atomic decay rate.

In Fig. 6.10, we study the probability to observe only one of the atoms excited $\langle e_1|\rho^S|e_1\rangle$ in function of $\omega - \omega_c$. For a perfect cavity (in red), we observe once again transition

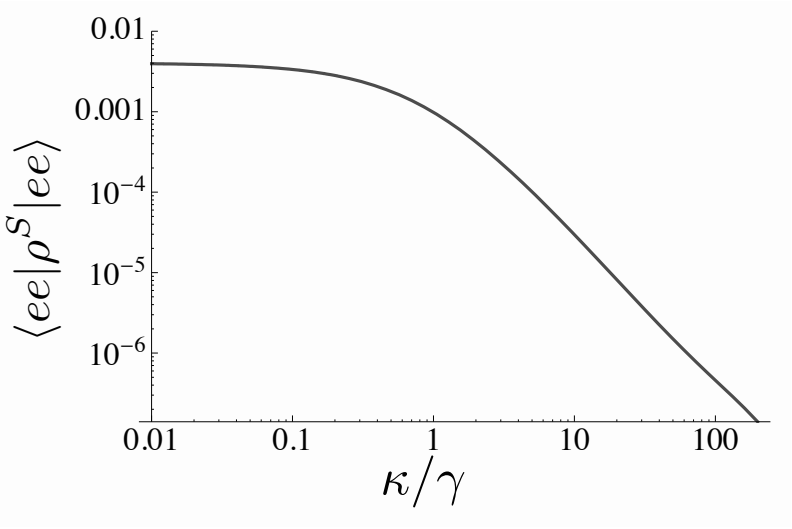

Figure 6.9: Spectrum of $\langle ee|\rho^S|ee\rangle$ in function of κ for the values in Tab. 6.1, $\Delta = 150 \times 2\pi\,\mathrm{MHz}$ at the resonance $\omega = \omega_c + \lambda_2/2$. For $\kappa \ll \gamma$ the population is saturated by the spontaneous emission, it then decreases following a power law as κ grows beyond γ.

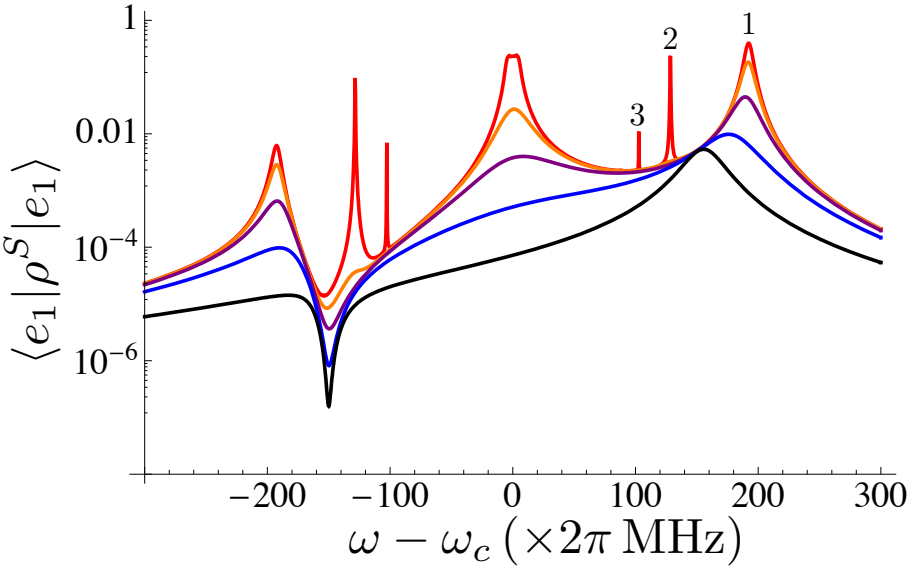

Figure 6.10: Spectra of $\langle e_1|\rho^S|e_1\rangle$ in function of $\omega - \omega_c$ for the values in Tab. 6.1, $\Delta = 150 \times 2\pi\,\mathrm{MHz}$ and different values of κ (in 2π MHz): 0 (Red); 20 (Orange); 55 (Purple); 150 (Blue); 400 (Black). The peaks are numbered in function of the order of the transitions at $\omega - \omega_c = \lambda_n/n$.

peaks for the transitions $|0\rangle \rightarrow |n,\pm\rangle$ at $\omega - \omega_c = \lambda_n/n$ for n up to 3, although the two higher order peaks are very thin and disappear completely for $\kappa = 20 \times 2\pi$ MHz which is easily understood since those are multi-photon processes measured on a single excitation spectrum, just as the two-photon peaks on $\langle a^\dagger a\rangle$ in Fig. 6.6 was several orders of magnitude smaller than the one-photon peaks on $\langle a^\dagger a\rangle$.

For greater values of cavity decay rate, all the peaks begin to fade away until only one peak is left around the first internal atomic frequency at $\omega - \omega_c = 150 \times 2\pi\,\text{MHz}$, as we would expect from a spectrum of an atom in free space. What we would not expect from such a spectrum however is the dip that forms around the second atomic internal frequency $\omega - \omega_c = -150 \times 2\pi\,\text{MHz}$. That new behavior is once again due to the cavity decay process in the system. Note that even though the presence of the $|ee\rangle$ state is strongly inhibited for finite κ at the frequency $2\omega = \omega_1 + \omega_2$, the presence of only one excited atom is not affected at all, which induces a strong blockade in the system, even if the two atoms do not interact directly with each other.

One interesting feature we also observe on the graph is that at the amplitude of the population of the $\langle e_1|\rho^S|e_1\rangle$ at the first atomic internal frequency $\omega - \omega_c = 150 \times 2\pi\,\text{MHz}$ seems to be completely independent from the value of κ. For a perfect cavity, there is no discernible peak at that location, but as the decay rate grows, the population stays the same while for all the other frequencies it weakens, which eventually yields a peak at the atomic frequency.

6.4 General Atomic Frequency Spread

In this section, we investigate the behavior of the system not being restrained by the constraint $\omega_1 + \omega_2 = 2\omega_c$. For this general setup of the atomic frequencies, we are no longer able to diagonalize the unperturbed Hamiltonian or perturbation theory. We will rely purely on numerical considerations and analogies with the previous case.

We define the atomic frequencies to be

$$\omega_1 = \omega_c + \Delta + \phi, \tag{6.76}$$

$$\omega_2 = \omega_c - \Delta + \phi, \tag{6.77}$$

which yield every possible value of ω_1 and ω_2 when Δ and ϕ are allowed to vary. The particular case $\omega_1 + \omega_2 = 2\omega_c$ is found when $\phi = 0$.

6.4.1 Eigenstates and Eigenvalues

We showed in Sec. 6.2 that the Hamiltonian H always commutes with the global excitation number operator $\hat{n}$ without making any assumptions on the atomic frequencies. This means that H keeps its block diagonal form described earlier, however we were unable to diagonalize the different blocks with general atomic internal frequencies. Although the analytical form of the eigenvalues and eigenstates are not generally known, except for the ground state $|0\rangle$, we may still numerically identify them. We keep the notation

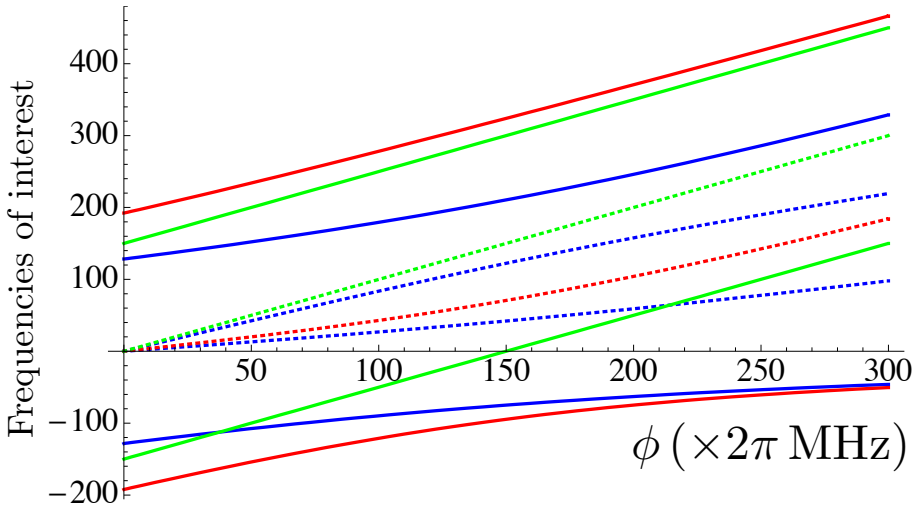

Figure 6.11: Numerical values of $\lambda^{(1,0)}$ (red, dotted), $\lambda^{(1,\pm)}$ (red), $\lambda^{(2,0_{a,b})}/2$ (blue, dotted) and $\lambda^{(2,\pm)}/2$ (red) as well as ω_1, ω_2 (green) and $(\omega_1+\omega_2)/2$ (green, dotted) in function of ϕ for $\alpha = 85\times 2\pi\,\mathrm{MHz}$, $\Delta = 150\times 2\pi\,\mathrm{MHz}$. The red and blue lines represent the values of $\omega-\omega_c$ a which one and two-photon transitions are expected and the green lines the values we might expect dips for different quantities. The dotted lines are transition values that are degenerate when $\Delta = 0$.

previously used and call the $n=1$ excited states $|1,0\rangle, |1,\pm\rangle$ and the n excited states $|n,0_{a,b}\rangle, |n,\pm\rangle$ with the respective eigenvalues 0, $\hbar\omega_c+\hbar\lambda^{(1,0)}$, $\hbar\omega_c+\hbar\lambda^{(1,\pm)}$, $n\hbar\omega_c+\hbar\lambda^{(n,0_{a,b})}$ and $n\hbar\omega_c+\hbar\lambda^{(n,\pm)}$. Although we do not now the analytical form of these eigenvalues, we can identify them from the values they have for $\phi=0$.

In Fig. 6.11, we show the numerical values of $\lambda^{(1,0)}$, $\lambda^{(1,\pm)}$, $\lambda^{(2,0_{a,b})}/2$ and $\lambda^{(2,\pm)}/2$ as well as ω_1, ω_2 and $(\omega_1+\omega_2)/2$ in function of ϕ for $\Delta = 150\times 2\pi\,\mathrm{MHz}$. We identify which eigenvalue is which from the initial values at $\phi=0$, with some uncertainty about $\lambda^{(2,0_a)}$ and $\lambda^{(2,0_b)}$ which are degenerate for $\phi=0$. We will shortly solve this problem.

We chose for the next numerical calculations to settle on the numerical parameter $\phi = 130\times 2\pi\,\mathrm{MHz}$ which spreads as evenly as possible all the numerical values plotted in an attempt to separate the possible peaks and dips as well as possible. We used in the previous calculations a high laser strength $\epsilon = 6\times 2\pi\,\mathrm{MHz}$ in order to maximize the visibility of the two-photon processes in the spectra. Unfortunately, using a high laser power also broadens the peaks and as we now investigate a more general case with a more complex structure, we will use the smaller value $\epsilon = 2\pi\,\mathrm{MHz}$ to separate the peaks more effectively.

In the particular case of two identical atoms, i. e. when $\Delta = 0$, we can partially diagonalize the blocks of the unperturbed Hamiltonian and find a few eigenstates. These

eigenvectors are

$$|1,0\rangle = \frac{1}{\sqrt{2}}\left(|0,eg\rangle - |0,ge\rangle\right), \tag{6.78}$$

$$|1,\pm\rangle = \frac{1}{\sqrt{2\alpha^2 + (\lambda^{(1,\pm)})^2}}\left(\alpha|0,eg\rangle + \alpha|0,ge\rangle - \lambda^{(1,\pm)}|1,gg\rangle\right), \tag{6.79}$$

$$|2,0_b\rangle = \frac{1}{\sqrt{2}}\left(|1,eg\rangle - |1,ge\rangle\right), \tag{6.80}$$

and the other ones were not found. We chose to call the last state $|2,0_b\rangle$ rather than $|2,0_a\rangle$ since it is actually the same as the case $\phi = 0$. Note that $|1,0\rangle$ and $|2,0_b\rangle$ are again antisymmetrical under the permutation of the two atoms and are again decoupled from the other states. We can also calculate the respective eigenvalues to the eigenstates and we find that $\lambda^{(1,0)} = \Delta$, $\lambda^{(1,\pm)} = (\Delta \pm \sqrt{8\alpha^2 + \Delta^2})/2$ and $\lambda^{(2,0_b)} = \Delta$. Numerically, starting from that situation, we checked that value of $\lambda^{(2,0_b)}$ is always smaller than $\lambda^{(2,0_a)}$ for other values of Δ and ϕ and the uncertainty about their respective denomination is lifted.

We can calculate the few off-diagonal terms coming from the perturbation W linking those eigenstates, which are expressed, in the unperturbed Hamiltonian eigenstates basis, as

$$\langle 0|W|1,0\rangle = 0, \tag{6.81}$$

$$\langle 0|W|1,\pm\rangle = -i\,\frac{\lambda^{(1,\pm)}}{\sqrt{2\alpha^2 + (\lambda^{(1,\pm)})^2}}\,\epsilon, \tag{6.82}$$

$$\langle 1,0|W|2,0_b\rangle = -i\epsilon, \tag{6.83}$$

$$\langle 1,\pm|W|2,0_b\rangle = 0, \tag{6.84}$$

which indicates that, because of their antisymmetry, the $|1,0\rangle$ and $|2,0_b\rangle$ states do not get populated by the perturbation by either one or two-photon processes.

Atomic, one and two-photon Spectroscopy

Let us now study the different spectra of the general steady state case. We show in Fig. 6.12 the $\langle a^\dagger a\rangle$ and $\langle (a^\dagger)^2 a^2\rangle$ spectra of the particular case $\Delta = 0$. As we expected, there is no peak at $\omega = \omega_c$, on the contrary we find there a strong dip in the populations at the atomic frequencies $\omega_1 = \omega_2 = \omega_c$, due once again to the cavity decay process. We find two-photon peaks in the $\langle (a^\dagger)^2 a^2\rangle$ spectrum (and a beginning of a three-photon peak around $\omega - \omega_c \simeq 140 \times 2\pi\,\mathrm{MHz}$), although the peak at $\lambda^{(2,-)}/2$ happens to be very close to the one-photon peak at $\lambda^{(1,-)}$ and those two are not resolved but yield a peak of consequently greater amplitude than the peak at $\lambda^{(2,+)}/2$.

Let us now investigate the more general case $\Delta = 150 \times 2\pi\,\mathrm{MHz}$ and $\phi = 130 \times 2\pi\,\mathrm{MHz}$, of which we plotted the $\langle a^\dagger a\rangle$ and $\langle (a^\dagger)^2 a^2\rangle$ spectra in Fig. 6.13. We count three one-photon peaks, all associated with one $n = 1$ eigenvalue and four two-photon peaks, again associated with the four $n = 2$ eigenvalues. We find two important dips in $\langle a^\dagger a\rangle$ located at the two

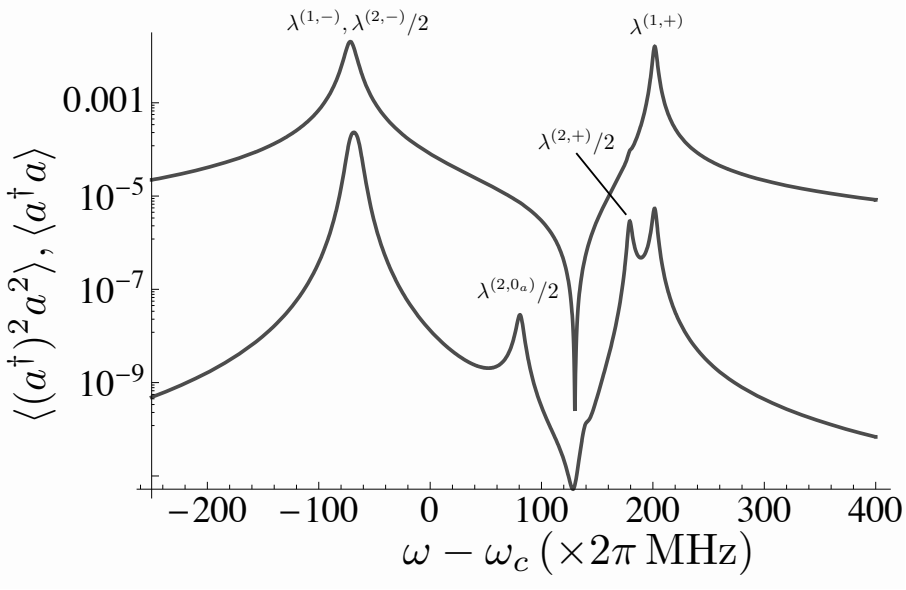

Figure 6.12: Spectra of $\langle a^\dagger a\rangle$ (top) and $\langle (a^\dagger)^2 a^2\rangle$ (bottom) in function of $\omega - \omega_c$ for the values in Tab. 6.1, $\epsilon = 2\pi\,\mathrm{MHz}$, $\Delta = 0$ and $\phi = 130 \times 2\pi\,\mathrm{MHz}$. We find two peaks at $\omega - \omega_c = \lambda^{(1,\pm)}$ corresponding to one-photon transitions and three peaks at $\omega - \omega_c = \lambda^{(2,\pm)}/2$ and $\lambda^{(2,0_a)}/2$ corresponding to the two-photon transitions. No trace of transitions involving the states $|1,0\rangle$ or $|n,0_b\rangle$. We also find a dip at the atomic frequencies $\omega_1 = \omega_2 = \omega_c + \Delta$.

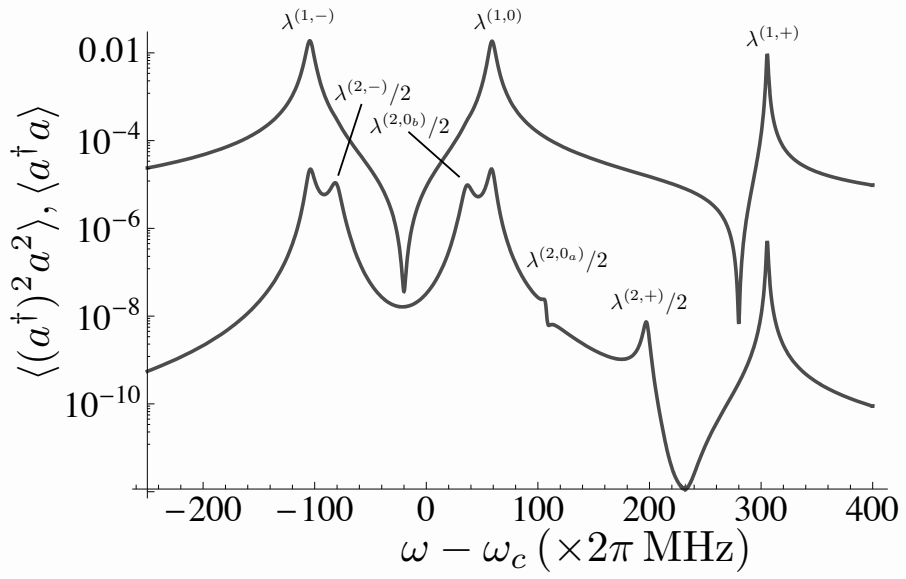

Figure 6.13: Spectra of $\langle a^\dagger a\rangle$ (top) and $\langle (a^\dagger)^2 a^2\rangle$ (bottom) in function of $\omega - \omega_c$ for the values in Tab. 6.1, $\epsilon = 2\pi\,\mathrm{MHz}$, $\Delta = 150 \times 2\pi\,\mathrm{MHz}$ and $\phi = 130 \times 2\pi\,\mathrm{MHz}$. We find three peaks at $\omega - \omega_c = \lambda^{(1,\pm)}$ and $\lambda^{(1,0)}$ corresponding to one-photon transitions and four peaks at $\omega - \omega_c = \lambda^{(2,\pm)}/2$ and $\lambda^{(2,0_a,b)}/2$ corresponding to two-photon transitions. We also find two dips at the atomic frequencies $\omega - \omega_c = 280 \times 2\pi\,\mathrm{MHz}$ and $\omega - \omega_c = -20 \times 2\pi\,\mathrm{MHz}$.

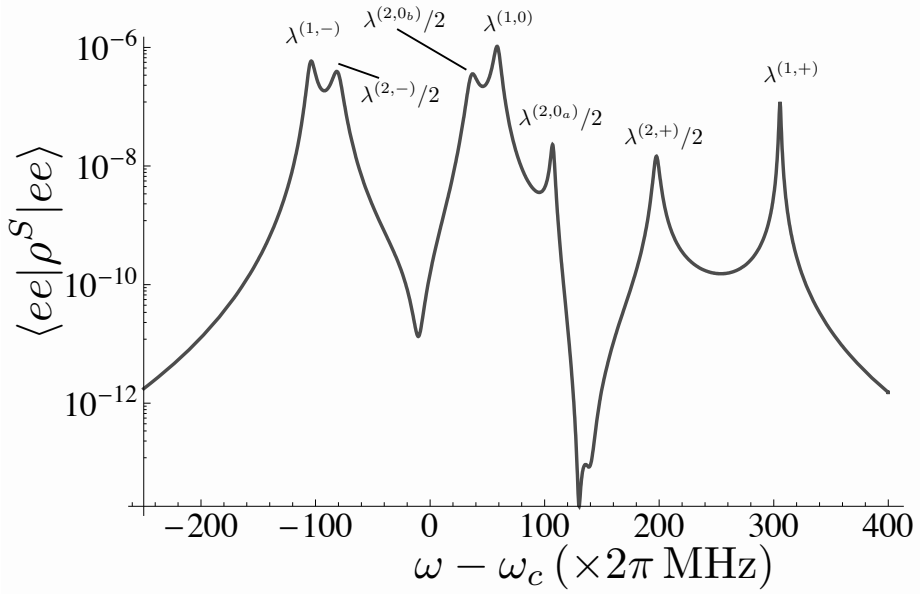

Figure 6.14: Spectrum of $\langle ee|\rho^S|ee\rangle$ in function of $\omega - \omega_c$ for the values in Tab. 6.1, $\epsilon = 2\pi\,\mathrm{MHz}$, $\Delta = 150 \times 2\pi\,\mathrm{MHz}$ and $\phi = 130 \times 2\pi\,\mathrm{MHz}$. We find three peaks at $\omega - \omega_c = \lambda^{(1,\pm)}$ and $\lambda^{(1,0)}$ corresponding to all possible one-photon transitions and four peaks at $\omega - \omega_c = \lambda^{(2,\pm)}/2$ and $\lambda^{(2,0_{a,b})}/2$ corresponding to all possible two-photon transitions. We also count three dips, two small ones at the atomic frequencies and an important one at the mean frequency $\omega - \omega_c = 130 \times 2\pi\,\mathrm{MHz}$.

atomic frequencies $\omega - \omega_c = 280 \times 2\pi\,\mathrm{MHz}$ and $\omega - \omega_c = -20 \times 2\pi\,\mathrm{MHz}$ which is a cavity decay related process. In the $\langle (a^\dagger)^2 a^2\rangle$ spectrum, the same dips are not visible, but we see the apparition of a new one around $\omega - \omega_c \simeq 225 \times 2\pi\,\mathrm{MHz}$ that does not seem to correspond to any particular value we used up until now.

In Fig. 6.14 we plotted the spectrum of $\langle ee|\rho^S|ee\rangle$ in function of $\omega - \omega_c$ also for $\Delta = 150 \times 2\pi\,\mathrm{MHz}$ and $\phi = 130 \times 2\pi\,\mathrm{MHz}$. We count seven peaks, three associated one-photon processes and four associated two-photon processes. This is the most general case where there is no interference between the different excitation paths that lead to an inhibition of a peak. We also count three different dips, two of them of weak amplitude located at the atomic frequencies $\omega - \omega_c = 280 \times 2\pi\,\mathrm{MHz}$ and $\omega - \omega_c = -20 \times 2\pi\,\mathrm{MHz}$, and a very strong one located at the half-sum of the frequencies $\omega - \omega_c = 130 \times 2\pi\,\mathrm{MHz}$, once again linked with the cavity decay process.

6.4.2 Cavity Induced Transparency

Let us investigate another property of two atoms in a cavity. We showed in Eq. (6.75) the spectrum of the mean number of photon $\langle a^\dagger a\rangle$ in an empty cavity. Using the same formalism we will derive the analytical expression of $\langle a^\dagger a\rangle$ in an empty cavity and show

that

$$\langle (a^\dagger)^2 a^2 \rangle = (\langle a^\dagger a \rangle)^2. \tag{6.85}$$

For that, we use Eq. (6.68) with $A = (a^\dagger)^2 a^2$ and we calculate

$$[A, a^\dagger a] = 0, \;\; [A, a^\dagger] = 2a^\dagger a^\dagger a, \;\; [A, a] = -2a^\dagger a a, \tag{6.86}$$

$$Aa^\dagger a - 2a^\dagger A a + a^\dagger a A = 2a^\dagger a^\dagger a a, \tag{6.87}$$

where we used the basic commutation relations $[a, a^\dagger] = 1$ to find the final results. We find

$$\frac{d}{dt}\langle (a^\dagger)^2 a^2 \rangle = 2\epsilon(\langle a^\dagger a^\dagger a \rangle + \langle a^\dagger a a \rangle) - 4\kappa \langle (a^\dagger)^2 a^2 \rangle, \tag{6.88}$$

and we have to calculate the time variation of $\langle a^\dagger a^\dagger a \rangle$. Let us pose $B = a^\dagger a^\dagger a$ and we have

$$[B, a^\dagger a] = -a^\dagger a^\dagger a, \;\; [B, a^\dagger] = a^\dagger a^\dagger, \;\; [B, a] = -2a^\dagger a, \tag{6.89}$$

$$Ba^\dagger a - 2a^\dagger B a + a^\dagger a B = 3a^\dagger a^\dagger a. \tag{6.90}$$

We have

$$\frac{d}{dt}\langle a^\dagger a^\dagger a \rangle = (i(\omega_c - \omega) - 3\kappa)\langle a^\dagger a^\dagger a \rangle + \epsilon(\langle a^\dagger a^\dagger \rangle + 2\langle a^\dagger a \rangle), \tag{6.91}$$

and with $\frac{d}{dt}\langle a^\dagger a a \rangle$ its complex conjugate. There is one more the time variation to calculate. With $C = a^2$ we have

$$[C, a^\dagger a] = 2aa, \;\; [C, a^\dagger] = 2a, \;\; [C, a] = 0, \tag{6.92}$$

$$Ca^\dagger a - 2a^\dagger C a + a^\dagger a C = 2aa, \tag{6.93}$$

and we have

$$\frac{d}{dt}\langle a^2 \rangle = 2\left(-i(\omega_c - \omega) - \kappa\right)\langle a^2 \rangle + 2\epsilon\langle a \rangle. \tag{6.94}$$

and with $\frac{d}{dt}\langle (a^\dagger)^2 \rangle$ its complex conjugate.

Globally, in the steady state, we have

$$\langle a \rangle = \frac{\epsilon}{\kappa + i(\omega_c - \omega)}, \tag{6.95}$$

$$\langle a^\dagger a \rangle = \frac{\epsilon^2}{\kappa^2 + (\omega_c - \omega)^2} = \langle a^\dagger \rangle \langle a \rangle, \tag{6.96}$$

$$\langle a^2 \rangle = \frac{\epsilon \langle a \rangle}{\kappa + i(\omega_c - \omega)} = \langle a \rangle^2, \tag{6.97}$$

$$\langle a^\dagger a^\dagger a \rangle = \frac{\epsilon(\langle a^\dagger a^\dagger \rangle + 2\langle a^\dagger a \rangle)}{3\kappa - i(\omega_c - \omega)} = \epsilon\langle a^\dagger \rangle \frac{\langle a^\dagger \rangle + 2\langle a \rangle}{3\kappa - i(\omega_c - \omega)} = \langle a^\dagger \rangle \langle a^\dagger a \rangle, \tag{6.98}$$

$$\langle (a^\dagger)^2 a^2 \rangle = \frac{\epsilon}{2\kappa}(\langle a^\dagger a^\dagger a \rangle + \langle a^\dagger a a \rangle) = \frac{\epsilon}{2\kappa}\langle a^\dagger a \rangle (\langle a^\dagger \rangle + \langle a \rangle) = \langle a^\dagger a \rangle^2, \tag{6.99}$$

and we have the desired result.

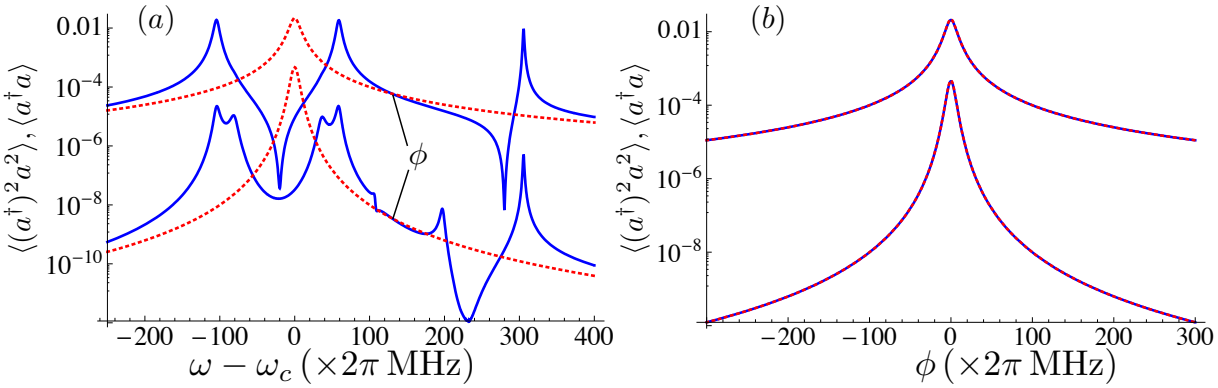

Figure 6.15: On (a), spectra of $\langle a^\dagger a\rangle$ (top) and $\langle(a^\dagger)^2a^2\rangle$ (bottom) in function of $\omega - \omega_c$ for the values in Tab. 6.1, $\epsilon = 2\pi\,\mathrm{MHz}$, $\Delta = 150 \times 2\pi\,\mathrm{MHz}$ and $\phi = 130 \times 2\pi\,\mathrm{MHz}$ (blue) along with the same spectra of an empty cavity (red, dotted) with the same settings and $\alpha = 0$. On (b), the same spectra of the system with the laser frequency set on $\omega = \omega_c + \phi = (\omega_1 + \omega_2)/2$ in function of ϕ (blue), along with the spectra of the empty cavity (red, dotted). At the frequency $2\omega = \omega_1 + \omega_2$, the system behaves as if the atoms were not in the cavity.

We showed in Fig. 6.15 (a) the same plot as in Fig. 6.13 (blue) along with the spectrum obtained by setting the atom-field coupling constant α to zero (red, dotted). We noted that at the frequency $\omega = (\omega_1 + \omega_2)/2 = \omega_c + \phi$ both red lines crossed the blue lines. In other words, at that particular frequency, the number of photons in the cavity is exactly the number of photons that would be expected in an empty cavity, furthermore the same result holds for the mean number of pairs of photons. It is easy to check numerically that the relation

$$\langle(a^\dagger)^2a^2\rangle = (\langle a^\dagger a\rangle)^2, \tag{6.100}$$

also holds for our two-atom system at the frequency $2\omega = \omega_1 + \omega_2$.

In Fig. 6.15 (b) we plotted $\langle a^\dagger a\rangle$ and $\langle(a^\dagger)^2a^2\rangle$ in function of ϕ for a laser frequency $\omega = \omega_c + \phi = (\omega_1 + \omega_2)/2$ (blue) along with the same quantities obtained for an empty cavity (red, dotted) for comparison. The two plots are identical, signature of some kind of cavity induced transparency (CIT) of the system.

Those figures were plotted with the atomic frequency difference $\Delta = 150 \times 2\pi\,\mathrm{MHz}$, however we may recall that the all the photon spectra we presented showed dips at the atomic frequencies ω_1 and ω_2 (although not very obvious on Fig. 6.6 due to the large value of ϵ), we would therefore suspect that the transparency effect would not be observed when the atoms have identical frequencies, i. e. when $\Delta = 0$. Indeed, the mean number of photons in a cavity with a laser on resonance with two identical atoms does not go beyond $\langle a^\dagger a\rangle \simeq 3\ 10^{-10}$, a value of about 6 orders of magnitude smaller than the one obtained for $\Delta = 150 \times 2\pi\,\mathrm{MHz}$.

In Fig. 6.16 we plotted the same plot as in Fig. 6.15 (b), but with a smaller gap in atomic frequencies $\Delta = 50 \times 2\pi\,\mathrm{MHz}$. We can see that on most of the spectrum the CIT

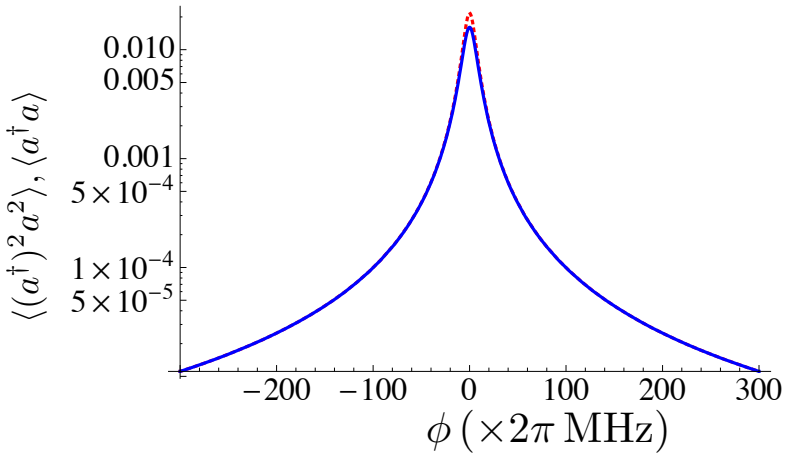

Figure 6.16: Spectra of $\langle a^\dagger a\rangle$ (top) and $\langle (a^\dagger)^2 a^2\rangle$ (bottom) of the system with the laser frequency set on $\omega = \omega_c + \phi = (\omega_1 + \omega_2)/2$ in function of ϕ (blue) along with the spectra of the empty cavity (red, dotted). The CIT effect is not perfectly observed around $\phi = 0$ since the atom frequencies are not spread out enough.

effect is observed, although around $\phi = 0$ the number of photons in the cavity is slightly smaller than what it would be in an empty cavity. We conclude that the CIT effect is stronger when the gap in the atomic frequencies is larger and not in competition with the cavity decay induced photon inhibition at the atomic frequencies.

We see on Fig. 6.11 that the $(\omega_1 + \omega_2)/2$ values for non-zero ϕ never coincide with another transition value, therefore we should not expect a strong competition between the CIT and other transition resonances.

6.5 Summary and Discussion

In this chapter, we have studied the behavior of two unidentical two-level atoms in a single mode cavity driven by a laser under realistic conditions of spontaneous emission and cavity losses. In free space, two-photon processes for independent atoms do not happen, as we checked by using perturbation theory and further with a master equation calculation. Our next objective was to show that two-level processes are possible in a cavity ad to study their occurrences in realistic experimental conditions.

In order to study the system using perturbation theory, we made the simplification of considering two atoms with frequencies evenly spread around the cavity mode frequency. We were then able to express analytically the eigenstates and eigenvalues of the unperturbed Hamiltonian, which allowed us to show that two-photon processes were possible for different dressed states of the system. In the free space case, the two-photon processes would have to happen at the mean of the atomic frequencies, but we found that in a cavity the transitions at that particular frequency were merely one-photon processes which could however be suppressed if the two atoms were identical with internal frequencies equal to

the cavity's.

We confirmed that analysis with the steady states of the master equation and we observed peaks due to multi-photon processes, up to five-photon processes in a perfect cavity[1]. The mean number of photons in the cavity, the mean number of pairs of photons, the population of a single excited atom as well as the population of two excited atoms in the system were studied.

Some effect that were not expected from the perturbation theory were observed for important cavity decay rates. Dips in the mean number of photons spectra were found whenever the laser hit the atomic frequencies. The population of two excited atoms was strongly weakened when the laser frequency was in the middle of the atomic frequencies but peaked on the atomic frequencies themselves for very poor quality cavities. Also for those cavities, the population of a single excited atom peaked when the laser resonated with its frequency but dipped for the other atom's frequency. The shifting of the peaks is understood easily as when the cavity loses more and more photons, it becomes similar with free space. However some kind of coupling still remains and causes dips that are not observed in free space.

The purely numerical study of steady states of the system without the simplification on the atomic frequencies was also conducted. The degeneracies on some dressed states were lifted and the number of one and two-photon peaks augmented as could have been expected. The results coming from the cavity decay processes were also observed and confirmed to exist in the general case.

A last effect, the cavity induced transparency, was observed. We showed that when the laser frequency was in the middle of the atomic frequencies, not only the population of the doubly excited state dropped but also the number of photons and of pairs of photons were found to be identical to the number that would have been found in an empty cavity, therefore yielding no particular multi-photon process, exactly as what we found in free space. The CIT effect was not found to be as strong when the atomic frequencies were very close from each other, as in this case the cavity decay induced drop in the mean photon number takes precedence.

Actual experimental realizations of atoms in resonant cavities have been realized in circuit cavity QED. In that type of experiments, like in [97, 99, 100] a lot of parameters, such at the atomic frequencies, are independently controllable. Monitoring the transmission at low enough power exhibits the usual vacuum Rabi splitting, specific to two atoms as the Rabi splitting depends on the number of atoms [101–106]. With an increase of the input power, the transmission could show the cavity two-photon resonance and exhibit all the effects we spoke of. A particular immediate realization of that two-photon effect could be realized in circuit cavity QED considering the setup used in [97] with two superconducting qubits instead of three. In that experiment, the frequency of each qubit is separately tunable, and we deliberately chose in this paper parameters close to what has been achieved.

[1]Five-photon processes are obviously the highest multi-photon processes one could obtain with a truncated basis with $n_{\max} = 5$. However, attempts were made with $n_{\max} = 7$ and no higher order process was noticed for the same value of ϵ.

Clearly, the existence of cavity induced two-photon transition implies the existence of cavity induced inter-qubits interaction. This would suggest that all inter-atomic forces can be manipulated by using cavities, as we have control over parameters like frequencies or coupling strengths. Cavities offer many possibilities, as whole ladders of dressed states and one or more external fields can be used to manipulate interactions inside the cavity [64,107].

Conclusion

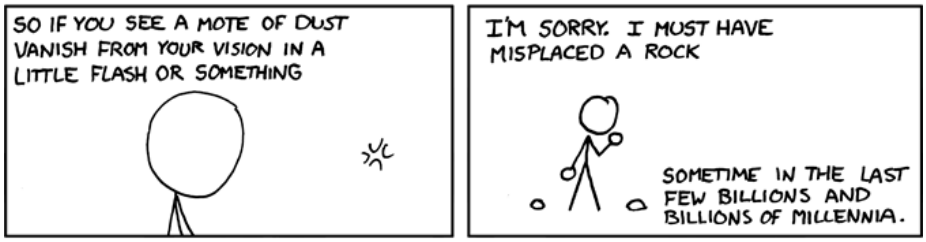

Randall Munroe, *A Bunch of Rocks* (part 8 of 9), `xkcd.com/505/`

In chapter 1, we made a contribution to quantum entanglement theory by introducing a new entanglement criterion, the Schrödinger-Robertson partial transpose inequality. We took advantage of the physicality of a partially transposed separable state to constrain the product of the variances of two operators to a minimal value. The violation of that constraint when measured on some state is the indisputable sign of entanglement in the state. We showed that not just any operator could be used in that inequality, and we gave a precise description of acceptable operators. We proved that there is always a pair of suitable operators that are able to detect the entanglement of any pure bipartite state of any dimension, giving a necessary and sufficient criterion for the detection of entanglement. We also proved that the criterion was necessary and sufficient in the case of pure three-qubit state. The Schrödinger-Robertson partial transpose inequality has a very wide range of application and we tested it on a few systems, multipartite mixed states, harmonic oscillators, multiphoton polarization states, continuous variable states or Schrödinger cat states with very encouraging results.

In chapter 2, we introduced an N-qubit generalization of the concurrence, originally defined for two qubits. We started off with three qubits and we gave a series of conditions that we proved to be necessary and sufficient for the entanglement of pure states. We used these conditions to construct nine matrices that lead to the definition of the three-qubit concurrences for pure states. We showed that those concurrences were not unrelated to other established measures of entanglement, such as the three-tangle or another type of multipartite concurrence defined in the literature. Following in the footsteps of the original concurrence, we generalized the application of our concurrences to mixed sates and we showed that any linear combination of the nine original matrices could be used to define a concurrence applicable on mixed states. Any observed non-zero concurrence in a

state immediately indicates the presence of entanglement in the system. We showed that in the case of symmetric states, the number of concurrences could be reduced to three, with which a non-zero value directly indicates the presence of genuine tripartite entanglement. We pushed the generalization to N-qubit states by determining all the necessary and sufficient conditions to entanglement of a pure state. Those conditions allowed us to define the concurrences for pure and mixed states of N-qubits. We concluded with an example application on a family of mixed states into which any N-qubit state can be depolarized and saw that the entanglement of those state could always be detected with our concurrences.

In chapter 3, we started to get interested in ways to produce entanglement in physical systems such as cold atoms. We investigated the dipole blockade effect observed in such systems and modelized it with an interaction term in the Hamiltonian and master equation of the system. We showed that if the doubly excited state was shifted out of resonance far enough, the system would evolve from the ground state into a mixture of ground state and maximally entangled state. We measured the intensity of the blockade as well as the concurrence in different situations and we concluded that indeed the amplitude of the blockade in the system was a good marker for the amount of entanglement shared in the atoms. We also saw that the blockade could be lifted by considering a strong enough laser excitation. This observation lead us to investigate the steady state of the system towards which all systems tend to. We were able to find the analytical expression of the steady state, which allowed us to give the expression for the amplitude of the blockade. Furthermore, we were able to give an analytical expression of the concurrence in the state. This expression can be used to calculate the laser strength that will maximize the amount of entanglement in the system for a given interaction strength. We concluded the chapter by giving another way to probe the blockade effect in the system, the photon-photon correlation. We showed a connection between values of the photon-photon correlation and the blockade, which provides a new way to measure the effect in an atomic system in the case where the spontaneous emission dominates over other dissipation effects.

In chapter 4, we extended our model to three-atom systems. We showed that it was enough to consider the sum of the pairwise atomic interactions to find the global interactive terms in the Hamiltonian. We studied the system in a mixed symmetry basis that helped us along the way to interpret several results. After a few considerations on general configurations of the system, we studied different cases: no interaction between the atoms, interaction between only two, same interaction between all atoms and aligned atoms with interaction between first neighbors only. For each case we were able to give a complete analytical expression of the steady state. We studied the different blockades in the system and saw that the maximally excited state tended to be very far away from resonance in genuine tripartite interactions. The blockades observed in pairs of atoms with the third atom traced out showed no great difference with the bipartite case except when we considered the atoms from the extremities of the chain of atoms. In that case, the population of these two atoms in their excited states was actually enhanced even though the atoms share no direct interaction. Then, we studied the two-atom concurrences in the different subsystems by tracing out one atom. We noted a general decrease of the amount of bipartite entanglement as a third atom was set to interact with the original pair. Anecdotally,

no entanglement was associated with the enhancing observed earlier. Finally, we studied tripartite entanglement using our concurrences defined the second chapter. We saw clear signs of genuine tripartite entanglement, especially of the W-type in the symmetric configuration, and thus we confirmed the interest of defining our concurrences.

In chapter 5, we investigated the EIT, which was shown to be able to detect Rydberg states. We wondered if, conversely, the long range interactions observed in Rydberg states could influence the EIT. We first gave an overview of the phenomenon and used our master equation formalism to give an analytical expression of the steady state for the a three-level atom in the ladder scheme excited by two lasers. By considering the steady state term responsible for EIT in the lowest order of the probe laser strength, we found the usual expression of the EIT. We then gave our model of dipole blockade interaction for two of such atoms in our Hamiltonian and steady state. After finding the eigenstates of the unperturbed basis, we investigated the possible two-photon processes and found that one possible excitation was forbidden for a non-zero interaction but that two others were always non-zero since they relied on only one possible excitation path. We then computed numerical simulations of the steady state and measured the blockade and its effect on EIT. We found that the blockade and antiblockade effects were important and in accordance with our perturbation theory considerations, although the EIT was only slightly affected. This can be explained by the fact that EIT is not a saturation effect, i. e. the population in the top level state is of less importance as the simple possibility for a transition. At that point, we considered another kind of possible interaction for the system, the dipole-dipole interaction, and presented our theoretical model. The effects of the interaction on the eigenstates of the unperturbed Hamiltonian were found to be deeper than those of the previously considered interaction since it increased the number of possible transitions. The two-photon transitions were also studied and we found that one of them was still forbidden while the other two were not. We found that the effect on the EIT in the steady state were considerably more important as we noted the apparition of three windows of transparency instead of one, which can be explained by the apparition of the new transition frequencies, in particular in the antisymmetric states of the system.

In chapter 6, we studied two-photon processes in cavity QED. After checking why such processes were forbidden for two unidentical atoms in free space, we gave our Hamiltonian modelizing the atoms, the cavity mode, the coupling between them and the laser excitation. We also gave the master equation which includes dissipations effects like atomic spontaneous emission and cavity losses in the model. We considered a constraint on the atomic frequencies that allowed us to analytically express the eigenstates and eigenvalues of the unperturbed Hamiltonian, which lead us to calculate, with perturbation theory, the possibility of two-photon processes within the cavity. We found that those processes were indeed possible when considering transitions to two of the dressed states of the system and we noted that the transitions to the other possible states could not be identified as two-photon processes but rather as two consecutive one-photon transitions. After a few numerical considerations, we studied the steady state of the system by computing different photonic and atomic spectra that confirmed the existence of two-photon processes. By studying the influence of lowering the cavity quality on the different spectra, we found

that some behaviors could be interpreted with a free space model, but others, such as the strong inhibition of the doubly excited state population at the mean atomic frequency, could not. We then numerically considered a more general setup by lifting the constraint on the atomic frequencies which lifted degeneracies and allowed us to confirm previous observations. One more effect was noted, the cavity induced transparency. For the same laser frequency that inhibits doubly excited states, the number of photons in the cavity is found to be the same as it should be in an empty cavity. This effect was found to be stronger when the atomic frequencies were far apart and annulled for identical frequencies.

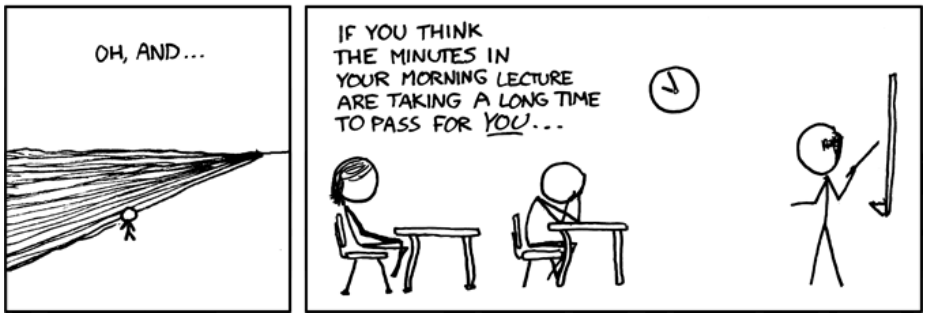

Randall Munroe, *A Bunch of Rocks* (part 9 of 9), `xkcd.com/505/`

Appendix A

Expression of Angular Eigenstates of Harmonic Oscillators

In this appendix, we derive some results on harmonic oscillators which are useful to show the abilities of entanglement detection of the SRPT criterion.

A.1 Two Dimensional Harmonic Oscillator

In two dimensions, the Hamiltonian describing a particle of mass m subject to an isotropic harmonic potential is

$$H = \frac{p_x^2}{2m} + \frac{p_y^2}{2m} + \frac{1}{2}m\omega^2\left(x^2 + y^2\right), \tag{A.1}$$

with x_i, p_i the position and momentum of the particle in the directions $i = x, y$ and ω a constant. Since H is the sum of two oscillators Hamiltonians along the directions x and y, it is clear that the eigenvalues of the hamiltonian will be written as

$$|n_x, n_y\rangle \equiv |n_x\rangle \otimes |n_y\rangle, \tag{A.2}$$

when the $|n_i\rangle$ are the eigenstates of the two one dimensional Hamiltonians. We may define the annihilation operators:

$$a_x = \frac{1}{\sqrt{2}}\left(\sqrt{\frac{m\omega}{\hbar}}x + \frac{i}{\sqrt{m\hbar\omega}}p_x\right), \tag{A.3}$$

$$a_y = \frac{1}{\sqrt{2}}\left(\sqrt{\frac{m\omega}{\hbar}}y + \frac{i}{\sqrt{m\hbar\omega}}p_y\right). \tag{A.4}$$

The creation operators $a_i^\dagger$ are the hermitian conjugates of the above operators. We have

$$[a_x, a_x^\dagger] = [a_y, a_y^\dagger] = 1, \tag{A.5}$$

while all other commutators between the four operators are zero. Let us finally define the number operators

$$N_x = a_x^\dagger a_x, \tag{A.6}$$
$$N_y = a_y^\dagger a_y, \tag{A.7}$$

which allow us to write H as

$$H = (N_x + N_y + 1)\hbar\omega. \tag{A.8}$$

The eigenstates have the properties

$$a_i|n_i\rangle = \sqrt{n_i}|n_i - 1\rangle, \tag{A.9}$$
$$a_i^\dagger|n_i\rangle = \sqrt{n_i + 1}|n_i + 1\rangle, \tag{A.10}$$
$$N_i|n_i\rangle = n_i|n_i\rangle, \tag{A.11}$$

and therefore, we have

$$|n_x, n_y\rangle = \frac{1}{\sqrt{n_x!\, n_y!}} \left(a_x^\dagger\right)^{n_x} \left(a_y^\dagger\right)^{n_y} |0, 0\rangle, \tag{A.12}$$

with $|0, 0\rangle$ the ground state of the oscillator.

We can also prove that

$$H|n_x, n_y\rangle = (n_x + n_y + 1)\hbar\omega|n_x, n_y\rangle. \tag{A.13}$$

If we define the total quantum number

$$n = n_x + n_y, \tag{A.14}$$

we note that one particular value of n corresponds to the $n + 1$ orthogonal eigenstates

$$|n, 0\rangle,\ |n - 1, 1\rangle, \ldots,\ |0, n\rangle, \tag{A.15}$$

which shows that the measure of the energy alone does not allow us to pinpoint one proper state. The discrimination between all these states could be achieved by measuring the energy separately in the x and y direction, but there is another method that takes advantage of the angular momentum L_z. That operator is defined by

$$L_z = xp_y - yp_x, \tag{A.16}$$

or in other terms

$$L_z = i\hbar(a_x a_y^\dagger - a_x^\dagger a_y), \tag{A.17}$$

and it is clear that the $|n_x, n_y\rangle$ states are not eigenstates of L_z.

However, it is possible to show that

$$[H, L_z] = 0, \tag{A.18}$$

which indicates there must be a common eigenstate basis for the two operators. That basis is made of the $|\psi_{k,M}\rangle$ eigenvectors which has the following properties:

$$H|\psi_{k,M}\rangle = \hbar\omega(2k+|M|+1)|\psi_{k,M}\rangle, \tag{A.19}$$
$$L_z|\psi_{k,M}\rangle = \hbar M|\psi_{k,M}\rangle. \tag{A.20}$$

We wish to express any $|\psi_{k,M}\rangle$ state in function of the $|n_x, n_y\rangle$ states. It is quite clear that $n = n_x + n_y = 2k + |M|$ and therefore for given k and M we have in general

$$|\psi_{k,M}\rangle = \sum_{i=0}^{n} c_i |n_x = n-i, n_y = i\rangle. \tag{A.21}$$

To find the analytical expression of the c_i coefficients, we need to define an intermediate basis as follow

$$a_r = \frac{1}{\sqrt{2}}\left(a_x - ia_y\right), \tag{A.22}$$
$$a_l = \frac{1}{\sqrt{2}}\left(a_x + ia_y\right), \tag{A.23}$$

where r and l stand for right and left, as those operators can be interpreted as annihilators of right and left "circular quanta". They are very similar to a_x and a_y, they follow the commutation rules

$$[a_r, a_r^\dagger] = [a_l, a_l^\dagger] = 1, \tag{A.24}$$

and all other combinations are zero. It is possible to express the regular ladder operators in function of the circular one and we find that

$$H = (N_r + N_l + 1)\hbar\omega, \tag{A.25}$$
$$L_z = \hbar(N_r - N_l), \tag{A.26}$$

with $N_r = a_r^\dagger a_r$ and $N_l = a_l^\dagger a_l$ the new number operators. We see that there is a $|\varphi_{n_r,n_l}\rangle$ basis in which both H and L_z are diagonal and which behaves exactly like the $|n_x, n_y\rangle$ basis. We also find

$$n = n_r + n_l = 2k + |M|, \tag{A.27}$$
$$M = n_r - n_l, \tag{A.28}$$

This result does allow to associate a definite $|\psi_{k,M}\rangle$ state to a single state $|\varphi_{n_r,n_l}\rangle$. There are two cases depending on the sign of M; if $M > 0$, it means $n_r > n_l$ and $|M| = n_r - n_l$ and $k = n_l$, if $M < 0$, then $|M| = n_l - n_r$ and $k = n_r$. Globally,

$$|\psi_{k,M}\rangle = |\varphi_{n_r=k+|M|,n_l=k}\rangle \text{ if } M > 0, \tag{A.29}$$
$$|\psi_{k,M}\rangle = |\varphi_{n_r=k,n_l=k+|M|}\rangle \text{ if } M < 0. \tag{A.30}$$

We see that a state with a positive helicity M has more "right" quanta than "left" quanta and inversely for $M < 0$. Now, to express a $|\varphi_{n_r,n_l}\rangle$ into a combination of $|n_x, n_y\rangle$ we have

$$
\begin{aligned}
|\varphi_{n_r,n_l}\rangle &= \frac{1}{\sqrt{n_r!\, n_l!}} \left(a_r^\dagger\right)^{n_r} \left(a_l^\dagger\right)^{n_l} |\varphi_{0,0}\rangle, && \text{(A.31)}\\
&= \frac{1}{\sqrt{2^n n_r!\, n_l!}} \left(a_x^\dagger + i a_y^\dagger\right)^{n_r} \left(a_x^\dagger - i a_y^\dagger\right)^{n_l} |0,0\rangle, && \text{(A.32)}\\
&= \frac{1}{\sqrt{2^n n_r!\, n_l!}} \sum_{k=0}^{n_r} \sum_{l=0}^{n_l} \binom{n_r}{k} \binom{n_l}{l} \left(a_x^\dagger\right)^{n-k-l} \left(a_y^\dagger\right)^{j+k} (i)^{k-l} |0,0\rangle, && \text{(A.33)}\\
&= \frac{1}{\sqrt{2^n n_r!\, n_l!}} \sum_{i=0}^{n} \sum_{j}^{\{-i,-i+2,\cdots,i\}} \binom{n_r}{\frac{i-j}{2}} \binom{n_l}{\frac{i+j}{2}} \left(a_x^\dagger\right)^{n-i} \left(a_y^\dagger\right)^{i} (i)^{j} |0,0\rangle, && \text{(A.34)}\\
&= \frac{1}{\sqrt{2^n n_r!\, n_l!}} \sum_{i=0}^{n} \sum_{j=0}^{i} \binom{n_r}{j} \binom{n_l}{i-j} \left(a_x^\dagger\right)^{n-i} \left(a_y^\dagger\right)^{i} (i)^{2j-i} |0,0\rangle, && \text{(A.35)}\\
&= \sum_{i=0}^{n} (-i)^i \sqrt{\frac{(n-i)!\, i!}{2^n n_r!\, n_l!}} \sum_{j=0}^{i} (-1)^j \binom{n_r}{j} \binom{n_l}{i-j} |n-i, i\rangle, && \text{(A.36)}\\
&= \sum_{i=0}^{n} (-i)^i \sqrt{\frac{\binom{n}{n_r}}{2^n \binom{n}{i}}} \sum_{j=0}^{i} (-1)^j \binom{n_r}{j} \binom{n_l}{i-j} |n-i, i\rangle, && \text{(A.37)}
\end{aligned}
$$

where on line (A.32) we simply used the definition of a_r and a_l and noted the ground state is the same in both basis, in (A.33) we used the binomial formula twice and in (A.34) we applied the change of variables $i = k + l$ and $j = k - l$. In order to span all values of (k, l) only once, we span all "antidiagonal" lines with $k + l = i$ $(i = 0, 1, \ldots, n)$ and along those lines we consider the elements $(k = \frac{i+j}{2}, l = \frac{i-j}{2})$ $(j = -i, -i + 2, \ldots, i - 2, i)$. The values of j should actually only go from $\max\{-i, i - 2n_l\}$ to $\min\{i, 2n_r - i\}$ in order not to go beyond $k = n_r$ and $l = n_l$ but we can simplify it since the binomial coefficients will yield zero if $k > n_r$ or $l > n_l$. In line (A.35) we applied yet another change of variable as $j' = \frac{i+j}{2}$ $(j = 0, 1, \ldots, i)$ and renamed j' as j, in (A.36) we applied the creation operators to the ground state and in (A.37) we multiplied the numerator and denominator in the root term by $n!$ and simplified the expression. The final sum on j may be expressed differently as we find that

$$
\sum_{j=0}^{i} (-1)^j \binom{n_r}{j} \binom{n_l}{i-j} = \binom{n_l}{i} {}_2F_1(-i, -n_r; n_l - i + 1; -1), \qquad \text{(A.38)}
$$

with ${}_2F_1$ the hypergeometric function, but we choose to keep the sum as it is for its implementation simplicity.

Now, we need to express directly the $|\psi_{k,n}\rangle$ state in the $|n_x, n_y\rangle$ basis. Depending on the sign of M, we need to consider the state $|\varphi_{k+|M|,k}\rangle$ or $|\varphi_{k,k+|M|}\rangle$. The easiest way to see the effect of a swap of n_r and n_l is in line (A.33) where the only difference is i^{k-l} becoming

$i^{l-k} = (-i)^{k-l}$. With that consideration, we finally have the c_i coefficients we wanted in (A.21) up to an overall phase:

$$c_i = (-\text{sign}(M)i)^i \sqrt{\frac{\binom{n}{k}}{2^n\binom{n}{i}}} \sum_{j=0}^{i} (-1)^j \binom{k+|M|}{j}\binom{k}{i-j}. \tag{A.39}$$

The last property we want to investigate is the relation

$$c_i = i^n (-1)^{n_l - i} c_{n-i}. \tag{A.40}$$

On the left hand side, we have

$$c_i = (-i)^i \sqrt{\frac{\binom{n}{n_r}}{2^n\binom{n}{i}}} \sum_{j=0}^{i} (-1)^j \binom{n_r}{j}\binom{n_l}{i-j}, \tag{A.41}$$

and on the right hand side

$$\begin{aligned} c_{n-i} &= (-i)^{n-i} \sqrt{\frac{\binom{n}{n_r}}{2^n\binom{n}{n-i}}} \sum_{j=0}^{n-i} (-1)^j \binom{n_r}{j}\binom{n_l}{n-i-j}, && \text{(A.42)} \\ &= (-i)^{n-i} \sqrt{\frac{\binom{n}{n_r}}{2^n\binom{n}{i}}} \sum_{j=n_l-i}^{n_r} (-1)^{n_r-j} \binom{n_r}{n_r-j}\binom{n_l}{n-i+j-n_r}, && \text{(A.43)} \\ &= (-i)^{n-i}(-1)^{n_r} \sqrt{\frac{\binom{n}{n_r}}{2^n\binom{n}{i}}} \sum_{j=n_l-i}^{n_r} (-1)^{j} \binom{n_r}{j}\binom{n_l}{i-j}, && \text{(A.44)} \end{aligned}$$

where in the second step we used the variable change $j' = n_r - j$ and in the last step simplified the expression. Aside from the phase, the only remaining difference is the borns of the sum but thanks to the binomial coefficients, that difference vanishes. Indeed, for both sums, the condition of having non zero terms is $\max\{0, i-n_l\} \leq j \leq \min\{i, n_r\}$, so that all terms considered outside those limits are zero. Of course, we have $|c_i| = |c_{n-i}|$.

A.2 Three Dimensional Harmonic Oscillator

In three dimensions, the Hamiltonian describing a particle of mass m subject to an isotropic harmonic potential is

$$H = \frac{p_x^2}{2m} + \frac{p_y^2}{2m} + \frac{p_z^2}{2m} + \frac{1}{2}m\omega^2\left(x^2+y^2+z^2\right), \tag{A.45}$$

with x_i, p_i the position and momentum of the particle in the directions $i = x, y, z$ and ω a constant. Once again, since H is the sum of three oscillators Hamiltonians, the eigenvalues of the hamiltonian will be written as

$$|n_x, n_y, n_z\rangle \equiv |n_x\rangle \otimes |n_y\rangle \otimes |n_z\rangle, \tag{A.46}$$

when the $|n_i\rangle$ are the eigenstates of the three one dimensional Hamiltonians. We may define the third annihilation operator:

$$a_z = \frac{1}{\sqrt{2}}\left(\sqrt{\frac{m\omega}{\hbar}}z + \frac{i}{\sqrt{m\hbar\omega}}p_z\right), \tag{A.47}$$

which behaves exactly as the others. We also define its number operator

$$N_z = a_z^\dagger a_z, \tag{A.48}$$

which allow us to write H as

$$H = \left(N_x + N_y + N_z + \frac{3}{2}\right)\hbar\omega. \tag{A.49}$$

The eigenstates are of the form

$$|n_x, n_y, n_z\rangle = \frac{1}{\sqrt{n_x!\, n_y!\, n_z!}}\left(a_x^\dagger\right)^{n_x}\left(a_y^\dagger\right)^{n_y}\left(a_z^\dagger\right)^{n_z}|0,0,0\rangle, \tag{A.50}$$

with $|0,0,0\rangle$ the ground state of the oscillator. This time for a definite energy $n = n_x + n_y + n_z$ there is a degree of degenerescence g_n of

$$g_n = \sum_{i=0}^{n}(i+1) = \frac{n(n+1)}{2} + (n+1) = \frac{1}{2}(n+1)(n+2). \tag{A.51}$$

Just as we introduced L_z in the two dimensional harmonic oscillator, we introduce the additional observable

$$\mathbf{L}^2 = \frac{1}{2}(L_+L_- + L_-L_+) + L_z^2, \tag{A.52}$$

with

$$L_+ = \hbar\sqrt{2}(a_z^\dagger a_l - a_r^\dagger a_z), \tag{A.53}$$
$$L_- = \hbar\sqrt{2}(a_l^\dagger a_z - a_z^\dagger a_r). \tag{A.54}$$

It can be checked that $[H, \mathbf{L}^2] = 0$ and $[L_z, \mathbf{L}^2] = 0$ which implies there must be a common set of eigenstates for H, L_z and $\mathbf{L}^2$. Those eigenstates are the $|\psi_{k,l,m}\rangle$ states and have the following properties

$$H|\psi_{k,l,m}\rangle = \hbar\omega(2k + l + \frac{3}{2})|\psi_{k,l,m}\rangle, \tag{A.55}$$
$$L_z|\psi_{k,l,m}\rangle = \hbar m|\psi_{k,l,m}\rangle, \tag{A.56}$$
$$\mathbf{L}^2|\psi_{k,l,m}\rangle = \hbar^2 l(l+1)|\psi_{k,l,m}\rangle, \tag{A.57}$$
$$L_\pm|\psi_{k,l,m}\rangle = \hbar\sqrt{l(l+1) - m(m\pm 1)}|\psi_{k,l,m\pm 1}\rangle. \tag{A.58}$$
$$\tag{A.59}$$

The last relation implies that m can take any integer value from $-l$ to l. So by repeatedly applying the L_- operator on a $|\psi_{k,l,l}\rangle$ state, we should be able to generate all states down to $|\psi_{k,l,-l}\rangle$. The first step is to find the expression of the $|\psi_{k,l,l}\rangle$ in the $|\varphi_{n_r,n_l,n_z}\rangle$ basis using the particular property $L_+|\psi_{k,l,l}\rangle = 0$. By identifying the quantum numbers we find

$$n = n_r + n_l + n_z = 2k + l, \tag{A.60}$$

$$m = n_r - n_l. \tag{A.61}$$

Since $n_r - n_l = m$ we can always write $n_r = K + m$, $n_r = K$ with K a positive integer and therefore we must have $n_z = n - m - 2K$, which cannot be negative hence we have $K \leq \frac{n-m}{2}$. We are now able to write

$$|\psi_{k,l,l}\rangle = \sum_{K=0}^{k} c_K |\varphi_{n_r=K+l,n_l=K,n_z=2k-2K}\rangle, \tag{A.62}$$

since $\frac{n-l}{2} = k$ and with normalized coefficient c_K. The effect of L_+ on such a decomposition is

$$\begin{aligned} L_+|\psi_{k,l,l}\rangle = \sum_{K=0}^{k} c_K \sqrt{2}\hbar \Big(& \sqrt{K}\sqrt{2k-2K+1}|\varphi_{K+l,K-1,2k-2K+1}\rangle \\ & - \sqrt{K+l+1}\sqrt{2k-2K}|\varphi_{K+l+1,K,2k-2K-1}\rangle \Big), \end{aligned} \tag{A.63}$$

which is zero if

$$c_K\sqrt{K+l+1}\sqrt{2k-2K} = c_{K+1}\sqrt{K+1}\sqrt{2k-2K-1}. \tag{A.64}$$

From that relation, we can express all c_K in function of c_0 and then normalize all coefficient. We have

$$c_K^2 = c_0^2 \prod_{j=0}^{K-1} \frac{(j+l+1)(2k-2j)}{(j+1)(2k-2j-1)}, \tag{A.65}$$

$$= c_0^2 \frac{(l+1)(l+2)\dots(l+K)(2k)(2k-2)\dots(2k-2K+2)}{(1)(2)\dots K(2k-1)(2k-3)\dots(2k-2K+1)}, \tag{A.66}$$

$$= c_0^2 \frac{(l+K)!}{l!\,K!} \frac{(2k)!!}{(2k-2K)!!} \frac{(2k-2K-1)!!}{(2k-1)!!}, \tag{A.67}$$

$$= c_0^2 \binom{l+K}{K} \frac{2^k k!}{2^{k-K}(k-K)!} \frac{(2k-2K)!}{2^{k-K}(k-K)!} \frac{2^k (k)!}{(2k)!}, \tag{A.68}$$

$$= c_0^2\, 2^{2K} \frac{\binom{l+K}{K}\binom{2k-2K}{k-K}}{\binom{2k}{k}}, \tag{A.69}$$

where $k!!$ is the double factorial of k which has the property

$$(2k)!! = (2k)(2k-2)\dots 2 = k!\,2^k, \tag{A.70}$$

$$(2k+1)!! = (2k+1)(2k-1)\dots 1 = \frac{(2k)!}{k!\,2^k}, \tag{A.71}$$

that we used in the process.

With that expression, we are now able to calculate the value of c_0 by normalizing the expression. We have

$$\sum_{K=0}^{k} c_K^2 = c_0^2 \sum_{K=0}^{k} 2^{2K} \frac{\binom{l+K}{K}\binom{2k-2K}{k-K}}{\binom{2k}{k}}, \tag{A.72}$$

$$= c_0^2 \frac{\binom{2(k+l+1)}{2k}}{\binom{k+l+1}{k}}, \tag{A.73}$$

Since that expression must be 1, we have he value of c_0. Finally, we get up to a global phase

$$|\psi_{k,l,l}\rangle = \sum_{K=0}^{k} 2^K \sqrt{\frac{\binom{l+K}{K}\binom{2k-2K}{k-K}\binom{k+l+1}{k}}{\binom{2k}{k}\binom{2(k+l+1)}{2k}}} |\varphi_{K+l,K,2k-2K}\rangle. \tag{A.74}$$

Appendix B

Steady State of the Blockaded Aligned Atoms

In this appendix, we present the analytical values of the steady state density matrix ρ_a^S of a system of three aligned atoms when two neighboring atoms interact via a Van der Waals potential of strength δ. The system is probed by a laser of Rabi frequency 2Ω and each atom dissipating rate is 2γ. That system is presented in Sec. 4.5.

The density matrix ρ governed by the master equation

$$\dot{\rho} = -i[H, \rho] - \gamma \sum_{i=1}^{3} (S_i^+ S_i^- \rho + \rho S_i^+ S_i^- - 2 S_i^- \rho S_i^+), \tag{B.1}$$

with the Hamiltonian

$$H = \sum_{j=1}^{3} \hbar\Omega \left(e^{i\mathbf{k}_L \cdot \mathbf{x}_j} S_j^+ + e^{-i\mathbf{k}_L \cdot \mathbf{x}_j} S_j^- \right) + \hbar\delta |e_1 e_3\rangle\langle e_1 e_3| + \hbar\delta |e_2 e_3\rangle\langle e_2 e_3|. \tag{B.2}$$

The density matrix is a 8×8 hermitian matrix which, when expressed in the mixed symmetry basis, is composed of two diagonal blocks of size 6×6 and 2×2. Therefore we have 8 real diagonal values, $15 + 1$ complex values above the diagonal and their complex conjugates under the diagonal.

We first express the common denominator $\mathcal{N}$ to all matrix elements

$$\begin{aligned}
\mathcal{N} = {} & 5441955840000\gamma^{32} + 7558272000\gamma^{30}\left(1289\delta^2 + 10944\Omega^2\right) + 5038848\gamma^{28}\left(1486037\delta^4 + 28544600\delta^2\Omega^2 + 111849600\Omega^4\right) \\
& + 46656\gamma^{26}\left(697985116\delta^6 + 228585654040\delta^4\Omega^2 + 20084095440\delta^2\Omega^4 + 487608422400\Omega^6\right) \\
& + 1296\gamma^{24}\left(68470060936\delta^8 + 34389881280\delta^6\Omega^2 + 5065127342280\delta^4\Omega^4 + 274360976064040\delta^2\Omega^6 + 467617444761600\Omega^8\right) \\
& + 432\gamma^{22}\left(36614689216\delta^{10} + 2696212619336\delta^8\Omega^2 + 595164395826400\delta^6\Omega^4 + 53413767664564\delta^4\Omega^6 + 2024535625228800\delta^2\Omega^8 + 2601293477068800\Omega^{10}\right) \\
& + 108\gamma^{20}\left(1727182800\delta^{12} + 184333789520\delta^{10}\Omega^2 + 58015026489580\delta^8\Omega^4 + 7669966339184\delta^6\Omega^6 + 477746821877760\delta^4\Omega^8\right. \\
& \left. + 13610214625075200\delta^2\Omega^{10} + 13810538299392000\Omega^{12}\right) + 216\gamma^{18}\left(6639744\delta^{14} + 1043571160\delta^{12}\Omega^2 + 46115931016\delta^{10}\Omega^4 + 850126923315\delta^8\Omega^6\right. \\
& \left. + 7699519634326\delta^6\Omega^8 + 358228489942240\delta^4\Omega^{10} + 8031919596441600\delta^2\Omega^{12} + 66461815701504\Omega^{14}\right) + 2\delta^4\Omega^{12}\left(27456\delta^{16} + 428866\delta^{14}\Omega^2\right. \\
& \left. + 3848994\delta^{12}\Omega^4 + 25227162\delta^{10}\Omega^6 + 122509127\delta^8\Omega^8 + 443184076\delta^6\Omega^{10} + 1124776800\delta^4\Omega^{12} + 1682159616\delta^2\Omega^{14} + 1012137984\Omega^{16}\right) \\
& + 72\gamma^{16}\left(952722\delta^{16} + 231734220\delta^{14}\Omega^2 + 14568245262\delta^{12}\Omega^4 + 367122369965\delta^{10}\Omega^6 + 45512506730480\delta^8\Omega^8 + 3047558250600960\delta^6\Omega^{10}\right. \\
& \left. + 1110477274270320\delta^4\Omega^{12} + 2022162684825600\delta^2\Omega^{14} + 1394743872061440\Omega^{16}\right) \\
& + \gamma^2\delta^2\Omega^{10}\left(412224\delta^{18} + 12402994\delta^{16}\Omega^2 + 149691748\delta^{14}\Omega^4 + 1189388877\delta^{12}\Omega^6 + 67798929910\delta^{10}\Omega^8 + 2802205128080\delta^8\Omega^{10}\right. \\
& \left. + 81286552896\delta^6\Omega^{12} + 1490568192000\delta^4\Omega^{14} + 1423389818880\delta^2\Omega^{16} + 502813163520\Omega^{18}\right) \\
& + 3\gamma^{14}\left(611712\delta^{18} + 257131440\delta^{16}\Omega^2 + 24121946592\delta^{14}\Omega^4 + 838616259336\delta^{12}\Omega^6 + 13866930233023\delta^{10}\Omega^8 + 1250689583399160\delta^8\Omega^{10}\right. \\
& \left. + 6509219299032480\delta^6\Omega^{12} + 19194162650818560\delta^4\Omega^{14} + 28999719470039040\delta^2\Omega^{16} + 16893852159836160\Omega^{18}\right) \\
& + \gamma^4\Omega^8\left(1101456\delta^{20} + 599238480\delta^{18}\Omega^2 + 108650183160\delta^{16}\Omega^4 + 10965739664\delta^{14}\Omega^6 + 748885201640\delta^{12}\Omega^8 + 35973030599880\delta^{10}\Omega^{10}\right. \\
& \left. + 1196708965344\delta^8\Omega^{12} + 25716954608640\delta^6\Omega^{14} + 313824031948800\delta^4\Omega^{16} + 1760780353536\delta^2\Omega^{18} + 2609192632320\Omega^{20}\right) \\
& + 2\gamma^6\Omega^6\left(671616\delta^{20} + 64443642\delta^{18}\Omega^2 + 18609138480\delta^{16}\Omega^4 + 2557200440700\delta^{14}\Omega^6 + 216265865515\delta^{12}\Omega^8 + 12324220628550\delta^{10}\Omega^{10}\right. \\
& \left. + 476187596673600\delta^8\Omega^{12} + 1190693485094400\delta^6\Omega^{14} + 1750663264665600\delta^4\Omega^{16} + 1283528274739200\delta^2\Omega^{18} + 324518333644800\Omega^{20}\right) \\
& + 2\gamma^8\Omega^4\left(402624\delta^{20} + 69371568\delta^{18}\Omega^2 + 3267179853\delta^{16}\Omega^4 + 655317672090\delta^{14}\Omega^6 + 72033825240500\delta^{12}\Omega^8 + 5010070439202\delta^{10}\Omega^{10}\right. \\
& \left. + 228903112834380\delta^8\Omega^{12} + 6698678719795200\delta^6\Omega^{14} + 11648702841292800\delta^4\Omega^{16} + 10457945800704000\delta^2\Omega^{18} + 3528983996006400\Omega^{20}\right) \\
& + 3\gamma^{10}\Omega^2\left(73728\delta^{20} + 25601328\delta^{18}\Omega^2 + 2060287896\delta^{16}\Omega^4 + 632383511130\delta^{14}\Omega^6 + 95893989645200\delta^{12}\Omega^8 + 8456511556497\delta^{10}\Omega^{10}\right. \\
& \left. + 468054217809240\delta^8\Omega^{12} + 16238803316313600\delta^6\Omega^{14} + 33334251385651200\delta^4\Omega^{16} + 35719531108761600\delta^2\Omega^{18} + 14817190477824000\Omega^{20}\right) \\
& + 6\gamma^{12}\left(3456\delta^{20} + 3341664\delta^{18}\Omega^2 + 522183042\delta^{16}\Omega^4 + 261787881120\delta^{14}\Omega^6 + 57888887501900\delta^{12}\Omega^8 + 6797240039437\delta^{10}\Omega^{10}\right. \\
& \left. + 470460440531440\delta^8\Omega^{12} + 19727489508600000\delta^6\Omega^{14} + 481691525300352000\delta^4\Omega^{16} + 611645843865600000\delta^2\Omega^{18} + 302078342725632000\Omega^{20}\right).
\end{aligned} \tag{B.3}$$

Let us first express the diagonal elements of ρ_a^S. For typography reasons, for each matrix element, we will have to pose a variable x. We pose $x = \frac{\mathcal{N}}{\Omega^6}\langle e|\rho_a^S|e\rangle$ and we have

$$
\begin{aligned}
x = {} & 5441955840000\gamma^{26} + 7558272000\gamma^{24}(809\delta^2 + 6624\Omega^2) + 5038848\gamma^{22}(577037\delta^4 + 10319600\delta^2\Omega^2 + 39273600\Omega^4) \\
& + 46656\gamma^{20}(16416847\delta^6 + 487337364\delta^4\Omega^2 + 4004407440\delta^2\Omega^4 + 9501373440\Omega^6) \\
& + 1296\gamma^{18}(94797961\delta^8 + 42308498888\delta^6\Omega^2 + 568289662928\delta^4\Omega^4 + 2888387942402\delta^2\Omega^6 + 4824793589768\Omega^8) \\
& + 432\gamma^{16}(28707360\delta^{10} + 1858487633\delta^8\Omega^2 + 36755201430\delta^6\Omega^4 + 302034330576\delta^4\Omega^6 + 1075527732096\delta^2\Omega^8 + 1349828167680\Omega^{10}) \\
& + 108\gamma^{14}(7261320\delta^{12} + 685015548\delta^{10}\Omega^2 + 19100382931\delta^8\Omega^4 + 227185546712\delta^6\Omega^6 + 1299750205248\delta^4\Omega^8 + 347135122944\delta^2\Omega^{10} \\
& \qquad + 33957326684\Omega^{12}) \\
& + \delta^4\Omega^8(2496\delta^{14} + 49306\delta^{12}\Omega^2 + 694171\delta^{10}\Omega^4 + 5529760\delta^8\Omega^6 + 28660998\delta^6\Omega^8 + 107167704\delta^4\Omega^{10} + 248864256\delta^2\Omega^{12} + 253034496\Omega^{14}) \\
& + 72\gamma^{12}(413712\delta^{14} + 59562252\delta^{12}\Omega^2 + 2330259585\delta^{10}\Omega^4 + 38037520574\delta^8\Omega^6 + 311537993838\delta^6\Omega^8 + 1335388898640\delta^4\Omega^{10} \\
& \quad + 2785264284672\delta^2\Omega^{12} + 2159197323264\Omega^{14}) + 4\gamma^2\delta^2\Omega^6(4110\delta^{16} + 170604\delta^{14}\Omega^2 + 2810705\delta^{12}\Omega^4 + 29174950\delta^{10}\Omega^6 + 188145883\delta^8\Omega^8 \\
& \quad + 811860975\delta^6\Omega^{10} + 2232679104\delta^4\Omega^{12} + 323843788\delta^2\Omega^{14} + 15712911360\Omega^{16}) + 72\gamma^{10}(8514\delta^{16} + 2092710\delta^{14}\Omega^2 + 119085409\delta^{12}\Omega^4 \\
& \quad + 2616787380\delta^{10}\Omega^6 + 28828815850\delta^8\Omega^8 + 1764200064\delta^6\Omega^{10} + 592694488824\delta^4\Omega^{12} + 98735457484\delta^2\Omega^{14} + 6042631864320\Omega^{16}) \\
& + \gamma^4\Omega^4(33264\delta^{18} + 2848752\delta^{16}\Omega^2 + 71261211\delta^{14}\Omega^4 + 941110210\delta^{12}\Omega^6 + 7675638795\delta^{10}\Omega^8 + 39716404500\delta^8\Omega^{10} + 1289880973446\delta^6\Omega^{12} \\
& \quad + 2347956495364\delta^4\Omega^{14} + 1862086164488\delta^2\Omega^{16} + 32614907904\Omega^{18}) + 12\gamma^6\Omega^2(1944\delta^{18} + 382287\delta^{16}\Omega^2 + 17056879\delta^{14}\Omega^4 + 315816633\delta^{12}\Omega^6 \\
& \quad + 3312939545\delta^{10}\Omega^8 + 211925854688\delta^8\Omega^{10} + 8269680451286\delta^6\Omega^{12} + 183516262848\delta^4\Omega^{14} + 19472552755\delta^2\Omega^{16} + 635311226\Omega^{18}) \\
& + 3\gamma^8(1728\delta^{18} + 968112\delta^{16}\Omega^2 + 88873848\delta^{14}\Omega^4 + 26734499886\delta^{12}\Omega^6 + 3829501429\delta^{10}\Omega^8 + 313051549164\delta^8\Omega^{10} + 15043839864406\delta^6\Omega^{12} \\
& \qquad + 407519768332\delta^4\Omega^{14} + 5458209767424\delta^2\Omega^{16} + 25514795335\Omega^{18}).
\end{aligned}
\tag{B.4}
$$

We pose $x = \frac{3\mathcal{N}}{\Omega^4}\langle W_2|\rho_a^S|W_2\rangle$ and we have

$$
\begin{aligned}
x = {} & 48977602560000\gamma^{28} + 68024448000\gamma^{26}\left(1129\delta^2 + 6864\Omega^2\right) + 15116544\gamma^{24}\left(3349111\delta^4 + 45420300\delta^2\Omega^2 + 127756800\Omega^4\right) \\
& + 419904\gamma^{22}\left(44114623\delta^6 + 1002767496\delta^4\Omega^2 + 6261045840\delta^2\Omega^4 + 10915223040\Omega^6\right) \\
& + 11664\gamma^{20}\left(3574675138\delta^8 + 122160361566\delta^6\Omega^2 + 1264417669806\delta^4\Omega^4 + 4889136585602\delta^2\Omega^6 + 5964958402568\Omega^8\right) \\
& + 2592\gamma^{18}\left(232656962\delta^{10} + 11397699876\delta^8\Omega^2 + 174529563291\delta^6\Omega^4 + 1110241194966\delta^4\Omega^6 + 3011508507456\delta^2\Omega^8 + 2748461289984\Omega^{10}\right) \\
& + 324\gamma^{16}\left(1748898806\delta^{12} + 121225957246\delta^{10}\Omega^2 + 2605477822578\delta^8\Omega^4 + 24190310310246\delta^6\Omega^6 + 107536720907526\delta^4\Omega^8 + 219152481776646\delta^2\Omega^{10}\right. \\
& \qquad \left. + 155865106759688\Omega^{12}\right) + 36\gamma^{14}\left(945826566\delta^{14} + 94265326686\delta^{12}\Omega^2 + 2790817224406\delta^{10}\Omega^4 + 35647041057578\delta^8\Omega^6 + 2290938301162806\delta^6\Omega^8\right. \\
& \qquad \left. + 7652301331248046\delta^4\Omega^{10} + 1221257102100486\delta^2\Omega^{12} + 69427145834496\Omega^{14}\right) + \delta^4\Omega^8\left(9984\delta^{16} + 268328\delta^{14}\Omega^2 + 31736906\delta^{12}\Omega^4\right. \\
& \qquad \left. + 231136436\delta^{10}\Omega^6 + 1220377806\delta^8\Omega^8 + 4789851386\delta^6\Omega^{10} + 12455250006\delta^4\Omega^{12} + 17176642566\delta^2\Omega^{14} + 7591034886\Omega^{16}\right) \\
& + 24\gamma^{12}\left(5194422\delta^{16} + 78374730\delta^{14}\Omega^2 + 3226473258\delta^{12}\Omega^4 + 55193625682\delta^{10}\Omega^6 + 479942768758\delta^8\Omega^8 + 2309621783707\delta^6\Omega^{10}\right. \\
& \qquad \left. + 6062101933183\delta^4\Omega^{12} + 776363199621\delta^2\Omega^{14} + 35747881943040\Omega^{16}\right) \\
& + \gamma^2\delta^2\Omega^6\left(65760\delta^{18} + 3226032\delta^{16}\Omega^2 + 54752262\delta^{14}\Omega^4 + 516091335\delta^{12}\Omega^6 + 3254348058\delta^{10}\Omega^8 + 14577123034\delta^8\Omega^{10} + 44068132140\delta^6\Omega^{12}\right. \\
& \qquad \left. + 78544288512\delta^4\Omega^{14} + 6568468070\delta^2\Omega^{16} + 1885549363\Omega^{18}\right) \\
& + 3\gamma^{10}\left(832896\delta^{18} + 213005808\delta^{16}\Omega^2 + 12745390176\delta^{14}\Omega^4 + 291729273420\delta^{12}\Omega^6 + 33090570284036\delta^{10}\Omega^8 + 2135241338579686\delta^8\Omega^{10}\right. \\
& \qquad \left. + 80951695304016\delta^6\Omega^{12} + 1716007763272326\delta^4\Omega^{14} + 178222683193344\delta^2\Omega^{16} + 66470265225216\Omega^{18}\right) \\
& + \gamma^4\Omega^4\left(133056\delta^{20} + 12484728\delta^{18}\Omega^2 + 338011668\delta^{16}\Omega^4 + 43531530216\delta^{14}\Omega^6 + 3417255177286\delta^{12}\Omega^8 + 180118760757\delta^{10}\Omega^{10}\right. \\
& \qquad \left. + 6333786912246\delta^8\Omega^{12} + 1363330915776\delta^6\Omega^{14} + 154687359744046\delta^4\Omega^{16} + 7456519618566\delta^2\Omega^{18} + 978447237120\Omega^{20}\right) \\
& + \gamma^6\Omega^2\left(93312\delta^{20} + 19291392\delta^{18}\Omega^2 + 923408112\delta^{16}\Omega^4 + 17651304993\delta^{14}\Omega^6 + 182106614192\delta^{12}\Omega^8 + 11726794718496\delta^{10}\Omega^{10}\right. \\
& \qquad \left. + 488436318625286\delta^8\Omega^{12} + 12543341048640\delta^6\Omega^{14} + 1781641252684806\delta^4\Omega^{16} + 117354904289286\delta^2\Omega^{18} + 2580654587904\Omega^{20}\right) \\
& + 3\gamma^8\left(6912\delta^{20} + 3988512\delta^{18}\Omega^2 + 385808124\delta^{16}\Omega^4 + 12197335112\delta^{14}\Omega^6 + 1780487839706\delta^{12}\Omega^8 + 147190446177186\delta^{10}\Omega^{10}\right. \\
& \qquad \left. + 7473840608764\delta^8\Omega^{12} + 230826769067046\delta^6\Omega^{14} + 4006813014489646\delta^4\Omega^{16} + 33590666428416\delta^2\Omega^{18} + 994155901747\Omega^{20}\right).
\end{aligned}
\tag{B.5}
$$

We pose $x = \frac{3\mathcal{N}}{\Omega^2}\langle W_1|\rho_a^S|W_1\rangle$ and we have

$$
\begin{aligned}
x = {} & 48977602560000\gamma^{30} + 68024448000\gamma^{28}\left(1289\delta^2 + 7584\Omega^2\right) + 45349632\gamma^{26}\left(1486037\delta^4 + 19221600\delta^2\Omega^2 + 52881600\Omega^4\right) \\
& + 419904\gamma^{24}\left(69798511\delta^6 + 14869888928\delta^4\Omega^2 + 9017591040\delta^2\Omega^4 + 155144678400\Omega^6\right) \\
& + 11664\gamma^{22}\left(6847006609\delta^8 + 215079564726\delta^6\Omega^2 + 213530433156\delta^4\Omega^4 + 8157715891200\delta^2\Omega^6 + 9894438696960\Omega^8\right) \\
& + 11664\gamma^{20}\left(1220489648\delta^{10} + 53830645198\delta^8\Omega^2 + 7778671187460\delta^6\Omega^4 + 4858210066080\delta^4\Omega^6 + 1322363647296\delta^2\Omega^8 + 120726501580800\Omega^{10}\right) \\
& + 324\gamma^{18}\left(5181548400\delta^{12} + 316302771440\delta^{10}\Omega^2 + 6297427063610\delta^8\Omega^4 + 56748628931280\delta^6\Omega^6 + 2531284947806400\delta^4\Omega^8\right. \\
& \left. + 5250173417164800\delta^2\Omega^{10} + 375742009958400\Omega^{12}\right) + 648\gamma^{16}\left(199192320\delta^{14} + 17071449200\delta^{12}\Omega^2 + 459182430920\delta^{10}\Omega^4 + 5610179634710\delta^8\Omega^6\right. \\
& \left. + 35953396822420\delta^6\Omega^8 + 1228398181233600\delta^4\Omega^{10} + 202241248243200\delta^2\Omega^{12} + 11650318995456\Omega^{14}\right) + 2\delta^4\Omega^{10}\left(237120\delta^{16} + 3213810\delta^{14}\Omega^2\right. \\
& \left. + 27934160\delta^{12}\Omega^4 + 185346870\delta^{10}\Omega^6 + 902024130\delta^8\Omega^8 + 3263363410\delta^6\Omega^{10} + 8004919080\delta^4\Omega^{12} + 10437419520\delta^2\Omega^{14} + 3795517440\Omega^{16}\right) \\
& + 108\gamma^{14}\left(57163320\delta^{16} + 7226820240\delta^{14}\Omega^2 + 2651302111880\delta^{12}\Omega^4 + 427369558922\delta^{10}\Omega^6 + 36689383207710\delta^8\Omega^8 + 1801857842059200\delta^6\Omega^{10}\right. \\
& \left. + 49199151632784\delta^4\Omega^{12} + 6593361438412800\delta^2\Omega^{14} + 310863557099520\Omega^{16}\right) \\
& + \gamma^2\delta^2\Omega^8\left(3956640\delta^{18} + 106738800\delta^{16}\Omega^2 + 1183639110\delta^{14}\Omega^4 + 9237708800\delta^{12}\Omega^6 + 52288405260\delta^{10}\Omega^8 + 213711204640\delta^8\Omega^{10}\right. \\
& \left. + 599847004680\delta^6\Omega^{12} + 999697605120\delta^4\Omega^{14} + 757016616960\delta^2\Omega^{16} + 188554936320\Omega^{18}\right) \\
& + 3\gamma^{12}\left(55054080\delta^{18} + 11485484640\delta^{16}\Omega^2 + 601166448000\delta^{14}\Omega^4 + 12804712890480\delta^{12}\Omega^6 + 141890488387510\delta^{10}\Omega^8 + 928230818982600\delta^8\Omega^{10}\right. \\
& \left. + 3659046913270080\delta^6\Omega^{12} + 8194854312161280\delta^4\Omega^{14} + 9060489794764800\delta^2\Omega^{16} + 3524533207695360\Omega^{18}\right) \\
& + \gamma^4\Omega^6\left(11796480\delta^{20} + 579801960\delta^{18}\Omega^2 + 9564077760\delta^{16}\Omega^4 + 91369665690\delta^{14}\Omega^6 + 610023616030\delta^{12}\Omega^8 + 2869918396230\delta^{10}\Omega^{10}\right. \\
& \left. + 9212392017000\delta^8\Omega^{12} + 18304264368000\delta^6\Omega^{14} + 19003009674240\delta^4\Omega^{16} + 8134298173440\delta^2\Omega^{18} + 978447237120\Omega^{20}\right) \\
& + 6\gamma^6\Omega^4\left(2609280\delta^{20} + 232241760\delta^{18}\Omega^2 + 6103026050\delta^{16}\Omega^4 + 76141615550\delta^{14}\Omega^6 + 627053261520\delta^{12}\Omega^8 + 3461409551220\delta^{10}\Omega^{10}\right. \\
& \left. + 12854006023900\delta^8\Omega^{12} + 29974987937280\delta^6\Omega^{14} + 38750708793600\delta^4\Omega^{16} + 22816554024960\delta^2\Omega^{18} + 4464165519360\Omega^{20}\right) \\
& + 3\gamma^8\Omega^2\left(3041280\delta^{20} + 53714160\delta^{18}\Omega^2 + 2375726904\delta^{16}\Omega^4 + 43905259217\delta^{14}\Omega^6 + 452010541816\delta^{12}\Omega^8 + 3002120404968\delta^{10}\Omega^{10}\right. \\
& \left. + 13112128718728\delta^8\Omega^{12} + 359514628236960\delta^6\Omega^{14} + 5603825931609600\delta^4\Omega^{16} + 4183796485324800\delta^2\Omega^{18} + 1080177721344000\Omega^{20}\right) \\
& + 6\gamma^{10}\left(311040\delta^{20} + 14308704\delta^{18}\Omega^2 + 1190693898\delta^{16}\Omega^4 + 34761972072\delta^{14}\Omega^6 + 491951521683\delta^{12}\Omega^8 + 4090631922759\delta^{10}\Omega^{10}\right. \\
& \left. + 21498413502436\delta^8\Omega^{12} + 700340088547680\delta^6\Omega^{14} + 13054818612873600\delta^4\Omega^{16} + 11933489170022400\delta^2\Omega^{18} + 3820591212134400\Omega^{20}\right).
\end{aligned}
\tag{B.6}
$$

We pose $x = \mathcal{N}\langle g|\rho_a^S|g\rangle$ and we have

$$
\begin{aligned}
x = {} & 5441955840000\gamma^{32} + 7558272000\gamma^{30}\left(1289\delta^2 + 8784\Omega^2\right) + 5038848\gamma^{28}\left(1486037\delta^4 + 22744100\delta^2\Omega^2 + 72321600\Omega^4\right) \\
& + 46656\gamma^{26}\left(69798511\delta^6 + 1804380552\delta^4\Omega^2 + 12889967040\delta^2\Omega^4 + 25561923840\Omega^6\right) \\
& + 1296\gamma^{24}\left(6847006609\delta^8 + 268516420920\delta^6\Omega^2 + 3213411666120\delta^4\Omega^4 + 14377719283200\delta^2\Omega^6 + 20053461288960\Omega^8\right) \\
& + 864\gamma^{22}\left(183073446\delta^{10} + 10399910356\delta^8\Omega^2 + 186111585675\delta^6\Omega^4 + 1387419727842\delta^4\Omega^6 + 4398629495904\delta^2\Omega^8 + 4614337331712\Omega^{10}\right) \\
& + 108\gamma^{20}\left(1727182800\delta^{12} + 140396162480\delta^{10}\Omega^2 + 3570582971270\delta^8\Omega^4 + 39292549828880\delta^6\Omega^6 + 207138789252000\delta^4\Omega^8 + 498417210063360\delta^2\Omega^{10}\right. \\
& \qquad \left. + 410675209297920\Omega^{12}\right) + 108\gamma^{18}\left(13279488\delta^{14} + 1568987480\delta^{12}\Omega^2 + 55811154056\delta^{10}\Omega^4 + 856009613817\delta^8\Omega^6 + 6598679395004\delta^6\Omega^8\right. \\
& \qquad \left. + 26422545713360\delta^4\Omega^{10} + 503903704427520\delta^2\Omega^{12} + 3361435320729600\Omega^{14}\right) + 2\delta^4\Omega^{12}\left(6240\delta^{16} + 89699\delta^{14}\Omega^2 + 774188\delta^{12}\Omega^4\right. \\
& \qquad \left. + 5081175\delta^{10}\Omega^6 + 25242547\delta^8\Omega^8 + 92379855\delta^6\Omega^{10} + 223101804\delta^4\Omega^{12} + 289877760\delta^2\Omega^{14} + 126517248\Omega^{16}\right) \\
& + 36\gamma^{16}\left(1905444\delta^{16} + 343953048\delta^{14}\Omega^2 + 17332641684\delta^{12}\Omega^4 + 362551028638\delta^{10}\Omega^6 + 3829775985949\delta^8\Omega^8 + 223010805351000\delta^6\Omega^{10}\right. \\
& \qquad \left. + 709539555144480\delta^4\Omega^{12} + 1103850215009280\delta^2\Omega^{14} + 609232423403520\Omega^{16}\right) \\
& + \gamma^2\delta^2\Omega^{10}\left(118704\delta^{18} + 30849460\delta^{16}\Omega^2 + 3405280900\delta^{14}\Omega^4 + 260998106\delta^{12}\Omega^6 + 14776403910\delta^{10}\Omega^8 + 607096754200\delta^8\Omega^{10} + 1690563142800\delta^6\Omega^{12}\right. \\
& \qquad \left. + 2800249574400\delta^4\Omega^{14} + 2229125529600\delta^2\Omega^{16} + 628516454400\Omega^{18}\right) \\
& + 3\gamma^{14}\left(611712\delta^{18} + 188535456\delta^{16}\Omega^2 + 14115308544\delta^{14}\Omega^4 + 405744738504\delta^{12}\Omega^6 + 5702368629559\delta^{10}\Omega^8 + 449195665528560\delta^8\Omega^{10}\right. \\
& \qquad \left. + 20748583466390400\delta^6\Omega^{12} + 540255769942464\delta^4\Omega^{14} + 6987346585067520\delta^2\Omega^{16} + 323767012294656\Omega^{18}\right) \\
& + \gamma^4\Omega^8\left(394704\delta^{20} + 18017172\delta^{18}\Omega^2 + 287183655\delta^{16}\Omega^4 + 2682674219\delta^{14}\Omega^6 + 17641720531\delta^{12}\Omega^8 + 82563893323\delta^{10}\Omega^{10}\right. \\
& \qquad \left. + 262814571888\delta^8\Omega^{12} + 5183431470720\delta^6\Omega^{14} + 54920616192000\delta^4\Omega^{16} + 253986471936\delta^2\Omega^{18} + 32614907904\Omega^{20}\right) \\
& + \gamma^6\Omega^6\left(603648\delta^{20} + 47497908\delta^{18}\Omega^2 + 1165271826\delta^{16}\Omega^4 + 14275726059\delta^{14}\Omega^6 + 112317724798\delta^{12}\Omega^8 + 609657778689\delta^{10}\Omega^{10}\right. \\
& \qquad \left. + 2233800502200\delta^8\Omega^{12} + 5152404663360\delta^6\Omega^{14} + 6696612741888\delta^4\Omega^{16} + 4122977697792\delta^2\Omega^{18} + 860218195968\Omega^{20}\right) \\
& + \gamma^8\Omega^4\left(452736\delta^{20} + 63380304\delta^{18}\Omega^2 + 2475471198\delta^{16}\Omega^4 + 42715585809\delta^{14}\Omega^6 + 421841093848\delta^{12}\Omega^8 + 2720480915532\delta^{10}\Omega^{10}\right. \\
& \qquad \left. + 11624794457748\delta^8\Omega^{12} + 313292430439200\delta^6\Omega^{14} + 4853317484966400\delta^4\Omega^{16} + 3697780742553600\delta^2\Omega^{18} + 1003940374118400\Omega^{20}\right) \\
& + 3\gamma^{10}\Omega^2\left(52992\delta^{20} + 14561136\delta^{18}\Omega^2 + 957968220\delta^{16}\Omega^4 + 24644838537\delta^{14}\Omega^6 + 324491624950\delta^{12}\Omega^8 + 2575015887824\delta^{10}\Omega^{10}\right. \\
& \qquad \left. + 13077660027472\delta^8\Omega^{12} + 414841883542560\delta^6\Omega^{14} + 7598330199187200\delta^4\Omega^{16} + 6949576507392000\delta^2\Omega^{18} + 2293000018329600\Omega^{20}\right) \\
& + 3\gamma^{12}\left(6912\delta^{20} + 4848192\delta^{18}\Omega^2 + 601934148\delta^{16}\Omega^4 + 24821937840\delta^{14}\Omega^6 + 463906190278\delta^{12}\Omega^8 + 4754177491525\delta^{10}\Omega^{10}\right. \\
& \qquad \left. + 29489152331396\delta^8\Omega^{12} + 1116526964965440\delta^6\Omega^{14} + 24250566493382400\delta^4\Omega^{16} + 26352612657561600\delta^2\Omega^{18} + 10323624827289600\Omega^{20}\right).
\end{aligned}
\tag{B.7}
$$

We pose $x = \frac{6\mathcal{N}}{\Omega^4}\langle\psi_2|\rho_a^S|\psi_2\rangle$ and we have

$$
\begin{aligned}
x = {} & 5441955840000\gamma^{26}\left(\delta^2+6\Omega^2\right)+7558272000\gamma^{24}\left(1109\delta^4+11958\delta^2\Omega^2+39744\Omega^4\right)\\
& +10077696\gamma^{22}\left(535081\delta^6+9250411\delta^4\Omega^2+53517600\delta^2\Omega^4+11782080\Omega^6\right)\\
& +46656\gamma^{20}\left(40904137\delta^8+1053182610\delta^6\Omega^2+9103891824\delta^4\Omega^4+35596925280\delta^2\Omega^6+5700824064\Omega^8\right)\\
& +2592\gamma^{18}\left(1582816888\delta^{10}+58275537938\delta^8\Omega^2+710375084106\delta^6\Omega^4+4032082969564\delta^4\Omega^6+11743332410884\delta^2\Omega^8+1447438076928\Omega^{10}\right)\\
& +1296\gamma^{16}\left(429081208\delta^{12}+22261542078\delta^{10}\Omega^2+370970341498\delta^8\Omega^4+2860437518166\delta^6\Omega^6+11966215308488\delta^4\Omega^8+2746475548416\delta^2\Omega^{10}\right.\\
& \left.+269656335360\Omega^{12}\right)+72\gamma^{14}\left(659908806\delta^{14}+48792936906\delta^{12}\Omega^2+1098710206826\delta^{10}\Omega^4+11136131341598\delta^8\Omega^6+617215730652\delta^6\Omega^8\right.\\
& \left.+20353730236416\delta^4\Omega^{10}+381751603845128\delta^2\Omega^{12}+30561594015744\Omega^{14}\right)+\delta^4\Omega^8\left(399366\delta^{16}+6280646\delta^{14}\Omega^2+50120426\delta^{12}\Omega^4\right.\\
& \left.+275187836\delta^{10}\Omega^6+1090503428\delta^8\Omega^8+3303912446\delta^6\Omega^{10}+8434753446\delta^4\Omega^{12}+16153528326\delta^2\Omega^{14}+15182069766\Omega^{16}\right)\\
& +12\gamma^{12}\left(205290726\delta^{16}+22647264126\delta^{14}\Omega^2+695979377646\delta^{12}\Omega^4+9135263691436\delta^{10}\Omega^6+64456050726786\delta^8\Omega^8+2775663542620 8\delta^6\Omega^{10}\right.\\
& \left.+7543702885881 6\delta^4\Omega^{12}+1182959593758 72\delta^2\Omega^{14}+777311036375 04\Omega^{16}\right)\\
& +\gamma^2\delta^2\Omega^6\left(2630406\delta^{18}+79616886\delta^{16}\Omega^2+926214726\delta^{14}\Omega^4+6510435546\delta^{12}\Omega^6+31379717676\delta^{10}\Omega^8+1049242308\delta^8\Omega^{10}\right.\\
& \left.+3082635045 6\delta^6\Omega^{12}+6582535833 6\delta^4\Omega^{14}+8388021787 2\delta^2\Omega^{16}+3771098726 4\Omega^{18}\right)\\
& +12\gamma^{10}\left(5840646\delta^{18}+1072143006\delta^{16}\Omega^2+46873651326\delta^{14}\Omega^4+7989158978 6\delta^{12}\Omega^6+7025718759776\delta^{10}\Omega^8+376756684928 0\delta^8\Omega^{10}\right.\\
& \left.+1328981046211 2\delta^6\Omega^{12}+3068033093424 0\delta^4\Omega^{14}+4068232932556 8\delta^2\Omega^{16}+2175347471155 2\Omega^{18}\right)\\
& +\gamma^4\Omega^4\left(5322246\delta^{20}+335671206\delta^{18}\Omega^2+6076473846\delta^{16}\Omega^4+575670541 5\delta^{14}\Omega^6+3469487933 6\delta^{12}\Omega^8+145519520532\delta^{10}\Omega^{10}\right.\\
& \left.+4561012242726\delta^8\Omega^{12}+1073489527296\delta^6\Omega^{14}+163059756134 4\delta^4\Omega^{16}+116617406054 4\delta^2\Omega^{18}+1956894474 24\Omega^{20}\right)\\
& +\gamma^6\Omega^2\left(3732486\delta^{20}+54044064\delta^{18}\Omega^2+1792952724\delta^{16}\Omega^4+24452203116\delta^{14}\Omega^6+192040963049\delta^{12}\Omega^8+9846596199 54\delta^{10}\Omega^{10}\right.\\
& \left.+3565702198536\delta^8\Omega^{12}+937294165555 2\delta^6\Omega^{14}+16379224026624\delta^4\Omega^{16}+1513933701120 0\delta^2\Omega^{18}+4574240833536\Omega^{20}\right)\\
& +6\gamma^8\left(138246\delta^{20}+5631264\delta^{18}\Omega^2+388455648\delta^{16}\Omega^4+88498798 90\delta^{14}\Omega^6+96342571912\delta^{12}\Omega^8+628008170375\delta^{10}\Omega^{10}\right.\\
& \left.+2711456583344\delta^8\Omega^{12}+8138002418976\delta^6\Omega^{14}+162721627257 60\delta^4\Omega^{16}+18213326585856\delta^2\Omega^{18}+7654438600704\Omega^{20}\right).
\end{aligned}
\tag{B.8}
$$

We pose $x = \frac{6\mathcal{N}}{\Omega^4}\langle\psi_1|\rho_a^S|\psi_1\rangle$ and we have

$$
\begin{aligned}
x = {} & 32651735040000\gamma^{28}+45349632000\gamma^{26}\left(1169\delta^2+7344\Omega^2\right)+30233088\gamma^{24}\left(1208787\delta^4+16021100\delta^2\Omega^2+49209600\Omega^4\right)\\
& +1399680\gamma^{22}\left(10107119\delta^6+215680752\delta^4\Omega^2+13553621 28\delta^2\Omega^4+2748584448\Omega^6\right)\\
& +7776\gamma^{20}\left(439275787\delta^8+13692162276\delta^6\Omega^2+1341306237 96\delta^4\Omega^4+546307675200\delta^2\Omega^6+8245288028 16\Omega^8\right)\\
& +10368\gamma^{18}\left(51966301\delta^{10}+2274258296\delta^8\Omega^2+31536223182\delta^6\Omega^4+1953031295 07\delta^4\Omega^6+586119140640\delta^2\Omega^8+69931656 1152\Omega^{10}\right)\\
& +648\gamma^{16}\left(86902040\delta^{12}+5294392066\delta^{10}\Omega^2+1001324475 09\delta^8\Omega^4+8538636542486\delta^6\Omega^6+382438639065 6\delta^4\Omega^8+902919937075 2\delta^2\Omega^{10}\right.\\
& \left.+8795045339136\Omega^{12}\right)+216\gamma^{14}\left(17841504\delta^{14}+1538331122\delta^{12}\Omega^2+394268762 50\delta^{10}\Omega^4+4462152549 23\delta^8\Omega^6+2685591684540\delta^6\Omega^8\right.\\
& \left.+93443725861 44\delta^4\Omega^{10}+17968350477312\delta^2\Omega^{12}+1450559265177 6\Omega^{14}\right)+\delta^4\Omega^8\left(399366\delta^{16}+672192\delta^{14}\Omega^2+5919778\delta^{12}\Omega^4\right.\\
& \left.+3680670 3\delta^{10}\Omega^6+1644964 74\delta^8\Omega^8+5232333 08\delta^6\Omega^{10}+1213055376\delta^4\Omega^{12}+1926779904\delta^2\Omega^{14}+15182069 76\Omega^{16}\right)\\
& +12\gamma^{12}\left(13768920\delta^{16}+1762394436\delta^{14}\Omega^2+62253416304\delta^{12}\Omega^4+9292806214 27\delta^{10}\Omega^6+7225832332830\delta^8\Omega^8+331412364936 00\delta^6\Omega^{10}\right.\\
& \left.+9329099369846 4\delta^4\Omega^{12}+1485373882245 12\delta^2\Omega^{14}+9948457834905 6\Omega^{16}\right)\\
& +\gamma^2\delta^2\Omega^6\left(1806726\delta^{18}+7590120\delta^{16}\Omega^2+99845556\delta^{14}\Omega^4+7785350 36\delta^{12}\Omega^6+4183611111\delta^{10}\Omega^8+157825514 56\delta^8\Omega^{10}\right.\\
& \left.+4243838560 8\delta^6\Omega^{12}+7962002380 8\delta^4\Omega^{14}+8896573440 0\delta^2\Omega^{16}+3771098726 4\Omega^{18}\right)\\
& +6\gamma^{10}\left(6670086\delta^{18}+140987736\delta^{16}\Omega^2+7188055176\delta^{14}\Omega^4+14349825822 6\delta^{12}\Omega^6+1428397312599\delta^{10}\Omega^8+8258674985068\delta^8\Omega^{10}\right.\\
& \left.+3031501095153 6\delta^6\Omega^{12}+7061589690451 2\delta^4\Omega^{14}+9348129069465 6\delta^2\Omega^{16}+5116138802380 8\Omega^{18}\right)\\
& +\gamma^4\Omega^4\left(2845446\delta^{20}+241032966\delta^{18}\Omega^2+5711169846\delta^{16}\Omega^4+6146851371\delta^{14}\Omega^6+4093070032 0\delta^{12}\Omega^8+184930170132\delta^{10}\Omega^{10}\right.\\
& \left.+5822785928886\delta^8\Omega^{12}+1269959090688 6\delta^6\Omega^{14}+1745383431168 4\delta^4\Omega^{16}+1171270139904\delta^2\Omega^{18}+1956894474 24\Omega^{20}\right)\\
& +3\gamma^6\Omega^2\left(622086\delta^{20}+107357766\delta^{18}\Omega^2+45524381 2\delta^{16}\Omega^4+7671122750\delta^{14}\Omega^6+676683464798\delta^{12}\Omega^8+375641011680\delta^{10}\Omega^{10}\right.\\
& \left.+1406139404624 0\delta^8\Omega^{12}+3591217037184\delta^6\Omega^{14}+5892596633088\delta^4\Omega^{16}+5197353320448\delta^2\Omega^{18}+1589976760320\Omega^{20}\right)\\
& +6\gamma^8\left(6912\delta^{20}+3196224\delta^{18}\Omega^2+260874180\delta^{16}\Omega^4+7242037738\delta^{14}\Omega^6+927863884 82\delta^{12}\Omega^8+6654202223 85\delta^{10}\Omega^{10}\right.\\
& \left.+3034282720856\delta^8\Omega^{12}+9197961163104\delta^6\Omega^{14}+1794035755123 2\delta^4\Omega^{16}+1960927543296 0\delta^2\Omega^{18}+8416812072960\Omega^{20}\right).
\end{aligned}
\tag{B.9}
$$

We pose $x = \frac{2\mathcal{N}}{\Omega^6}\langle\phi_2|\rho_a^S|\phi_2\rangle$ and we have

$$
\begin{aligned}
x = {} & 10883911680000\gamma^{26} + 136048896000\gamma^{24}\left(81\delta^2 + 736\Omega^2\right) + 10077696\gamma^{22}\left(470537\delta^4 + 9345600\delta^2\Omega^2 + 39273600\Omega^4\right) \\
& + 93312\gamma^{20}\left(12545653\delta^6 + 402593664\delta^4\Omega^2 + 3659556240\delta^2\Omega^4 + 9501373440\Omega^6\right) \\
& + 7776\gamma^{18}\left(246666699\delta^8 + 1106163476\delta^6\Omega^2 + 15991966044\delta^4\Omega^4 + 88882133760\delta^2\Omega^6 + 160826452992\Omega^8\right) \\
& + 432\gamma^{16}\left(52434405\delta^{10} + 3030142166\delta^8\Omega^2 + 59906748564\delta^6\Omega^4 + 521984289312\delta^4\Omega^6 + 2005578102528\delta^2\Omega^8 + 2699656335360\Omega^{10}\right) \\
& + 72\gamma^{14}\left(26834490\delta^{12} + 1986757242\delta^{10}\Omega^2 + 49376764811\delta^8\Omega^4 + 577169846376\delta^6\Omega^6 + 3445661173248\delta^4\Omega^8 + 9800920249344\delta^2\Omega^{10}\right. \\
& \qquad \left. + 1018719800524 8\Omega^{12}\right) \\
& + \delta^4\Omega^8\left(22464\delta^{14} + 303082\delta^{12}\Omega^2 + 2530011\delta^{10}\Omega^4 + 15372072\delta^8\Omega^6 + 65965196\delta^6\Omega^8 + 214441776\delta^4\Omega^{10} + 482319360\delta^2\Omega^{12} + 506068992\Omega^{14}\right) \\
& + 36\gamma^{12}\left(3038148\delta^{14} + 310435884\delta^{12}\Omega^2 + 9608933749\delta^{10}\Omega^4 + 137883924566\delta^8\Omega^6 + 1092377959520\delta^6\Omega^8 + 4818973249728\delta^4\Omega^{10}\right. \\
& \left. + 10577583673344\delta^2\Omega^{12} + 863678929305 6\Omega^{14}\right) + \gamma^2\delta^2\Omega^6\left(147960\delta^{16} + 4000008\delta^{14}\Omega^2 + 44023094\delta^{12}\Omega^4 + 330792939\delta^{10}\Omega^6 + 17330324328\delta^8\Omega^8\right. \\
& \left. + 65512988888\delta^6\Omega^{10} + 172472601604\delta^4\Omega^{12} + 2532711628 8\delta^2\Omega^{14} + 125703290 88\Omega^{16}\right) + 12\gamma^{10}\left(292572\delta^{16} + 48002508\delta^{14}\Omega^2 + 1971027195\delta^{12}\Omega^4\right. \\
& \left. + 34092264362\delta^{10}\Omega^6 + 3261944488 08\delta^8\Omega^8 + 191205146520 0\delta^6\Omega^{10} + 65388641578 56\delta^4\Omega^{12} + 113442597273 60\delta^2\Omega^{14} + 725115823718 4\Omega^{16}\right) \\
& + \gamma^4\Omega^4\left(299376\delta^{18} + 16985256\delta^{16}\Omega^2 + 284427855\delta^{14}\Omega^4 + 27189269 38\delta^{12}\Omega^6 + 176180294 40\delta^{10}\Omega^8 + 797863558 08\delta^8\Omega^{10}\right. \\
& \qquad \left. + 246997843200\delta^6\Omega^{12} + 4523911464 96\delta^4\Omega^{14} + 3669814149 12\delta^2\Omega^{16} + 652298158 08\Omega^{18}\right) \\
& + 3\gamma^6\Omega^2\left(69984\delta^{18} + 9086028\delta^{16}\Omega^2 + 2757417528\delta^{14}\Omega^4 + 36650152 55\delta^{12}\Omega^6 + 3020952130 6\delta^{10}\Omega^8 + 1681534775 92\delta^8\Omega^{10} + 6246015091 20\delta^6\Omega^{12}\right. \\
& \left. + 1394381938176\delta^4\Omega^{14} + 1518168047616\delta^2\Omega^{16} + 508248981504\Omega^{18}\right) + 6\gamma^8\left(7776\delta^{18} + 28288 08\delta^{16}\Omega^2 + 176292762\delta^{14}\Omega^4 + 3834991052\delta^{12}\Omega^6\right. \\
& \left. + 429142649 03\delta^{10}\Omega^8 + 3040934269 28\delta^8\Omega^{10} + 1392888111 9936\delta^6\Omega^{12} + 3811189318272\delta^4\Omega^{14} + 52705572618 24\delta^2\Omega^{16} + 255147953356 8\Omega^{18}\right).
\end{aligned}
\tag{B.10}
$$

We pose $x = \frac{2\mathcal{N}}{\Omega^4}\langle\phi_1|\rho_a^S|\phi_1\rangle$ and we have

$$
\begin{aligned}
x = {} & 10883911680000\gamma^{28} + 15116544000\gamma^{26}\left(1289\delta^2 + 7344\Omega^2\right) + 10077696\gamma^{24}\left(1486037\delta^4 + 18637100\delta^2\Omega^2 + 49209600\Omega^4\right) \\
& + 93312\gamma^{22}\left(69798511\delta^6 + 1437172560\delta^4\Omega^2 + 8409511440\delta^2\Omega^4 + 13742922240\Omega^6\right) \\
& + 2592\gamma^{20}\left(684700609\delta^8 + 20663794332\delta^6\Omega^2 + 197487126036\delta^4\Omega^4 + 718744933440\delta^2\Omega^6 + 824528802816\Omega^8\right) \\
& + 1728\gamma^{18}\left(183073446\delta^{10} + 76995003558\delta^8\Omega^2 + 1062423482316\delta^6\Omega^4 + 6291289505346\delta^4\Omega^6 + 16141447117448\delta^2\Omega^8 + 13986331223040\Omega^{10}\right) \\
& + 216\gamma^{16}\left(172718280\delta^{12} + 9972423126\delta^{10}\Omega^2 + 187170660179\delta^8\Omega^4 + 1580865636128\delta^6\Omega^6 + 6589128711168\delta^4\Omega^8 + 1281692306073 6\delta^2\Omega^{10}\right. \\
& \qquad \left. + 879504533913 6\Omega^{12}\right) + 72\gamma^{14}\left(39838464\delta^{14} + 3204047190\delta^{12}\Omega^2 + 79890980190\delta^{10}\Omega^4 + 897845412985\delta^8\Omega^6 + 5296264572252\delta^6\Omega^8\right. \\
& \qquad \left. + 167493574040 64\delta^4\Omega^{10} + 2588587837747 2\delta^2\Omega^{12} + 1450559265177 6\Omega^{14}\right) + \delta^4\Omega^8\left(19968\delta^{16} + 288400\delta^{14}\Omega^2 + 2413242\delta^{12}\Omega^4\right. \\
& \qquad \left. + 15101755\delta^{10}\Omega^6 + 69824052\delta^8\Omega^8 + 240949628\delta^6\Omega^{10} + 594740016\delta^4\Omega^{12} + 871603200\delta^2\Omega^{14} + 506068992\Omega^{16}\right) \\
& + 12\gamma^{12}\left(11432664\delta^{16} + 1346929380\delta^{14}\Omega^2 + 449077488 96\delta^{12}\Omega^4 + 6483358983 31\delta^{10}\Omega^6 + 5004469498170\delta^8\Omega^8 + 223545940559 04\delta^6\Omega^{10}\right. \\
& \qquad \left. + 563055011363 52\delta^4\Omega^{12} + 7125915241267 2\delta^2\Omega^{14} + 331615261163 52\Omega^{16}\right) \\
& + \gamma^2\delta^2\Omega^6\left(131520\delta^{18} + 4004712\delta^{16}\Omega^2 + 46346580\delta^{14}\Omega^4 + 353838468\delta^{12}\Omega^6 + 1944325979\delta^{10}\Omega^8 + 7754541060\delta^8\Omega^{10} + 219255224 88\delta^6\Omega^{12}\right. \\
& \qquad \left. + 395087938 56\delta^4\Omega^{14} + 369879367 68\delta^2\Omega^{16} + 125703290 88\Omega^{18}\right) \\
& + 6\gamma^{10}\left(611712\delta^{18} + 1182602 16\delta^{16}\Omega^2 + 55032426 00\delta^{14}\Omega^4 + 1013435824 34\delta^{12}\Omega^6 + 975885796671\delta^{10}\Omega^8 + 566913158400 4\delta^8\Omega^{10}\right. \\
& \qquad \left. + 202075467613 92\delta^6\Omega^{12} + 418322466979 20\delta^4\Omega^{14} + 440683781160 96\delta^2\Omega^{16} + 170537960079 36\Omega^{18}\right) \\
& + \gamma^4\Omega^4\left(266112\delta^{20} + 17247360\delta^{18}\Omega^2 + 320085840\delta^{16}\Omega^4 + 3177915291\delta^{14}\Omega^6 + 21233983106\delta^{12}\Omega^8 + 99806554512\delta^{10}\Omega^{10}\right. \\
& \qquad \left. + 326031087768\delta^8\Omega^{12} + 691409481984\delta^6\Omega^{14} + 832642954888\delta^4\Omega^{16} + 455653195776\delta^2\Omega^{18} + 652298158 08\Omega^{20}\right) \\
& + \gamma^6\Omega^2\left(186624\delta^{20} + 28014048\delta^{18}\Omega^2 + 966968220\delta^{16}\Omega^4 + 13864916754\delta^{14}\Omega^6 + 117945652609\delta^{12}\Omega^8 + 670022560992\delta^{10}\Omega^{10}\right. \\
& \qquad \left. + 25742690406 72\delta^8\Omega^{12} + 639664877836 8\delta^6\Omega^{14} + 931553913600 0\delta^4\Omega^{16} + 667317790310 4\delta^2\Omega^{18} + 158997676032 0\Omega^{20}\right) \\
& + 6\gamma^8\left(6912\delta^{20} + 2934720\delta^{18}\Omega^2 + 212210964\delta^{16}\Omega^4 + 5119312274\delta^{14}\Omega^6 + 600406005 54\delta^{12}\Omega^8 + 429526288597\delta^{10}\Omega^{10}\right. \\
& \qquad \left. + 199089484972 0\delta^8\Omega^{12} + 586080390259 2\delta^6\Omega^{14} + 101542704111136\delta^4\Omega^{16} + 89145247334 40\delta^2\Omega^{18} + 280560402432 0\Omega^{20}\right).
\end{aligned}
\tag{B.11}
$$

Of course, the condition $\mathrm{Tr}\left(\rho_a^S\right) = 1$ verifies. The following terms are the off diagonal terms above the diagonal. We pose $x = \frac{\sqrt{3}\mathcal{N}}{\Omega^5}\langle e|\rho_a^S|W_2\rangle$ and we have

$$
\begin{aligned}
x = {} & 16325867520000\gamma^{27} - 10883911680000i\gamma^{26}\delta + 22674816000\gamma^{25}(809\delta^2 + 6624\Omega^2) - 15116544000i\gamma^{24}(809\delta^3 + 6624\delta\Omega^2) \\
& + 15116544\gamma^{23}(577037\delta^4 + 10319600\delta^2\Omega^2 + 39273600\Omega^4) - 10077696i\gamma^{22}(577037\delta^5 + 10309600\delta^3\Omega^2 + 39273600\delta\Omega^4) \\
& + 139968\gamma^{21}(16416847\delta^6 + 487337364\delta^4\Omega^2 + 4004407440\delta^2\Omega^4 + 9501373440\Omega^6) \\
& - 93312i\gamma^{20}(16416847\delta^7 + 486810864\delta^5\Omega^2 + 3991706640\delta^3\Omega^4 + 9501373440\delta\Omega^6) \\
& + 3888\gamma^{19}(94797961\delta^8 + 42308498888\delta^6\Omega^2 + 568289662924\delta^4\Omega^4 + 2888387942402\delta^2\Omega^6 + 4824793589768\Omega^8) \\
& - 2592i\gamma^{18}(94797961\delta^9 + 42297323946\delta^7\Omega^2 + 565978842366\delta^5\Omega^4 + 2869603113603\delta^3\Omega^6 + 4824793589768\delta\Omega^8) \\
& + 1296\gamma^{17}(287073601\delta^{10} + 18584876338\delta^8\Omega^2 + 367552014306\delta^6\Omega^4 + 3020343305764\delta^4\Omega^6 + 10755277320962\delta^2\Omega^8 + 13498281676801\Omega^{10}) \\
& - 432i\gamma^{16}(57414720\delta^{11} + 37220970234\delta^9\Omega^2 + 733386280984\delta^7\Omega^4 + 5985532454405\delta^5\Omega^6 + 21288203066883\delta^3\Omega^8 + 26996563353605\delta\Omega^{10}) \\
& + 324\gamma^{15}(72613201\delta^{12} + 6850155481\delta^{10}\Omega^2 + 191003829316\delta^8\Omega^4 + 2271855467126\delta^6\Omega^6 + 12997502052484\delta^4\Omega^8 + 34713512294402\delta^2\Omega^{10} \\
& \quad + 33957326684161\Omega^{12}) - 144i\gamma^{14}(108919801\delta^{13} + 10311397381\delta^{11}\Omega^2 + 287047163816\delta^9\Omega^4 + 3383913379657\delta^7\Omega^6 + 19192812174725\delta^5\Omega^8 \\
& \quad + 51341328679681\delta^3\Omega^{10} + 50935990026241\delta\Omega^{12}) \\
& - 2i\delta^5\Omega^8(2496\delta^{14} + 56634\delta^{12}\Omega^2 + 702476\delta^{10}\Omega^4 + 5167889\delta^8\Omega^6 + 26384987\delta^6\Omega^8 + 99430404\delta^4\Omega^{10} + 235738368\delta^2\Omega^{12} + 248168448\Omega^{14}) \\
& + 3\gamma\delta^4\Omega^8(2496\delta^{14} + 49306\delta^{12}\Omega^2 + 694171\delta^{10}\Omega^4 + 5529760\delta^8\Omega^6 + 28660998\delta^6\Omega^8 + 107167704\delta^4\Omega^{10} + 248864256\delta^2\Omega^{12} + 253034496\Omega^{14}) \\
& + 216\gamma^{13}(413712\delta^{14} + 59562252\delta^{12}\Omega^2 + 2330259585\delta^{10}\Omega^4 + 38037520574\delta^8\Omega^6 + 311537993838\delta^6\Omega^8 + 1335388986404\delta^4\Omega^{10} \\
& \quad + 27852642846721\delta^2\Omega^{12} + 21591973232641\Omega^{14}) - 72i\gamma^{12}(827424\delta^{15} + 119782746\delta^{13}\Omega^2 + 4697283043\delta^{11}\Omega^4 + 76079207675\delta^9\Omega^6 \\
& \quad + 614130374450\delta^7\Omega^8 + 2611231725504\delta^5\Omega^{10} + 5476043427840\delta^3\Omega^{12} + 4318394646528\delta\Omega^{14}) + 12\gamma^3\delta^2\Omega^6(4110\delta^{16} + 170604\delta^{14}\Omega^2 \\
& \quad + 2810705\delta^{12}\Omega^4 + 29174950\delta^{10}\Omega^6 + 188145883\delta^8\Omega^8 + 811860975\delta^6\Omega^{10} + 2232679104\delta^4\Omega^{12} + 3238437888\delta^2\Omega^{14} + 1571291136\Omega^{16}) \\
& - 2i\gamma^2\delta^3\Omega^6(16440\delta^{16} + 731808\delta^{14}\Omega^2 + 11977095\delta^{12}\Omega^4 + 114668180\delta^{10}\Omega^6 + 709145514\delta^8\Omega^8 + 3039764466\delta^6\Omega^{10} + 8464354848\delta^4\Omega^{12} \\
& \quad + 12560818176\delta^2\Omega^{14} + 6200229888\Omega^{16}) + 216\gamma^{11}(8514\delta^{16} + 2092710\delta^{14}\Omega^2 + 119085409\delta^{12}\Omega^4 + 2616787380\delta^{10}\Omega^6 + 28828815850\delta^8\Omega^8 \\
& \quad + 176420006416\delta^6\Omega^{10} + 592694488824\delta^4\Omega^{12} + 987354574848\delta^2\Omega^{14} + 604263186432\Omega^{16}) \\
& - 12i\gamma^{10}(102168\delta^{17} + 25273152\delta^{15}\Omega^2 + 1449138210\delta^{13}\Omega^4 + 31759644389\delta^{11}\Omega^6 + 343855171530\delta^9\Omega^8 + 2066715390240\delta^7\Omega^{10} \\
& \quad + 6911413013664\delta^5\Omega^{12} + 1162458434764\delta^3\Omega^{14} + 725115823718\delta\Omega^{16}) \\
& - 6i\gamma^4\delta\Omega^4(11088\delta^{18} + 982324\delta^{16}\Omega^2 + 25170492\delta^{14}\Omega^4 + 320193055\delta^{12}\Omega^6 + 2484079588\delta^{10}\Omega^8 + 12571334080\delta^8\Omega^{10} + 40900490976\delta^6\Omega^{12} \\
& \quad + 75592806912\delta^4\Omega^{14} + 61016702976\delta^2\Omega^{16} + 10871635968\Omega^{18}) + 3\gamma^5\Omega^4(33264\delta^{18} + 2848752\delta^{16}\Omega^2 + 71261211\delta^{14}\Omega^4 + 941110210\delta^{12}\Omega^6 \\
& \quad + 7675638795\delta^{10}\Omega^8 + 39716404500\delta^8\Omega^{10} + 128988097344\delta^6\Omega^{12} + 234795649536\delta^4\Omega^{14} + 186208616448\delta^2\Omega^{16} + 32614907904\Omega^{18}) \\
& + 36\gamma^7\Omega^2(1944\delta^{18} + 382287\delta^{16}\Omega^2 + 17056879\delta^{14}\Omega^4 + 315816633\delta^{12}\Omega^6 + 3312939545\delta^{10}\Omega^8 + 21192585468\delta^8\Omega^{10} + 82696804512\delta^6\Omega^{12} \\
& \quad + 183516262848\delta^4\Omega^{14} + 194725527552\delta^2\Omega^{16} + 63531122688\Omega^{18}) - 12i\gamma^6\delta\Omega^2(3888\delta^{18} + 775686\delta^{16}\Omega^2 + 35355090\delta^{14}\Omega^4 + 652165047\delta^{12}\Omega^6 \\
& \quad + 6599031126\delta^{10}\Omega^8 + 40946381309\delta^8\Omega^{10} + 158375400372\delta^6\Omega^{12} + 354322947456\delta^4\Omega^{14} + 382072578048\delta^2\Omega^{16} + 127062245376\Omega^{18}) \\
& + 9\gamma^9(1728\delta^{18} + 968112\delta^{16}\Omega^2 + 88873848\delta^{14}\Omega^4 + 2673449988\delta^{12}\Omega^6 + 38295014291\delta^{10}\Omega^8 + 313051549164\delta^8\Omega^{10} + 1504383998640\delta^6\Omega^{12} \\
& + 4075197683328\delta^4\Omega^{14} + 5458209767424\delta^2\Omega^{16} + 2551479533568\Omega^{18}) - 12i\gamma^8(864\delta^{19} + 486432\delta^{17}\Omega^2 + 45222786\delta^{15}\Omega^4 + 1370249899\delta^{13}\Omega^6 \\
& + 193323010254\delta^{11}\Omega^8 + 15371628673096\delta^9\Omega^{10} + 726835328844\delta^7\Omega^{12} + 19712833637764\delta^5\Omega^{14} + 267570509414432\delta^3\Omega^{16} + 12757397667840\delta\Omega^{18}).
\end{aligned}
\tag{B.12}
$$

We pose $x = \frac{\sqrt{3}\mathcal{N}}{\Omega^4}\langle e|\rho_a^S|W_1\rangle$ and we have

$$
\begin{aligned}
x = &-16325867520000\gamma^{28} + 163258675200000i\gamma^{27}\delta - 22674816000\gamma^{26}(689\delta^2 + 6624\Omega^2) + 22674816000i\gamma^{25}(829\delta^3 + 6624\delta\Omega^2)\\
&- 15116544\gamma^{24}(379787\delta^4 + 8663600\delta^2\Omega^2 + 3927360\Omega^4) + 40310784i\gamma^{23}(228717\delta^5 + 3961475\delta^3\Omega^2 + 14727600\delta\Omega^4)\\
&- 139968\gamma^{22}(6621931\delta^6 + 307038564\delta^4\Omega^2 + 32974826400\delta^2\Omega^4 + 9501373440\Omega^6)\\
&+ 139968i\gamma^{21}(18049333\delta^7 + 515121414\delta^5\Omega^2 + 40851842400\delta^3\Omega^4 + 9501373440\delta\Omega^6)\\
&- 3888\gamma^{20}(6091795\delta^8 + 1487191284\delta^6\Omega^2 + 337352917320\delta^4\Omega^4 + 2318305536000\delta^2\Omega^6 + 482479358976\Omega^8)\\
&+ 7776i\gamma^{19}(54791161\delta^9 + 2333398257\delta^7\Omega^2 + 29925866406\delta^5\Omega^4 + 1465734542400\delta^3\Omega^6 + 241239679488\delta\Omega^8)\\
&+ 5184\gamma^{18}(2824860\delta^{10} + 116309568\delta^8\Omega^2 - 25977856416\delta^6\Omega^4 - 412187789888\delta^4\Omega^6 - 2085720131520\delta^2\Omega^8 - 337457041920\Omega^{10})\\
&+ 432i\gamma^{17}(1061254800\delta^{11} + 64984599370\delta^9\Omega^2 + 12161316333960\delta^7\Omega^4 + 948011474592\delta^5\Omega^6 + 325644942643200\delta^3\Omega^8 + 40494845030400\delta\Omega^{10})\\
&+ 108\gamma^{16}(22295160\delta^{12} + 1114378904\delta^{10}\Omega^2 + 87644373696\delta^8\Omega^4 - 1283230584960\delta^6\Omega^6 - 1875566814336\delta^4\Omega^8 - 771439735296000\delta^2\Omega^{10}\\
&- 101871980052480\Omega^{12}) + 2\delta^6\Omega^{10}(18752\delta^{12} + 2390300\delta^{10}\Omega^2 + 154692500\delta^8\Omega^4 + 76229100\delta^6\Omega^6 + 29135012\delta^4\Omega^8 + 7101225600\delta^2\Omega^{10} + 773222400\Omega^{12})\\
&+ 72i\gamma^{15}(436957200\delta^{13} + 38517639360\delta^{11}\Omega^2 + 1008556038550\delta^9\Omega^4 + 112374498513360\delta^7\Omega^6 + 6070300183872\delta^5\Omega^8 + 1569212433900720\delta^3\Omega^{10}\\
&+ 152807970078720\delta\Omega^{12}) + 36\gamma^{14}(47364480\delta^{14} + 4514345520\delta^{12}\Omega^2 + 1090547455400\delta^{10}\Omega^4 + 78326519607000\delta^8\Omega^6 - 9822728613600\delta^6\Omega^8\\
&- 312508519574400\delta^4\Omega^{10} - 116179867054080\delta^2\Omega^{12} - 129551839395840\Omega^{14})\\
&+ i\gamma\delta^5\Omega^8(17472\delta^{14} + 3496020\delta^{12}\Omega^2 + 35607380\delta^{10}\Omega^4 + 228750410\delta^8\Omega^6 + 1043402810\delta^6\Omega^8 + 3540069240\delta^4\Omega^{10} + 787458816\delta^2\Omega^{12} + 812630016\Omega^{14})\\
&+ 2\gamma^2\delta^4\Omega^8(146040\delta^{14} + 36564450\delta^{12}\Omega^2 + 330244890\delta^{10}\Omega^4 + 1898394300\delta^8\Omega^6 + 8015086270\delta^6\Omega^8 + 2251387860\delta^4\Omega^{10} + 333274982400\delta^2\Omega^{12}\\
&+ 14677770240\Omega^{14}) + 36i\gamma^{13}(36853920\delta^{15} + 4866934320\delta^{13}\Omega^2 + 177428528060\delta^{11}\Omega^4 + 26906927990100\delta^9\Omega^6 + 2041511952682\delta^7\Omega^8\\
&+ 82529149281600\delta^5\Omega^{10} + 16743572987904\delta^3\Omega^{12} + 1295518393958400\delta\Omega^{14}) + 24\gamma^{12}(2431620\delta^{16} + 429728760\delta^{14}\Omega^2 + 18194784300\delta^{12}\Omega^4\\
&+ 276191099710\delta^{10}\Omega^6 + 1638937472100\delta^8\Omega^8 + 23736547371600\delta^6\Omega^{10} - 138088621778400\delta^4\Omega^{12} - 56473951887360\delta^2\Omega^{14} - 5438368677888\Omega^{16})\\
&+ \gamma^4\delta^2\Omega^6(7384800\delta^{16} + 358115100\delta^{14}\Omega^2 + 5107418010\delta^{12}\Omega^4 + 37010858800\delta^{10}\Omega^6 + 177564595380\delta^8\Omega^8 + 563581363320\delta^6\Omega^{10} + 99163004371200\delta^4\Omega^{12}\\
&+ 6356905574400\delta^2\Omega^{14} - 254803968000\Omega^{16}) + i\gamma^3\delta^3\Omega^6(1047840\delta^{16} + 41737080\delta^{14}\Omega^2 + 606230490\delta^{12}\Omega^4 + 5082250040\delta^{10}\Omega^6 + 28055573160\delta^8\Omega^8\\
&+ 108964444620\delta^6\Omega^{10} + 283529638080\delta^4\Omega^{12} + 407367843840\delta^2\Omega^{14} + 197897748480\Omega^{16}) + 12i\gamma^{11}(2598480\delta^{17} + 569768400\delta^{15}\Omega^2 + 29889679920\delta^{13}\Omega^4\\
&+ 607965706090\delta^{11}\Omega^6 + 6119175862680\delta^9\Omega^8 + 34381436802600\delta^7\Omega^{10} + 109315983137760\delta^5\Omega^{12} + 17812174675968\delta^3\Omega^{14} + 1087673735577600\delta\Omega^{16})\\
&+ 3\gamma^{10}(2592000\delta^{18} + 108607680\delta^{16}\Omega^2 + 814152840\delta^{14}\Omega^4 + 2013928655200\delta^{12}\Omega^6 + 20768150589100\delta^{10}\Omega^8 + 100640059768000\delta^8\Omega^{10}\\
&+ 208961185632000\delta^6\Omega^{12} - 7849862910720\delta^4\Omega^{14} - 912347106508800\delta^2\Omega^{16} - 76544386007040\Omega^{18})\\
&+ 3\gamma^8\Omega^2(13593600\delta^{18} + 2327281200\delta^{16}\Omega^2 + 96783576000\delta^{14}\Omega^4 + 1502064260000\delta^{12}\Omega^6 + 11072658484900\delta^{10}\Omega^8 + 45424005081200\delta^8\Omega^{10}\\
&+ 96738825360000\delta^6\Omega^{12} + 51940923264000\delta^4\Omega^{14} - 10609665638400\delta^2\Omega^{16} - 7623734722560\Omega^{18})\\
&+ \gamma^6\Omega^4(80337600\delta^{18} + 7264870800\delta^{16}\Omega^2 + 175915535700\delta^{14}\Omega^4 + 1783472693800\delta^{12}\Omega^6 + 10207344516000\delta^{10}\Omega^8 + 36586250407920\delta^8\Omega^{10}\\
&+ 72606633552320\delta^6\Omega^{12} + 5126530176000\delta^4\Omega^{14} - 1774391132160\delta^2\Omega^{16} - 978447237120\Omega^{18})\\
&+ 3i\gamma^5\delta\Omega^4(6729600\delta^{18} + 529507600\delta^{16}\Omega^2 + 12313006200\delta^{14}\Omega^4 + 140893240900\delta^{12}\Omega^6 + 980226943400\delta^{10}\Omega^8 + 4510213940400\delta^8\Omega^{10} + 13685215152000\delta^6\Omega^{12}\\
&+ 24292893196800\delta^4\Omega^{14} + 19153295769600\delta^2\Omega^{16} + 3261490790400\Omega^{18}) + 6i\gamma^7\delta\Omega^2(2332800\delta^{18} + 403837200\delta^{16}\Omega^2 + 16658976600\delta^{14}\Omega^4 + 281544537900\delta^{12}\Omega^6\\
&+ 2589931362400\delta^{10}\Omega^8 + 14673519136100\delta^8\Omega^{10} + 52864594014000\delta^6\Omega^{12} + 113038434777600\delta^4\Omega^{14} + 118552257331200\delta^2\Omega^{16} + 38118673612800\Omega^{18})\\
&+ 12i\gamma^9(259200\delta^{19} + 12472200\delta^{17}\Omega^2 + 103661598000\delta^{15}\Omega^4 + 2885522414000\delta^{13}\Omega^6 + 37543924283000\delta^{11}\Omega^8 + 274756371482000\delta^9\Omega^{10}\\
&+ 1210639622118000\delta^7\Omega^{12} + 3127457430432000\delta^5\Omega^{14} + 4119235817472000\delta^3\Omega^{16} + 1913609650176000\delta\Omega^{18}).
\end{aligned}
\tag{B.13}
$$

We pose $x = \frac{\mathcal{N}}{\Omega^3}\langle e|\rho_a^S|g\rangle$ and we have

$$
\begin{aligned}
x = {} & 5441955840000i\gamma^{29} + 5441955840000\gamma^{28}\delta + 7558272000i\gamma^{27}(689\delta^2 + 6624\Omega^2) + 7558272000\gamma^{26}(829\delta^3 + 6624\delta\Omega^2) \\
& + 5038848i\gamma^{25}(379787\delta^4 + 8663600\delta^2\Omega^2 + 39273600\Omega^4) + 40310784\gamma^{24}(76239\delta^5 + 1320700\delta^3\Omega^2 + 4909200\delta\Omega^4) \\
& + 46656i\gamma^{23}(6621931\delta^6 + 307308564\delta^4\Omega^2 + 3297482640\delta^2\Omega^4 + 950137344\Omega^6) \\
& + 46656\gamma^{22}(18049333\delta^7 + 515933664\delta^5\Omega^2 + 4081440240\delta^3\Omega^4 + 9501373440\delta\Omega^6) \\
& + 1296i\gamma^{21}(6091795\delta^8 + 1481012784\delta^6\Omega^2 + 339508597324\delta^4\Omega^4 + 23183055360\delta^2\Omega^6 + 4824793589768\Omega^8) \\
& + 2592\gamma^{20}(54791161\delta^9 + 2341994118\delta^7\Omega^2 + 299813142064\delta^5\Omega^4 + 14604750144\delta^3\Omega^6 + 2412396794888\delta\Omega^8) \\
& - 432i\gamma^{19}(11299440\delta^{10} + 69737575\delta^8\Omega^2 - 1054035752\delta^6\Omega^4 - 16810957771\delta^4\Omega^6 - 834288052608\delta^2\Omega^8 - 13498281676\Omega^{10}) \\
& + 432\gamma^{18}(35375160\delta^{11} + 2177458273\delta^9\Omega^2 + 40827442683\delta^7\Omega^4 + 3158485513\delta^5\Omega^6 + 1077575889024\delta^3\Omega^8 + 13498281676\delta\Omega^{10}) \\
& - 108i\gamma^{17}(7431720\delta^{12} + 401620776\delta^{10}\Omega^2 + 32420473118\delta^8\Omega^4 - 4780078901\delta^6\Omega^6 - 652154649408\delta^4\Omega^8 - 25714657843\delta^2\Omega^{10} \\
& \quad - 3395732668416\Omega^{12}) - 2i\gamma\delta^6\Omega^{10}(9504\delta^{12} + 65673\delta^{10}\Omega^2 + 220519\delta^8\Omega^4 + 1150897\delta^6\Omega^6 + 4661356\delta^4\Omega^8 + 8957184\delta^2\Omega^{10} + 5971968\Omega^{12}) \\
& + 216\gamma^{16}(4855080\delta^{13} + 429772056\delta^{11}\Omega^2 + 11336901001\delta^9\Omega^4 + 1258581697748\delta^7\Omega^6 + 67082873884\delta^5\Omega^8 + 17237073392\delta^3\Omega^{10} \\
& \quad + 1697866334208\delta\Omega^{12}) - 72i\gamma^{15}(789408\delta^{14} + 82089024\delta^{12}\Omega^2 + 2034280770\delta^{10}\Omega^4 + 128950370\delta^8\Omega^6 - 3341092005\delta^6\Omega^8 \\
& \quad - 565547613456\delta^4\Omega^{10} - 19363311175\delta^2\Omega^{12} - 2159197323264\Omega^{14}) \\
& + 2\delta^5\Omega^{10}(-1248\delta^{14} - 3695\delta^{12}\Omega^2 + 1802\delta^{10}\Omega^4 - 49328\delta^8\Omega^6 + 192762\delta^6\Omega^8 + 2268312\delta^4\Omega^{10} + 2709504\delta^2\Omega^{12} - 4866048\Omega^{14}) \\
& - i\gamma^3\delta^4\Omega^8(158160\delta^{14} + 2950752\delta^{12}\Omega^2 + 16540629\delta^{10}\Omega^4 + 75103508\delta^8\Omega^6 + 312444294\delta^6\Omega^8 + 81989738\delta^4\Omega^{10} + 11002844\delta^2\Omega^{12} \\
& \quad + 511377408\Omega^{14}) + 36\gamma^{14}(1228464\delta^{15} + 161911416\delta^{13}\Omega^2 + 5972248404\delta^{11}\Omega^4 + 911544854\delta^9\Omega^6 + 68374019179\delta^7\Omega^8 \\
& \quad + 2716895611680\delta^5\Omega^{10} + 549287793100\delta^3\Omega^{12} + 43183946465\delta\Omega^{14}) - 72i\gamma^{13}(27018\delta^{16} + 5307036\delta^{14}\Omega^2 + 236162988\delta^{12}\Omega^4 \\
& \quad + 33593800\delta^{10}\Omega^6 + 1624007468\delta^8\Omega^8 + 80341469\delta^6\Omega^{10} - 1834432755\delta^4\Omega^{12} - 627488354304\delta^2\Omega^{14} - 60426318643\Omega^{16}) \\
& + \gamma^2\delta^3\Omega^8(-8016\delta^{16} - 92478\delta^{14}\Omega^2 + 832989\delta^{12}\Omega^4 + 5537476\delta^{10}\Omega^6 + 30236874\delta^8\Omega^8 + 167338272\delta^6\Omega^{10} + 36598118\delta^4\Omega^{12} \\
& \quad + 79847424\delta^2\Omega^{14} - 16986931\Omega^{16}) - 6i\gamma^5\delta^2\Omega^6(63360\delta^{16} + 2802305\delta^{14}\Omega^2 + 29716068\delta^{12}\Omega^4 + 158605607\delta^{10}\Omega^6 + 669829738\delta^8\Omega^8 \\
& \quad + 2017866991\delta^6\Omega^{10} + 3387060096\delta^4\Omega^{12} + 2075682816\delta^2\Omega^{14} - 141557760\Omega^{16}) + \gamma^4\delta^3\Omega^6(9936\delta^{16} + 394248\delta^{14}\Omega^2 + 14488137\delta^{12}\Omega^4 \\
& \quad + 156845442\delta^{10}\Omega^6 + 863978062\delta^8\Omega^8 + 368110326\delta^6\Omega^{10} + 98051132\delta^4\Omega^{12} + 11571738624\delta^2\Omega^{14} + 3280601088\Omega^{16}) \\
& + 72\gamma^{12}(14436\delta^{17} + 3114456\delta^{15}\Omega^2 + 164999238\delta^{13}\Omega^4 + 3424758241\delta^{11}\Omega^6 + 34546441555\delta^9\Omega^8 + 190384609250\delta^7\Omega^{10} + 5945878921\delta^5\Omega^{12} \\
& \quad + 968070850560\delta^3\Omega^{14} + 604263186432\delta\Omega^{16}) - 3i\gamma^{11}(8640\delta^{18} + 4107024\delta^{16}\Omega^2 + 333264528\delta^{14}\Omega^4 + 7962841536\delta^{12}\Omega^6 \\
& \quad + 703063035\delta^{10}\Omega^8 + 27304355240\delta^8\Omega^{10} + 4265969214\delta^6\Omega^{12} - 587623925376\delta^4\Omega^{14} - 30411570216\delta^2\Omega^{16} - 2551479533568\Omega^{18}) \\
& - 6i\gamma^9\Omega^2(26208\delta^{18} + 5017626\delta^{16}\Omega^2 + 208098504\delta^{14}\Omega^4 + 2803058573\delta^{12}\Omega^6 + 165799379\delta^{10}\Omega^8 + 57255686032\delta^8\Omega^{10} \\
& \quad + 1091675130\delta^6\Omega^{12} + 33976204416\delta^4\Omega^{14} - 1768277606\delta^2\Omega^{16} - 127062245376\Omega^{18}) \\
& - 3i\gamma^7\Omega^4(121392\delta^{18} + 11387184\delta^{16}\Omega^2 + 243026421\delta^{14}\Omega^4 + 1908381166\delta^{12}\Omega^6 + 8853993383\delta^{10}\Omega^8 + 2873757155\delta^8\Omega^{10} + 542377303\delta^6\Omega^{12} \\
& \quad + 33955803648\delta^4\Omega^{14} - 1971545702\delta^2\Omega^{16} - 108716359\Omega^{18}) + \gamma^6\delta\Omega^4(50976\delta^{18} + 3672972\delta^{16}\Omega^2 + 98974890\delta^{14}\Omega^4 + 1349636340\delta^{12}\Omega^6 \\
& \quad + 9614688383\delta^{10}\Omega^8 + 441017169\delta^8\Omega^{10} + 13359242\delta^6\Omega^{12} + 2265528\delta^4\Omega^{14} + 163284\delta^2\Omega^{16} + 32614907\Omega^{18}) \\
& + 3\gamma^8\delta\Omega^2(14400\delta^{18} + 2362248\delta^{16}\Omega^2 + 99429720\delta^{14}\Omega^4 + 1817717536\delta^{12}\Omega^6 + 17381244999\delta^{10}\Omega^8 + 970807273\delta^8\Omega^{10} + 343187357\delta^6\Omega^{12} \\
& \quad + 72047586\delta^4\Omega^{14} + 7415989\delta^2\Omega^{16} + 254124\Omega^{18}) + 6\gamma^{10}(1728\delta^{19} + 798120\delta^{17}\Omega^2 + 65879856\delta^{15}\Omega^4 + 1891971576\delta^{13}\Omega^6 \\
& + 253803294\delta^{11}\Omega^8 + 18470085\delta^9\Omega^{10} + 794970059\delta^7\Omega^{12} + 20202867\delta^5\Omega^{14} + 2655326\delta^3\Omega^{16} + 127573\delta\Omega^{18}).
\end{aligned}
\tag{B.14}
$$

We pose $x = -\frac{\sqrt{3}\mathcal{N}}{\sqrt{2}\delta\Omega^5}\langle e|\rho_a^S|\psi_2\rangle$ and we have

$$
\begin{aligned}
x = {} & 2720977920000\gamma^{26} - 1360488960000i\gamma^{25}\delta + 3779136000\gamma^{24}(869\delta^2 + 6624\Omega^2) - 5668704000i\gamma^{23}(263\delta^3 + 2088\delta\Omega^2) \\
& + 5038848\gamma^{22}(337831\delta^4 + 5568800\delta^2\Omega^2 + 19636800\Omega^4) - 2519424i\gamma^{21}(272081\delta^5 + 4776925\delta^3\Omega^2 + 16990800\delta\Omega^4) \\
& + 23328\gamma^{20}(21314305\delta^6 + 5748218640\delta^4\Omega^2 + 43430738400\delta^2\Omega^4 + 95013734400\Omega^6) \\
& - 11664i\gamma^{19}(14784361\delta^7 + 437809116\delta^5\Omega^2 + 3407903280\delta^3\Omega^4 + 7438919040\delta\Omega^6) \\
& + 2592\gamma^{18}(34787761\delta^8 + 1384675254\delta^6\Omega^2 + 16833872700\delta^4\Omega^4 + 78259929840\delta^2\Omega^6 + 120619839744\Omega^8) \\
& - 1944i\gamma^{17}(13335600\delta^9 + 606795097\delta^7\Omega^2 + 7851330636\delta^5\Omega^4 + 37131348096\delta^3\Omega^6 + 56969415936\delta\Omega^8) \\
& + 432\gamma^{16}(24355380\delta^{10} + 1375546388\delta^8\Omega^2 + 240628224812\delta^6\Omega^4 + 1772286062044\delta^4\Omega^6 + 5766662073600\delta^2\Omega^8 + 6749140838400\Omega^{10}) \\
& - 648i\gamma^{15}(3673260\delta^{11} + 250370630\delta^9\Omega^2 + 4877723581\delta^7\Omega^4 + 37781645148\delta^5\Omega^6 + 124381570752\delta^3\Omega^8 + 145171229184\delta\Omega^{10}) \\
& + \delta^6\Omega^8(4992\delta^{12} + 52212\delta^{10}\Omega^2 + 294574\delta^8\Omega^4 + 1593589\delta^6\Omega^6 + 6895342\delta^4\Omega^8 + 16971528\delta^2\Omega^{10} + 17005824\Omega^{12}) + 36\gamma^{14}(21911760\delta^{12} \\
& \qquad + 1758048282\delta^{10}\Omega^2 + 421590377274\delta^8\Omega^4 + 43540230069696\delta^6\Omega^6 + 2218292032752\delta^4\Omega^8 + 54475844025600\delta^2\Omega^{10} + 509359900262400\Omega^{12}) \\
& - 108i\gamma^{13}(1203120\delta^{13} + 126028710\delta^{11}\Omega^2 + 3577475931\delta^9\Omega^4 + 40823323822\delta^7\Omega^6 + 217012055784\delta^5\Omega^8 + 538311895200\delta^3\Omega^{10} \\
& \qquad + 504412987392\delta\Omega^{12}) \\
& - 6i\gamma\delta^3\Omega^8(4992\delta^{14} + 82522\delta^{12}\Omega^2 + 718350\delta^{10}\Omega^4 + 4047558\delta^8\Omega^6 + 14868671\delta^6\Omega^8 + 35595156\delta^4\Omega^{10} + 53247744\delta^2\Omega^{12} + 38928384\Omega^{14}) \\
& + 72\gamma^{12}(507636\delta^{14} + 60387606\delta^{12}\Omega^2 + 1970869939\delta^{10}\Omega^4 + 26826718907\delta^8\Omega^6 + 187742148611\delta^6\Omega^8 + 716908877184\delta^4\Omega^{10} \\
& \qquad + 1394432985600\delta^2\Omega^{12} + 1079598661632\Omega^{14}) - 18i\gamma^{11}(213192\delta^{15} + 37812960\delta^{13}\Omega^2 + 1590294750\delta^{11}\Omega^4 + 25597816393\delta^9\Omega^6 \\
& \qquad + 196450895286\delta^7\Omega^8 + 776790563304\delta^5\Omega^{10} + 1530799291008\delta^3\Omega^{12} + 1197937410048\delta\Omega^{14}) - 6i\gamma^3\delta\Omega^6(27732\delta^{16} + 939750\delta^{14}\Omega^2 \\
& \qquad + 11611607\delta^{12}\Omega^4 + 84141852\delta^{10}\Omega^6 + 382498405\delta^8\Omega^8 + 1096254966\delta^6\Omega^{10} + 1946311200\delta^4\Omega^{12} + 1920098304\delta^2\Omega^{14} + 679477248\Omega^{16}) \\
& + \gamma^2\delta^2\Omega^6(32880\delta^{16} + 905436\delta^{14}\Omega^2 + 8101086\delta^{12}\Omega^4 + 51105811\delta^{10}\Omega^6 + 256334751\delta^8\Omega^8 + 866076576\delta^6\Omega^{10} + 1711680768\delta^4\Omega^{12} \\
& \qquad + 1788991488\delta^2\Omega^{14} + 934281216\Omega^{16}) - 6i\gamma^5\delta\Omega^4(51048\delta^{16} + 3423936\delta^{14}\Omega^2 + 67177614\delta^{12}\Omega^4 + 653060911\delta^{10}\Omega^6 + 3748446036\delta^8\Omega^8 \\
& \qquad + 13084608006\delta^6\Omega^{10} + 27512642304\delta^4\Omega^{12} + 32323995648\delta^2\Omega^{14} + 15882780672\Omega^{16}) \\
& - 36i\gamma^7\delta\Omega^2(5832\delta^{16} + 844545\delta^{14}\Omega^2 + 29020916\delta^{12}\Omega^4 + 408943338\delta^{10}\Omega^6 + 3077958087\delta^8\Omega^8 + 13386813344\delta^6\Omega^{10} + 33778078164\delta^4\Omega^{12} \\
& \qquad + 46417330944\delta^2\Omega^{14} + 27030896640\Omega^{16}) + 12\gamma^{10}(78840\delta^{16} + 15509790\delta^{14}\Omega^2 + 714211593\delta^{12}\Omega^4 + 12521261615\delta^{10}\Omega^6 \\
& \qquad + 111362198526\delta^8\Omega^8 + 579630798936\delta^6\Omega^{10} + 1741350653856\delta^4\Omega^{12} + 2764123978752\delta^2\Omega^{14} + 1812789559296\Omega^{16}) \\
& - 18i\gamma^9(2592\delta^{17} + 1030392\delta^{15}\Omega^2 + 70083114\delta^{13}\Omega^4 + 1593245321\delta^{11}\Omega^6 + 16721357732\delta^9\Omega^8 + 93982858478\delta^7\Omega^{10} + 291486598656\delta^5\Omega^{12} \\
& + 473695725312\delta^3\Omega^{14} + 318155931648\delta\Omega^{16}) + 3\gamma^4\Omega^4(22176\delta^{18} + 1401392\delta^{16}\Omega^2 + 23121108\delta^{14}\Omega^4 + 193849523\delta^{12}\Omega^6 + 1161957839\delta^{10}\Omega^8 \\
& \qquad + 4859749838\delta^8\Omega^{10} + 12798809376\delta^6\Omega^{12} + 19668667392\delta^4\Omega^{14} + 16454320128\delta^2\Omega^{16} + 5435817984\Omega^{18}) \\
& + 3\gamma^6\Omega^2(15552\delta^{18} + 2352360\delta^{16}\Omega^2 + 77967822\delta^{14}\Omega^4 + 1007693859\delta^{12}\Omega^6 + 7683305181\delta^{10}\Omega^8 + 39495037520\delta^8\Omega^{10} + 129976277184\delta^6\Omega^{12} \\
& + 255067398144\delta^4\Omega^{14} + 274712518656\delta^2\Omega^{16} + 127062245376\Omega^{18}) + 3\gamma^8(3456\delta^{18} + 1500768\delta^{16}\Omega^2 + 108349128\delta^{14}\Omega^4 + 2495444770\delta^{12}\Omega^6 \\
& + 26898818039\delta^{10}\Omega^8 + 175454520910\delta^8\Omega^{10} + 717293466600\delta^6\Omega^{12} + 1739143289088\delta^4\Omega^{14} + 2283473534976\delta^2\Omega^{16} + 1275739766784\Omega^{18}).
\end{aligned}
\tag{B.15}
$$

We pose $x = \frac{\sqrt{6}\mathcal{N}}{\delta^2\Omega^6}\langle e|\rho_a^S|\psi_1\rangle$ and we have

$$
\begin{aligned}
x = &-4534963200000\gamma^{24} + 503884800000i\gamma^{23}\delta - 24564384000\gamma^{22}(11\delta^2 + 256\Omega^2) + 6298560000i\gamma^{21}(71\delta^3 + 694\delta\Omega^2) \\
&- 559872\gamma^{20}(53059\delta^4 + 7799700\delta^2\Omega^2 + 44017200\Omega^4) + 233280i\gamma^{19}(697699\delta^5 + 147134656\delta^3\Omega^2 + 50152800\delta\Omega^4) \\
&+ 11664\gamma^{18}(1196879\delta^6 - 96149854\delta^4\Omega^2 - 1475315520\delta^2\Omega^4 - 4018913280\Omega^6) \\
&+ 432i\gamma^{17}(72824035\delta^7 + 2539475499\delta^5\Omega^2 + 182611406888\delta^3\Omega^4 + 28956225600\delta\Omega^6) \\
&+ 216\gamma^{16}(23144818\delta^8 - 5306492616\delta^6\Omega^2 - 228189726004\delta^4\Omega^4 - 1503800691844\delta^2\Omega^6 - 2362661498888\Omega^8) \\
&+ 144i\gamma^{15}(24150495\delta^9 + 1278444662\delta^7\Omega^2 + 150869713985\delta^5\Omega^4 + 48431432520\delta^3\Omega^6 + 1406611008\delta\Omega^8) \\
&+ 144\gamma^{14}(4843527\delta^{10} + 9617117\delta^8\Omega^2 - 508468635\delta^6\Omega^4 - 66356789508\delta^4\Omega^6 - 2461399665124\delta^2\Omega^8 - 2349669150720\Omega^{10}) \\
&+ 72i\gamma^{13}(3038670\delta^{11} + 240681325\delta^9\Omega^2 + 43049672647\delta^7\Omega^4 + 2334269994\delta^5\Omega^6 + 11441810544\delta^3\Omega^8 - 1056439987208\delta\Omega^{10}) \\
&+ 24\gamma^{12}(2064582\delta^{12} + 56942631\delta^{10}\Omega^2 - 2442169541\delta^8\Omega^4 - 615357293616\delta^6\Omega^6 - 42295976370\delta^4\Omega^8 - 1005215545152\delta^2\Omega^{10} \\
&- 575571640320\Omega^{12}) - \delta^4\Omega^8(9536\delta^{12} + 121562\delta^{10}\Omega^2 + 970991\delta^8\Omega^4 + 6901158\delta^6\Omega^6 + 32249960\delta^4\Omega^8 + 77099712\delta^2\Omega^{10} + 70963200\Omega^{12}) \\
&+ 12i\gamma^{11}(600300\delta^{13} + 74248980\delta^{11}\Omega^2 + 1977020605\delta^9\Omega^4 + 17602811241\delta^7\Omega^6 + 303121329248\delta^5\Omega^8 - 2318433829928\delta^3\Omega^{10} - 6388745564168\delta\Omega^{12}) \\
&+ 6\gamma^{10}(292176\delta^{14} + 20486640\delta^{12}\Omega^2 - 3857476968\delta^{10}\Omega^4 - 212278563798\delta^8\Omega^6 - 2393452602048\delta^6\Omega^8 - 10628265789604\delta^4\Omega^{10} \\
&- 1754650861056\delta^2\Omega^{12} - 5609243934720\Omega^{14}) + 6i\gamma^7\delta\Omega^2(5472\delta^{14} + 708678\delta^{12}\Omega^2 + 55365963\delta^{10}\Omega^4 + 8328586398\delta^8\Omega^6 + 1640304698\delta^6\Omega^8 \\
&- 228534219604\delta^4\Omega^{10} - 1126117612804\delta^2\Omega^{12} - 1361555619840\Omega^{14}) \\
&- 2i\gamma\delta^3\Omega^6(2496\delta^{14} - 858\delta^{12}\Omega^2 - 229693\delta^{10}\Omega^4 - 19137678\delta^8\Omega^6 - 70399304\delta^6\Omega^8 - 39422644\delta^4\Omega^{10} + 4098009616\delta^2\Omega^{12} + 780779520\Omega^{14}) \\
&- \gamma^2\delta^2\Omega^6(18672\delta^{14} + 1499676\delta^{12}\Omega^2 + 191142308\delta^{10}\Omega^4 + 15941446898\delta^8\Omega^6 + 900589156\delta^6\Omega^8 + 28435904164\delta^4\Omega^{10} + 4188123648\delta^2\Omega^{12} \\
&+ 1911029760\Omega^{14}) - \gamma^4\delta^2\Omega^4(-25248\delta^{14} + 2746992\delta^{12}\Omega^2 + 1079036198\delta^{10}\Omega^4 + 128204952208\delta^8\Omega^6 + 9087131730\delta^6\Omega^8 + 361892896564\delta^4\Omega^{10} \\
&+ 69719407488\delta^2\Omega^{12} + 47394422784\Omega^{14}) + 12i\gamma^9(7920\delta^{15} + 1746210\delta^{13}\Omega^2 + 720429446\delta^{11}\Omega^4 + 111821466809\delta^9\Omega^6 + 5617557875\delta^7\Omega^8 \\
&- 1703273246405\delta^5\Omega^{10} - 174641887008\delta^3\Omega^{12} - 28599599923208\delta\Omega^{14}) + 6\gamma^8(4032\delta^{16} + 775152\delta^{14}\Omega^2 - 3948072\delta^{12}\Omega^4 - 104982779304\delta^{10}\Omega^6 \\
&- 1785450268008\delta^8\Omega^8 - 12622488917604\delta^6\Omega^{10} - 4039926774244\delta^4\Omega^{12} - 488380455936\delta^2\Omega^{14} - 74232889344\Omega^{16}) \\
&- 2i\gamma^3\delta\Omega^4(6144\delta^{16} + 188328\delta^{14}\Omega^2 - 953340\delta^{12}\Omega^4 - 21708451\delta^{10}\Omega^6 - 1136910998\delta^8\Omega^8 - 49147584\delta^6\Omega^{10} + 13953499204\delta^4\Omega^{12} \\
&+ 3888663552\delta^2\Omega^{14} + 2463105024\Omega^{16}) - 6i\gamma^5\delta\Omega^2(768\delta^{16} + 101584\delta^{14}\Omega^2 + 733227\delta^{12}\Omega^4 - 26266829\delta^{10}\Omega^6 - 2311101828\delta^8\Omega^8 \\
&- 1232185266\delta^6\Omega^{10} + 506572233604\delta^4\Omega^{12} + 180211023364\delta^2\Omega^{14} + 16652500992\Omega^{16}) - \gamma^6(-650884\delta^{16}\Omega^2 - 11024884\delta^{14}\Omega^4 + 1791081244\delta^{12}\Omega^6 \\
&+ 445296161904\delta^{10}\Omega^8 + 43717913796\delta^8\Omega^{10} + 2239804868644\delta^6\Omega^{12} + 549747880704\delta^4\Omega^{14} + 49992140390 4\delta^2\Omega^{16} + 2446118092 8\Omega^{18}).
\end{aligned}
\tag{B.16}
$$

We pose $x = \frac{3i\mathcal{N}}{\Omega^3}\langle W_2|\rho_a^S|W_1\rangle$ and we have

$$
\begin{aligned}
x = {} & 48977602560000\gamma^{29} - 16325867520000i\gamma^{28}\delta + 68024448000\gamma^{27}\left(1169\delta^2 + 7104\Omega^2\right) - 22674816000i\gamma^{26}\left(1109\delta^3 + 7584\delta\Omega^2\right) \\
& + 45349632\gamma^{25}\left(1208787\delta^4 + 16096600\delta^2\Omega^2 + 45897600\Omega^4\right) - 10077696i\gamma^{24}\left(1605243\delta^5 + 23971400\delta^3\Omega^2 + 78782400\delta\Omega^4\right) \\
& + 419904\gamma^{23}\left(505355595\delta^6 + 11090984280\delta^4\Omega^2 + 68681930400\delta^2\Omega^4 + 123290726400\Omega^6\right) \\
& - 139968i\gamma^{22}\left(40904137\delta^7 + 1013568192\delta^5\Omega^2 + 7148913840\delta^3\Omega^4 + 15156771840\delta\Omega^6\right) \\
& + 11664\gamma^{21}\left(4392757870\delta^8 + 142461690480\delta^6\Omega^2 + 1434039542280\delta^4\Omega^4 + 5559692947200\delta^2\Omega^6 + 7105123215360\Omega^8\right) \\
& - 15552i\gamma^{20}\left(79140844\delta^9 + 2949205977\delta^7\Omega^2 + 33835160211\delta^5\Omega^4 + 152108360640\delta^3\Omega^6 + 2346363210240\delta\Omega^8\right) \\
& + 3888\gamma^{19}\left(2078652040\delta^{10} + 94840304380\delta^8\Omega^2 + 1385065696440\delta^6\Omega^4 + 8637487115760\delta^4\Omega^6 + 23769243590400\delta^2\Omega^8 + 23147868856320\Omega^{10}\right) \\
& - 432i\gamma^{18}\left(386173080\delta^{11} + 20878183405\delta^9\Omega^2 + 352380258651\delta^7\Omega^4 + 2534424159312\delta^5\Omega^6 + 8230865459328\delta^3\Omega^8 + 983923681075 2\delta\Omega^{10}\right) \\
& + 324\gamma^{17}\left(26070612\delta^{12} + 1647466761 6\delta^{10}\Omega^2 + 330725800787\delta^8\Omega^4 + 2945368832664\delta^6\Omega^6 + 12948740884800\delta^4\Omega^8 + 271172445511168\delta^2\Omega^{10}\right. \\
& \left. + 20985823346688\Omega^{12}\right) - 144i\gamma^{16}\left(98986320\delta^{13} + 7785610296\delta^{11}\Omega^2 + 186174391397\delta^9\Omega^4 + 1928675387127\delta^7\Omega^6 + 98998402940 64\delta^5\Omega^8\right. \\
& \left. + 2482889146211 44\delta^3\Omega^{10} + 23838336516096\delta\Omega^{12}\right) - 2i\delta^5\Omega^{10}\left(46240\delta^{14} + 602413\delta^{12}\Omega^2 + 4493396\delta^{10}\Omega^4 + 25729582\delta^8\Omega^6 + 110461712\delta^6\Omega^8\right. \\
& \left. + 334080384\delta^4\Omega^{10} + 617992704\delta^2\Omega^{12} + 510935040\Omega^{14}\right) + 144\gamma^{15}\left(40143384\delta^{14} + 355613886 0\delta^{12}\Omega^2 + 960841204 22\delta^{10}\Omega^4\right. \\
& \left. + 11507127442 83\delta^8\Omega^6 + 7140746050137\delta^6\Omega^8 + 238177640382 48\delta^4\Omega^{10} + 396153675694 08\delta^2\Omega^{12} + 2499718496256 0\Omega^{14}\right) \\
& - 36i\gamma^{14}\left(20529072\delta^{15} + 2451044424\delta^{13}\Omega^2 + 831147330 24\delta^{11}\Omega^4 + 1189104544243\delta^9\Omega^6 + 8625503366800\delta^7\Omega^8 + 339650522258 88\delta^5\Omega^{10}\right. \\
& \left. + 6833274769152 0\delta^3\Omega^{12} + 5370397596057 6\delta\Omega^{14}\right) + 2\gamma\delta^4\Omega^8\left(17472\delta^{16} + 310594\delta^{14}\Omega^2 + 2949555\delta^{12}\Omega^4 + 19431411\delta^{10}\Omega^6 + 93890612\delta^8\Omega^8\right. \\
& \left. + 337433938\delta^6\Omega^{10} + 85178445 6\delta^4\Omega^{12} + 126784972 8\delta^2\Omega^{14} + 75910348 8\Omega^{16}\right) - i\gamma^2\delta^3\Omega^8\left(743856\delta^{16} + 19228854\delta^{14}\Omega^2 + 191750321\delta^{12}\Omega^4\right. \\
& \left. + 1292918176\delta^{10}\Omega^6 + 6369267066\delta^8\Omega^8 + 2207862218 4\delta^6\Omega^{10} + 492403104 00\delta^4\Omega^{12} + 591253585 92\delta^2\Omega^{14} + 253105274 88\Omega^{16}\right) \\
& + 48\gamma^{13}\left(5163345\delta^{16} + 671699466\delta^{14}\Omega^2 + 24574116063\delta^{12}\Omega^4 + 3844552464 85\delta^{10}\Omega^6 + 31498984558 65\delta^8\Omega^8 + 1474463705 0814\delta^6\Omega^{10}\right. \\
& \left. + 390701372653 80\delta^4\Omega^{12} + 52971247254 528\delta^2\Omega^{14} + 275903289262 08\Omega^{16}\right) \\
& - 24i\gamma^{12}\left(876096\delta^{17} + 176833872\delta^{15}\Omega^2 + 88505961 78\delta^{13}\Omega^4 + 1741922352 49\delta^{11}\Omega^6 + 1697179939011\delta^9\Omega^8 + 932233907140 2\delta^7\Omega^{10}\right. \\
& \left. + 294175235154 96\delta^5\Omega^{12} + 484731818864 64\delta^3\Omega^{14} + 3134873655705 6\delta\Omega^{16}\right) \\
& + \gamma^3\delta^2\Omega^6\left(209568\delta^{18} + 7752216\delta^{16}\Omega^2 + 104941290\delta^{14}\Omega^4 + 869332903\delta^{12}\Omega^6 + 5017908516\delta^{10}\Omega^8 + 208336539 82\delta^8\Omega^{10}\right. \\
& \left. + 606391802 88\delta^6\Omega^{12} + 111696721920\delta^4\Omega^{14} + 107093975040\delta^2\Omega^{16} + 37710987264\Omega^{18}\right) \\
& - i\gamma^4\delta\Omega^6\left(1999344\delta^{18} + 98922996\delta^{16}\Omega^2 + 15225572 91\delta^{14}\Omega^4 + 1280685211 0\delta^{12}\Omega^6 + 739521692 10\delta^{10}\Omega^8 + 29611474 9692\delta^8\Omega^{10}\right. \\
& \left. + 773128494720\delta^6\Omega^{12} + 116248371 60096\delta^4\Omega^{14} + 796421652480\delta^2\Omega^{16} + 130459631616\Omega^{18}\right) \\
& - i\gamma^6\delta\Omega^4\left(2354688\delta^{18} + 216435876\delta^{16}\Omega^2 + 55474689 48\delta^{14}\Omega^4 + 641796948 92\delta^{12}\Omega^6 + 451306805 403\delta^{10}\Omega^8 + 212335875 5112\delta^8\Omega^{10}\right. \\
& \left. + 64945908250 56\delta^6\Omega^{12} + 117651935185 92\delta^4\Omega^{14} + 106234064732 16\delta^2\Omega^{16} + 31473386127 36\Omega^{18}\right) \\
& - 3i\gamma^8\delta\Omega^2\left(422208\delta^{18} + 75657312\delta^{16}\Omega^2 + 3331882776\delta^{14}\Omega^4 + 58073694816\delta^{12}\Omega^6 + 531162351893\delta^{10}\Omega^8 + 3020849744 176\delta^8\Omega^{10}\right. \\
& \left. + 109490645852 16\delta^6\Omega^{12} + 236907325601 28\delta^4\Omega^{14} + 265430912532 48\delta^2\Omega^{16} + 10968291606 528\Omega^{18}\right) \\
& + 3\gamma^{11}\left(2001024\delta^{18} + 425918736\delta^{16}\Omega^2 + 21956275824\delta^{14}\Omega^4 + 446852242168\delta^{12}\Omega^6 + 46523509599 29\delta^{10}\Omega^8 + 2845002719097 2\delta^8\Omega^{10}\right. \\
& \left. + 105778610773104\delta^6\Omega^{12} + 229222477186560\delta^4\Omega^{14} + 25656337081 9584\delta^2\Omega^{16} + 10997721464 8320\Omega^{18}\right) \\
& - 24i\gamma^{10}\left(10368\delta^{19} + 4713210\delta^{17}\Omega^2 + 386724702\delta^{15}\Omega^4 + 10836025994\delta^{13}\Omega^6 + 139732622347\delta^{11}\Omega^8 + 10064424241 97\delta^9\Omega^{10}\right. \\
& \left. + 44141700542 22\delta^7\Omega^{12} + 11454866219952\delta^5\Omega^{14} + 15590693154816\delta^3\Omega^{16} + 8207963062272\delta\Omega^{18}\right) \\
& + 2\gamma^5\Omega^4\left(201888\delta^{20} + 15078300\delta^{18}\Omega^2 + 331534167\delta^{16}\Omega^4 + 3686541870\delta^{14}\Omega^6 + 26255417635\delta^{12}\Omega^8 + 1288488831 63\delta^{10}\Omega^{10}\right. \\
& \left. + 43515022458 6\delta^8\Omega^{12} + 948070541376\delta^6\Omega^{14} + 11705288555 52\delta^4\Omega^{16} + 660292632576\delta^2\Omega^{18} + 97844723712\Omega^{20}\right) \\
& + \gamma^7\Omega^2\left(279936\delta^{20} + 46479456\delta^{18}\Omega^2 + 1838491680\delta^{16}\Omega^4 + 30164056197\delta^{14}\Omega^6 + 279367083806\delta^{12}\Omega^8 + 1670746103379\delta^{10}\Omega^{10}\right. \\
& \left. + 6664805416212\delta^8\Omega^{12} + 171026563305 60\delta^6\Omega^{14} + 25694431967232\delta^4\Omega^{16} + 1912679615692 8\delta^2\Omega^{18} + 486777500467 2\Omega^{20}\right) \\
& + 6\gamma^9\left(10368\delta^{20} + 4800816\delta^{18}\Omega^2 + 386057982\delta^{16}\Omega^4 + 10497335192\delta^{14}\Omega^6 + 136563937615\delta^{12}\Omega^8 + 1042197173058\delta^{10}\Omega^{10}\right. \\
& \left. + 50450000924 36\delta^8\Omega^{12} + 15415707749520\delta^6\Omega^{14} + 27765646467840\delta^4\Omega^{16} + 2562051774873 6\delta^2\Omega^{18} + 879799880908 8\Omega^{20}\right).
\end{aligned}
\tag{B.17}
$$

We pose $x = \frac{-\sqrt{3}\mathcal{N}}{\Omega^2}\langle W_2|\rho_a^S|g\rangle$ and we have

$$
\begin{aligned}
x = {} & 16325867520000\gamma^{30} - 5441955840000i\gamma^{29}\delta + 22674816000\gamma^{28}\left(1169\delta^2 + 7344\Omega^2\right) - 7558272000i\gamma^{27}\left(1109\delta^3 + 8784\delta\Omega^2\right) \\
& + 15116544\gamma^{26}\left(1208787\delta^4 + 16321100\delta^2\Omega^2 + 49209600\Omega^4\right) - 10077696i\gamma^{25}\left(535081\delta^5 + 9050050\delta^3\Omega^2 + 34540800\delta\Omega^4\right) \\
& + 699840\gamma^{24}\left(101071119\delta^6 + 2218097520\delta^4\Omega^2 + 14121701280\delta^2\Omega^4 + 27485844480\Omega^6\right) \\
& - 46656i\gamma^{23}\left(409041370\delta^7 + 11307953520\delta^5\Omega^2 + 90720698400\delta^3\Omega^4 + 222260198400\delta\Omega^6\right) \\
& + 3888\gamma^{22}\left(4392757870\delta^8 + 141018102360\delta^6\Omega^2 + 1429588137960\delta^4\Omega^4 + 5785728912000\delta^2\Omega^6 + 82452880281600\Omega^8\right) \\
& - 5184i\gamma^{21}\left(791408440\delta^9 + 32591677760\delta^7\Omega^2 + 419048196210\delta^5\Omega^4 + 2134559498400\delta^3\Omega^6 + 3771569226240\delta\Omega^8\right) \\
& + 2592\gamma^{20}\left(10393260200\delta^{10} + 465825714100\delta^8\Omega^2 + 6746359410000\delta^6\Omega^4 + 42675272933400\delta^4\Omega^6 + 124736921568000\delta^2\Omega^8 + 139863312230400\Omega^{10}\right) \\
& - 432i\gamma^{19}\left(1287243600\delta^{11} + 76580908670\delta^9\Omega^2 + 1434027816270\delta^7\Omega^4 + 11499920940600\delta^5\Omega^6 + 42024737381760\delta^3\Omega^8 + 56921423984640\delta\Omega^{10}\right) \\
& + 108\gamma^{18}\left(2607061200\delta^{12} + 160792105760\delta^{10}\Omega^2 + 3163351136430\delta^8\Omega^4 + 27948844889520\delta^6\Omega^6 + 125555724518400\delta^4\Omega^8 + 285244793256960\delta^2\Omega^{10}\right. \\
& \qquad \left. + 263851360174080\Omega^{12}\right) - 864i\gamma^{17}\left(54992400\delta^{13} + 4757969760\delta^{11}\Omega^2 + 125624175470\delta^9\Omega^4 + 1432500117460\delta^7\Omega^6 + 8140886290800\delta^5\Omega^8\right. \\
& \qquad \left. + 22781387715840\delta^3\Omega^{10} + 24492088350720\delta\Omega^{12}\right) \\
& - 2\delta^6\Omega^{10}\left(2496\delta^{14} + 26142\delta^{12}\Omega^2 + 235426\delta^{10}\Omega^4 + 1645581\delta^8\Omega^6 + 7237386\delta^6\Omega^8 + 24598388\delta^4\Omega^{10} + 65593248\delta^2\Omega^{12} + 87054336\Omega^{14}\right) \\
& - 3i\gamma\delta^5\Omega^{10}\left(16000\delta^{14} + 196708\delta^{12}\Omega^2 + 1484542\delta^{10}\Omega^4 + 9060887\delta^8\Omega^6 + 41380759\delta^6\Omega^8 + 134481844\delta^4\Omega^{10} + 275867904\delta^2\Omega^{12}\right. \\
& \qquad \left. + 261144576\Omega^{14}\right) + 108\gamma^{16}\left(17841504\delta^{14} + 1532615016\delta^{12}\Omega^2 + 40164663560\delta^{10}\Omega^4 + 468878167637\delta^8\Omega^6 + 2878459853988\delta^6\Omega^8\right. \\
& \qquad \left. + 9901491398304\delta^4\Omega^{10} + 18378524924928\delta^2\Omega^{12} + 14505592651776\Omega^{14}\right) - 36i\gamma^{15}\left(6843024\delta^{15} + 901481784\delta^{13}\Omega^2 + 33757396164\delta^{11}\Omega^4\right. \\
& \qquad \left. + 526754701513\delta^9\Omega^6 + 4165066865442\delta^7\Omega^8 + 18029096748960\delta^5\Omega^{10} + 401175580008960\delta^3\Omega^{12} + 348799886622720\delta\Omega^{14}\right) \\
& - 2\gamma^2\delta^4\Omega^8\left(8016\delta^{16} + 267030\delta^{14}\Omega^2 + 3020475\delta^{12}\Omega^4 + 28148570\delta^{10}\Omega^6 + 163055247\delta^8\Omega^8 + 648154423\delta^6\Omega^{10} + 1912278228\delta^4\Omega^{12}\right. \\
& \qquad \left. + 32708183040\delta^2\Omega^{14} + 163764633600\Omega^{16}\right) - 6i\gamma^3\delta^3\Omega^8\left(661760\delta^{16} + 16329630\delta^{14}\Omega^2 + 160338790\delta^{12}\Omega^4 + 1125074080\delta^{10}\Omega^6 + 5868594210\delta^8\Omega^8\right. \\
& \qquad \left. + 21730423410\delta^6\Omega^{10} + 52752460320\delta^4\Omega^{12} + 69998469120\delta^2\Omega^{14} + 32133611520\Omega^{16}\right) + 108\gamma^{14}\left(7649400\delta^{16} + 957480560\delta^{14}\Omega^2 + 33586947760\delta^{12}\Omega^4\right. \\
& \qquad \left. + 504157140380\delta^{10}\Omega^6 + 3972378052830\delta^8\Omega^8 + 18279378758480\delta^6\Omega^{10} + 50705002369440\delta^4\Omega^{12} + 80065687080960\delta^2\Omega^{14} + 55269210193920\Omega^{16}\right) \\
& - 36i\gamma^{13}\left(1946880\delta^{17} + 436002720\delta^{15}\Omega^2 + 24213408120\delta^{13}\Omega^4 + 517289225280\delta^{11}\Omega^6 + 5413082279830\delta^9\Omega^8 + 32159561961500\delta^7\Omega^{10}\right. \\
& \qquad \left. + 110866691791200\delta^5\Omega^{12} + 200420446740480\delta^3\Omega^{14} + 141637103124480\delta\Omega^{16}\right) + 4\gamma^4\delta^2\Omega^6\left(49680\delta^{18} - 106116\delta^{16}\Omega^2 - 3921873\delta^{14}\Omega^4\right. \\
& \left. - 61668201\delta^{12}\Omega^6 - 549610070\delta^{10}\Omega^8 - 2832896475\delta^8\Omega^{10} - 9801900513\delta^6\Omega^{12} - 19830104928\delta^4\Omega^{14} - 14635496448\delta^2\Omega^{16} + 6370099200\Omega^{18}\right) \\
& - 3i\gamma^5\delta\Omega^6\left(3306720\delta^{18} + 168985440\delta^{16}\Omega^2 + 2564824710\delta^{14}\Omega^4 + 22002002790\delta^{12}\Omega^6 + 133455664480\delta^{10}\Omega^8 + 568547223040\delta^8\Omega^{10}\right. \\
& \qquad \left. + 1602055051200\delta^6\Omega^{12} + 2628574018560\delta^4\Omega^{14} + 1942473277440\delta^2\Omega^{16} + 326149079040\Omega^{18}\right) \\
& - 3i\gamma^7\delta\Omega^4\left(3404160\delta^{18} + 345240840\delta^{16}\Omega^2 + 9182072640\delta^{14}\Omega^4 + 107972894300\delta^{12}\Omega^6 + 791213023970\delta^{10}\Omega^8 + 3950472427460\delta^8\Omega^{10}\right. \\
& \qquad \left. + 12993597652080\delta^6\Omega^{12} + 25552331159040\delta^4\Omega^{14} + 24948984545280\delta^2\Omega^{16} + 7732451082240\Omega^{18}\right) \\
& - 3i\gamma^9\delta\Omega^2\left(1584000\delta^{18} + 321461280\delta^{16}\Omega^2 + 15453295680\delta^{14}\Omega^4 + 282074765560\delta^{12}\Omega^6 + 2686391840690\delta^{10}\Omega^8 + 16192904122320\delta^8\Omega^{10}\right. \\
& \qquad \left. + 63087906144240\delta^6\Omega^{12} + 148071621369600\delta^4\Omega^{14} + 179944291860480\delta^2\Omega^{16} + 79085630914560\Omega^{18}\right) \\
& + 3\gamma^{12}\left(6670080\delta^{18} + 1352275200\delta^{16}\Omega^2 + 65763868320\delta^{14}\Omega^4 + 1259440435200\delta^{12}\Omega^6 + 12263574042430\delta^{10}\Omega^8 + 70081806091080\delta^8\Omega^{10}\right. \\
& \qquad \left. + 253615042700640\delta^6\Omega^{12} + 592773623452800\delta^4\Omega^{14} + 833072655237120\delta^2\Omega^{16} + 511613880238080\Omega^{18}\right) \\
& - 72i\gamma^{11}\left(11520\delta^{19} + 5850900\delta^{17}\Omega^2 + 537381480\delta^{15}\Omega^4 + 16347243540\delta^{13}\Omega^6 + 223367027570\delta^{11}\Omega^8 + 1709151069840\delta^9\Omega^{10} + 8073162049400\delta^7\Omega^{12}\right. \\
& \qquad \left. + 22780360857840\delta^5\Omega^{14} + 33790977146880\delta^3\Omega^{16} + 19191012065280\delta\Omega^{18}\right) \\
& + 3\gamma^6\Omega^4\left(339840\delta^{20} + 18006960\delta^{18}\Omega^2 + 249531940\delta^{16}\Omega^4 + 1350760330\delta^{14}\Omega^6 - 4867503660\delta^{12}\Omega^8 - 86423155400\delta^{10}\Omega^{10} - 449997835960\delta^8\Omega^{12}\right. \\
& \qquad \left. - 1113092636160\delta^6\Omega^{14} - 744822881280\delta^4\Omega^{16} + 81738989568\delta^2\Omega^{18} + 326149079040\Omega^{20}\right) \\
& + 3\gamma^8\Omega^2\left(2880000\delta^{20} + 422438400\delta^{18}\Omega^2 + 14142507600\delta^{16}\Omega^4 + 193852004900\delta^{14}\Omega^6 + 1401670390000\delta^{12}\Omega^8 + 5687288978600\delta^{10}\Omega^{10}\right. \\
& \qquad \left. + 14592195042400\delta^8\Omega^{12} + 31085028700800\delta^6\Omega^{14} + 86192132889600\delta^4\Omega^{16} + 162836191641600\delta^2\Omega^{18} + 79498838016000\Omega^{20}\right) \\
& + 3\gamma^{10}\left(691200\delta^{20} + 300931200\delta^{18}\Omega^2 + 22255290000\delta^{16}\Omega^4 + 550514229600\delta^{14}\Omega^6 + 6456367977400\delta^{12}\Omega^8 + 43164227802300\delta^{10}\Omega^{10}\right. \\
& \qquad \left. + 182994552257600\delta^8\Omega^{12} + 533653016851200\delta^6\Omega^{14} + 1120243605926400\delta^4\Omega^{16} + 1528739669606400\delta^2\Omega^{18} + 841681207296000\Omega^{20}\right).
\end{aligned}
\tag{B.18}
$$

We pose $x = \frac{3\sqrt{2}i\mathcal{N}}{\delta\Omega^4}\langle W_2|\rho_a^S|\psi_2\rangle$ and we have

$$
\begin{aligned}
x = {} & 16325867520000\gamma^{27} + 2720977920000i\gamma^{26}\delta + 22674816000\gamma^{25}\left(1109\delta^2 + 6624\Omega^2\right) + 3779136000i\gamma^{24}\left(1109\delta^3 + 8304\delta\Omega^2\right) \\
& + 30233088\gamma^{23}\left(535081\delta^4 + 7129800\delta^2\Omega^2 + 19636800\Omega^4\right) + 5038848i\gamma^{22}\left(535081\delta^5 + 8370550\delta^3\Omega^2 + 31618800\delta\Omega^4\right) \\
& + 139968\gamma^{21}\left(409041137\delta^6 + 916565364\delta^4\Omega^2 + 5557069440\delta^2\Omega^4 + 9501373440\Omega^6\right) \\
& + 23328i\gamma^{20}\left(409041137\delta^7 + 10239161885\delta^5\Omega^2 + 7894754640\delta^3\Omega^4 + 18757232640\delta\Omega^6\right) \\
& + 15552\gamma^{19}\left(79140844\delta^8 + 2686707747\delta^6\Omega^2 + 26884016343\delta^4\Omega^4 + 100138422960\delta^2\Omega^6 + 120619839744\Omega^8\right) \\
& + 2592i\gamma^{18}\left(791408449\delta^9 + 28898285047\delta^7\Omega^2 + 345271777115\delta^5\Omega^4 + 1670492764805\delta^3\Omega^6 + 2783633091845\delta\Omega^8\right) \\
& + 3888\gamma^{17}\left(42908120\delta^{10} + 2118621226\delta^8\Omega^2 + 31372033999\delta^6\Omega^4 + 189658497960\delta^4\Omega^6 + 493465735872\delta^2\Omega^8 + 449942722560\Omega^{10}\right) \\
& + 648i\gamma^{16}\left(429081205\delta^{11} + 22150437345\delta^9\Omega^2 + 371137657715\delta^7\Omega^4 + 2744422360805\delta^5\Omega^6 + 9336804220805\delta^3\Omega^8 + 11691886602245\delta\Omega^{10}\right) \\
& + 864\gamma^{15}\left(164977205\delta^{12} + 11831677235\delta^{10}\Omega^2 + 247724048295\delta^8\Omega^4 + 2165608562495\delta^6\Omega^6 + 9022328171285\delta^4\Omega^8 + 17625727483205\delta^2\Omega^{10}\right. \\
& \qquad \left. + 12733997506565\Omega^{12}\right) + 144i\gamma^{14}\left(1649772015\delta^{13} + 121209449295\delta^{11}\Omega^2 + 2744755666115\delta^9\Omega^4 + 27716988608695\delta^7\Omega^6 + 143415029977205\delta^5\Omega^8\right. \\
& \qquad \left. + 367892973360035\delta^3\Omega^{10} + 362233418342455\delta\Omega^{12}\right) \\
& + 12\gamma\delta^4\Omega^8\left(12480\delta^{14} + 172686\delta^{12}\Omega^2 + 1288751\delta^{10}\Omega^4 + 6833333\delta^8\Omega^6 + 24577082\delta^6\Omega^8 + 54949872\delta^4\Omega^{10} + 68270400\delta^2\Omega^{12} + 35721216\Omega^{14}\right) \\
& + i\delta^5\Omega^8\left(19968\delta^{14} + 240016\delta^{12}\Omega^2 + 1796986\delta^{10}\Omega^4 + 11231491\delta^8\Omega^6 + 51263298\delta^6\Omega^8 + 156895672\delta^4\Omega^{10} + 293904192\delta^2\Omega^{12} + 259928064\Omega^{14}\right) \\
& + 432\gamma^{13}\left(17107565\delta^{14} + 1853094065\delta^{12}\Omega^2 + 54491464255\delta^{10}\Omega^4 + 653339666285\delta^8\Omega^6 + 3860105129025\delta^6\Omega^8 + 11964047733365\delta^4\Omega^{10}\right. \\
& \qquad \left. + 18335850370565\delta^2\Omega^{12} + 10795986616325\Omega^{14}\right) + 12i\gamma^{12}\left(102645365\delta^{15} + 11238178685\delta^{13}\Omega^2 + 344659949645\delta^{11}\Omega^4 + 4519996238635\delta^9\Omega^6\right. \\
& \qquad \left. + 31415295820085\delta^7\Omega^8 + 122853264687365\delta^5\Omega^{10} + 248204129679365\delta^3\Omega^{12} + 197453473873925\delta\Omega^{14}\right) + 12\gamma^3\delta^2\Omega^6\left(71904\delta^{16} + 2238432\delta^{14}\Omega^2\right. \\
& \qquad \left. + 24070890\delta^{12}\Omega^4 + 1597565545\delta^{10}\Omega^6 + 70673052985\delta^8\Omega^8 + 1999390176\delta^6\Omega^{10} + 34143582245\delta^4\Omega^{12} + 31801420805\delta^2\Omega^{14} + 12740198405\Omega^{16}\right) \\
& + i\gamma^2\delta^3\Omega^6\left(131520\delta^{16} + 3675672\delta^{14}\Omega^2 + 36522084\delta^{12}\Omega^4 + 261028380\delta^{10}\Omega^6 + 1397708553\delta^8\Omega^8 + 5147231792\delta^6\Omega^{10} + 12012109248\delta^4\Omega^{12}\right. \\
& \qquad \left. + 15328074240\delta^2\Omega^{14} + 7134511104\Omega^{16}\right) + 36\gamma^{11}\left(584064\delta^{16} + 106149960\delta^{14}\Omega^2 + 4530105264\delta^{12}\Omega^4 + 73274409650\delta^{10}\Omega^6\right. \\
& \qquad \left. + 577442620083\delta^8\Omega^8 + 2510969531988\delta^6\Omega^{10} + 6062337503568\delta^4\Omega^{12} + 7473848832000\delta^2\Omega^{14} + 3625579118592\Omega^{16}\right) \\
& + 6i\gamma^{10}\left(584064\delta^{17} + 106476552\delta^{15}\Omega^2 + 4611588120\delta^{13}\Omega^4 + 77638162626\delta^{11}\Omega^6 + 678019630541\delta^9\Omega^8 + 3560994832016\delta^7\Omega^{10}\right. \\
& \qquad \left. + 11016797171952\delta^5\Omega^{12} + 1796141636812\delta^3\Omega^{14} + 116478723686405\delta\Omega^{16}\right) \\
& + 36\gamma^5\Omega^4\left(45120\delta^{18} + 2928680\delta^{16}\Omega^2 + 52751735\delta^{14}\Omega^4 + 467691181\delta^{12}\Omega^6 + 2585825478\delta^{10}\Omega^8 + 9092014864\delta^8\Omega^{10} + 1962875740\delta^6\Omega^{12}\right. \\
& \qquad \left. + 243076458\delta^4\Omega^{14} + 14966194176\delta^2\Omega^{16} + 2717908992\Omega^{18}\right) + i\gamma^4\delta\Omega^4\left(266112\delta^{18} + 16304544\delta^{16}\Omega^2 + 272761056\delta^{14}\Omega^4 + 2414667411\delta^{12}\Omega^6\right. \\
& \qquad \left. + 15225336100\delta^{10}\Omega^8 + 66845798670\delta^8\Omega^{10} + 189625470048\delta^6\Omega^{12} + 312559822080\delta^4\Omega^{14} + 246009692160\delta^2\Omega^{16} + 57076088832\Omega^{18}\right) \\
& + 36\gamma^7\Omega^2\left(31104\delta^{18} + 4519680\delta^{16}\Omega^2 + 150220206\delta^{14}\Omega^4 + 1983117260\delta^{12}\Omega^6 + 14315178471\delta^{10}\Omega^8 + 63133467985\delta^8\Omega^{10} + 169584858852\delta^6\Omega^{12}\right. \\
& \qquad \left. + 26370505324\delta^4\Omega^{14} + 2119056629765\delta^2\Omega^{16} + 635311226885\Omega^{18}\right) + 144\gamma^9\left(1728\delta^{18} + 700992\delta^{16}\Omega^2 + 47925438\delta^{14}\Omega^4 + 1066339216\delta^{12}\Omega^6\right. \\
& \qquad \left. + 10882342662\delta^{10}\Omega^8 + 62200605184\delta^8\Omega^{10} + 209625616077\delta^6\Omega^{12} + 404448324552\delta^4\Omega^{14} + 404696217600\delta^2\Omega^{16} + 159467470848\Omega^{18}\right) \\
& + i\gamma^6\delta\Omega^2\left(186624\delta^{18} + 26731296\delta^{16}\Omega^2 + 858185268\delta^{14}\Omega^4 + 11084494002\delta^{12}\Omega^6 + 85988684539\delta^{10}\Omega^8 + 453896749716\delta^8\Omega^{10}\right. \\
& \qquad \left. + 1557709007592\delta^6\Omega^{12} + 3184751142144\delta^4\Omega^{14} + 3364344668160\delta^2\Omega^{16} + 1309692395520\Omega^{18}\right) \\
& + 12i\gamma^8\left(3456\delta^{19} + 1401984\delta^{17}\Omega^2 + 95490690\delta^{15}\Omega^4 + 2120435725\delta^{13}\Omega^6 + 22510668346\delta^{11}\Omega^8 + 147423631295\delta^9\Omega^{10}\right. \\
& \qquad \left. + 617584596488\delta^7\Omega^{12} + 1548136299792\delta^5\Omega^{14} + 2049987852288\delta^3\Omega^{16} + 1065566306304\delta\Omega^{18}\right).
\end{aligned}
\tag{B.19}
$$

We pose $x = \frac{3\mathcal{N}}{\sqrt{2}\delta\Omega^5}\langle W_2|\rho_a^S|\psi_1\rangle$ and we have

$$
\begin{aligned}
x = &-2720977920000\gamma^{26} + 453496320000i\gamma^{25}\delta - 1259712000\gamma^{24}\left(3047\delta^2 + 19872\Omega^2\right) + 629856000i\gamma^{23}\left(709\delta^3 - 1176\delta\Omega^2\right) \\
&- 30233088\gamma^{22}\left(76951\delta^4 + 1009300\delta^2\Omega^2 + 3272800\Omega^4\right) + 279936i\gamma^{21}\left(638993\delta^5 - 3821475\delta^3\Omega^2 - 23151600\delta\Omega^4\right) \\
&- 23328\gamma^{20}\left(33994869\delta^6 + 681898364\delta^4\Omega^2 + 4289717040\delta^2\Omega^4 + 9501373440\Omega^6\right) \\
&+ 11664i\gamma^{19}\left(3224139\delta^7 - 48759892\delta^5\Omega^2 - 545783760\delta^3\Omega^4 - 598907520\delta\Omega^6\right) \\
&- 432\gamma^{18}\left(3866690369\delta^8 + 10790956464\delta^6\Omega^2 + 976919985536\delta^4\Omega^4 + 418961371680\delta^2\Omega^6 + 723719038464\Omega^8\right) \\
&+ 648i\gamma^{17}\left(6887322\delta^9 - 226364549\delta^7\Omega^2 - 3832750284\delta^5\Omega^4 - 816348556\delta^3\Omega^6 + 13397481216\delta\Omega^8\right) \\
&- 72\gamma^{16}\left(312168714\delta^{10} + 11775109193\delta^8\Omega^2 + 1362679026786\delta^6\Omega^4 + 80595715975\delta^4\Omega^6 + 2807463234816\delta^2\Omega^8 + 404948450304\Omega^{10}\right) \\
&+ 72i\gamma^{15}\left(4132458\delta^{11} - 265085186\delta^9\Omega^2 - 6613175991\delta^7\Omega^4 - 22255216740\delta^5\Omega^6 + 1067420505608\delta^3\Omega^8 + 366673402368\delta\Omega^{10}\right) \\
&+ \delta^6\Omega^8\left(4544\delta^{12} + 69350\delta^{10}\Omega^2 + 676417\delta^8\Omega^4 + 5307569\delta^6\Omega^6 + 25354618\delta^4\Omega^8 + 60128184\delta^2\Omega^{10} + 53957376\Omega^{12}\right) - 36\gamma^{14}\left(534405\right. \\
&\left. 48\delta^{12} + 2759242050\delta^{10}\Omega^2 + 390401613598\delta^8\Omega^4 + 26334594243\delta^6\Omega^6 + 1279499408880\delta^4\Omega^8 + 40851407473\delta^2\Omega^{10} + 509359900262\Omega^{12}\right) \\
&+ 12i\gamma^{13}\left(854388\delta^{13} - 82059036\delta^{11}\Omega^2 - 3401198369\delta^9\Omega^4 - 187892026986\delta^7\Omega^6 + 19261858399\delta^5\Omega^8 + 1457808868512\delta^3\Omega^{10}\right. \\
&\left. + 223743032524\delta\Omega^{12}\right) + 6i\gamma^9\delta\Omega^2\left(1149060\delta^{14} + 58267310\delta^{12}\Omega^2 + 4436510418\delta^{10}\Omega^4 + 321995208\delta^8\Omega^6 + 63564262010\delta^6\Omega^8\right. \\
&\left. + 4157582151136\delta^4\Omega^{10} + 101631826252\delta^2\Omega^{12} + 8060020162\Omega^{14}\right) - 24\gamma^{12}\left(4187790\delta^{14} + 312354429\delta^{12}\Omega^2 + 5447460881\delta^{10}\Omega^4\right. \\
&\left. + 365472386\delta^8\Omega^6 + 17057881505\delta^6\Omega^8 + 913667703408\delta^4\Omega^{10} + 29688527600\delta^2\Omega^{12} + 3238795984896\Omega^{14}\right) \\
&+ 6i\gamma^{11}\left(23328\delta^{15} + 5914200\delta^{13}\Omega^2 + 453476\delta^{11}\Omega^4 - 867886061\delta^9\Omega^6 + 50037899602\delta^7\Omega^8 + 6684052979\delta^5\Omega^{10} + 2360845263744\delta^3\Omega^{12}\right. \\
&\left. + 247196344320\delta\Omega^{14}\right) + \gamma^2\delta^2\Omega^6\left(-4224\delta^{16} + 590808\delta^{14}\Omega^2 + 10094372\delta^{12}\Omega^4 + 100653610\delta^{10}\Omega^6 + 616094685\delta^8\Omega^8 + 1961744784\delta^6\Omega^{10}\right. \\
&\left. + 2640363264\delta^4\Omega^{12} + 434350080\delta^2\Omega^{14} - 934281216\Omega^{16}\right) + 2i\gamma\delta^3\Omega^6\left(2496\delta^{16} + 4582\delta^{14}\Omega^2 - 103689\delta^{12}\Omega^4 - 729708\delta^{10}\Omega^6 - 1798414\delta^8\Omega^8\right. \\
&\left. + 8413789\delta^6\Omega^{10} + 70665852\delta^4\Omega^{12} + 16685798\delta^2\Omega^{14} + 116785152\Omega^{16}\right) + 2i\gamma^7\delta\Omega^2\left(153648\delta^{16} + 14178264\delta^{14}\Omega^2 + 1771704758\delta^{12}\Omega^4\right. \\
&\left. + 409442548\delta^{10}\Omega^6 + 67644176768\delta^8\Omega^8 + 8554241920\delta^6\Omega^{10} + 396092810088\delta^4\Omega^{12} + 7440572390\delta^2\Omega^{14} + 462094958592\Omega^{16}\right) \\
&- 6\gamma^{10}\left(481536\delta^{16} + 58491060\delta^{14}\Omega^2 + 1330847266\delta^{12}\Omega^4 + 82875255\delta^{10}\Omega^6 + 5849368\delta^8\Omega^8 + 2830408905\delta^6\Omega^{10} + 102948289862\delta^4\Omega^{12}\right. \\
&\left. + 3823339567104\delta^2\Omega^{14} + 36255791185\Omega^{16}\right) + \gamma^4\Omega^4\left(-67200\delta^{18} - 703872\delta^{16}\Omega^2 + 34726935\delta^{14}\Omega^4 + 613667149\delta^{12}\Omega^6\right. \\
&\left. + 5146493817\delta^{10}\Omega^8 + 214134498\delta^8\Omega^{10} + 36904379040\delta^6\Omega^{12} + 3943074816\delta^4\Omega^{14} - 39510540288\delta^2\Omega^{16} - 1630745395\Omega^{18}\right) \\
&+ 2i\gamma^3\delta\Omega^4\left(6144\delta^{18} + 252852\delta^{16}\Omega^2 + 366234\delta^{14}\Omega^4 - 5987860\delta^{12}\Omega^6 - 20680032\delta^{10}\Omega^8 + 197758475\delta^8\Omega^{10} + 1840524402\delta^6\Omega^{12}\right. \\
&\left. + 55394735\delta^4\Omega^{14} + 6312370176\delta^2\Omega^{16} + 2038431744\Omega^{18}\right) + 2i\gamma^5\delta\Omega^2\left(2304\delta^{18} + 483144\delta^{16}\Omega^2 + 9724497\delta^{14}\Omega^4 + 148287\delta^{12}\Omega^6\right. \\
&\left. - 16197335\delta^{10}\Omega^8 + 1788550800\delta^8\Omega^{10} + 182617013\delta^6\Omega^{12} + 66881826432\delta^4\Omega^{14} + 9953506713\delta^2\Omega^{16} + 476483420\Omega^{18}\right) \\
&- \gamma^6\Omega^2\left(102528\delta^{18} + 6940560\delta^{16}\Omega^2 + 45996618\delta^{14}\Omega^4 - 1114678094\delta^{12}\Omega^6 - 17894676069\delta^{10}\Omega^8 - 1040167519\delta^8\Omega^{10} - 220607717184\delta^6\Omega^{12}\right. \\
&\left. + 490275624\delta^4\Omega^{14} + 59984636\delta^2\Omega^{16} + 3811867\Omega^{18}\right) - 3\gamma^8\left(11520\delta^{18} + 3072960\delta^{16}\Omega^2 + 103287696\delta^{14}\Omega^4 + 617253036\delta^{12}\Omega^6\right. \\
&\left. - 54787527\delta^{10}\Omega^8 - 7043403865\delta^8\Omega^{10} - 182105576088\delta^6\Omega^{12} + 31193533\delta^4\Omega^{14} + 1590385508\delta^2\Omega^{16} + 12757397\Omega^{18}\right).
\end{aligned}
\tag{B.20}
$$

We pose $x = \frac{\sqrt{3}i\mathcal{N}}{\Omega}\langle W_1|\rho_a^S|g\rangle$ and we have

$$
\begin{aligned}
x = {} & 16325867520000\gamma^{31} - 10883911680000i\gamma^{28}\delta\Omega^2 + 22674816000\gamma^{29}\left(1289\delta^2 + 8064\Omega^2\right) \\
& + 15116544\gamma^{27}\left(1486037\delta^4 + 20450600\delta^2\Omega^2 + 60225600\Omega^4\right) - 15116544000i\gamma^{26}\left(1109\delta^3\Omega^2 + 7344\delta\Omega^4\right) \\
& + 139968\gamma^{25}\left(69798511\delta^6 + 1584002556\delta^4\Omega^2 + 10265286240\delta^2\Omega^4 + 19057559040\Omega^6\right) \\
& - 20155392i\gamma^{24}\left(535081\delta^5\Omega^2 + 7716550\delta^3\Omega^4 + 24604800\delta\Omega^6\right) \\
& - 10368i\gamma^{20}\delta\Omega^2\left(791408440\delta^8 + 28276315386\delta^6\Omega^2 + 312931884694\delta^4\Omega^4 + 1372400431200\delta^2\Omega^6 + 2061322007048\Omega^8\right) \\
& + 3888\gamma^{23}\left(6847006090\delta^8 + 229519657446\delta^6\Omega^2 + 2437173489966\delta^4\Omega^4 + 9980074540806\delta^2\Omega^6 + 13192740034568\Omega^8\right) \\
& - 93312i\gamma^{22}\left(40904137\delta^7\Omega^2 + 975591360\delta^5\Omega^4 + 6662892240\delta^3\Omega^6 + 13742922240\delta\Omega^8\right) \\
& - 864i\gamma^{18}\delta\Omega^2\left(12872436\delta^{10} + 664246344\delta^8\Omega^2 + 10753266635\delta^6\Omega^4 + 75473585514\delta^4\Omega^6 + 240432811833\delta^2\Omega^8 + 279726624460\Omega^{10}\right) \\
& + 1296\gamma^{21}\left(366146892\delta^{10} + 17273169953\delta^8\Omega^2 + 267716092230\delta^6\Omega^4 + 17890807696564\delta^4\Omega^6 + 523214355052\delta^2\Omega^8 + 52708526530560\Omega^{10}\right) \\
& - 864i\gamma^{16}\delta\Omega^2\left(10998480\delta^{12} + 821491998\delta^{10}\Omega^2 + 18696529623\delta^8\Omega^4 + 1886063354186\delta^6\Omega^6 + 95478956683284\delta^4\Omega^8 + 2354568883200\delta^2\Omega^{10}\right. \\
& \left. + 219876133478 4\Omega^{12}\right) + 324\gamma^{19}\left(172718280\delta^{12} + 11308775176\delta^{10}\Omega^2 + 242575613979\delta^8\Omega^4 + 2343127083296\delta^6\Omega^6 + 111569103848 16\delta^4\Omega^8\right. \\
& \left. + 249309327052 80\delta^2\Omega^{10} + 199841103175 68\Omega^{12}\right) - 2i\delta^5\Omega^{12}\left(20608\delta^{14} + 321892\delta^{12}\Omega^2 + 2595572\delta^{10}\Omega^4 + 14514901\delta^8\Omega^6 + 61185983\delta^6\Omega^8\right. \\
& \left. + 185822772\delta^4\Omega^{10} + 3353541 12\delta^2\Omega^{12} + 248168448\Omega^{14}\right) - 216i\gamma^{14}\delta\Omega^2\left(2281008\delta^{14} + 257197472\delta^{12}\Omega^2 + 82186881 24\delta^{10}\Omega^4\right. \\
& \left. + 1139356288 55\delta^8\Omega^6 + 8184302249 38\delta^6\Omega^8 + 31972292185 28\delta^4\Omega^{10} + 6325080329472\delta^2\Omega^{12} + 48351975505 92\Omega^{14}\right) \\
& + 216\gamma^{17}\left(199192 32\delta^{14} + 18369550 80\delta^{12}\Omega^2 + 5355165066 88\delta^{10}\Omega^4 + 7046695173 15\delta^8\Omega^6 + 4812704327430\delta^6\Omega^8 + 174907393632 48\delta^4\Omega^{10}\right. \\
& \left. + 311471860400 64\delta^2\Omega^{12} + 204453643345 92\Omega^{14}\right) + \gamma\delta^4\Omega^{10}\left(32448\delta^{16} + 470486\delta^{14}\Omega^2 + 4055528\delta^{12}\Omega^4 + 26041786\delta^{10}\Omega^6 + 122463047\delta^8\Omega^8\right. \\
& \left. + 4252379 26\delta^6\Omega^{10} + 1033207176\delta^4\Omega^{12} + 145275955 2\delta^2\Omega^{14} + 759103488\Omega^{16}\right) - 4i\gamma^2\delta^3\Omega^{10}\left(78096\delta^{16} + 2310309\delta^{14}\Omega^2 + 25756066\delta^{12}\Omega^4\right. \\
& \left. + 1778413 29\delta^{10}\Omega^6 + 8704458 95\delta^8\Omega^8 + 3015927141\delta^6\Omega^{10} + 6633327312\delta^4\Omega^{12} + 7560622080\delta^2\Omega^{14} + 3100114944\Omega^{16}\right) \\
& - 24i\gamma^{12}\delta\Omega^2\left(584064\delta^{16} + 110701368\delta^{14}\Omega^2 + 5157576432\delta^{12}\Omega^4 + 975355932 32\delta^{10}\Omega^6 + 9440844179 55\delta^8\Omega^8 + 5191763937318\delta^6\Omega^{10}\right. \\
& \left. + 162716011287 84\delta^4\Omega^{12} + 263250156625 92\delta^2\Omega^{14} + 16580763058176\Omega^{16}\right) + 108\gamma^{15}\left(1905444\delta^{16} + 260120664\delta^{14}\Omega^2 + 10418466500\delta^{12}\Omega^4\right. \\
& \left. + 182229138454\delta^{10}\Omega^6 + 16709996628 93\delta^8\Omega^8 + 866681155912 8\delta^6\Omega^{10} + 250976272076 64\delta^4\Omega^{12} + 365959477463 04\delta^2\Omega^{14} + 200325136711 68\Omega^{16}\right) \\
& - 6i\gamma^4\delta\Omega^8\left(156208\delta^{18} + 7589704\delta^{16}\Omega^2 + 127798381\delta^{14}\Omega^4 + 1137508883\delta^{12}\Omega^6 + 6654642452\delta^{10}\Omega^8 + 267290411 20\delta^8\Omega^{10} + 692463067 20\delta^6\Omega^{12}\right. \\
& \left. + 100975993344\delta^4\Omega^{14} + 665091440 64\delta^2\Omega^{16} + 108716359 68\Omega^{18}\right) + \gamma^3\delta^2\Omega^8\left(227760\delta^{18} + 68253 36\delta^{16}\Omega^2 + 7926885 3\delta^{14}\Omega^4 + 614598700\delta^{12}\Omega^6\right. \\
& \left. + 3412378350\delta^{10}\Omega^8 + 136314025 94\delta^8\Omega^{10} + 380307256 68\delta^6\Omega^{12} + 663476544 00\delta^4\Omega^{14} + 585554780 16\delta^2\Omega^{16} + 188554936 32\Omega^{18}\right) \\
& - 2i\gamma^6\delta\Omega^6\left(644544\delta^{18} + 53644092\delta^{16}\Omega^2 + 1367522232\delta^{14}\Omega^4 + 166644533 08\delta^{12}\Omega^6 + 120654331143\delta^{10}\Omega^8 + 5733027775 86\delta^8\Omega^{10}\right. \\
& \left. + 17484927657 84\delta^6\Omega^{12} + 310580225510 4\delta^4\Omega^{14} + 27158665789 44\delta^2\Omega^{16} + 7949883801 60\Omega^{18}\right) \\
& - 6i\gamma^8\delta\Omega^4\left(130752\delta^{18} + 21156912\delta^{16}\Omega^2 + 866624832\delta^{14}\Omega^4 + 150661977 52\delta^{12}\Omega^6 + 14156362504 9\delta^{10}\Omega^8 + 817520721488\delta^8\Omega^{10}\right. \\
& \left. + 29674501579 92\delta^6\Omega^{12} + 633684831 0912\delta^4\Omega^{14} + 691965163 9296\delta^2\Omega^{16} + 280560402 4320\Omega^{18}\right) \\
& - 24i\gamma^{10}\delta\Omega^2\left(6912\delta^{18} + 2934252\delta^{16}\Omega^2 + 220900320\delta^{14}\Omega^4 + 5869958224\delta^{12}\Omega^6 + 753936054 91\delta^{10}\Omega^8 + 549505648630\delta^8\Omega^{10}\right. \\
& \left. + 24195400894 80\delta^6\Omega^{12} + 62227183620 96\delta^4\Omega^{14} + 829198732 4928\delta^2\Omega^{16} + 426344900 1984\Omega^{18}\right) \\
& + 3\gamma^{13}\left(1835136\delta^{18} + 414894096\delta^{16}\Omega^2 + 23907669984\delta^{14}\Omega^4 + 558141538344\delta^{12}\Omega^6 + 664587515719 7\delta^{10}\Omega^8 + 45767187850980\delta^8\Omega^{10}\right. \\
& \left. + 18877157621 6544\delta^6\Omega^{12} + 44796680847 7056\delta^4\Omega^{14} + 543559556800 512\delta^2\Omega^{16} + 250130544721920\Omega^{18}\right) \\
& + 3\gamma^5\Omega^6\left(191232\delta^{20} + 10655876\delta^{18}\Omega^2 + 191343892\delta^{16}\Omega^4 + 1886362799\delta^{14}\Omega^6 + 125909651 58\delta^{12}\Omega^8 + 587963062 73\delta^{10}\Omega^{10}\right. \\
& \left. + 18904723664 4\delta^8\Omega^{12} + 389168911680\delta^6\Omega^{14} + 446884047360\delta^4\Omega^{16} + 231393853440\delta^2\Omega^{18} + 32614907 904\Omega^{20}\right) \\
& + 2\gamma^7\Omega^4\left(323136\delta^{20} + 32911632\delta^{18}\Omega^2 + 965855613\delta^{16}\Omega^4 + 131454260 31\delta^{14}\Omega^6 + 109108825924\delta^{12}\Omega^8 + 607556848290\delta^{10}\Omega^{10}\right. \\
& \left. + 22805027137 14\delta^8\Omega^{12} + 54944652476 16\delta^6\Omega^{14} + 767710482163 2\delta^4\Omega^{16} + 52492882083 84\delta^2\Omega^{18} + 12414049320 96\Omega^{20}\right) \\
& + 3\gamma^9\Omega^2\left(110592\delta^{20} + 21904848\delta^{18}\Omega^2 + 1091077992\delta^{16}\Omega^4 + 221684112 59\delta^{14}\Omega^6 + 241639577320\delta^{12}\Omega^8 + 165203983104 8\delta^{10}\Omega^{10}\right. \\
& \left. + 7373031996248\delta^8\Omega^{12} + 209106118981 92\delta^6\Omega^{14} + 348138093669 12\delta^4\Omega^{16} + 29396938162176\delta^2\Omega^{18} + 9211800453120\Omega^{20}\right) \\
& + 6\gamma^{11}\left(10368\delta^{20} + 5186592\delta^{18}\Omega^2 + 479526030\delta^{16}\Omega^4 + 15536954520\delta^{14}\Omega^6 + 2385720081 49\delta^{12}\Omega^8 + 208955399135 5\delta^{10}\Omega^{10}\right. \\
& \left. + 11377149456 992\delta^8\Omega^{12} + 385009448242 08\delta^6\Omega^{14} + 762015015426 24\delta^4\Omega^{16} + 773927014072 32\delta^2\Omega^{18} + 29789100048384\Omega^{20}\right).
\end{aligned}
\tag{B.21}
$$

We pose $x = \frac{3\mathcal{N}}{\sqrt{2}\delta\Omega^3}\langle W_1|\rho_a^S|\psi_2\rangle$ and we have

$$
\begin{aligned}
x = {} & 8162933760000\gamma^{28} + 4081466880000i\gamma^{27}\delta + 11337408000\gamma^{26}\left(1109\delta^2 + 6864\Omega^2\right) + 5668704000i\gamma^{25}\left(1109\delta^3 + 7424\delta\Omega^2\right) \\
& + 5038848\gamma^{24}\left(1605243\delta^4 + 21641150\delta^2\Omega^2 + 63878400\Omega^4\right) + 2519424i\gamma^{23}\left(1605243\delta^5 + 23071900\delta^3\Omega^2 + 75680400\delta\Omega^4\right) \\
& + 69984\gamma^{22}\left(40904137\delta^6 + 911009196\delta^4\Omega^2 + 5689013040\delta^2\Omega^4 + 10915223040\Omega^6\right) \\
& + 34992i\gamma^{21}\left(40904137\delta^7 + 961303804\delta^5\Omega^2 + 6584332440\delta^3\Omega^4 + 13744333440\delta\Omega^6\right) \\
& + 7776\gamma^{20}\left(79140844\delta^8 + 2634940782\delta^6\Omega^2 + 26299699035\delta^4\Omega^4 + 1042668424480\delta^2\Omega^6 + 14912396006 4\Omega^8\right) \\
& + 3888i\gamma^{19}\left(79140844\delta^9 + 2760428169\delta^7\Omega^2 + 29936176395\delta^5\Omega^4 + 1285914182 40\delta^3\Omega^6 + 191408655744\delta\Omega^8\right) \\
& + 216\gamma^{18}\left(3861730 80\delta^{10} + 185169969 34\delta^8\Omega^2 + 2662810142 07\delta^6\Omega^4 + 1634847303888\delta^4\Omega^6 + 4745053528128\delta^2\Omega^8 + 549692257996 8\Omega^{10}\right) \\
& + 324i\gamma^{17}\left(128724360\delta^{11} + 6435575616\delta^9\Omega^2 + 999120451 19\delta^7\Omega^4 + 6640482441 12\delta^5\Omega^6 + 2018480961600\delta^3\Omega^8 + 228899278080 0\delta\Omega^{10}\right) \\
& - \delta^6\Omega^{10}\left(2624\delta^{12} + 148034\delta^{10}\Omega^2 + 1714930\delta^8\Omega^4 + 10479875\delta^6\Omega^6 + 42352570\delta^4\Omega^8 + 106268520\delta^2\Omega^{10} + 120837888\Omega^{12}\right) \\
& + 144\gamma^{16}\left(49493160\delta^{12} + 34235642 28\delta^{10}\Omega^2 + 6808030552 3\delta^8\Omega^4 + 5780612016 87\delta^6\Omega^6 + 2524145296572\delta^4\Omega^8 + 587176146144 0\delta^2\Omega^{10}\right. \\
& \qquad \left. + 584494150348 8\Omega^{12}\right) + 72i\gamma^{15}\left(49493160\delta^{13} + 3559834800\delta^{11}\Omega^2 + 761549720 53\delta^9\Omega^4 + 7017447216 48\delta^7\Omega^6 + 324935359470 0\delta^5\Omega^8\right. \\
& \qquad \left. + 749465203564 8\delta^3\Omega^{10} + 674159322470 4\delta\Omega^{12}\right) + 36\gamma^{14}\left(10264536\delta^{14} + 1067955432\delta^{12}\Omega^2 + 29296239318\delta^{10}\Omega^4 + 326820959891\delta^8\Omega^6\right. \\
& \qquad \left. + 1885968917894\delta^6\Omega^8 + 64566885341 76\delta^4\Omega^{10} + 129326236427 52\delta^2\Omega^{12} + 115711909724 16\Omega^{14}\right) + 24i\gamma^{13}\left(7698402\delta^{15} + 831965580\delta^{13}\Omega^2\right. \\
& \left. + 245355085 68\delta^{11}\Omega^4 + 299002499747\delta^9\Omega^6 + 186952582388 4\delta^7\Omega^8 + 65205936638 28\delta^5\Omega^{10} + 11891430964080\delta^3\Omega^{12} + 864664160256 0\delta\Omega^{14}\right) \\
& + 2i\gamma\delta^3\Omega^8\left(17472\delta^{16} + 186178\delta^{14}\Omega^2 + 1119675\delta^{12}\Omega^4 + 5434983\delta^{10}\Omega^6 + 18806972\delta^8\Omega^8 + 43220647\delta^6\Omega^{10} + 56242020\delta^4\Omega^{12} - 8361216\delta^2\Omega^{14}\right. \\
& \qquad \left. - 116785152\Omega^{16}\right) + \gamma^2\delta^2\Omega^8\left(16464\delta^{16} - 7246388\delta^{14}\Omega^2 - 20850131\delta^{12}\Omega^4 - 18838389 1\delta^{10}\Omega^6 - 95021184 3\delta^8\Omega^8 - 28374495 36\delta^6\Omega^{10}\right. \\
& \left. - 41756601 60\delta^4\Omega^{12} - 12226498 56\delta^2\Omega^{14} + 934281216\Omega^{16}\right) + 6\gamma^{12}\left(1752192\delta^{16} + 305314848\delta^{14}\Omega^2 + 119884017 12\delta^{12}\Omega^4 + 173190814706\delta^{10}\Omega^6\right. \\
& \qquad \left. + 12255029734 95\delta^8\Omega^8 + 52850911716 72\delta^6\Omega^{10} + 154731391644 96\delta^4\Omega^{12} + 28672736569344\delta^2\Omega^{14} + 2383192129536 0\Omega^{16}\right) \\
& + 3i\gamma^{11}\left(1752192\delta^{17} + 317207664\delta^{15}\Omega^2 + 13418879064\delta^{13}\Omega^4 + 214283429800\delta^{11}\Omega^6 + 170223364756 7\delta^9\Omega^8 + 791493903804 8\delta^7\Omega^{10}\right. \\
& \qquad \left. + 217732220757 12\delta^5\Omega^{12} + 319803332129 28\delta^3\Omega^{14} + 18611850608640\delta\Omega^{16}\right) \\
& + 2i\gamma^5\delta\Omega^4\left(201888\delta^{18} + 125571 48\delta^{16}\Omega^2 + 204962667\delta^{14}\Omega^4 + 1613985582\delta^{12}\Omega^6 + 8544533500\delta^{10}\Omega^8 + 310871898 69\delta^8\Omega^{10}\right. \\
& \left. + 745059857 94\delta^6\Omega^{12} + 1023754026 24\delta^4\Omega^{14} + 497636904 96\delta^2\Omega^{16} - 150334341 12\Omega^{18}\right) + i\gamma^3\delta\Omega^6\left(209568\delta^{18} + 5917368\delta^{16}\Omega^2 + 52501458\delta^{14}\Omega^4\right. \\
& \left. + 310292611\delta^{12}\Omega^6 + 1326482382\delta^{10}\Omega^8 + 3901894798\delta^8\Omega^{10} + 7400697180\delta^6\Omega^{12} + 6530889024\delta^4\Omega^{14} - 2559983616\delta^2\Omega^{16} - 407686348 8\Omega^{18}\right) \\
& + \gamma^4\Omega^6\left(286800\delta^{18} + 4387428\delta^{16}\Omega^2 - 36763203\delta^{14}\Omega^4 - 976728283\delta^{12}\Omega^6 - 7180826439\delta^{10}\Omega^8 - 26788521066\delta^8\Omega^{10} - 4679188012 8\delta^6\Omega^{12}\right. \\
& \left. - 13787698176\delta^4\Omega^{14} + 3772691251 2\delta^2\Omega^{16} + 163074539 52\Omega^{18}\right) + \gamma^6\Omega^4\left(703872\delta^{18} + 36543756\delta^{16}\Omega^2 + 3990109 44\delta^{14}\Omega^4 + 4154314 39\delta^{12}\Omega^6\right. \\
& \qquad \left. - 1460441089 8\delta^{10}\Omega^8 - 8967918519 0\delta^8\Omega^{10} - 1730419260 48\delta^6\Omega^{12} + 1135359521 28\delta^4\Omega^{14} + 671621455872\delta^2\Omega^{16} + 430109097984\Omega^{18}\right) \\
& + i\gamma^7\delta\Omega^2\left(279936\delta^{18} + 401290 56\delta^{16}\Omega^2 + 1277418720\delta^{14}\Omega^4 + 1564388679 3\delta^{12}\Omega^6 + 1072607222 48\delta^{10}\Omega^8 + 483851834649\delta^8\Omega^{10}\right. \\
& \qquad \left. + 142911808278 0\delta^6\Omega^{12} + 254794289112 0\delta^4\Omega^{14} + 223758302515 2\delta^2\Omega^{16} + 50271230361 6\Omega^{18}\right) \\
& + 6\gamma^8\Omega^2\left(89568\delta^{18} + 11780928\delta^{16}\Omega^2 + 324400602\delta^{14}\Omega^4 + 3055344816\delta^{12}\Omega^6 + 12539576381\delta^{10}\Omega^8 + 28204106722\delta^8\Omega^{10} + 97593389808\delta^6\Omega^{12}\right. \\
& \left. + 48394202630 4\delta^4\Omega^{14} + 11274033807 36\delta^2\Omega^{16} + 828463251456\Omega^{18}\right) + 6\gamma^{10}\left(20736\delta^{18} + 8065080\delta^{16}\Omega^2 + 502307016\delta^{14}\Omega^4 + 9603997624\delta^{12}\Omega^6\right. \\
& \left. + 794351703 89\delta^{10}\Omega^8 + 375786892549\delta^8\Omega^{10} + 1306682508816\delta^6\Omega^{12} + 373260939926 4\delta^4\Omega^{14} + 705125329920 0\delta^2\Omega^{16} + 5539188768768\Omega^{18}\right) \\
& + 6i\gamma^9\left(10368\delta^{19} + 41942880\delta^{17}\Omega^2 + 2827700 22\delta^{15}\Omega^4 + 6087309524\delta^{13}\Omega^6 + 598382435 92\delta^{11}\Omega^8 + 345612339207\delta^9\Omega^{10}\right. \\
& \qquad \left. + 126327969298 4\delta^7\Omega^{12} + 280135866230 4\delta^5\Omega^{14} + 328589650713 6\delta^3\Omega^{16} + 14213668700 16\delta\Omega^{18}\right).
\end{aligned}
\tag{B.22}
$$

We pose $x = \frac{3i\mathcal{N}}{\sqrt{2}\delta\Omega^4}\langle W_1|\rho_a^S|\psi_1\rangle$ and we have

$$
\begin{aligned}
x = {} & 8162933760000\gamma^{27} + 1360488960000i\gamma^{26}\delta + 11337408000\gamma^{25}\left(1109\delta^2 + 6624\Omega^2\right) + 1889568000i\gamma^{24}\left(1109\delta^3 + 11184\delta\Omega^2\right) \\
& + 15116544\gamma^{23}\left(535081\delta^4 + 6789800\delta^2\Omega^2 + 19636800\Omega^4\right) + 2519424i\gamma^{22}\left(535081\delta^5 + 10257550\delta^3\Omega^2 + 38530800\delta\Omega^4\right) \\
& + 69984\gamma^{21}\left(40904137\delta^6 + 838967364\delta^4\Omega^2 + 5056381440\delta^2\Omega^4 + 9501373440\Omega^6\right) \\
& + 11664i\gamma^{20}\left(40904137\delta^7 + 11511381720\delta^5\Omega^2 + 8674071840\delta^3\Omega^4 + 19300515840\delta\Omega^6\right) \\
& + 7776\gamma^{19}\left(79140844\delta^8 + 2379204603\delta^6\Omega^2 + 22568100543\delta^4\Omega^4 + 87493631760\delta^2\Omega^6 + 1206198397448\Omega^8\right) \\
& + 1296i\gamma^{18}\left(79140844\delta^9 + 3002957532\delta^7\Omega^2 + 34146352179\delta^5\Omega^4 + 154554365520\delta^3\Omega^6 + 241715332224\delta\Omega^8\right) \\
& + 648\gamma^{17}\left(1287243608\delta^{10} + 54732137868\delta^8\Omega^2 + 735963249216\delta^6\Omega^4 + 4407780993840\delta^4\Omega^6 + 12496106424960\delta^2\Omega^8 + 13498281676800\Omega^{10}\right) \\
& + 324i\gamma^{16}\left(429081208\delta^{11} + 21437896868\delta^9\Omega^2 + 330075751398\delta^7\Omega^4 + 2260424568720\delta^5\Omega^6 + 7272189907200\delta^3\Omega^8 + 8708453959680\delta\Omega^{10}\right) \\
& + 216\gamma^{15}\left(32995440\delta^{12} + 1990304382\delta^{10}\Omega^2 + 363780297678\delta^8\Omega^4 + 30050603545880\delta^6\Omega^6 + 1302610681296\delta^4\Omega^8 + 28937284594560\delta^2\Omega^{10}\right. \\
& \qquad \left. + 254679950131200\Omega^{12}\right) + 216i\gamma^{14}\left(54992408\delta^{13} + 3672190758\delta^{11}\Omega^2 + 73312606169\delta^9\Omega^4 + 671681474728\delta^7\Omega^6 + 3283975831440\delta^5\Omega^8\right. \\
& \qquad \left. + 8199977466240\delta^3\Omega^{10} + 786959788032\delta\Omega^{12}\right) \\
& + 4i\delta^5\Omega^8\left(12488\delta^{14} + 140318\delta^{12}\Omega^2 + 783718\delta^{10}\Omega^4 + 3035348\delta^8\Omega^6 + 10325406\delta^6\Omega^8 + 38002184\delta^4\Omega^{10} + 97264562\delta^2\Omega^{12} + 100869120\Omega^{14}\right) \\
& + 9\gamma\delta^4\Omega^8\left(14728\delta^{14} + 272788\delta^{12}\Omega^2 + 2332168\delta^{10}\Omega^4 + 12935808\delta^8\Omega^6 + 54527256\delta^6\Omega^8 + 169101728\delta^4\Omega^{10} + 308463368\delta^2\Omega^{12} + 216023040\Omega^{14}\right) \\
& + 108\gamma^{13}\left(34215128\delta^{14} + 3057244448\delta^{12}\Omega^2 + 75671663178\delta^{10}\Omega^4 + 819922568588\delta^8\Omega^6 + 4808120989126\delta^6\Omega^8 + 16271242908008\delta^4\Omega^{10}\right. \\
& \qquad \left. + 29459600962568\delta^2\Omega^{12} + 2159197323264\Omega^{14}\right) + 6i\gamma^{12}\left(1026453688\delta^{15} + 9680067008\delta^{13}\Omega^2 + 250293781988\delta^{11}\Omega^4 + 2898344778078\delta^9\Omega^6\right. \\
& \qquad \left. + 18760473391268\delta^7\Omega^8 + 71908806530888\delta^5\Omega^{10} + 146421472435208\delta^3\Omega^{12} + 114852556800008\delta\Omega^{14}\right) + 9\gamma^3\delta^2\Omega^6\left(194408\delta^{16} + 4370848\delta^{14}\Omega^2\right. \\
& \qquad \left. + 47544018\delta^{12}\Omega^4 + 321612378\delta^{10}\Omega^6 + 1527124758\delta^8\Omega^8 + 5253309708\delta^6\Omega^{10} + 11729162888\delta^4\Omega^{12} + 13476648968\delta^2\Omega^{14} + 5662310408\Omega^{16}\right) \\
& + i\gamma^2\delta^3\Omega^6\left(310088\delta^{16} + 8693768\delta^{14}\Omega^2 + 76809548\delta^{12}\Omega^4 + 406708158\delta^{10}\Omega^6 + 1633278848\delta^8\Omega^8 + 6153992848\delta^6\Omega^{10} + 18589756808\delta^4\Omega^{12}\right. \\
& \qquad \left. + 30466045448\delta^2\Omega^{14} + 17411604488\Omega^{16}\right) + 108\gamma^{11}\left(973448\delta^{16} + 143709728\delta^{14}\Omega^2 + 4989282908\delta^{12}\Omega^4 + 69992023768\delta^{10}\Omega^6 + 522883322038\delta^8\Omega^8\right. \\
& \qquad \left. + 2371420229688\delta^6\Omega^{10} + 6540855413048\delta^4\Omega^{12} + 9839629578248\delta^2\Omega^{14} + 6042631864328\Omega^{16}\right) \\
& + 3i\gamma^{10}\left(5840648\delta^{17} + 877865048\delta^{15}\Omega^2 + 30640456568\delta^{13}\Omega^4 + 444503554208\delta^{11}\Omega^6 + 3532341963938\delta^9\Omega^8 + 17786230716168\delta^7\Omega^{10}\right. \\
& \qquad \left. + 56631166812968\delta^5\Omega^{12} + 96337341480968\delta^3\Omega^{14} + 61562523156488\delta\Omega^{16}\right) \\
& + 9\gamma^5\Omega^4\left(532808\delta^{18} + 26202608\delta^{16}\Omega^2 + 387040148\delta^{14}\Omega^4 + 3283164088\delta^{12}\Omega^6 + 18367313758\delta^{10}\Omega^8 + 71954237948\delta^8\Omega^{10} + 189448371848\delta^6\Omega^{12}\right. \\
& \qquad \left. + 292828884488\delta^4\Omega^{14} + 219166801928\delta^2\Omega^{16} + 54358179848\Omega^{18}\right) + i\gamma^4\delta\Omega^4\left(731528\delta^{18} + 38868488\delta^{16}\Omega^2 + 620346548\delta^{14}\Omega^4 + 4690568738\delta^{12}\Omega^6\right. \\
& \qquad \left. + 23574308818\delta^{10}\Omega^8 + 97190161268\delta^8\Omega^{10} + 323024366888\delta^6\Omega^{12} + 656926444808\delta^4\Omega^{14} + 589172244488\delta^2\Omega^{16} + 122305904648\Omega^{18}\right) \\
& + 12i\gamma^6\delta\Omega^2\left(60488\delta^{18} + 6435368\delta^{16}\Omega^2 + 176151568\delta^{14}\Omega^4 + 2083141008\delta^{12}\Omega^6 + 13887694688\delta^{10}\Omega^8 + 66580135568\delta^8\Omega^{10} + 244918358658\delta^6\Omega^{12}\right. \\
& \qquad \left. + 581571612488\delta^4\Omega^{14} + 678645043208\delta^2\Omega^{16} + 248433868808\Omega^{18}\right) + 9\gamma^7\Omega^2\left(495368\delta^{18} + 55110008\delta^{16}\Omega^2 + 1461297128\delta^{14}\Omega^4 + 16840706218\delta^{12}\Omega^6\right. \\
& \qquad \left. + 116852795198\delta^{10}\Omega^8 + 540065656868\delta^8\Omega^{10} + 1672456451048\delta^6\Omega^{12} + 3195479589128\delta^4\Omega^{14} + 3228837396488\delta^2\Omega^{16} + 1270622453768\Omega^{18}\right) \\
& + 9\gamma^9\left(138248\delta^{18} + 45034568\delta^{16}\Omega^2 + 2425743248\delta^{14}\Omega^4 + 44987622608\delta^{12}\Omega^6 + 417642375478\delta^{10}\Omega^8 + 2376073250948\delta^8\Omega^{10}\right. \\
& \qquad \left. + 8776920388088\delta^6\Omega^{12} + 20143416458888\delta^4\Omega^{14} + 25181878026248\delta^2\Omega^{16} + 12757397667848\Omega^{18}\right) \\
& + 3i\gamma^8\left(69128\delta^{19} + 22354568\delta^{17}\Omega^2 + 1174924088\delta^{15}\Omega^4 + 22205490708\delta^{13}\Omega^6 + 212016508558\delta^{11}\Omega^8 + 1259402603078\delta^9\Omega^{10}\right. \\
& \qquad \left. + 5288890642768\delta^7\Omega^{12} + 14460525687368\delta^5\Omega^{14} + 20600860631048\delta^3\Omega^{16} + 10391914414088\delta\Omega^{18}\right).
\end{aligned}
\tag{B.23}
$$

We pose $x = \frac{\sqrt{3}\mathcal{N}}{\sqrt{2}\delta\Omega^2}\langle g|\rho_a^S|\psi_2\rangle$ and we have

$$
\begin{aligned}
x = {} & 2720977920000i\gamma^{29} - 1360488960000\gamma^{28}\delta + 3779136000i\gamma^{27}\left(1109\delta^2 + 6624\Omega^2\right) - 1889568000\gamma^{26}\left(1109\delta^3 + 7344\delta\Omega^2\right) \\
& + 5038848i\gamma^{25}\left(535081\delta^4 + 6869800\delta^2\Omega^2 + 19636800\Omega^4\right) - 2519424\gamma^{24}\left(535081\delta^5 + 7491550\delta^3\Omega^2 + 24694800\delta\Omega^4\right) \\
& + 23328i\gamma^{23}\left(40904137\delta^6 + 858623364\delta^4\Omega^2 + 5050387440\delta^2\Omega^4 + 9501373440\Omega^6\right) \\
& - 11664\gamma^{22}\left(40904137\delta^7 + 924493860\delta^5\Omega^2 + 6207375240\delta^3\Omega^4 + 13079370240\delta\Omega^6\right) \\
& + 2592i\gamma^{21}\left(79140844\delta^8 + 2463944931\delta^6\Omega^2 + 22572157743\delta^4\Omega^4 + 83893754160\delta^2\Omega^6 + 120619839744\Omega^8\right) \\
& - 1296\gamma^{20}\left(79140844\delta^9 + 2626388928\delta^7\Omega^2 + 27225077463\delta^5\Omega^4 + 114350771520\delta^3\Omega^6 + 171969899904\delta\Omega^8\right) \\
& + 216i\gamma^{19}\left(1287243608\delta^{10} + 57404352268\delta^8\Omega^2 + 739933563696\delta^6\Omega^4 + 4042609213328\delta^4\Omega^6 + 11013412527368\delta^2\Omega^8 + 13498281676800\Omega^{10}\right) \\
& - 108\gamma^{18}\left(1287243608\delta^{11} + 60691821928\delta^9\Omega^2 + 877743850958\delta^7\Omega^4 + 5478506393408\delta^5\Omega^6 + 16154246914568\delta^3\Omega^8 + 18488580065288\delta\Omega^{10}\right) \\
& + 216i\gamma^{17}\left(109984808\delta^{12} + 7054446728\delta^{10}\Omega^2 + 123223627908\delta^8\Omega^4 + 877061521318\delta^6\Omega^6 + 3219216239528\delta^4\Omega^8 + 7187611754888\delta^2\Omega^{10}\right. \\
& \qquad \left. + 8489331671048\Omega^{12}\right) - 108\gamma^{16}\left(109984808\delta^{13} + 7408198328\delta^{11}\Omega^2 + 143874341248\delta^9\Omega^4 + 1181704929838\delta^7\Omega^6 + 4973607066248\delta^5\Omega^8\right. \\
& \qquad \left. + 10908053832968\delta^3\Omega^{10} + 9837198213128\delta\Omega^{12}\right) \\
& + 3i\gamma\delta^4\Omega^{10}\left(3968\delta^{14} + 6476\delta^{12}\Omega^2 - 188758\delta^{10}\Omega^4 - 1591643\delta^8\Omega^6 - 10126681\delta^6\Omega^8 - 41767036\delta^4\Omega^{10} - 78411648\delta^2\Omega^{12} - 38854656\Omega^{14}\right) \\
& + 4\delta^5\Omega^{10}\left(1248\delta^{14} + 14031\delta^{12}\Omega^2 + 78371\delta^{10}\Omega^4 + 303534\delta^8\Omega^6 + 1032540\delta^6\Omega^8 + 3800218\delta^4\Omega^{10} + 9726456\delta^2\Omega^{12} + 10086912\Omega^{14}\right) \\
& + 36i\gamma^{15}\left(3421512\delta^{14} + 32990671\delta^{12}\Omega^2 + 78282137\delta^{10}\Omega^4 + 68653498967\delta^8\Omega^6 + 275589161934\delta^6\Omega^8 + 670273677696\delta^4\Omega^{10}\right. \\
& \qquad \left. + 1505327572224\delta^2\Omega^{12} + 2159197323264\Omega^{14}\right) - 216\gamma^{14}\left(285126\delta^{15} + 28705996\delta^{13}\Omega^2 + 749421446\delta^{11}\Omega^4 + 7613016971\delta^9\Omega^6\right. \\
& \qquad \left. + 38664342699\delta^7\Omega^8 + 112856505460\delta^5\Omega^{10} + 181125883344\delta^3\Omega^{12} + 126444128256\delta\Omega^{14}\right) + 3i\gamma^5\delta^2\Omega^6\left(21264\delta^{16} + 247008\delta^{14}\Omega^2\right. \\
& \left. - 8888235\delta^{12}\Omega^4 - 224278137\delta^{10}\Omega^6 - 1903283746\delta^8\Omega^8 - 9711092644\delta^6\Omega^{10} - 27203724864\delta^4\Omega^{12} - 32780291328\delta^2\Omega^{14} - 10469965824\Omega^{16}\right) \\
& + 6i\gamma^3\delta^2\Omega^8\left(3328\delta^{16} + 81261\delta^{14}\Omega^2 - 1057681\delta^{12}\Omega^4 - 15011731\delta^{10}\Omega^6 - 105603927\delta^8\Omega^8 - 484775523\delta^6\Omega^{10} - 1143864864\delta^4\Omega^{12}\right. \\
& \qquad \left. - 986918400\delta^2\Omega^{14} - 155713536\Omega^{16}\right) + 2\gamma^2\delta^3\Omega^8\left(8016\delta^{16} + 384102\delta^{14}\Omega^2 + 3732969\delta^{12}\Omega^4 + 20638472\delta^{10}\Omega^6 + 84616656\delta^8\Omega^8\right. \\
& \left. + 300165313\delta^6\Omega^{10} + 826351044\delta^4\Omega^{12} + 1284762240\delta^2\Omega^{14} + 753795072\Omega^{16}\right) + 18i\gamma^{13}\left(194688\delta^{16} + 31493040\delta^{14}\Omega^2 + 1059797232\delta^{12}\Omega^4\right. \\
& \qquad \left. + 11317458168\delta^{10}\Omega^6 + 39313835929\delta^8\Omega^8 - 152562392808\delta^6\Omega^{10} - 2516978372648\delta^4\Omega^{12} + 2016505681928\delta^2\Omega^{14} + 120852637286 4\Omega^{16}\right) \\
& - 3\gamma^{12}\left(584064\delta^{17} + 98164512\delta^{15}\Omega^2 + 3589427376\delta^{13}\Omega^4 + 43866268464\delta^{11}\Omega^6 + 228347177599\delta^9\Omega^8 + 606155016324\delta^7\Omega^{10}\right. \\
& \left. + 665189517312\delta^5\Omega^{12} - 269403515136\delta^3\Omega^{14} - 67113241804 8\delta\Omega^{16}\right) - 3\gamma^8\delta\Omega^2\left(28800\delta^{18} + 3429504\delta^{16}\Omega^2 + 64908444\delta^{14}\Omega^4 - 620720596\delta^{12}\Omega^6\right. \\
& \qquad \left. - 6375576740\delta^{10}\Omega^8 - 50672515702\delta^8\Omega^{10} - 221822190248\delta^6\Omega^{12} - 578592408432\delta^4\Omega^{14} - 778622303232\delta^2\Omega^{16} - 377120489472\Omega^{18}\right) \\
& + 2\gamma^4\delta\Omega^6\left(-9936\delta^{18} + 766632\delta^{16}\Omega^2 + 23051820\delta^{14}\Omega^4 + 201037587\delta^{12}\Omega^6 + 1069910686\delta^{10}\Omega^8 + 4255487244\delta^8\Omega^{10} + 12623689926\delta^6\Omega^{12}\right. \\
& \left. + 23299093728\delta^4\Omega^{14} + 20279697408\delta^2\Omega^{16} + 4076863488\Omega^{18}\right) + 3i\gamma^7\Omega^4\left(63936\delta^{18} + 2400252\delta^{16}\Omega^2 - 2007840\delta^{14}\Omega^4 - 659230028\delta^{12}\Omega^6\right. \\
& \qquad \left. - 8373953045\delta^{10}\Omega^8 - 516101261728\delta^8\Omega^{10} - 1723011638888\delta^6\Omega^{12} - 2656995436808\delta^4\Omega^{14} - 1243098316808\delta^2\Omega^{16} + 54358179848\Omega^{18}\right) \\
& + 3\gamma^6\delta\Omega^4\left(-33984\delta^{18} - 1045848\delta^{16}\Omega^2 + 16296422\delta^{14}\Omega^4 + 4521335398\delta^{12}\Omega^6 + 36459493168\delta^{10}\Omega^8 + 180389795728\delta^8\Omega^{10} + 614839300488\delta^6\Omega^{12}\right. \\
& \left. + 1320678416648\delta^4\Omega^{14} + 1449271664648\delta^2\Omega^{16} + 513005322248\Omega^{18}\right) + 3i\gamma^9\Omega^2\left(55872\delta^{18} + 6320880\delta^{16}\Omega^2 + 120795432\delta^{14}\Omega^4 - 40429246\delta^{12}\Omega^6\right. \\
& \qquad \left. - 152967772978\delta^{10}\Omega^8 - 1433414203028\delta^8\Omega^{10} - 6098797324088\delta^6\Omega^{12} - 11746576955528\delta^4\Omega^{14} - 6881463336968\delta^2\Omega^{16} + 1270622453768\Omega^{18}\right) \\
& + 18i\gamma^{11}\left(2304\delta^{18} + 834840\delta^{16}\Omega^2 + 44467188\delta^{14}\Omega^4 + 599288904\delta^{12}\Omega^6 + 11327845688\delta^{10}\Omega^8 - 241263408638\delta^8\Omega^{10} - 1780125563368\delta^6\Omega^{12}\right. \\
& \left. - 4489755335528\delta^4\Omega^{14} - 2699514408968\delta^2\Omega^{16} + 212623294464\Omega^{18}\right) - 3\gamma^{10}\left(6912\delta^{19} + 2591136\delta^{17}\Omega^2 + 147761604\delta^{15}\Omega^4 + 2181085320\delta^{13}\Omega^6\right. \\
& \left. + 8386460338\delta^{11}\Omega^8 - 195160841378\delta^9\Omega^{10} - 2823304561848\delta^7\Omega^{12} - 11179752444968\delta^5\Omega^{14} - 19852961172488\delta^3\Omega^{16} - 1243623849984\delta\Omega^{18}\right).
\end{aligned}
\tag{B.24}
$$

We pose $x = \frac{\sqrt{3}\mathcal{N}}{\sqrt{2}\delta\Omega^2}\langle g|\rho_a^S|\psi_1\rangle$ and we have

$$
\begin{aligned}
x = {} & 2720977920000\gamma^{28} + 1360488960000i\gamma^{27}\delta + 3779136000\gamma^{26}\left(1109\delta^2 + 7344\Omega^2\right) + 1889568000i\gamma^{25}\left(1109\delta^3 + 9504\delta\Omega^2\right) \\
& + 5038848\gamma^{24}\left(535081\delta^4 + 7041550\delta^2\Omega^2 + 24604800\Omega^4\right) + 2519424i\gamma^{23}\left(535081\delta^5 + 9066800\delta^3\Omega^2 + 32758800\delta\Omega^4\right) \\
& + 23328\gamma^{22}\left(40904137\delta^6 + 822298860\delta^4\Omega^2 + 5559672240\delta^2\Omega^4 + 13742922240\Omega^6\right) \\
& + 11664i\gamma^{21}\left(40904137\delta^7 + 1056342348\delta^5\Omega^2 + 7701209640\delta^3\Omega^4 + 16751456640\delta\Omega^6\right) \\
& + 2592\gamma^{20}\left(79140844\delta^8 + 2223903708\delta^6\Omega^2 + 21759257619\delta^4\Omega^4 + 104715562320\delta^2\Omega^6 + 20613220704\Omega^8\right) \\
& + 1296i\gamma^{19}\left(79140844\delta^9 + 2855192355\delta^7\Omega^2 + 31746478347\delta^5\Omega^4 + 140162391360\delta^3\Omega^6 + 21108846758 4\delta\Omega^8\right) \\
& + 216\gamma^{18}\left(1287243 60\delta^{10} + 49226196 86\delta^8\Omega^2 + 621087258 69\delta^6\Omega^4 + 4188103103 52\delta^4\Omega^6 + 167872654137 6\delta^2\Omega^8 + 279726624460 8\Omega^{10}\right) \\
& + 108i\gamma^{17}\left(1287243 60\delta^{11} + 6320616808\delta^9\Omega^2 + 9666762043 5\delta^7\Omega^4 + 6469866639 36\delta^5\Omega^6 + 1983602948544\delta^3\Omega^8 + 2209771279872\delta\Omega^{10}\right) \\
& - \delta^6\Omega^{10}\left(3904\delta^{12} + 95578\delta^{10}\Omega^2 + 1022588\delta^8\Omega^4 + 7031671\delta^6\Omega^6 + 31020602\delta^4\Omega^8 + 75508296\delta^2\Omega^{10} + 76250880\Omega^{12}\right) + 432\gamma^{16}\left(5499240\delta^{12}\right. \\
& \qquad \left. + 289737750\delta^{10}\Omega^2 + 44838972 27\delta^8\Omega^4 + 351646748 05\delta^6\Omega^6 + 2027263997 16\delta^4\Omega^8 + 753885953856\delta^2\Omega^{10} + 10993806673 92\Omega^{12}\right) \\
& + 216i\gamma^{15}\left(5499240\delta^{13} + 3719138 12\delta^{11}\Omega^2 + 752637985 5\delta^9\Omega^4 + 6793027088 6\delta^7\Omega^6 + 3142148229 00\delta^5\Omega^8 + 712179891072\delta^3\Omega^{10}\right. \\
& \qquad \left. + 598998053376\delta\Omega^{12}\right) + 108\gamma^{14}\left(1140504\delta^{14} + 87274480\delta^{12}\Omega^2 + 1647551580\delta^{10}\Omega^4 + 125385804 69\delta^8\Omega^6 + 739341379 34\delta^6\Omega^8\right. \\
& \qquad \left. + 491286201856\delta^4\Omega^{10} + 1863960585600\delta^2\Omega^{12} + 241759877 75296\Omega^{14}\right) + 24i\gamma^{13}\left(2566134\delta^{15} + 251638128\delta^{13}\Omega^2 + 67513072 47\delta^{11}\Omega^4\right. \\
& \qquad \left. + 780488907 14\delta^9\Omega^6 + 4784362690 71\delta^7\Omega^8 + 162944067 6612\delta^5\Omega^{10} + 275786065 1376\delta^3\Omega^{12} + 167044338 8928\delta\Omega^{14}\right) \\
& - \gamma^2\delta^2\Omega^8\left(32784\delta^{16} + 1162494\delta^{14}\Omega^2 + 17435333\delta^{12}\Omega^4 + 149468889\delta^{10}\Omega^6 + 793059049\delta^8\Omega^8 + 23719848 24\delta^6\Omega^{10} + 3240132480\delta^4\Omega^{12}\right. \\
& \qquad \left. + 710387712\delta^2\Omega^{14} - 934281216\Omega^{16}\right) \\
& + i\gamma\delta^3\Omega^8\left(4992\delta^{16} + 66460\delta^{14}\Omega^2 + 438160\delta^{12}\Omega^4 + 1943441\delta^{10}\Omega^6 + 5000704\delta^8\Omega^8 - 4425298\delta^6\Omega^{10} - 856841 52\delta^4\Omega^{12} - 248744448\delta^2\Omega^{14}\right. \\
& \left. - 233570304\Omega^{16}\right) + 6\gamma^{12}\left(584064\delta^{16} + 73090800\delta^{14}\Omega^2 + 1756008000\delta^{12}\Omega^4 + 9698443130\delta^{10}\Omega^6 - 21464959629\delta^8\Omega^8 + 403391090 16\delta^6\Omega^{10}\right. \\
& \qquad \left. + 331851175 2432\delta^4\Omega^{12} + 143343773798 40\delta^2\Omega^{14} + 165807630581 76\Omega^{16}\right) + 3i\gamma^{11}\left(584064\delta^{17} + 93306960\delta^{15}\Omega^2 + 34637037 84\delta^{13}\Omega^4\right. \\
& \left. + 508686546 76\delta^{11}\Omega^6 + 3865890179 05\delta^9\Omega^8 + 172646411 9240\delta^7\Omega^{10} + 433658712 5472\delta^5\Omega^{12} + 502616386 4832\delta^3\Omega^{14} + 146839545 4464\delta\Omega^{16}\right) \\
& + i\gamma^7\delta\Omega^2\left(79488\delta^{18} + 9414720\delta^{16}\Omega^2 + 262338276\delta^{14}\Omega^4 + 29721342 81\delta^{12}\Omega^6 + 1909063861 9\delta^{10}\Omega^8 + 75898754439\delta^8\Omega^{10} + 1571363880 36\delta^6\Omega^{12}\right. \\
& \qquad \left. + 157501491 616\delta^4\Omega^{14} - 5026471925 76\delta^2\Omega^{16} - 5593106350 08\Omega^{18}\right) + 3i\gamma^5\delta\Omega^4\left(30528\delta^{18} + 1625656\delta^{16}\Omega^2 + 242902 70\delta^{14}\Omega^4\right. \\
& \left. + 185267431\delta^{12}\Omega^6 + 883063692\delta^{10}\Omega^8 + 2365310944\delta^8\Omega^{10} + 5682404 28\delta^6\Omega^{12} - 1626775756 8\delta^4\Omega^{14} - 393247825 92\delta^2\Omega^{16} - 2632974336 0\Omega^{18}\right) \\
& - 3\gamma^4\Omega^6\left(10192\delta^{18} + 1466500\delta^{16}\Omega^2 + 34387615\delta^{14}\Omega^4 + 393582107\delta^{12}\Omega^6 + 2578417319\delta^{10}\Omega^8 + 9350238370\delta^8\Omega^{10} + 1560671596 8\delta^6\Omega^{12}\right. \\
& \qquad \left. + 39530649 60\delta^4\Omega^{14} - 1240576819 2\delta^2\Omega^{16} - 543581784\Omega^{18}\right) + i\gamma^3\delta\Omega^6\left(38496\delta^{18} + 971184\delta^{16}\Omega^2 + 9116862\delta^{14}\Omega^4 + 51861599\delta^{12}\Omega^6\right. \\
& \qquad \left. + 184919259\delta^{10}\Omega^8 + 225289066\delta^8\Omega^{10} - 1323878916\delta^6\Omega^{12} - 6445893312\delta^4\Omega^{14} - 977942937 6\delta^2\Omega^{16} - 4076863488\Omega^{18}\right) \\
& + \gamma^6\Omega^4\left(81216\delta^{18} - 2614308\delta^{16}\Omega^2 - 237128676\delta^{14}\Omega^4 - 4247037307\delta^{12}\Omega^6 - 3680743849 8\delta^{10}\Omega^8 - 1651691986 62\delta^8\Omega^{10} - 3266285192 64\delta^6\Omega^{12}\right. \\
& \left. - 454640060160\delta^4\Omega^{14} + 5756771450 88\delta^2\Omega^{16} + 397494190080\Omega^{18}\right) + 6\gamma^8\Omega^2\left(21024\delta^{18} + 1422936\delta^{16}\Omega^2 - 11747934\delta^{14}\Omega^4 - 1057964615\delta^{12}\Omega^6\right. \\
& \qquad \left. - 145914695 51\delta^{10}\Omega^8 - 863370142 60\delta^8\Omega^{10} - 2000948013 60\delta^6\Omega^{12} + 5743030521 6\delta^4\Omega^{14} + 805002043392\delta^2\Omega^{16} + 7014010060 80\Omega^{18}\right) \\
& + 6\gamma^{10}\left(6912\delta^{18} + 1904904\delta^{16}\Omega^2 + 65600532\delta^{14}\Omega^4 + 566125 84\delta^{12}\Omega^6 - 1329109660 4\delta^{10}\Omega^8 - 1308356399 63\delta^8\Omega^{10} - 3448826608 32\delta^6\Omega^{12}\right. \\
& \left. + 709280114976\delta^4\Omega^{14} + 417992887296 0\delta^2\Omega^{16} + 426344900 1984\Omega^{18}\right) + 6i\gamma^9\left(3456\delta^{19} + 1208592\delta^{17}\Omega^2 + 69215814\delta^{15}\Omega^4 + 1334677652\delta^{13}\Omega^6\right. \\
& \qquad \left. + 122887601 83\delta^{11}\Omega^8 + 668028275 30\delta^9\Omega^{10} + 217863911576\delta^7\Omega^{12} + 35467485772 8\delta^5\Omega^{14} + 111274184448\delta^3\Omega^{16} - 22079161958 4\delta\Omega^{18}\right).
\end{aligned}
\tag{B.25}
$$

We pose $x = \frac{3i\mathcal{N}}{\Omega^5}\langle g|\psi_2|\psi_1\rangle$ and we have

$$
\begin{aligned}
x = {} & 163258675200000\gamma^{27} - 5441955840000i\gamma^{26}\delta + 68024448000\gamma^{25}\left(323\delta^2 + 2208\Omega^2\right) - 57946752000i\gamma^{24}\left(109\delta^3 + 864\delta\Omega^2\right) \\
& + 5038848\gamma^{23}\left(2510111\delta^4 + 36802800\delta^2\Omega^2 + 117820800\Omega^4\right) - 5038848i\gamma^{22}\left(617537\delta^5 + 10377600\delta^3\Omega^2 + 39273600\delta\Omega^4\right) \\
& + 139968\gamma^{21}\left(29122235\delta^6 + 694936764\delta^4\Omega^2 + 4694109840\delta^2\Omega^4 + 9501373440\Omega^6\right) \\
& - 46656i\gamma^{20}\left(18238995\delta^7 + 492416864\delta^5\Omega^2 + 3960727440\delta^3\Omega^4 + 9501373440\delta\Omega^6\right) \\
& + 3888\gamma^{19}\left(207960905\delta^8 + 7282133928\delta^6\Omega^2 + 784586677324\delta^4\Omega^4 + 3332235801600\delta^2\Omega^6 + 482479358976\Omega^8\right) \\
& - 432i\gamma^{18}\left(32819549 5\delta^9 + 1283110212 0\delta^7\Omega^2 + 166904520 5160\delta^5\Omega^4 + 851391941760\delta^3\Omega^6 + 144743807692 8\delta\Omega^8\right) \\
& + 1296\gamma^{17}\left(78825621\delta^{10} + 3866512517\delta^8\Omega^2 + 596300524266\delta^6\Omega^4 + 401121464400\delta^4\Omega^6 + 122100509376 0\delta^2\Omega^8 + 134982816768 0\Omega^{10}\right) \\
& - 144i\gamma^{16}\left(10312086 3\delta^{11} + 558215646 2\delta^9\Omega^2 + 106223268441 4\delta^7\Omega^4 + 881150044896\delta^5\Omega^6 + 318537835891 2\delta^3\Omega^8 + 404948450304 0\delta\Omega^{10}\right) \\
& + 36\gamma^{15}\left(227893716\delta^{12} + 15397662800\delta^{10}\Omega^2 + 3228359719 47\delta^8\Omega^4 + 3081782155608\delta^6\Omega^6 + 14909126639040\delta^4\Omega^8 + 349209616988 16\delta^2\Omega^{10}\right. \\
& \qquad \left. + 305615940157 44\Omega^{12}\right) - 36i\gamma^{14}\left(26987772\delta^{13} + 1998677376\delta^{11}\Omega^2 + 532653342 67\delta^9\Omega^4 + 6543695323 84\delta^7\Omega^6 + 38643710741 76\delta^5\Omega^8\right. \\
& \qquad \left. + 104706479232 00\delta^3\Omega^{10} + 101871980052 48\delta\Omega^{12}\right) \\
& + 2i\delta^5\Omega^8\left(4544\delta^{14} + 36254\delta^{12}\Omega^2 - 4385\delta^{10}\Omega^4 - 1658371\delta^8\Omega^6 - 16229981\delta^6\Omega^8 - 8450336 4\delta^4\Omega^{10} - 2232276 48\delta^2\Omega^{12} - 233570304\Omega^{14}\right) \\
& + 12\gamma^{13}\left(33566724\delta^{14} + 3136060128\delta^{12}\Omega^2 + 875740970 77\delta^{10}\Omega^4 + 1128803547522\delta^8\Omega^6 + 779209425709 2\delta^6\Omega^8 + 293970082386 24\delta^4\Omega^{10}\right. \\
& \qquad \left. + 5520601831 2192\delta^2\Omega^{12} + 388655518187 52\Omega^{14}\right) - 12i\gamma^{12}\left(3168108\delta^{15} + 326245920\delta^{13}\Omega^2 + 11996806031\delta^{11}\Omega^4 + 2109503174 58\delta^9\Omega^6\right. \\
& \qquad \left. + 186317668947 6\delta^7\Omega^8 + 829994765961 6\delta^5\Omega^{10} + 173799186001 92\delta^3\Omega^{12} + 12955183939584\delta\Omega^{14}\right) + i\gamma^2\delta^3\Omega^6\left(25248\delta^{16} + 703104\delta^{14}\Omega^2\right. \\
& \qquad \left. - 94394\delta^{12}\Omega^4 - 712198 39\delta^{10}\Omega^6 - 779854896\delta^8\Omega^8 - 4541437572\delta^6\Omega^{10} - 1438918041 6\delta^4\Omega^{12} - 216038154 24\delta^2\Omega^{14} - 100222894 08\Omega^{16}\right) \\
& - 2\gamma\delta^4\Omega^6\left(4992\delta^{16} + 35084\delta^{14}\Omega^2 + 145440\delta^{12}\Omega^4 + 948531\delta^{10}\Omega^6 + 2923633\delta^8\Omega^8 - 1230438 1\delta^6\Omega^{10} - 124445316\delta^4\Omega^{12} - 36293760 0\delta^2\Omega^{14}\right. \\
& \qquad \left. - 379551744\Omega^{16}\right) + 12\gamma^{11}\left(911088\delta^{16} + 119591088\delta^{14}\Omega^2 + 4473642775\delta^{12}\Omega^4 + 780270830 54\delta^{10}\Omega^6 + 737678631992\delta^8\Omega^8\right. \\
& \qquad \left. + 4051912843056\delta^6\Omega^{10} + 125379813034 08\delta^4\Omega^{12} + 192843678597 12\delta^2\Omega^{14} + 1087673735576 0\Omega^{16}\right) \\
& - 12i\gamma^{10}\left(66816\delta^{17} + 10114080\delta^{15}\Omega^2 + 515920063\delta^{13}\Omega^4 + 1305132488 3\delta^{11}\Omega^6 + 168277908718\delta^9\Omega^8 + 112944898836 0\delta^7\Omega^{10}\right. \\
& \qquad \left. + 3941232978096\delta^5\Omega^{12} + 648159440486 4\delta^3\Omega^{14} + 362557911859 2\delta\Omega^{16}\right) \\
& + i\gamma^4\delta\Omega^4\left(15936\delta^{18} + 1123128\delta^{16}\Omega^2 - 7080042\delta^{14}\Omega^4 - 5916911 98\delta^{12}\Omega^6 - 757100132 7\delta^{10}\Omega^8 - 502300844 52\delta^8\Omega^{10} - 186002369856\delta^6\Omega^{12}\right. \\
& \qquad \left. - 350891730432\delta^4\Omega^{14} - 263308050432\delta^2\Omega^{16} - 326149079 04\Omega^{18}\right) \\
& + \gamma^3\delta^2\Omega^4\left(-24576\delta^{18} - 1041360\delta^{16}\Omega^2 - 5709336\delta^{14}\Omega^4 - 21711122\delta^{12}\Omega^6 - 39049749\delta^{10}\Omega^8 + 79393100 8\delta^8\Omega^{10} + 742658586 0\delta^6\Omega^{12}\right. \\
& \qquad \left. + 263126407 68\delta^4\Omega^{14} + 399229378 56\delta^2\Omega^{16} + 188554936 32\Omega^{18}\right) - i\gamma^6\delta\Omega^2\left(8064\delta^{18} + 491712\delta^{16}\Omega^2 + 54239460\delta^{14}\Omega^4 + 2356233029\delta^{12}\Omega^6\right. \\
& \qquad \left. + 37042345086\delta^{10}\Omega^8 + 2929153995 36\delta^8\Omega^{10} + 1282183349184\delta^6\Omega^{12} + 294831393868 8\delta^4\Omega^{14} + 298164436992 0\delta^2\Omega^{16} + 762373472256\Omega^{18}\right) \\
& + 3\gamma^9\left(41472\delta^{18} + 7199952\delta^{16}\Omega^2 + 371710780\delta^{14}\Omega^4 + 10547311268\delta^{12}\Omega^6 + 145921614933\delta^{10}\Omega^8 + 11297486619 64\delta^8\Omega^{10}\right. \\
& \qquad \left. + 529167964920 0\delta^6\Omega^{12} + 138435929199 36\delta^4\Omega^{14} + 175005443358 72\delta^2\Omega^{16} + 765443860070 4\Omega^{18}\right) \\
& - 3i\gamma^8\left(2304\delta^{19} + 606816\delta^{17}\Omega^2 + 43326372\delta^{15}\Omega^4 + 1695841752\delta^{13}\Omega^6 + 333323146 01\delta^{11}\Omega^8 + 329749148956\delta^9\Omega^{10} + 175458208920 0\delta^7\Omega^{12}\right. \\
& \qquad \left. + 492777191462 4\delta^5\Omega^{14} + 639331024896 0\delta^3\Omega^{16} + 255147953356 8\delta\Omega^{18}\right) \\
& + \gamma^7\left(-262080\delta^{18}\Omega^2 - 23452080\delta^{16}\Omega^4 + 40748352\delta^{14}\Omega^6 + 888942260 9\delta^{12}\Omega^8 + 107792180514\delta^{10}\Omega^{10} + 767750815464 6\delta^8\Omega^{12}\right. \\
& \qquad \left. + 323139605414 4\delta^6\Omega^{14} + 722977060838 4\delta^4\Omega^{16} + 736684454707 2\delta^2\Omega^{18} + 228712041676 8\Omega^{20}\right) \\
& + \gamma^5\left(-9216\delta^{20}\Omega^2 - 1676832\delta^{18}\Omega^4 - 33919692\delta^{16}\Omega^6 - 693723907\delta^{14}\Omega^8 + 841642970\delta^{12}\Omega^{10} + 133884257 79\delta^{10}\Omega^{12} + 101406921876\delta^8\Omega^{14}\right. \\
& \qquad \left. + 394833485376\delta^6\Omega^{16} + 746616282624\delta^4\Omega^{18} + 57493330329 6\delta^2\Omega^{20} + 97844723712\Omega^{22}\right).
\end{aligned}
\tag{B.26}
$$

We pose $x = \frac{i\mathcal{N}}{\Omega^5}\langle g|\phi_2|\phi_1\rangle$ and we have

$$
\begin{aligned}
x = {} & 5441955840000\gamma^{27} - 5441955840000i\gamma^{26}\delta + 7558272000\gamma^{25}\left(649\delta^2 + 6624\Omega^2\right) - 7558272000i\gamma^{24}\left(769\delta^3 + 6624\delta\Omega^2\right) \\
& + 5038848\gamma^{23}\left(364037\delta^4 + 8371600\delta^2\Omega^2 + 3927360\Omega^4\right) - 1679616i\gamma^{22}\left(1583861\delta^5 + 29542800\delta^3\Omega^2 + 1178208000\delta\Omega^4\right) \\
& + 46656\gamma^{21}\left(8674459\delta^6 + 317849964\delta^4\Omega^2 + 33147050400\delta^2\Omega^4 + 950137344\Omega^6\right) \\
& - 46656i\gamma^{20}\left(14924375\delta^7 + 450048564\delta^5\Omega^2 + 38441210400\delta^3\Omega^4 + 950137344\delta\Omega^6\right) \\
& + 1296\gamma^{19}\left(53202233\delta^8 + 2406130968\delta^6\Omega^2 + 391228299720\delta^4\Omega^4 + 24445400832\delta^2\Omega^6 + 482479358976\Omega^8\right) \\
& - 1296i\gamma^{18}\left(907889590\delta^9 + 39127471680\delta^7\Omega^2 + 531590009400\delta^5\Omega^4 + 27858696768\delta^3\Omega^6 + 482479358976\delta\Omega^8\right) \\
& + 1296\gamma^{17}\left(79090150\delta^{10} + 3905515116\delta^8\Omega^2 + 77171823780\delta^6\Omega^4 + 7331665291200\delta^4\Omega^6 + 310016790144\delta^2\Omega^8 + 4499427225600\Omega^{10}\right) \\
& - 432i\gamma^{16}\left(31492455\delta^{11} + 1829038133\delta^9\Omega^2 + 34709243058\delta^7\Omega^4 + 285096754656\delta^5\Omega^6 + 10393840615680\delta^3\Omega^8 + 134982816768\delta\Omega^{10}\right) \\
& + 36\gamma^{15}\left(31885020\delta^{12} + 1918467840\delta^{10}\Omega^2 + 41452380829\delta^8\Omega^4 + 472783052616\delta^6\Omega^6 + 29920717307520\delta^4\Omega^8 + 918778681036800\delta^2\Omega^{10}\right. \\
& \qquad \left. + 10187198005248\Omega^{12}\right) - 108i\gamma^{14}\left(10016220\delta^{13} + 779137576\delta^{11}\Omega^2 + 19356704609\delta^9\Omega^4 + 217299594976\delta^7\Omega^6 + 1229764187520\delta^5\Omega^8\right. \\
& \qquad \left. + 33491392957440\delta^3\Omega^{10} + 3395732668416\delta\Omega^{12}\right) \\
& - 2i\delta^5\Omega^8\left(4992\delta^{14} + 66484\delta^{12}\Omega^2 + 527540\delta^{10}\Omega^4 + 3142936\delta^8\Omega^6 + 13612995\delta^6\Omega^8 + 43746108\delta^4\Omega^{10} + 95074560\delta^2\Omega^{12} + 97320960\Omega^{14}\right) \\
& + 2\gamma\delta^4\Omega^8\left(9984\delta^{14} + 126888\delta^{12}\Omega^2 + 917920\delta^{10}\Omega^4 + 4921156\delta^8\Omega^6 + 18652099\delta^6\Omega^8 + 53637036\delta^4\Omega^{10} + 116727552\delta^2\Omega^{12} + 126517248\Omega^{14}\right) \\
& + 36\gamma^{13}\left(2210724\delta^{14} + 191311380\delta^{12}\Omega^2 + 9484814579\delta^{10}\Omega^4 + 618088834180\delta^8\Omega^6 + 46930197184\delta^6\Omega^8 + 2148195452448\delta^4\Omega^{10}\right. \\
& \qquad \left. + 50070551040000\delta^2\Omega^{12} + 4318394646528\Omega^{14}\right) - 36i\gamma^{12}\left(1555884\delta^{15} + 170685108\delta^{13}\Omega^2 + 5489037269\delta^{11}\Omega^4 + 782619146900\delta^9\Omega^6\right. \\
& \qquad \left. + 59626273335807\delta^7\Omega^8 + 2513864919648\delta^5\Omega^{10} + 53423114342400\delta^3\Omega^{12} + 4318394646528\delta\Omega^{14}\right) - i\gamma^2\delta^3\Omega^6\left(65760\delta^{16} + 1833528\delta^{14}\Omega^2\right. \\
& \qquad \left. + 19850394\delta^{12}\Omega^4 + 145041709\delta^{10}\Omega^6 + 755918640\delta^8\Omega^8 + 2837214348\delta^6\Omega^{10} + 7294863744\delta^4\Omega^{12} + 10502148096\delta^2\Omega^{14} + 5265948672\Omega^{16}\right) \\
& + \gamma^3\delta^2\Omega^6\left(1315209\delta^{16} + 33175920\delta^{14}\Omega^2 + 327802740\delta^{12}\Omega^4 + 2140931390\delta^{10}\Omega^6 + 9804489008\delta^8\Omega^8 + 33038549886\delta^6\Omega^{10} + 8316543744\delta^4\Omega^{12}\right. \\
& \qquad \left. + 1237336473600\delta^2\Omega^{14} + 62851645440\Omega^{16}\right) + 12\gamma^{11}\left(241488\delta^{16} + 35446248\delta^{14}\Omega^2 + 1256514741\delta^{12}\Omega^4 + 18391540082\delta^{10}\Omega^6\right. \\
& \qquad \left. + 153221553708\delta^8\Omega^8 + 8535314267040\delta^6\Omega^{10} + 298269722491200\delta^4\Omega^{12} + 5420132278272\delta^2\Omega^{14} + 36255791185920\Omega^{16}\right) \\
& - 12i\gamma^{10}\left(138240\delta^{17} + 24324912\delta^{15}\Omega^2 + 1058296335\delta^{13}\Omega^4 + 18753217276\delta^{11}\Omega^6 + 176980422032\delta^9\Omega^8 + 1001394250704\delta^7\Omega^{10}\right. \\
& \qquad \left. + 33040355908320\delta^5\Omega^{12} + 561845127168\delta^3\Omega^{14} + 36255791185920\delta\Omega^{16}\right) \\
& + 3\gamma^5\Omega^4\left(88704\delta^{18} + 4712168\delta^{16}\Omega^2 + 71055548\delta^{14}\Omega^4 + 592605576\delta^{12}\Omega^6 + 3314130215\delta^{10}\Omega^8 + 13356650436\delta^8\Omega^{10} + 39336581952\delta^6\Omega^{12}\right. \\
& \qquad \left. + 725318323200\delta^4\Omega^{14} + 6025759948800\delta^2\Omega^{16} + 108716359680\Omega^{18}\right) - i\gamma^4\delta\Omega^4\left(133056\delta^{18} + 7890456\delta^{16}\Omega^2 + 135444348\delta^{14}\Omega^4 + 1277995680\delta^{12}\Omega^6\right. \\
& \qquad \left. + 8175513451\delta^{10}\Omega^8 + 36598095660\delta^8\Omega^{10} + 1109356490880\delta^6\Omega^{12} + 19954713139200\delta^4\Omega^{14} + 163552296960\delta^2\Omega^{16} + 3261490790400\Omega^{18}\right) \\
& + 3\gamma^7\Omega^2\left(62208\delta^{18} + 7556880\delta^{16}\Omega^2 + 207514236\delta^{14}\Omega^4 + 2401748723\delta^{12}\Omega^6 + 16957763126\delta^{10}\Omega^8 + 83383135720\delta^8\Omega^{10}\right. \\
& \qquad \left. + 293814291072\delta^6\Omega^{12} + 6603168867840\delta^4\Omega^{14} + 73926593740800\delta^2\Omega^{16} + 254124490752\Omega^{18}\right) \\
& - i\gamma^6\delta\Omega^2\left(93312\delta^{18} + 12761856\delta^{16}\Omega^2 + 405751572\delta^{14}\Omega^4 + 5484447327\delta^{12}\Omega^6 + 44799586370\delta^{10}\Omega^8 + 245233535904\delta^8\Omega^{10}\right. \\
& \qquad \left. + 889450394976\delta^6\Omega^{12} + 19452679441920\delta^4\Omega^{14} + 212440950374400\delta^2\Omega^{16} + 762373472256\Omega^{18}\right) \\
& + 3\gamma^9\left(13824\delta^{18} + 4689504\delta^{16}\Omega^2 + 263711676\delta^{14}\Omega^4 + 4996532116\delta^{12}\Omega^6 + 47533515515\delta^{10}\Omega^8 + 295135304692\delta^8\Omega^{10}\right. \\
& \qquad \left. + 1281392225232\delta^6\Omega^{12} + 3547180953216\delta^4\Omega^{14} + 50829047562240\delta^2\Omega^{16} + 255147953356800\Omega^{18}\right) \\
& - 3i\gamma^8\left(6912\delta^{19} + 2662560\delta^{17}\Omega^2 + 176257092\delta^{15}\Omega^4 + 3992597180\delta^{13}\Omega^6 + 44983802989\delta^{11}\Omega^8 + 312994921284\delta^9\Omega^{10}\right. \\
& \qquad \left. + 1392003685872\delta^7\Omega^{12} + 37075981029120\delta^5\Omega^{14} + 508758324019200\delta^3\Omega^{16} + 255147953356800\delta\Omega^{18}\right).
\end{aligned}
\tag{B.27}
$$

Appendix C

Steady State of a Three-level Atom Excited by Two Lasers

In this appendix, we present the analytical values of the steady state density matrix ρ governed by the master equation

$$\begin{aligned}\dot{\rho} &= \frac{-i}{\hbar}[H,\rho] - \gamma_a(|a\rangle\langle a|\rho - 2|b\rangle\langle a|\rho|a\rangle\langle b| + \rho|a\rangle\langle a|) \\ &\quad + \gamma_b(|b\rangle\langle b|\rho - 2|c\rangle\langle b|\rho|b\rangle\langle c| + \rho|b\rangle\langle b|). \end{aligned} \tag{C.1}$$

with the Hamiltonian

$$H = -\hbar\delta|a\rangle\langle a| - \hbar\Delta|b\rangle\langle b| + \hbar\Omega_1\left(|b\rangle\langle c| + |c\rangle\langle b|\right) + \hbar\Omega_2\left(|a\rangle\langle b| + |b\rangle\langle a|\right), \tag{C.2}$$

as presented in Sec. 5.1. We first express the common denominator $\mathcal{N}$ to all matrix elements

$$\begin{aligned}\mathcal{N} = {} & \gamma_a^5\gamma_b\left(\Delta^2 + \gamma_b^2 + 2\Omega_1^2\right) \\ & + \gamma_a^3\gamma_b\left(\left(\Delta^2 + \gamma_b^2 + 2\Omega_1^2\right)\left(2\delta^2 + 2\delta\Delta + \Delta^2 + \gamma_b^2 + 2\Omega_1^2\right) - \left(\Delta(2\delta + \Delta) - 5\gamma_b^2 - 6\Omega_1^2\right)\Omega_2^2 + \Omega_2^4\right) \\ & + \gamma_b^2\Omega_2^2\left((\delta+\Delta)^2\gamma_b^2 + \Omega_1^4 + \left(-\Delta(\delta+\Delta) + \Omega_2^2\right)^2 + 2\Omega_1^2\left((\delta+\Delta)^2 + \Omega_2^2\right)\right) \\ & + 2\gamma_a^4\left(\gamma_b^4 + \Omega_1^2\Omega_2^2 + \gamma_b^2\left(\Delta^2 + 2\Omega_1^2 + \Omega_2^2\right)\right) \\ & + \gamma_a^2\left(\Omega_1^2\Omega_2^2\left(2\delta^2 + 2\delta\Delta + \Delta^2 + 2\Omega_1^2 + 2\Omega_2^2\right) + \gamma_b^4\left(2(\delta+\Delta)^2 + 2\Omega_1^2 + 3\Omega_2^2\right)\right. \\ & \qquad \left. + \gamma_b^2\left(2\left((\delta+\Delta)^2 + \Omega_1^2\right)\left(\Delta^2 + 2\Omega_1^2\right) + \left(2\delta^2 - 4\delta\Delta - 3\Delta^2 + 7\Omega_1^2\right)\Omega_2^2 + 4\Omega_2^4\right)\right) \\ & + \gamma_a\gamma_b\left((\delta+\Delta)^2\gamma_b^4 + 2\Omega_1^6 + \left(\delta^2 + \Omega_2^2\right)\left(-\Delta(\delta+\Delta) + \Omega_2^2\right)^2\right. \\ & \quad + \Omega_1^4\left(-4\delta^2 - 4\delta\Delta + \Delta^2 + 4\Omega_2^2\right) + \Omega_1^2\left(2\delta\left(\delta^3 + 2\delta^2\Delta - \Delta^3\right) + 4(\delta+\Delta)^2\Omega_2^2 + 3\Omega_2^4\right) \\ & \quad \left. + \gamma_b^2\left((\delta+\Delta)^2\left(\delta^2 + \Delta^2\right) + \Omega_1^4 + \left(\delta^2 - \Delta^2\right)\Omega_2^2 + 3\Omega_2^4 + 2\Omega_1^2\left(\Delta(\delta+\Delta) + 2\Omega_2^2\right)\right)\right), \end{aligned} \tag{C.3}$$

The diagonal elements of ρ_c are

$$\frac{\mathcal{N}}{\Omega_1^2\Omega_2^2}\langle a|\rho|a\rangle = \gamma_b\left(\gamma_a\left(\delta^2 + (\gamma_a+\gamma_b)^2\right) + (\gamma_a+\gamma_b)\Omega_1^2\right) + (\gamma_a+\gamma_b)^2\Omega_2^2, \tag{C.4}$$

We pose $x = \frac{\mathcal{N}}{\Omega_1^2\Omega_2}\langle b|\rho|b\rangle$ and we have

$$\begin{aligned} x = {} & \gamma_a^5\gamma_b + (\delta+\Delta)^2\gamma_b^2\Omega_2^2 + \gamma_a^4\left(2\gamma_b^2+\Omega_2^2\right) + \gamma_a^3\gamma_b\left(2\delta^2+2\delta\Delta+\Delta^2+\gamma_b^2+2\Omega_1^2+3\Omega_2^2\right) \\ & + \gamma_a\gamma_b\left((\delta+\Delta)^2\gamma_b^2 + \left(-\delta(\delta+\Delta)+\Omega_1^2\right)^2 + \left((\delta+\Delta)^2+2\Omega_1^2\right)\Omega_2^2+\Omega_2^4\right) \\ & + \gamma_a^2\left(\Omega_2^2\left(\delta^2+\Omega_1^2+\Omega_2^2\right) + 2\gamma_b^2\left((\delta+\Delta)^2+\Omega_1^2+\Omega_2^2\right)\right). \end{aligned} \tag{C.5}$$

We pose $x = \mathcal{N}\langle c|\rho|c\rangle$ and we have

$$\begin{aligned} x = {} & \gamma_a^5\gamma_b\left(\Delta^2+\gamma_b^2+\Omega_1^2\right) \\ & + \gamma_a^3\gamma_b\left(\left(\Delta^2+\gamma_b^2+\Omega_1^2\right)\left(2\delta^2+2\delta\Delta+\Delta^2+\gamma_b^2+2\Omega_1^2\right) - \left(\Delta(2\delta+\Delta)-5\gamma_b^2-2\Omega_1^2\right)\Omega_2^2+\Omega_2^4\right) \\ & + \gamma_b^2\Omega_2^2\left((\delta+\Delta)^2\gamma_b^2 + \left(-\Delta(\delta+\Delta)+\Omega_2^2\right)^2 + \Omega_1^2\left((\delta+\Delta)^2+\Omega_2^2\right)\right) \\ & + \gamma_a^4\left(2\gamma_b^4+\Omega_1^2\Omega_2^2+2\gamma_b^2\left(\Delta^2+\Omega_1^2+\Omega_2^2\right)\right) \\ & + \gamma_a^2\left(\Omega_1^2\left((\delta+\Delta)^2+\Omega_1^2\right)\Omega_2^2 + \gamma_b^4\left(2(\delta+\Delta)^2+2\Omega_1^2+3\Omega_2^2\right)\right. \\ & \qquad \left. + \gamma_b^2\left(2\left(\Delta^2+\Omega_1^2\right)\left((\delta+\Delta)^2+\Omega_1^2\right) + \left(2\delta^2-4\delta\Delta-3\Delta^2+3\Omega_1^2\right)\Omega_2^2+4\Omega_2^4\right)\right) \\ & + \gamma_a\gamma_b\left((\delta+\Delta)^2\gamma_b^4 + \Omega_1^6 + \Omega_1^4\left(-2\delta^2-2\delta\Delta+\Delta^2+\Omega_2^2\right) + \left(\delta^2+\Omega_2^2\right)\left(-\Delta(\delta+\Delta)+\Omega_2^2\right)^2\right. \\ & \qquad + \Omega_1^2\left(\delta(\delta-\Delta)(\delta+\Delta)(\delta+2\Delta) + \left(2\delta^2+6\delta\Delta+3\Delta^2\right)\Omega_2^2\right) \\ & \qquad \left. + \gamma_b^2\left((\delta+\Delta)^2\left(\delta^2+\Delta^2\right) + \Omega_1^4 + \left(\delta^2-\Delta^2\right)\Omega_2^2 + 3\Omega_2^4 + \Omega_1^2\left(-\delta^2+\Delta^2+3\Omega_2^2\right)\right)\right). \end{aligned} \tag{C.6}$$

Of course, the condition $\mathrm{Tr}\,(\rho) = 1$ verifies. The following terms are the off diagonal terms above the diagonal. We pose $x = \frac{\mathcal{N}}{\Omega_1^2\Omega_2}\langle a|\rho|b\rangle$ and we have

$$\begin{aligned} x = {} & \gamma_a\gamma_b\left((\delta+\Delta-i\gamma_a)\left(\delta^2+(\gamma_a+\gamma_b)^2\right) - i\left(-i\delta+\gamma_a+\gamma_b\right)\Omega_1^2\right) \\ & + \left((\delta-i\gamma_a)\gamma_a^2 + (\delta+\Delta-2i\gamma_a)\gamma_a\gamma_b + (\delta+\Delta-i\gamma_a)\gamma_b^2\right)\Omega_2^2. \end{aligned} \tag{C.7}$$

We pose $x = \frac{\mathcal{N}}{\Omega_1\Omega_2}\langle a|\rho|c\rangle$ and we have

$$\begin{aligned} x = {} & -\gamma_a^4\gamma_b(\gamma_b+i\Delta) + \gamma_a^3\gamma_b\left(-(2\gamma_b+i\delta)(\gamma_b+i\Delta)+\Omega_1^2-\Omega_2^2\right) - \gamma_b^2\Omega_2^2\left(i\gamma_b\delta-\delta\Delta+\Omega_1^2+\Omega_2^2\right) \\ & + \gamma_a\gamma_b\left(-i\gamma_b^3\delta+\delta^3\Delta+\Omega_1^4+\Omega_1^2\Omega_2^2-\Omega_2^4+\gamma_b^2\left(\delta\Delta-\Omega_1^2-2\Omega_2^2\right)+\Delta^2\left(\Omega_1^2-\Omega_2^2\right)\right. \\ & \qquad \left. - \delta^2\left(2\Delta^2+\Omega_1^2+\Omega_2^2\right)+\delta\Delta\left(\Delta^2+3\Omega_2^2\right)\right. \\ & \qquad \left. - i\gamma_b\left(\delta^3-2\delta^2\Delta+\delta\Delta^2-2\delta\Omega_1^2+2\Delta\Omega_1^2+(\delta+\Delta)\Omega_2^2\right) - \gamma_a^2\left(\gamma_b^4+i\gamma_b^3(2\delta+\Delta)-\Omega_1^2\Omega_2^2\right.\right. \\ & \qquad \left.\left. + \gamma_b^2\left(\delta^2-4\delta\Delta+\Delta^2+3\Omega_2^2\right)+i\gamma_b\left(\delta^2\Delta-2\delta\left(\Delta^2+\Omega_1^2\right)+\Delta\left(\Delta^2+2\Omega_1^2+\Omega_2^2\right)\right)\right). \end{aligned} \tag{C.8}$$

We pose $x = \frac{\mathcal{N}}{\Omega_1}\langle b|\rho|c\rangle$ and we have

$$
\begin{aligned}
x = {} & \gamma_a^5 \left(\Delta - i\gamma_b\right)\gamma_b + (\delta+\Delta)\gamma_b^2\Omega_2^2\left((\delta+\Delta)\left(\Delta - i\gamma_b\right) - \Omega_2^2\right) + \gamma_a^4\gamma_b\left(2\left(\Delta - i\gamma_b\right)\gamma_b - i\Omega_2^2\right) \\
& + \gamma_a^3\gamma_b\left(\left(\Delta - i\gamma_b\right)\left(2\delta^2 + 2\delta\Delta + \Delta^2 + \gamma_b^2 + 2\Omega_1^2\right) - (\delta + 3i\gamma_b)\,\Omega_2^2\right) \\
& + \gamma_a^2\left((2\delta+\Delta)\Omega_1^2\Omega_2^2 - i\gamma_b\Omega_2^2\left(\delta^2 + \Omega_1^2 + \Omega_2^2\right) - 2i\gamma_b^3\left((\delta+\Delta)^2 + \Omega_1^2 + \Omega_2^2\right)\right. \\
& \qquad \left. + \gamma_b^2\left(2\Delta(\delta+\Delta)^2 + 2\Delta\Omega_1^2 - (2\delta+\Delta)\Omega_2^2\right)\right) + \gamma_a\gamma_b\left(-i(\delta+\Delta)^2\gamma_b^3 + \Delta\Omega_1^4\right. \\
& \qquad \left. + (\delta+\Delta)\gamma_b^2\left(\Delta(\delta+\Delta) - \Omega_2^2\right) + (\delta+\Delta)\left(\Delta(\delta+\Delta) - \Omega_2^2\right)\left(\delta^2 + \Omega_2^2\right)\right. \\
& \left. + 2(\delta+\Delta)\Omega_1^2\left(-\delta\Delta + \Omega_2^2\right) - i\gamma_b\left(\left(-\delta(\delta+\Delta) + \Omega_1^2\right)^2 + \left((\delta+\Delta)^2 + 2\Omega_1^2\right)\Omega_2^2 + \Omega_2^4\right)\right).
\end{aligned}
\tag{C.9}
$$

Bibliography

[1] F. Mintert, A. R. R. Carvalho, M. Kuś, and A. Buchleitner, Phys. Rep. **415**, 207–259 (2005).

[2] S. L. Braunstein and P. van Loock, Rev. Mod. Phys. **77**, 513 (2005).

[3] A. Pati, Phys. Lett. A **278**, 118 (2000).

[4] A. Peres, Phys. Rev. Lett. **77**, 1413–1415 (1996).

[5] J. Bell, Physics **1**, 195–200 (1964).

[6] W. Dür, Phys. Rev. Lett. **87**, 230402 (2001).

[7] O. Gühne, P. Hyllus, D. Bruß, A. Ekert, M. Lewenstein, C. Macchiavello, and A. Sanpera, Phys. Rev. A **66**, 062305 (2002).

[8] R. Simon, Phys. Rev. Lett. **84**, 2726–2729 (2000).

[9] L.-M. Duan, G. Giedke, J. I. Cirac, and P. Zoller, Phys. Rev. Lett. **84**, 2722–2725 (2000).

[10] H. F. Hofmann, Phys. Rev. A **68**, 034307 (2003).

[11] M. Hillery and M. S. Zubairy, Phys. Rev. Lett. **96**, 050503 (2006).

[12] A. A. Klyachko, B. Öztop, and A. S. Shumovsky, Phys. Rev. A **75**, 032315 (2007).

[13] G. A. Durkin and C. Simon, Phys. Rev. Lett. **95**, 180402 (2005).

[14] V. Giovannetti, S. Mancini, D. Vitali, and P. Tombesi, Phys. Rev. A **67**, 022320 (2003).

[15] E. Shchukin and W. Vogel, Phys. Rev. Lett. **95**, 230502 (2005).

[16] O. Gühne, Phys. Rev. Lett. **92**, 117903 (2004).

[17] G. S. Agarwal and A. Biswas, New J. Phys. **7**, 211 (2005).

[18] H. Nha and J. Kim, Phys. Rev. A **74**, 012317 (2006).

[19] H. Nha, Phys. Rev. A **76**, 014305 (2007).

[20] L. Song, X. Wang, D. Yan, and Z.-S. Pu, J. Phys. B **41**, 015505 (2008).

[21] E. Schrödinger, Sitzungsber. Preuss. Akad. Wiss., Phys. Math. Kl. **19**, 296 (1930).

[22] M. Horodecki, P. Horodecki, and R. Horodecki, Phys. Lett. A **223**, 1 (1996).

[23] A. Mair, A. Vaziri, G. Weihs, and A. Zeilinger, Nature **412**, 313–316 (2001).

[24] T. Tsegaye, J. Söderholm, M. Atatüre, A. Trifonov, G. Björk, A. V. Sergienko, B. E. A. Saleh, and M. C. Teich, Phys. Rev. Lett. **85**, 5013–5017 (2000).

[25] C. C. Gerry and R. Grobe, Phys. Rev. A **75**, 034303 (2007).

[26] W. Dür, G. Vidal, and J. I. Cirac, Phys. Rev. A **62**, 062314 (2000).

[27] A. Acín, A. Andrianov, L. Costa, E. Jané, J. I. Latorre, and R. Tarrach, Phys. Rev. Lett. **85**, 1560–1563 (2000).

[28] R. F. Werner, Phys. Rev. A **40**, 4277–4281 (1989).

[29] G. Tóth and O. Gühne, Phys. Rev. Lett. **94**, 060501 (2005).

[30] A. R. U. Devi, R. Prabhu, and A. K. Rajagopal, Phys. Rev. Lett. **98**, 060501 (2007).

[31] G. S. Agarwal and S. A. Ponomarenko, Phys. Rev. A **67**, 032103 (2003).

[32] D. Bruß, J. Math. Phys. **43**, 4237–4251 (2002).

[33] W. K. Wootters, Phys. Rev. Lett. **80**, 2245–2248 (1998).

[34] V. Coffman, J. Kundu, and W. K. Wootters, Phys. Rev. A **61**, 052306 (2000).

[35] R. Lohmayer, A. Osterloh, J. Siewert, and A. Uhlmann, Phys. Rev. Lett. **97**, 260502 (2006).

[36] A. Osterloh, J. Siewert, and A. Uhlmann, Phys. Rev. A **77**, 032310 (2008).

[37] S. Albeverio and S.-M. Fei, J. Opt. B: Quantum Semiclassical Opt. **3**, 223 (2001).

[38] A. Uhlmann, Phys. Rev. A **62**, 032307 (2000).

[39] P. Rungta, V. Bužek, C. M. Caves, M. Hillery, and G. J. Milburn, Phys. Rev. A **64**, 042315 (2001).

[40] S. J. Akhtarshenas, J. Phys. A **38**, 6777 (2005).

[41] X.-H. Gao and S.-M. Fei, Eur. Phys. J. Spec. Top. **159**, 71–77 (2008).

[42] C.-s. Yu and H.-s. Song, Phys. Rev. A **72**, 022333 (2005).

[43] S. P. Walborn, P. H. Souto Ribeiro, L. Davidovich, F. Mintert, and A. Buchleitner, Nature **440**, 1022–1024 (2006).

[44] W. Dür, J. I. Cirac, and R. Tarrach, Phys. Rev. Lett. **83**, 3562–3565 (1999).

[45] A. Acín, D. Bruß, M. Lewenstein, and A. Sanpera, Phys. Rev. Lett. **87**, 040401 (2001).

[46] P. Jorrand and M. Mhalla, Int. J. Found. Comput. Sci. **14**, 797–814 (2003).

[47] A. R. U. Devi, R. Prabhu, and A. K. Rajagopal, Phys. Rev. Lett. **98**, 060501 (2007).

[48] C. H. Bennett, D. P. DiVincenzo, J. A. Smolin, and W. K. Wootters, Phys. Rev. A **54**, 3824–3851 (1996).

[49] J. Neumann, *Mathematische Grundlagen der Quantenmechanik*, Springer (1995).

[50] S. Hill and W. K. Wootters, Phys. Rev. Lett. **78**, 5022–5025 (1997).

[51] T. G. Kolda and B. W. Bader, SIAM Rev. **51**, 455–500 (2009).

[52] R. Oldenburger, The Annals of Mathematics **35**, pp. 622–653 (1934).

[53] C. H. Bennett, D. P. DiVincenzo, T. Mor, P. W. Shor, J. A. Smolin, and B. M. Terhal, Phys. Rev. Lett. **82**, 5385–5388 (1999).

[54] G. V. Varada and G. S. Agarwal, Phys. Rev. A **45**, 6721–6729 (1992).

[55] D. Jaksch, J. I. Cirac, P. Zoller, S. L. Rolston, R. Côté, and M. D. Lukin, Phys. Rev. Lett. **85**, 2208–2211 (2000).

[56] I. E. Protsenko, G. Reymond, N. Schlosser, and P. Grangier, Phys. Rev. A **65**, 052301 (2002).

[57] M. D. Lukin, M. Fleischhauer, R. Cote, L. M. Duan, D. Jaksch, J. I. Cirac, and P. Zoller, Phys. Rev. Lett. **87**, 037901 (2001).

[58] C. Hettich, C. Schmitt, J. Zitzmann, S. Kuhn, I. Gerhardt, and V. Sandoghdar, Science **298**, 385–389 (2002).

[59] M. Saffman and T. G. Walker, Phys. Rev. A **66**, 065403 (2002).

[60] D. Tong, S. M. Farooqi, J. Stanojevic, S. Krishnan, Y. P. Zhang, R. Côté, E. E. Eyler, and P. L. Gould, Phys. Rev. Lett. **93**, 063001 (2004).

[61] K. Singer, M. Reetz-Lamour, T. Amthor, L. G. Marcassa, and M. Weidemüller, Phys. Rev. Lett. **93**, 163001 (2004).

[62] T. C. Liebisch, A. Reinhard, P. R. Berman, and G. Raithel, Phys. Rev. Lett. **95**, 253002 (2005).

[63] T. Vogt, M. Viteau, J. Zhao, A. Chotia, D. Comparat, and P. Pillet, Phys. Rev. Lett. **97**, 083003 (2006).

[64] K. M. Birnbaum, A. Boca, R. Miller, A. D. Boozer, T. E. Northup, and H. J. Kimble, Nature **436**, 87–90 (2005).

[65] E. Urban, T. A. Johnson, T. Henage, L. Isenhower, D. D. Yavuz, T. G. Walker, and M. Saffman, Nat. Phys. **5**, 110–114 (2009).

[66] A. Gaetan, Y. Miroshnychenko, T. Wilk, A. Chotia, M. Viteau, D. Comparat, P. Pillet, A. Browaeys, and P. Grangier, Nat. Phys. **5**, 115–118 (2009).

[67] T. Pohl and P. R. Berman, Phys. Rev. Lett. **102**, 013004 (2009).

[68] S. Das, G. S. Agarwal, and M. O. Scully, Phys. Rev. Lett. **101**, 153601 (2008).

[69] G. S. Agarwal, *Quantum Statistical Theories of Spontaneous Emission and Their Relation to Other Approaches*, Springer, Berlin (1974).

[70] J. v. Zanthier, T. Bastin, and G. S. Agarwal, Phys. Rev. A **74**, 061802 (2006).

[71] C. Skornia, J. v. Zanthier, G. S. Agarwal, E. Werner, and H. Walther, Phys. Rev. A **64**, 063801 (2001).

[72] M. Lax, Phys. Rev. **172**, 350–361 (1968).

[73] R. J. Glauber, Phys. Rev. **130**, 2529–2539 (1963).

[74] T. G. Walker and M. Saffman, Phys. Rev. A **77**, 032723 (2008).

[75] C. Ates, T. Pohl, T. Pattard, and J. M. Rost, Phys. Rev. Lett. **98**, 023002 (2007).

[76] T. Amthor, C. Giese, C. S. Hofmann, and M. Weidemüller, Phys. Rev. Lett. **104**, 013001 (2010).

[77] M. Saffman and K. Mølmer, Phys. Rev. Lett. **102**, 240502 (2009).

[78] S. Wüster, C. Ates, A. Eisfeld, and J. M. Rost, Phys. Rev. Lett. **105**, 053004 (2010).

[79] G. S. Agarwal, Phys. Rev. A **55**, 2467–2470 (1997).

[80] H. Lee and M. Scully, Found. Phys. **28**, 585–600 (1998).

[81] O. Kocharovskaya and P. Mandel, Phys. Rev. A **42**, 523–535 (1990).

[82] H. X. Chen, A. V. Durrant, J. P. Marangos, and J. A. Vaccaro, Phys. Rev. A **58**, 1545–1548 (1998).

[83] J. Gea-Banacloche, Y.-q. Li, S.-z. Jin, and M. Xiao, Phys. Rev. A **51**, 576–584 (1995).

[84] S. E. Harris, Physics Today **50**, 36–42 (1997).

[85] M. Fleischhauer, A. Imamoglu, and J. P. Marangos, Rev. Mod. Phys. **77**, 633–673 (2005).

[86] S. E. Harris, J. E. Field, and A. Imamoğlu, Phys. Rev. Lett. **64**, 1107–1110 (1990).

[87] J. Marangos, Nature **397**, 559–560 (1999).

[88] M. Mücke, E. Figueroa, J. Bochmann, C. Hahn, K. Murr, S. Ritter, C. J. Villas-Boas, and G. Rempe, Nature **465**, 755–758 (2010).

[89] A. K. Mohapatra, T. R. Jackson, and C. S. Adams, Phys. Rev. Lett. **98**, 113003 (2007).

[90] A. Yariv, *Quantum Electronics*, John Wiley & Sons, Singapore, 3rd edition (1989).

[91] F. C. Grynberg Gilbert, Aspect Alain, *Introduction aux lasers et à l'optique quantique*, Ellipses, Cours de l'Ecole Polytechnique (1997).

[92] R. D. L. Kronig, J. Opt. Soc. Am. **12**, 547–556 (1926).

[93] H. Kramers, Atti Cong. Intern. Fisica Como **2**, 545–557 (1927).

[94] R. Loudon, *The Quantum Theory of Light*, Oxford University Press, London (2000).

[95] M. S. Kim and G. S. Agarwal, Phys. Rev. A **57**, 3059–3064 (1998).

[96] M. Orrit, Science **298**, 369–370 (2002).

[97] J. M. Fink, R. Bianchetti, M. Baur, M. Göppl, L. Steffen, S. Filipp, P. J. Leek, A. Blais, and A. Wallraff, Phys. Rev. Lett. **103**, 083601 (2009).

[98] S. Filipp, P. Maurer, P. J. Leek, M. Baur, R. Bianchetti, J. M. Fink, M. Göppl, L. Steffen, J. M. Gambetta, A. Blais, and A. Wallraff, Phys. Rev. Lett. **102**, 200402 (2009).

[99] J. M. Fink, M. Goppl, M. Baur, R. Bianchetti, P. J. Leek, A. Blais, and A. Wallraff, Nature **454**, 315–318 (2008).

[100] M. Baur, S. Filipp, R. Bianchetti, J. M. Fink, M. Göppl, L. Steffen, P. J. Leek, A. Blais, and A. Wallraff, Phys. Rev. Lett. **102**, 243602 (2009).

[101] J. J. Sanchez-Mondragon, N. B. Narozhny, and J. H. Eberly, Phys. Rev. Lett. **51**, 550–553 (1983).

[102] G. S. Agarwal, Phys. Rev. Lett. **53**, 1732–1734 (1984).

[103] M. G. Raizen, R. J. Thompson, R. J. Brecha, H. J. Kimble, and H. J. Carmichael, Phys. Rev. Lett. **63**, 240–243 (1989).

[104] A. Boca, R. Miller, K. M. Birnbaum, A. D. Boozer, J. McKeever, and H. J. Kimble, Phys. Rev. Lett. **93**, 233603 (2004).

[105] P. Maunz, T. Puppe, I. Schuster, N. Syassen, P. W. H. Pinkse, and G. Rempe, Phys. Rev. Lett. **94**, 033002 (2005).

[106] R. J. Thompson, Q. A. Turchette, O. Carnal, and H. J. Kimble, Phys. Rev. A **57**, 3084–3104 (1998).

[107] E. Solano, G. S. Agarwal, and H. Walther, Phys. Rev. Lett. **90**, 027903 (2003).